

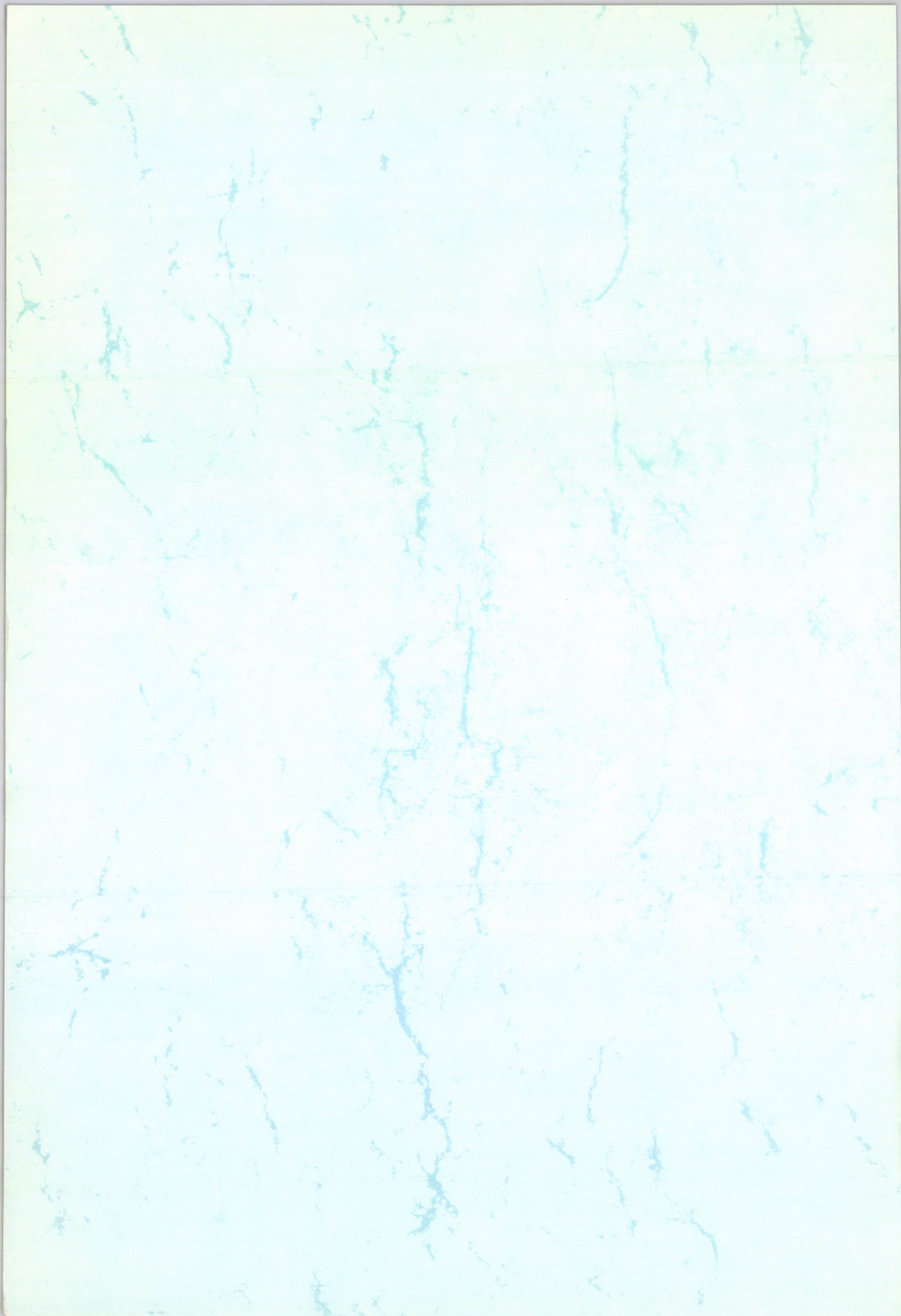
ATOMKI

ANNUAL REPORT

1993



INSTITUTE OF NUCLEAR RESEARCH
OF THE HUNGARIAN ACADEMY OF SCIENCES
DEBRECEN, HUNGARY



INSTITUTE OF NUCLEAR RESEARCH
OF THE HUNGARIAN ACADEMY OF SCIENCES
DEBRECEN, HUNGARY

ANNUAL REPORT 1993

ATOMKI

Postal address:

Debrecen
P.O.Box 51
H-4001
Hungary

Edited by: Z. Gácsi

HU ISSN0 0231-3596

ATOMKI

Preface

Since the 94 contributions to this Annual Report and their distribution among the research topics properly represent our results in 1993, an introduction by the director can only serve two purposes: (i) emphasize (or advertize) some of the results, (ii) report on developments not obvious from the research reports.

It is not easy, however, to single out any results and say: these are the most significant ones. The main branch of our research is nuclear and atomic physics, but the topics range from general physics to the development of instruments, it includes environmental research and touches upon biology and medicine. In such a broad range the highlighting of anything is questionable and may be futile. Therefore, I leave it to the reader to find the reports of their interest, or judge the results. General information about the Institute can be found in the first section; it gives some insight into the organisation, personnel and finance of the Institute.

A few important developments took place in 1993, however, which affected the whole institute, and may not be evident from the research reports. Here I will give a short summary of these.

The lack of a computer network and a central computer was a serious problem for the institute. A grant from FEFA (Fund for the Development of Higher Education) made possible the installation of a state-of-the-art **computer network**. At the same time, we obtained a grant from IIF (Fund for Information Infrastructure Development) for a central computer, and we acquired a four-processor **Silicon Graphics Challenge-L** machine, which will serve as a central computer for the Institute and for the physics departments of Kossuth University.

With the physics departments of Kossuth University we worked out the program of a new type of PhD training in physics. The **PhD program has been approved** by the Hungarian Accreditation Committee, and from October, 1993 fifteen students started their studies in this new framework.

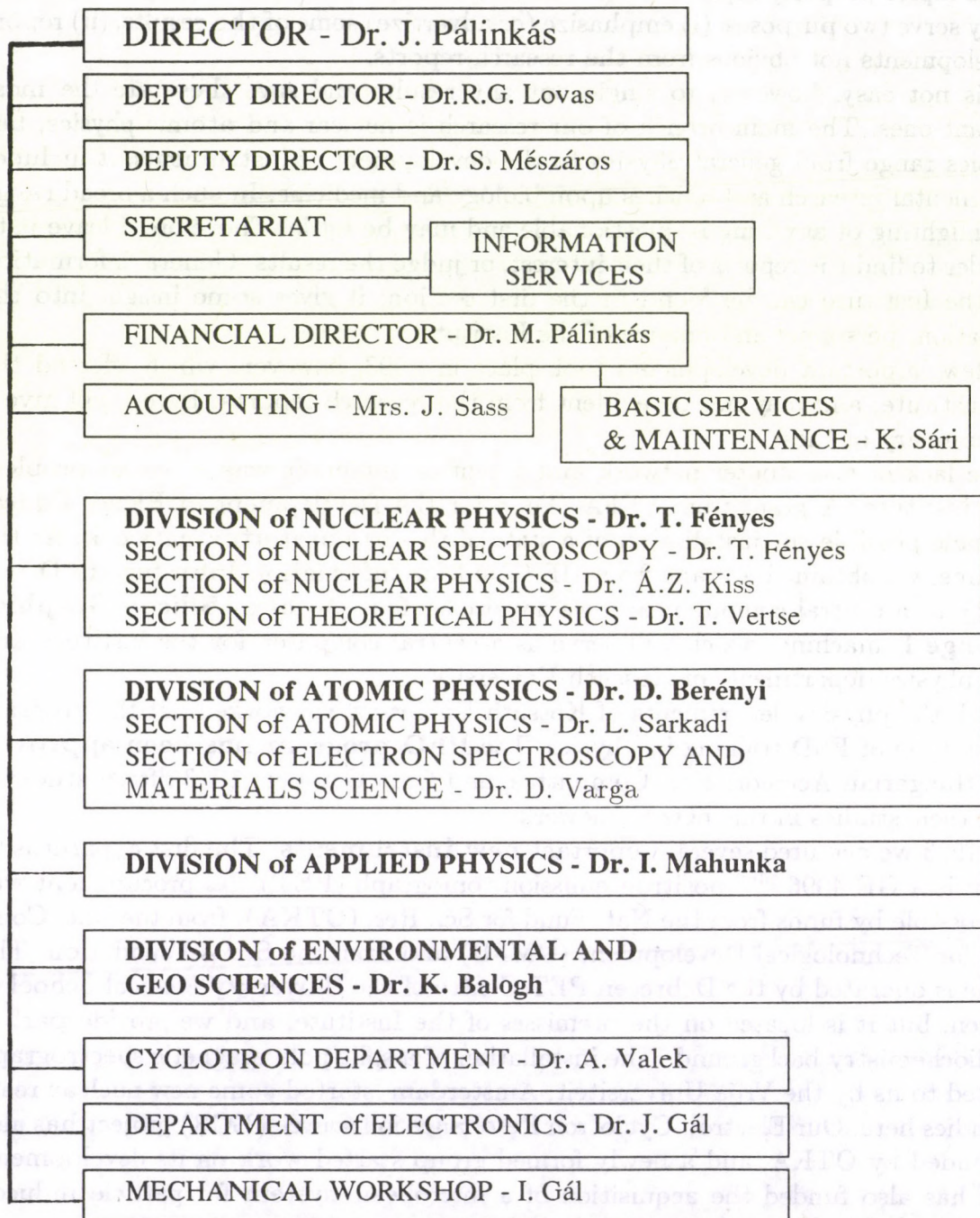
In 1993 we acquired several important **new instruments**. The first apparatus to mention is a GE 4096^{plus} positron emission tomograph (PET). Its procurement was made possible by funds from the Nat. Fund for Sci. Res. (OTKA), from the Nat. Committee for Technological Development (OMFB) and from the Soros Foundation. The machine is operated by the Debrecen PET Centre of the University Medical School of Debrecen, but it is located on the premisses of the Institute, and we provide part of the radiochemistry background. The installation of a split-pole magnetic spectrograph presented to us by the Vrije Universiteit, Amsterdam, started some new nuclear reaction studies here. Our Electron Cyclotron Resonance ion source (ECR) project has also been funded by OTKA, and a newly formed group started work on its development. OTKA has also funded the acquisition of a microbeam system for particle induced X-ray emission studies.

These new apparatuses start to work in 1994 and we all look forward to seeing the first results.

Debrecen, March 9, 1994

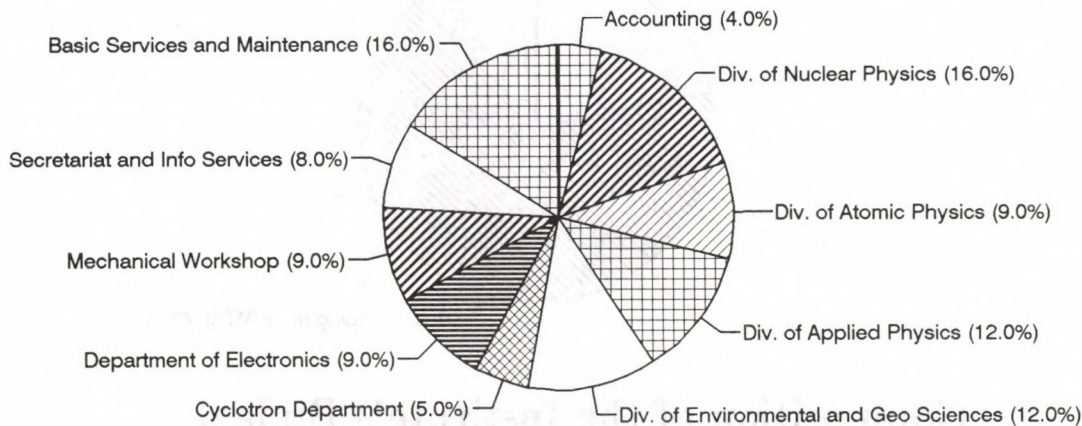

Dr. József Pálincás
Director

The organisation structure of the
Institute of Nuclear Research
of the Hungarian Academy of Sciences

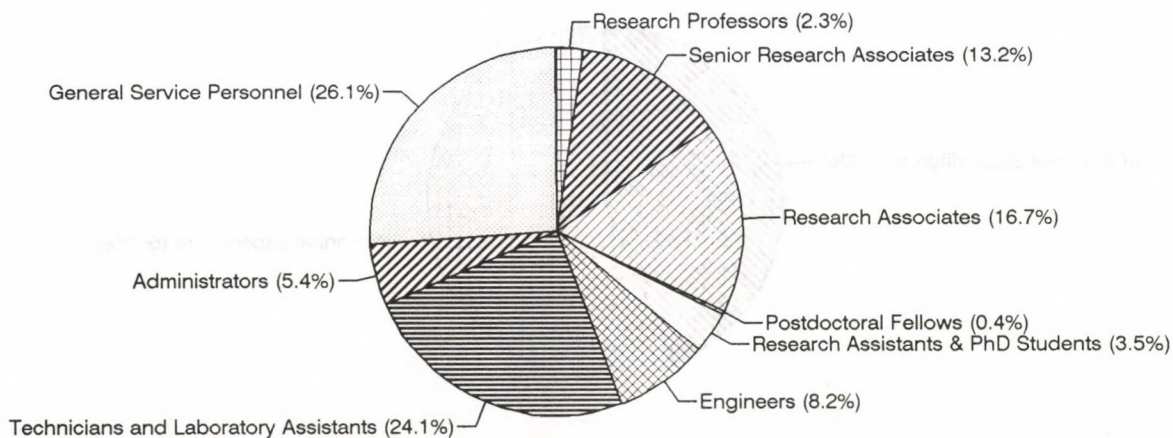


Personnel

The Institute at present employs a total of 240 persons. The affiliation of personnel to units of organisation and the composition of personnel are given below.



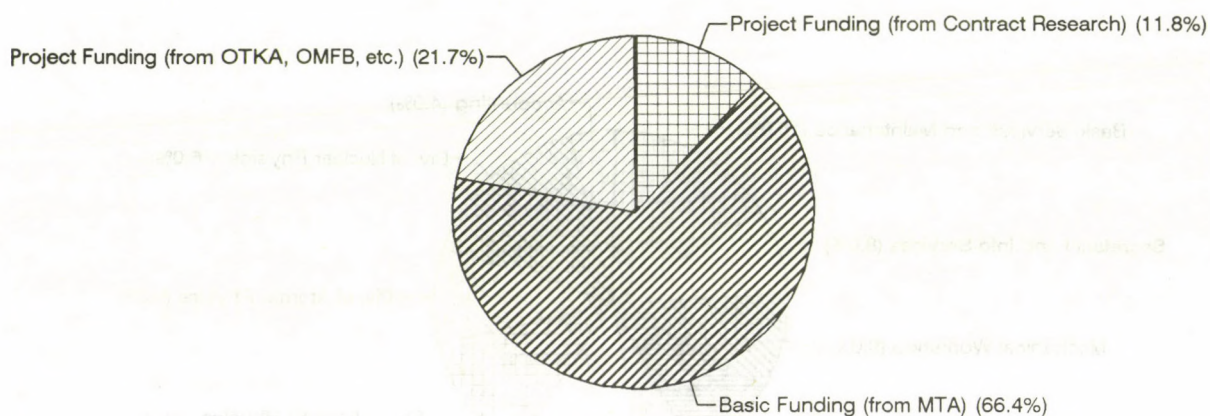
Affiliation of Personnel to Units of Organisation



Composition of Personnel

Finance

The total budget of the Institute in 1993 was 152 Million Hungarian Forints. The composition of the budget and the breakdown of expenditure according to different categories are given below.

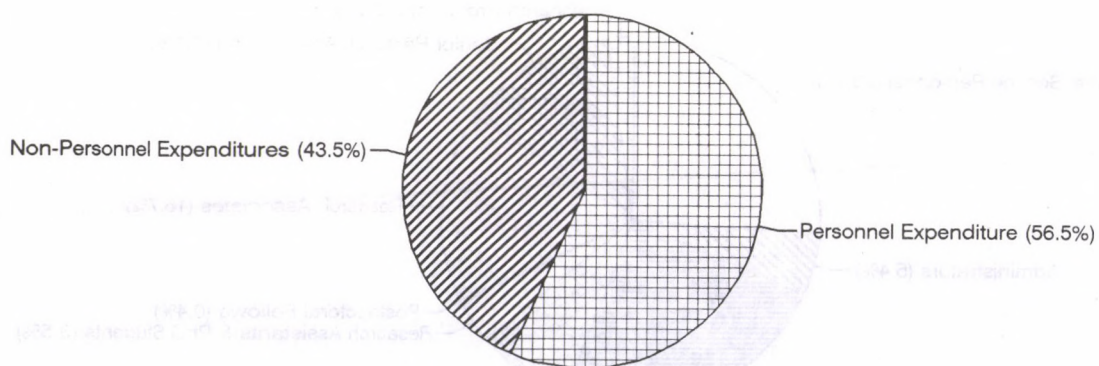


Composition of the Institute's Budget

MTA: Hungarian Academy of Sciences

OTKA: National Fund for Scientific Research

OMFB: National Committee for Technological Development



Breakdown of Expenditure into Personnel and Non-Personnel Expenditures

CONTENTS

REPORTS:

General Physics	1
Nuclear Physics	5
Atomic Physics	41
Materials Science and Analysis	79
Earth and Cosmic Sciences, Environmental Research	101
Biological and Medical Research	129
Development of Methods and Instruments	137

PUBLICATIONS AND SEMINARS:

Papers Published in 1993	169
Conference Contributions and Talks	175
Theses Completed	193
Hebdomadal Seminars	195
Author Index	199

CONTENTS

REPORTS

General Physics	1
Special Physics	5
Atomic Physics	41
Classical Science and Applications	79
Classical Science and Applications	107
Biological and Medical Research	139
Mathematics of Physics and Astronomical	157
Physics	169
Classical Science and Applications	175
Classical Science and Applications	183
Classical Science and Applications	191
Classical Science and Applications	199

GENERAL PHYSICS

On solvable potentials associated with $su(1, 1)$ algebras

G. Lévai

Group theoretical methods represent an invaluable tool of analyzing physical systems that admit some kind of symmetry. In many cases physical operators can be expressed in terms of group generators, which satisfy the commutation relations of an algebra. Depending on the nature of the actual physical problem, the elements of such algebras are realized in terms of matrices, creation/annihilation operators, differential operators, etc.

Motivated by the potential group method [1] and supersymmetric quantum mechanics [2], which apply different symmetry concepts to solve essentially the same series of one-dimensional quantum mechanical potential problems, we have considered the realization of the $su(1, 1)$ algebra in terms of linear differential operators

$$J_{\pm} = e^{\pm i\phi} \left(\pm h(x) \frac{\partial}{\partial x} \pm g(x) + f(x) J_z + c(x) \right),$$
$$J_z = -i \frac{\partial}{\partial x},$$

which act on basis states of the form

$$|jm\rangle = e^{im\phi} \psi_{jm}(x).$$

The operators J_+ , J_- and J_z form an $su(1, 1)$ algebra if the functions $h(x)$, $f(x)$ and $c(x)$ satisfy two simple differential equations.

The Casimir operator of the $su(1, 1)$ algebra realized in this way takes the form of a second-order differential operator, and this result can be used, for example, to derive the Schrödinger equation for some potentials. In this case the solutions of the Schrödinger equation are assigned to the states $|jm\rangle$, which form a basis for the irreducible representations of $su(1, 1)$, and are connected by the ladder operators J_+ and J_- . The range of similar $su(1, 1)$ algebras can be extended by performing variable and similarity transformations of the operators and basis states. These transformations do not necessarily leave the commutation relations intact, but when they do, we arrive at new second-order differential operators automatically associated with $su(1, 1)$ algebras. In particular, these techniques can be employed to formulate in group theoretical terms the procedure, which transforms the second-order differential equation of some special function into the Schrödinger equation with some potential. Since we have studied such transformations previously [3] to derive shape-invariant potentials [4] from the differential equation of orthogonal polynomials (such as the $P_n^{(\alpha, \beta)}(y)$ Jacobi, $L_n^{(\alpha)}(y)$ generalized Laguerre and $H_n(y)$ Hermite polynomials), this procedure offers a natural way of exploring $su(1, 1)$ algebraic structures associated with the most well-known

solvable potentials of non-relativistic quantum mechanics. This method also allows a unified, systematic treatment of earlier isolated results.

Our study [5] has recovered potential algebras in six cases associated with PI and LI class potentials [3], while spectrum generating algebras have been identified in five cases in relation with the LI and HI classes, and also for the special, common version of PI and PII class [3]. (These examples include the Pöschl–Teller, Morse, and harmonic oscillator potentials, for instance.) The present form of the generators was found to be inappropriate to derive the four shape-invariant potentials belonging to the LII case (the Coulomb problem), and to the general PII class [3]. We have studied the relation between the ladder operators of the algebraic approach (J_+ , J_-) and those of supersymmetric quantum mechanics (A^\dagger , A) [2], and we have found, that they are essentially the same when J_+ and J_- are the members of a potential algebra.

In certain cases we have obtained the compact $su(2) \simeq so(3)$ algebra rather than the non-compact $su(1, 1) \simeq so(2, 1)$. The series of states linked by the J_+ and J_- ladder operators is finite in this case, which result has a straightforward group theoretical interpretation. An example for this was one of the PI class potentials, where, up to a similarity transformation, the compact potential algebra and the wavefunctions could be recognized as the angular momentum algebra and the spherical harmonics, respectively. This example shows that although most of the algebraic structures found in this study had been known previously, the present procedure offers a novel approach to some of them.

We have discussed the connection of the $su(1, 1)$ (and $su(2)$) algebras to other algebraic structures identified earlier in relation with these potentials. We have also pointed out the possibility of generalizing the present procedure in several directions, such as considering other realizations of the $su(1, 1)$ algebra, other algebraic structures and larger classes of potentials. Our results concerning shape-invariant potentials may be helpful in identifying new $su(1, 1)$ algebras associated with the less well-known class of non-shape-invariant potentials.

References

1. see J. Wu, Y. Alhassid and F. Gürsey: *Ann. Phys. (N. Y.)* **196** (1989) 163, and references therein.
2. see, for example, A. Lahiri, P. K. Roy and B. Bagchi: *J. Mod. Phys. A* **5** (1990) 1383 for a review.
3. G. Lévai: *J. Phys. A:Math. Gen.* **22** (1989) 689.
4. L. Gendenshtein: *JETP Lett.* **38** (1983) 356.
5. G. Lévai: “*Solvable potentials associated with $su(1, 1)$ algebras: a systematic study*”, submitted to the *J. Phys. A:Math. Gen.*

Genetic algorithm with local optimization

K. F. Pál

Genetic algorithms are optimization methods inspired by natural evolution. They work on a population of possible solutions of the problem in hand. They create new solutions from bits and pieces of the existing members of the population and select the best individuals for further manipulations. This way they can "breed" better and better solutions.

We tested a hybrid algorithm on a massively multimodal spin lattice problem [1]. It had been shown earlier that the same method gives excellent results for the traveling salesman problem [2,3]. In the algorithm the creation of a new individual involves an operation that unites properties of pairs of individuals ("crossover") and a local optimization. This way only locally optimum solutions compete. The test problem was to find the energy minimum of a set of 450 spins scattered randomly on a 20 by 30 two dimensional lattice. Only spins occupying neighbouring lattice sites interact with each other, the interaction is ferromagnetic between horizontal and vertical neighbours and antiferromagnetic between the diagonal ones. The vacancy sites are kept fixed. A property of such a system is that in any region of the lattice there can be more very different and equally good spin combinations, and only the structure of the whole lattice decides which one belongs to the global optimum. Therefore, global optimum can only be achieved with high probability if the selection scheme of the algorithm is able to keep as many good spin combinations in the population as possible, that is to maintain a high degree of genetic diversity.

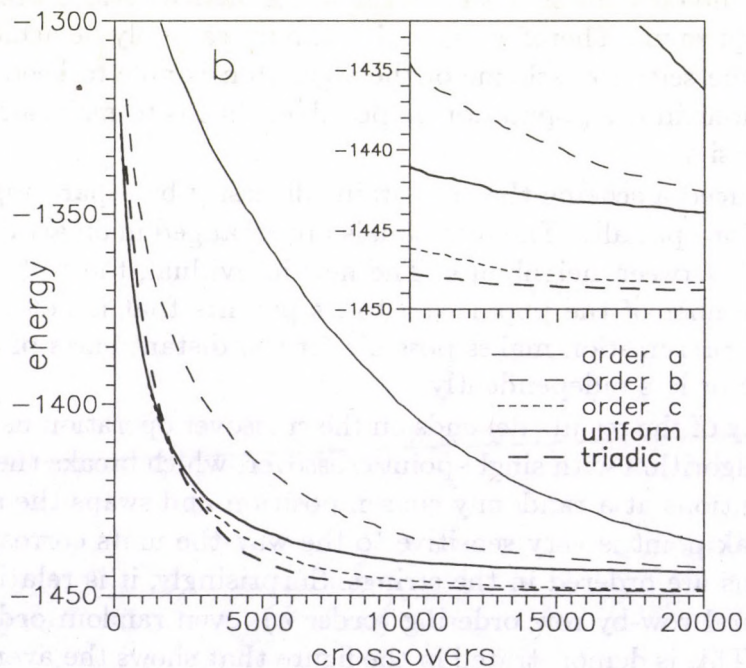
We introduced a scheme that maintains diversity by separating the members of the population spatially. The individuals are arranged in an array and crossover is only allowed between neighbours. The new individual, the "offspring" replaces the nearest member of the population to its parents that is not better than the offspring. This prescription makes possible for the distant parts of the population to evolve more or less independently.

The quality of the results depends on the crossover operation used. The performance of the algorithm with single-point crossover, which breaks the strings coding the parent solutions at a randomly chosen position and swaps the substrings that follow the break point is very sensitive to the way the units corresponding to the individual spins are ordered in the strings. Surprisingly, it is relatively poor with the most natural row-by-row ordering (order a), even random ordering (order b) works better. This is demonstrated in the figure that shows the average of the best energies found as a function of the number of crossovers from 150 calculations with each crossover method. The best results with single-point crossover were achieved unexpectedly using a fairly involved ordering (order c) that unites strongly interlocking pieces of the parent lattices. Unfortunately, its construction gives no recipe how to get a good ordering if we want to use the hybrid scheme to other problems. We can only conclude that it may be difficult to find one. The unexpected way

of the ordering-dependence is caused by some interplay between the crossover and the local optimization.

Uniform crossover — taking each bit from either of the parent strings with equal probability — is ordering-invariant and works reasonably well, but the convergence slows down too much in the final stage of the search. We constructed another ordering-invariant crossover that is able to preserve good spin combinations created by the local optimization. This triadic crossover involves a third individual besides the parents. It gave extremely good results, probably global optimum was achieved in 96% of our calculations. We expect this crossover to work well in the hybrid algorithm for other problems as well whose locally optimum solutions tend to have common features.

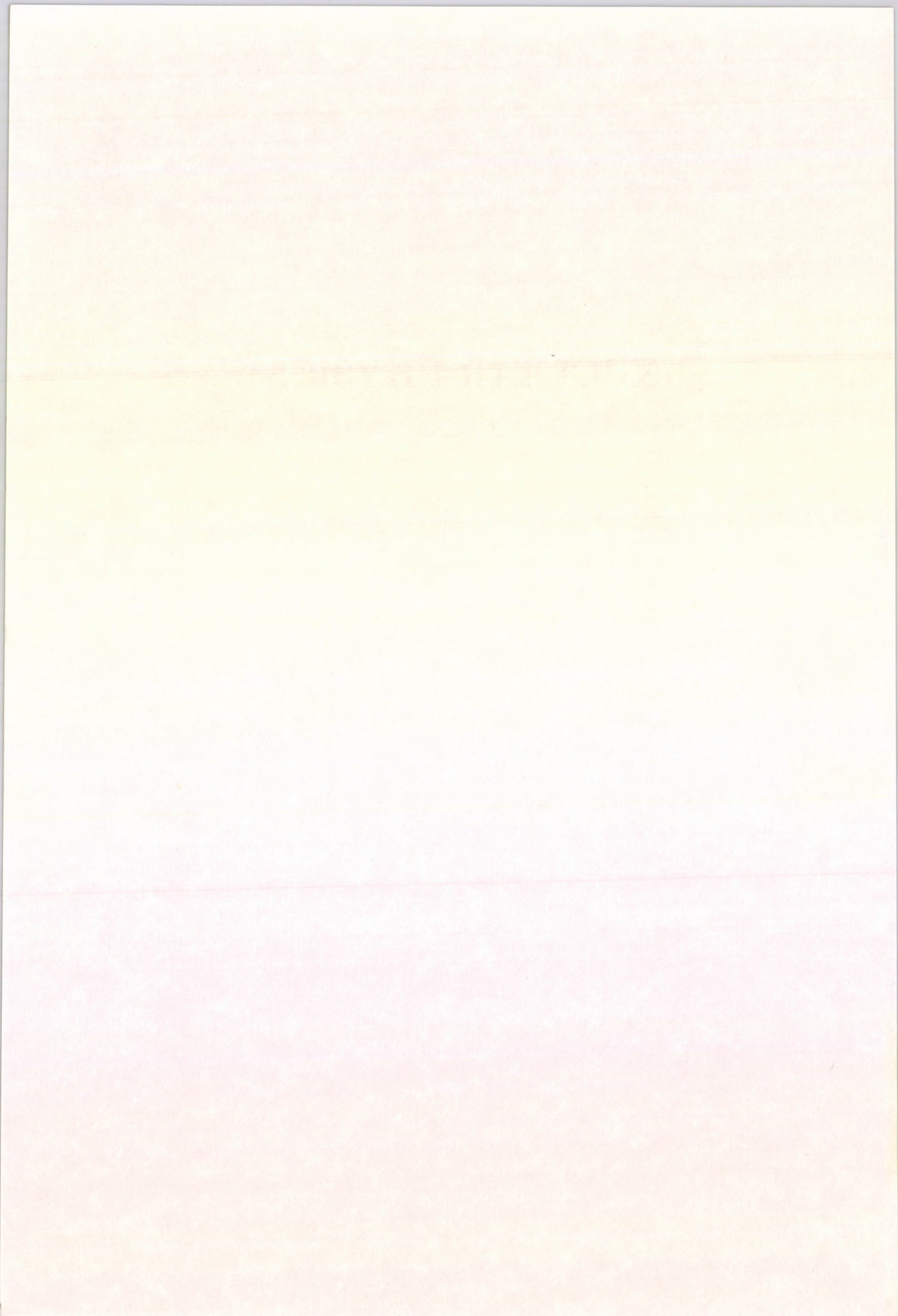
The results indicate that the hybrid scheme is very suitable if one wants to find global or very nearly global optima of difficult, massively multimodal problems. If a local optimization is available, it can be unified in a straightforward way with the genetic search. The main limitation of its usefulness is that if there is no fast enough local optimization method for the particular problem, computation time may be prohibitively long. However, as computers are getting faster, this limitation becomes less and less serious. Evolutionary optimization methods will become especially competitive in the age of parallel computation.



References

1. K. F. Pál, submitted to *Biol. Cybern.*
2. R. M. Brady, *Nature* 317 (1985) 804.
3. K. F. Pál, *Biol. Cybern.* 69 (1993) 539.

NUCLEAR PHYSICS



Stopping powers of CR-39 Nuclear Track Detector Material

Zs. Fülöp, Á.Z. Kiss, E. Somorjai, I. Hunyadi,

E. Rauhala * and J. Räsänen *

*Accelerator Laboratory, Department of Physics, University of Helsinki,
FIN-00014 Helsinki, Finland

This year we continued and finished our cooperation project with the Accelerator Laboratory of the Helsinki University to measure the stopping powers of CR-39 nuclear track detector material for protons and helium ions in Debrecen and for ${}^7\text{Li}$, ${}^{11}\text{B}$, ${}^{12}\text{C}$, ${}^{14}\text{N}$, ${}^{16}\text{O}$, ${}^{23}\text{Na}$, ${}^{27}\text{Al}$ and ${}^{28}\text{Si}$ ions in Helsinki.

The measurements were performed in the transmission geometry as in our earlier work [1]. The ion stopping powers obtained are compared to the predictions of two recent semiempirical models. The predictions are found to clearly underestimate the observed stopping powers for ${}^7\text{Li}$, ${}^{11}\text{B}$, ${}^{12}\text{C}$, ${}^{23}\text{Na}$, ${}^{27}\text{Al}$ and ${}^{28}\text{Si}$ ions [2].

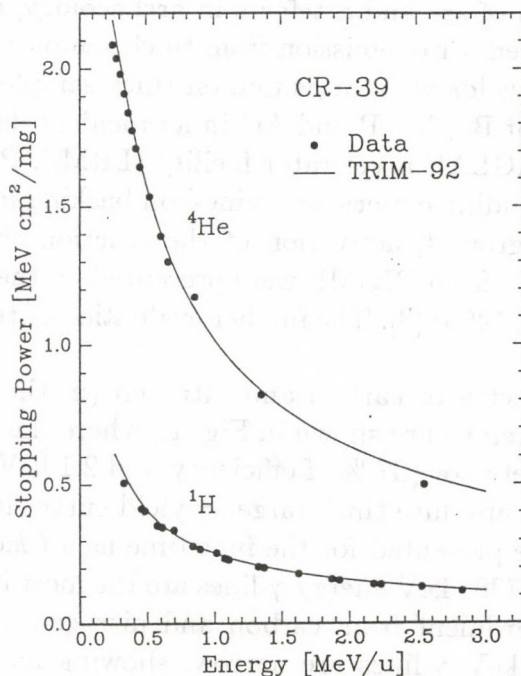


Fig. 1. Stopping powers of CR-39 for ${}^1\text{H}$ and ${}^4\text{He}$ ions. The curves represent the stopping powers as predicted by TRIM-92 code.

References

1. E. Rauhala, J. Räsänen, Zs. Fülöp, Á.Z. Kiss and I. Hunyadi, Nucl. Tracks and Rad. Meas. **20** (1992) 611.
2. J. Räsänen, E. Rauhala, Zs. Fülöp, Á.Z. Kiss E. Somorjai and I. Hunyadi, submitted to Nucl. Tracks and Rad. Meas.

Thick target yields of deuteron induced gamma-ray emission from light elements

Á.Z. Kiss, I. Biron *, T. Calligaro * and J. Salomon *

*Laboratoire de Recherche des Musées de France, Palais du Louvre, 75041
Paris Cedex 01, France

Deuteron induced γ -ray emission (DIGME) is known to be a very suitable method for the determination of C, N and O since the early work of Sparks et al. [1] and sensitive also for B, Na, Mg, Al and Si [2]. Nevertheless few results have been published on its analytical applications up to now, probably because of the associated neutron hazard and the risk to cause detector damage by the neutrons.

To provide basic data for the application of DIGME in different fields like geology, mineralogy, materials sciences, environmental and life sciences and primarily for the analysis of works of art and artefacts in archaeology, a systematic investigation of deuteron induced γ -ray emission from thick samples has been performed. Absolute prompt γ -ray yields were measured on thick samples with elements of Z between 3 and 19 (except Be, Ne, P and Ar) in an incident deuteron energy range of 0.7–3.4 MeV at the AGLAE accelerator facility (LRMF, Paris).

The first results including experience gained on backing materials (Fe, Ni, Cu, Ta, etc.), neutron background, activation of the reaction chamber and a direct comparison with γ -yields from PIGME were presented on the IBA-11 Conference (Balatonfüred, Hungary, 1993) [3]. The further evaluation of the experimental data is under course.

In this report γ -spectra of carbon and nitrogen (in the form of TaN) bombarded by 1.8 MeV deuterons are shown in Fig. 1., where the γ -rays were detected with an n-type HPGe detector (37 % of efficiency and 2.1 keV of energy resolution at 1.33 MeV). In Fig. 2. absolute thick target γ -yield curves for some γ -energies of carbon and nitrogen are presented for the first time as a function of deuteron energy. The 3089 keV and 7301 keV energy γ -lines are the most intense ones emerging during deuteron bombardment from carbon and nitrogen, respectively. The less intense 3854 and 5270 keV γ -lines are narrow, showing no Doppler-broadening, thus in the case of high background from other constituents of the sample can help the identification of carbon and nitrogen.

References

1. R.J. Sparks and G.J. McCallum, New Zealand J. of Sci. 12 (1969) 470.
2. F. Abel, G. Amsel, E. d'Artemare, C. Ortega et J. Siska, Rapport Scientifique, GDR 86, 1987-1989, p. 156-161.
3. Á.Z. Kiss, I. Biron, T. Calligaro and J. Salomon, Nucl. Inst. and Meth. in press.

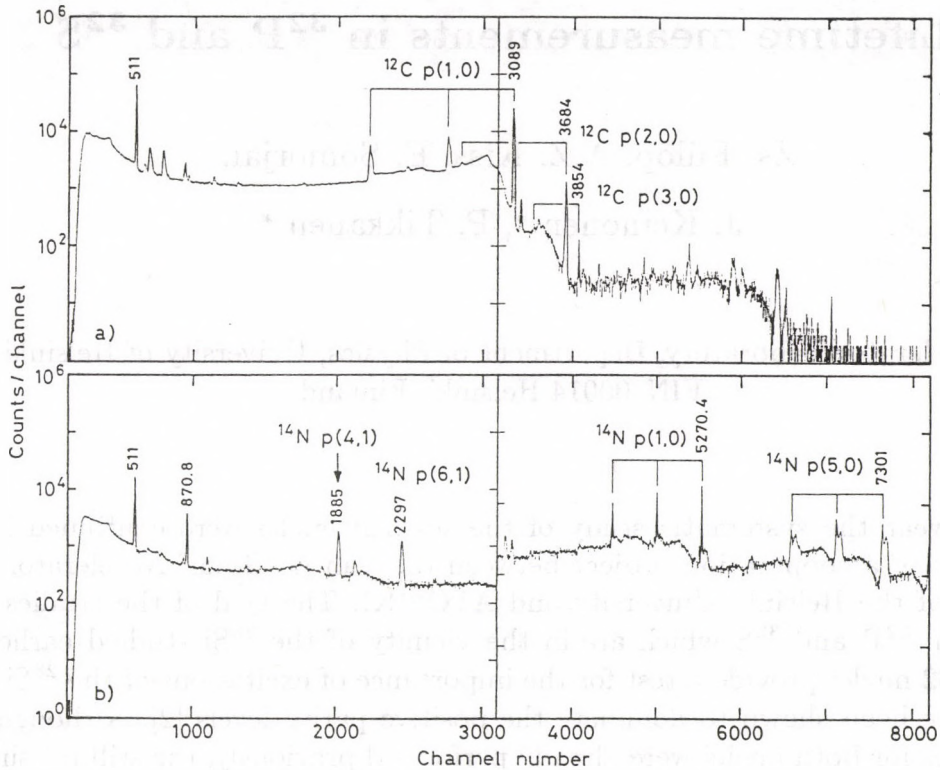


Fig. 1. γ -spectra obtained from the bombardment of carbon (a) and nitrogen (b) with 1.8 MeV deuterons. The numbers in the figure denote γ -ray energies in keV. The notation e.g.: $^{12}\text{C p}(1,0)$ means $^{12}\text{C}(d, p\gamma_{1-0})^{13}\text{C}$. (The 870.8 keV energy γ -line is from oxygen contamination.)

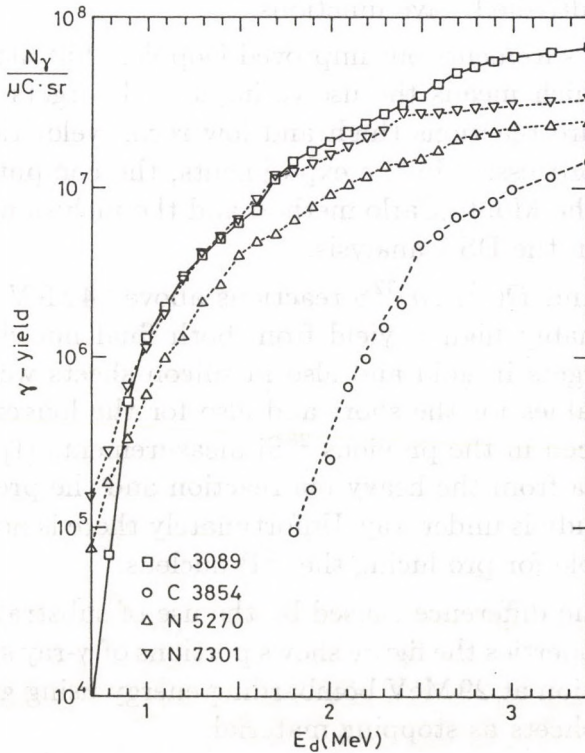


Fig. 2. Absolute thick-target γ -yield curves for carbon and nitrogen as a function of deuteron energy.

Lifetime measurements in ^{32}P and ^{32}S

Zs. Fülöp, Á.Z. Kiss, E. Somorjai,

J. Keinonen *, P. Tikkanen *

*Accelerator Laboratory, Department of Physics, University of Helsinki,
FIN-00014 Helsinki, Finland

This year the systematic study of the sd-shell nuclei were continued in the framework of a cooperation project between the Van de Graaff Accelerator Laboratories of the Helsinki University and ATOMKI. The goal of the studies were two nuclei: ^{32}P and ^{32}S which are in the vicinity of the ^{28}Si studied earlier [1]. The $A = 32$ nuclei provide a test for the importance of excitations of the ^{28}Si core, which have been shown to dominate the positive parity levels [2]. Although several studies for both nuclei were already performed previously, the still missing, or poorly determined branching ratio, mean lifetime, etc. values [3] necessitate a more precise reinvestigation. The aim of this study is to clear the apparent discrepancy in the reported lifetime values, and to be able to test shell model calculations based on large-basis multi-shell wave functions.

For the lifetime measurements our improved Doppler shift attenuation (DSA) method was applied which means the use of implanted targets and both heavy ion and radiative capture reactions (high and low recoil velocities, two different kind of slowing-down processes) in the experiments, the computer simulation of γ -ray line shapes with the Monte Carlo method and the inclusion of experimental stopping power values in the DSA analysis.

The $D(^{31}\text{P}, p)^{32}\text{P}$ and $D(^{31}\text{P}, n)^{32}\text{S}$ reactions above 24 MeV bombarding energy produced a reasonably high γ -yield from both final nuclei simultaneously. Implanted deuteron targets in gold and also in silicon sheets were used in order to get more accurate values for the short and also for the longer (> 400 fs) lifetimes as it was introduced in the previous ^{28}Si measurements [1]. The evaluation of the experimental data from the heavy ion reaction and the preparation for the $^{31}\text{P}(p, \gamma)^{32}\text{S}$ reaction study is under way. Unfortunately there is no proton or alpha capture reaction available for producing the ^{32}P nucleus.

As an example of the difference caused by the use of substrates having either fast or slow stopping properties the figure shows portions of γ -ray spectra measured at 0° to the beam direction at 29 MeV bombarding energy using gold (dotted line) and silicon (solid line) sheets as stopping material.

References

1. P. Tikkanen, J. Keinonen, A. Kangasmäki, Zs. Fülöp, Á.Z. Kiss and E. Somorjai, Phys. Rev. **C47** (1993) 145.
2. B.H. Wildenthal, J.B. McGrory, E.C. Halbert and H.D. Graber, Phys. Rev. **C4** (1971) 1708.
3. P.M. Endt, Nucl. Phys. **A521** (1990) 45.

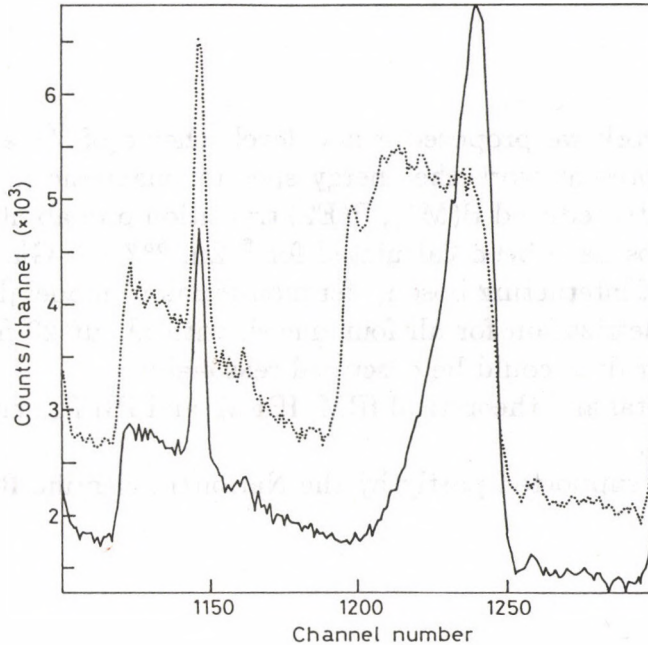


Fig. 1. Portions of γ -ray spectra recorded in the DSA measurement of the 1.15 MeV ^{32}P state ($\tau \sim 230$ fs, 1.15 \rightarrow 0.51 MeV transition) in the case of gold (dotted line) and silicon (solid line) as stopping material. The narrow 517.08 keV γ -line showing no Doppler-broadening is from a radioactive source for comparison.

Consistent description of the structure of ^{64}Zn , ^{65}Zn , ^{65}Ga and ^{66}Ga nuclei

J. Timár, T. Fényes, Zs. Dombrádi, S. Brant⁺, V. Paar⁺ and

Lj. Šimičić⁺

⁺ Department of Physics, Faculty of Science, University of Zagreb, 41000 Zagreb, Croatia

In an earlier work we proposed a new level scheme of ^{66}Ga from (p,n γ) reaction [1]. In the present work the energy spectra, magnetic dipole and electric quadrupole moments, reduced B(M1), B(E2) transition probabilities, and gamma-ray branching ratios have been calculated for ^{64}Zn , ^{65}Zn , ^{65}Ga , and ^{66}Ga nuclei in the framework of interacting boson(-fermion-fermion) model [IB(FF)M]. Using a consistent parametrization for all four nuclei, with about 20 fitted parameters hundreds of nuclear data could be described reasonably.

The experimental and theoretical IBM, IBFM, and IBFFM energy spectra are compared in Fig. 1.

This work was supported partly by the National Scientific Research Foundation (OTKA).

References

1. J. Timár, T. Fényes, Zs. Dombrádi, J. Kumpulainen and J. Julin, ATOMKI Ann. Rep. 1992, p. 12

The level scheme of ^{70}As nucleus

Zs. Podolyák and T. Fényes

In the last two years we have studied the γ -, $\gamma\gamma$ -coincidence, internal conversion electron and γ -ray angular distribution spectra of the $^{70}\text{Ge}(p,n\gamma)^{70}\text{As}$ reaction [1]. On the basis of experimental results now we propose a new level scheme of ^{70}As , which contains 61 new γ -ray transitions and 16 new levels. The level spin and parity values have been determined from the decay properties of states, measured 29 internal conversion coefficients, Hauser-Feshbach analysis, γ -ray angular distribution results and other available data.

Fig. 1 shows the low-energy part of the level scheme. The results of the Hauser-Feshbach analysis are presented in Fig. 2.

This work was supported by the OTKA foundation.

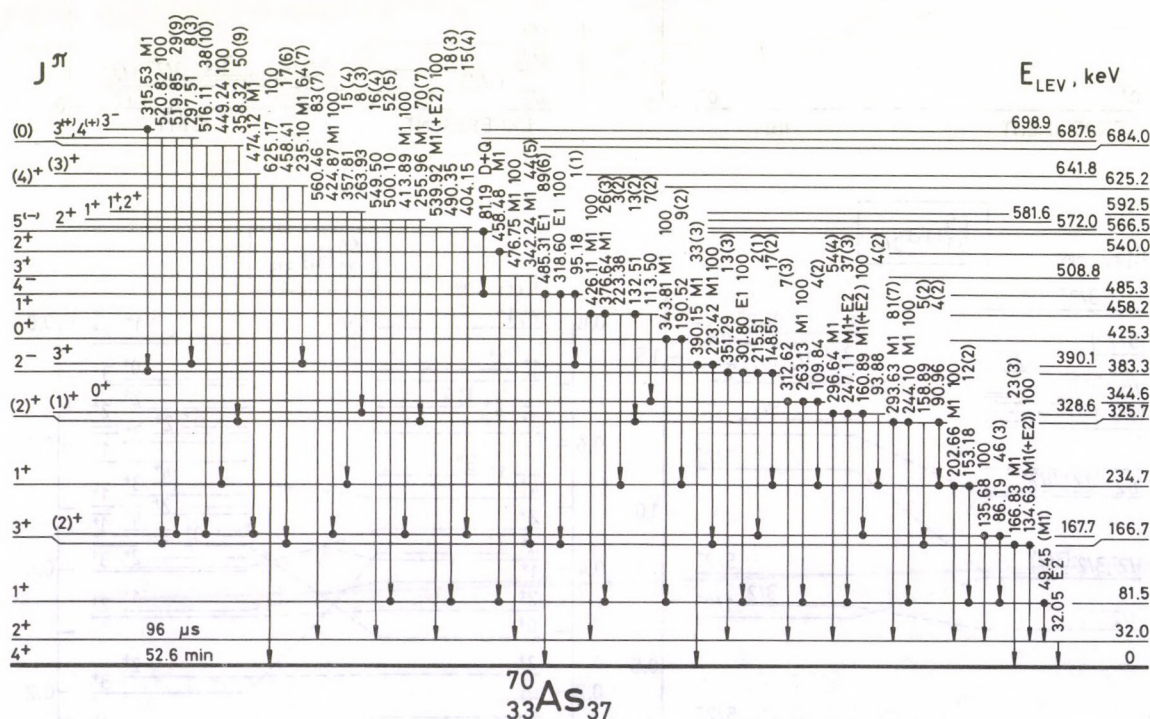


Fig. 1. Low-energy part of the proposed level scheme of ^{70}As . Behind the γ -ray energies and multipolarities γ -branching ratios (and their errors) are given. D and Q mean dipole and quadrupole transitions, respectively. Solid circles at the ends of arrows indicate $\gamma\gamma$ -coincidence relations.

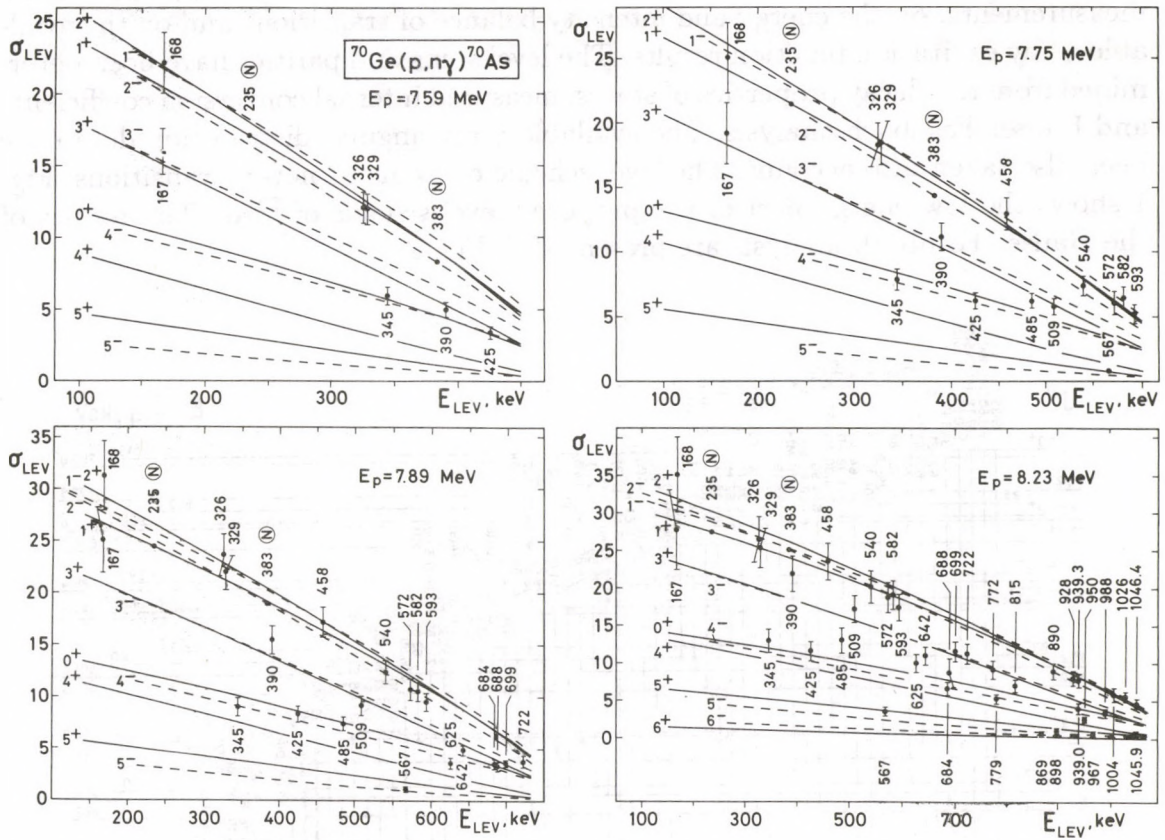


Fig. 2. Experimental relative cross sections (σ_{LEV}) of the $^{70}\text{Ge}(p, n\gamma)^{70}\text{As}$ reaction (dots with error bars) as a function of the ^{70}As level energy (E_{LEV}). The curves show Hauser-Feshbach theoretical results. Encircled N means normalization point.

References

1. Zs. Podolyák, J. Timár and T. X. Quang, ATOMKI Ann. Rep. 1992, p. 16

Excited states of ^{72}As from $(p,n\gamma)$ reaction

D. Sohler and T. Fényes

Based on our earlier experimental results [1] we propose a new level scheme of ^{72}As . The level scheme has been constructed mainly on the basis of $\gamma\gamma$ -coincidence measurements, on the energy and intensity balance of transitions and on the available γ -ray excitation function results. The level spins and parities have been determined from the decay properties of states, measured internal conversion coefficients and Hauser-Feshbach analysis. The available γ -ray angular distribution data have been also taken into account. The level scheme contains 57 new γ -transitions. Fig. 1 shows the low-energy part of the proposed level scheme of ^{72}As . The results of the Hauser-Feshbach analysis are presented in Fig. 2.

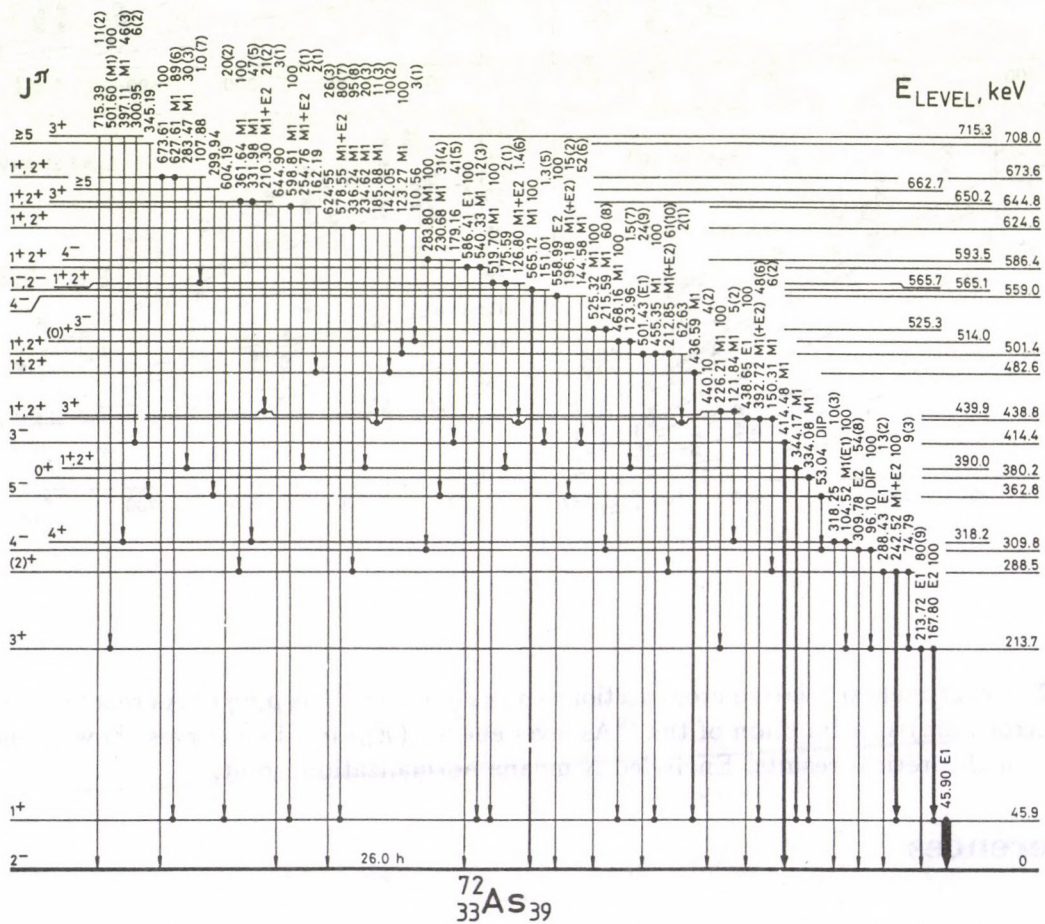


Fig. 1. Low-energy part of the proposed level scheme of ^{72}As . Solid circles at the ends of arrows indicate $\gamma\gamma$ -coincidence relations. Behind the γ -ray energies and multiplicities relative γ -branching ratios (and their errors) are given.

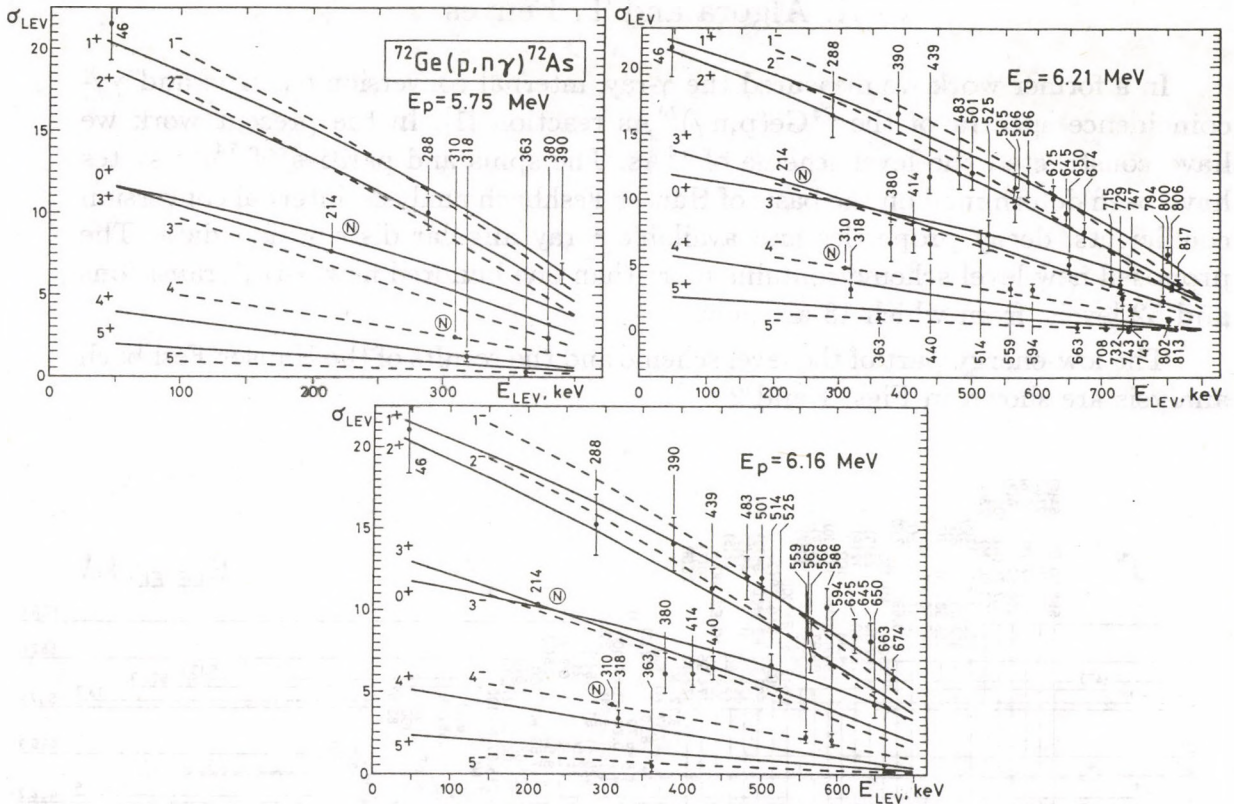


Fig. 2. Experimental relative cross sections (σ_{LEV}) of the $^{72}\text{Ge}(p,\gamma)^{72}\text{As}$ reaction (dots with error bars) as a function of the ^{72}As level energy (E_{LEV}). The curves show Hauser-Feshbach theoretical results. Encircled N means normalization point. The results obtained at different bombarding proton energies are shown separately.

This work was supported by the OTKA Foundation.

References

1. D. Sohler, A. Algora and Z. Gácsi, ATOMKI Ann. Rep. 1992, p. 18

The level scheme of ^{74}As from $(p,n\gamma)$ reaction

A. Algora and T. Fényes

In a former work we measured the γ -ray, internal conversion electron and $\gamma\gamma$ -coincidence spectra of the $^{74}\text{Ge}(p,n\gamma)^{74}\text{As}$ reaction [1]. In the present work we have constructed the level scheme of ^{74}As . The spins and parities of ^{74}As states have been determined on the basis of Hauser-Feshbach analysis, internal conversion coefficients, decay properties and available γ -ray angular distribution data. The proposed new level scheme contains more than one hundred new γ -ray transitions and 52 levels, from which 18 are new.

The low-energy part of the level scheme and the results of the Hauser-Feshbach analysis are shown in Figs. 1 and 2.

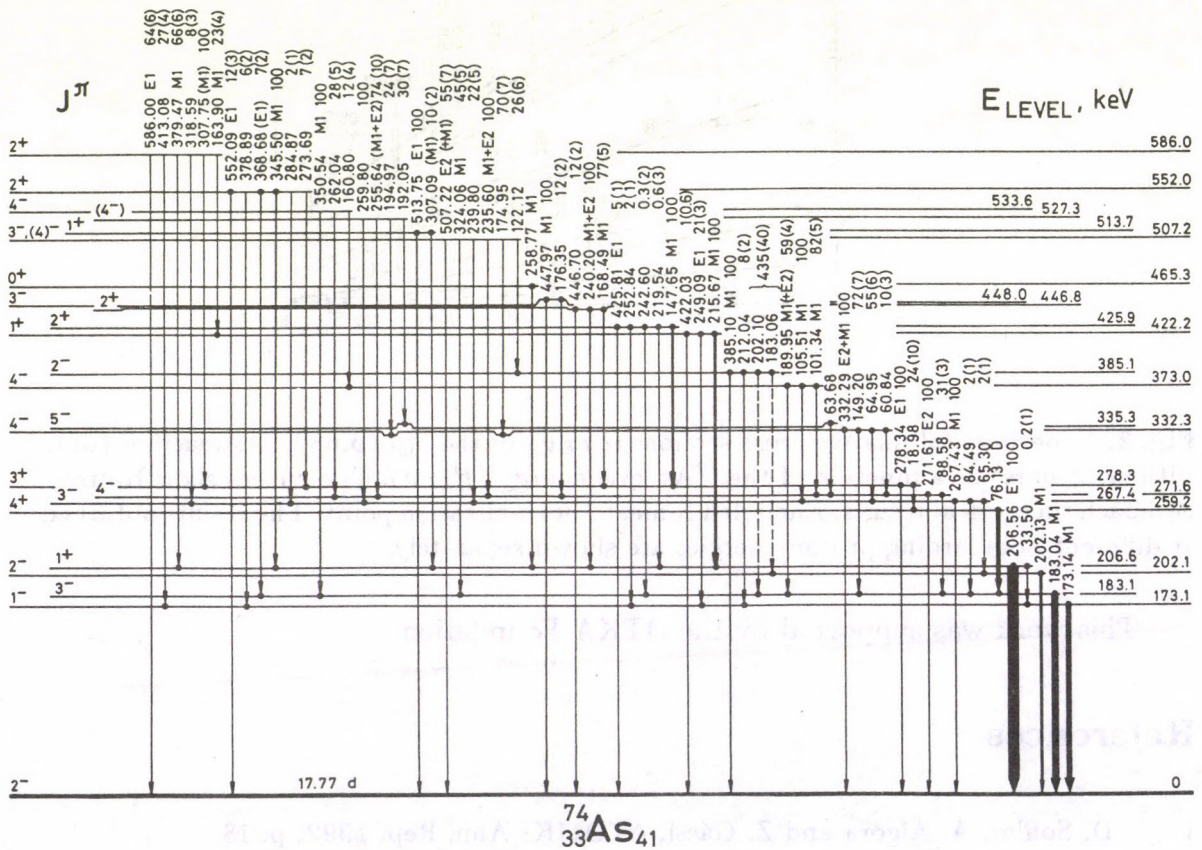


Fig. 1. Low-energy part of the proposed level scheme of ^{74}As . Solid circles at the ends of arrows indicate $\gamma\gamma$ -coincidence relations. D means dipole transition. Behind the γ -ray energies and multipolarities γ -branching ratios (and their errors) are given.

The support of OTKA Foundation is acknowledged.

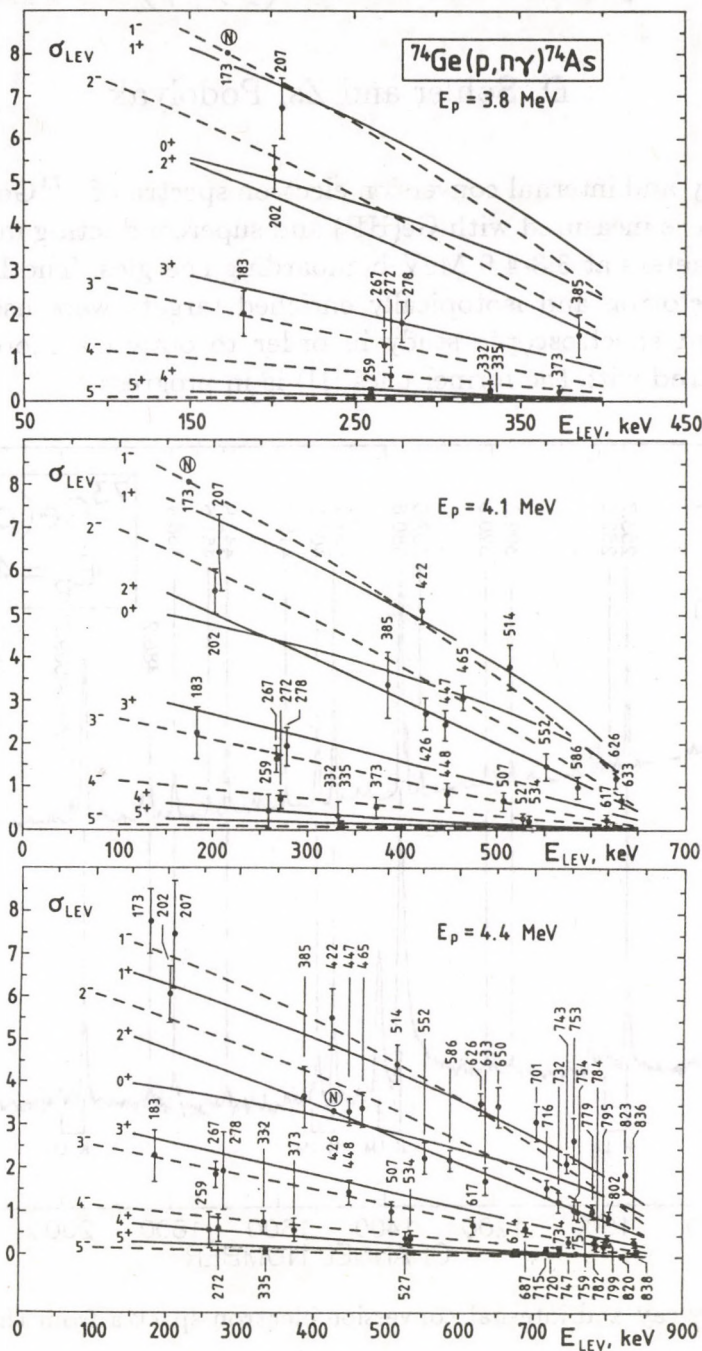


Fig. 2. Experimental relative cross sections (σ_{LEV}) of the $^{74}\text{Ge}(p, n\gamma)^{74}\text{As}$ reaction (dots with error bars) as a function of the ^{74}As level energy (E_{LEV}). The curves show Hauser-Feshbach theoretical results. Encircled N means normalization point. The results obtained at different bombarding proton energies are shown separately.

1. A. Algora, D. Sohler and Z. Gácsi, ATOMKI Ann. Rep. 1992, p. 20

Study of ^{73}As from $(p,n\gamma)$ reaction

D. Sohler and Zs. Podolyák

Gamma-ray and internal conversion electron spectra of $^{73}\text{Ge}(p,n\gamma)^{73}\text{As}$ reaction (Fig. 1) were measured with Ge(HP) and superconducting magnetic lens plus Si(Li) spectrometers at 3.3-4.0 MeV bombarding energies. The Debrecen 104-cm isochronous cyclotron and isotopically enriched targets were used in the experiments. Detailed spectroscopic study in order to obtain a more complete level scheme (compared with the former ones [1]) is in progress.

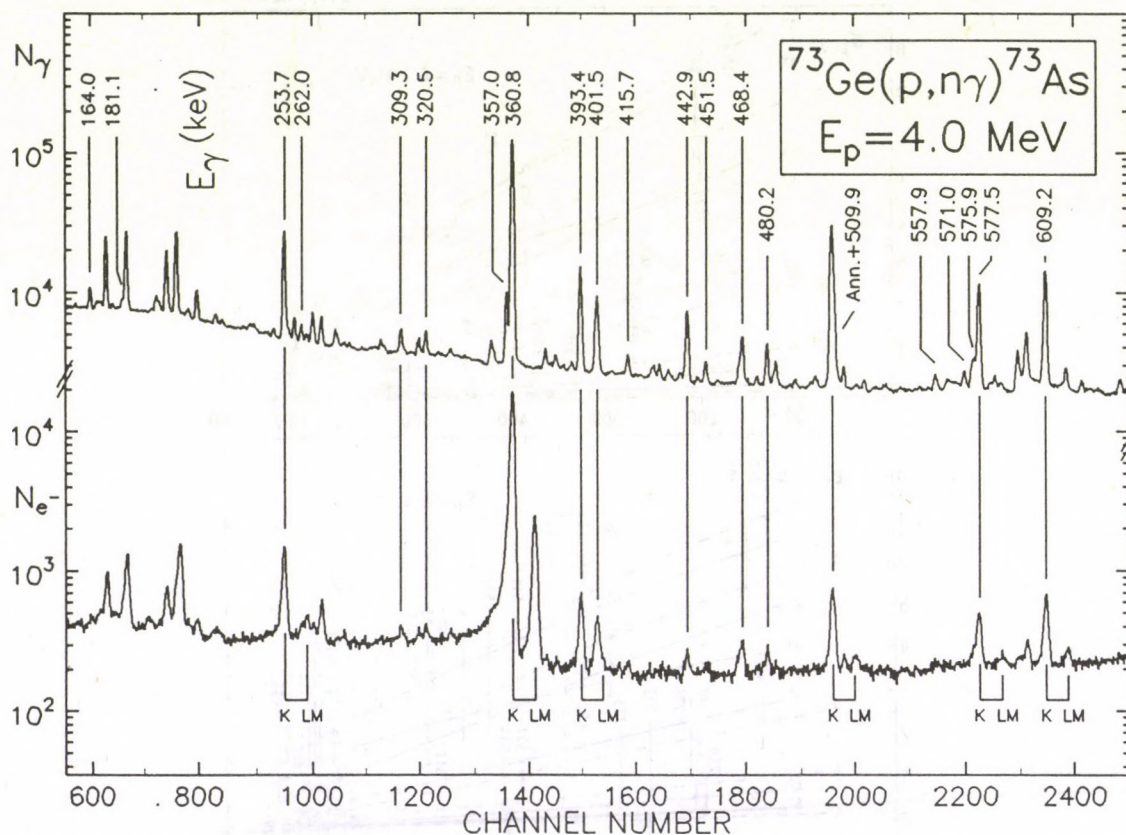


Fig. 1. Typical γ -ray and internal conversion electron spectra from the $^{73}\text{Ge}(p,n\gamma)^{73}\text{As}$ reaction.

Reference

1. M. M. King, Nucl. Data Sheets **51** (1987) 161

Supersymmetry calculations on ^{74}Se , ^{75}Se , ^{73}As and ^{74}As

A. Algora, T. Fényes, Zs. Dombrádi

As a continuation of our earlier studies on the structure of ^{74}As [1,2], we tested the possible description of the ^{74}As levels by means of the supersymmetry scheme $U_{\pi}^B(6) \times U_{\pi}^F(12) \times U_{\nu}^B(6) \times U_{\nu}^F(12)$ using the $U(5)$ limit for the bosonic core.

The basic idea of this approximation is to determine the boson-boson and boson-fermion interactions from the neighbouring even-even and odd-mass nuclei, and then on the basis of supersymmetry relations predict the energy spectrum of the odd-odd nucleus. The energy spectra of the four neighbouring nuclei (even-even, even-odd, odd-even, odd-odd) are interrelated by the \mathcal{N} number (sum of the boson and fermion numbers), and are described by the same hamiltonian. The main advantage of this symmetry based approximation is that the eigenvalue problem can be solved analitically.

According to Van Isacker and Jolie [3] the eigenvalues of the hamiltonian are given by the following formula

$$E = A_{\nu\pi} \sum_i N_i(N_i + 7 - 2i) + A_{\nu} \sum_i N_{i\nu}(N_{i\nu} + 7 - 2i) + A_{\pi} \sum_i N_{i\pi}(N_{i\pi} + 7 - 2i) + B_1 \sum_i n_i + B_2 \sum_i n_i(n_i + 6 - 2i) + C[v_1(v_1 + 3) + v_2(v_2 + 1)] + DL(L + 1) + ES(S + 1) + FJ(J + 1) \text{ MeV,}$$

where N_i , $N_{i\nu}$, $N_{i\pi}$, n_i , v_1 , v_2 , L , S , J are quantum numbers and $A_{\nu\pi}$, A_{ν} , A_{π} , B_1 , B_2 , C , D , E , F parameters, which are not determined by the symmetry.

The parameters were fitted firstly to the experimental levels of the ^{74}Se , ^{75}Se , ^{73}As , then the ^{74}As spectrum was generated using the obtained parameters ($A_{\nu\pi} + A_{\nu} = 26$, $A_{\nu\pi} + A_{\pi} = 55$, $B_1 = 500$, $B_2 = 0$, $C = 4$, $D = -26$, $F = 40$). The experimental and the calculated spectra are compared in Fig.1. The quantum numbers were assigned to the states of ^{74}As tentatively on the basis of energies, spins and parities.

References

1. A. Algora, T. X. Quang, D. Sohler and Z. Gácsi, ATOMKI Ann. Rep. 1991, p. 16.
2. A. Algora, D. Sohler and Z. Gácsi, ATOMKI Ann. Rep. 1992, p. 20.
3. P. Van Isacker and J. Jolie, Nucl. Phys. A503 (1989) 429.

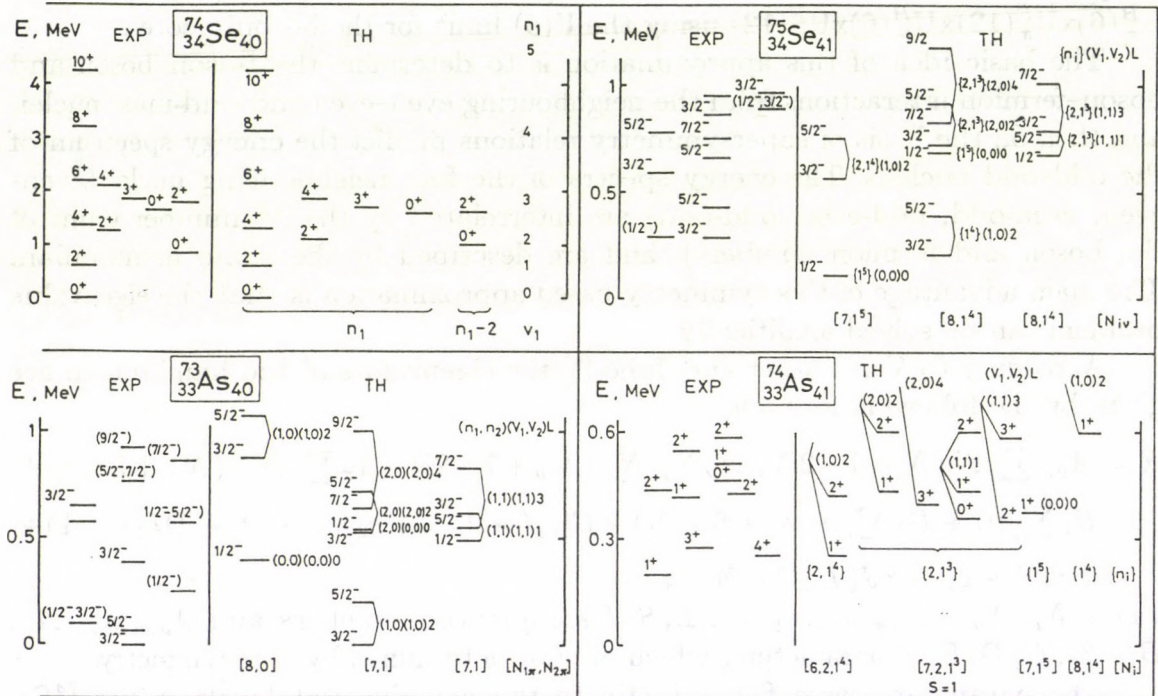


Fig. 1 Comparison of the experimental energy spectra of ^{74}Se , ^{75}Se , ^{73}As and ^{74}As with the calculated ones. The levels are labelled with $[N_i]$, $[N_{i\pi}]$, $[N_{i\nu}]$, $\{n_i\}$, (v_1, v_2) , L, S, J , the irreducible representations of the groups $U_{\pi\nu}^{BF}(6)$, $U_{\pi}^{BF}(6)$, $U_{\nu}^{BF}(6)$, $U_{\pi\nu}^{BF}(5)$, $O_{\pi\nu}^{BF}(5)$, $O_{\pi\nu}^{BF}(3)$, $SU_{\pi\nu}^{BF}(2)$ and Spin (3).

Astrophysical p-process: $^{70}\text{Ge}(\alpha, \gamma)^{74}\text{Se}$

Zs. Fülöp, Á.Z. Kiss, C.E. Rolfs *,

E. Somorjai, H.P. Trautvetter *

*Institut für Physik mit Ionenstrahlen, Ruhr-Universität, Bochum,
Germany

The study of the $^{70}\text{Ge}(\alpha, \gamma)^{74}\text{Se}$ reaction was continued in 1993 in the framework of a Hungarian-German project. The importance and the goal of the investigation has been already discussed [1].

The neutron and the resulted γ -ray background were reduced by using evaporated ^{70}Ge targets onto thin Au-foils. Measurements with the new transmission targets have been performed at the cyclotron in Debrecen and the tandem accelerator in Bochum within the energy range of $4.9 \leq E_\alpha \leq 7.96 \text{ MeV}$. The obtained γ -ray spectra contain only one line belonging to ^{74}Se , namely the $635 \text{ keV } 1 \rightarrow 0$ transition; the primary transitions are strongly fragmented. From the preliminary analyses the yield of the $635 \text{ keV } \gamma$ -line as a function of bombarding energy is shown in Fig. 1.

The precise analyses of the measured spectra are in progress. New experiments are planned for obtaining the total γ -ray yield of the reaction.

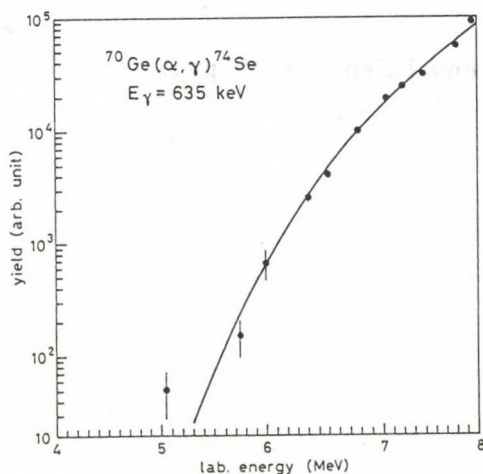


Fig. 1. The preliminary yield curve of the $E_\gamma = 635 \text{ keV } 1 \rightarrow 0$ transition in ^{74}Se . The solid line is to guide the eye.

Reference

1. Zs. Fülöp, Á.Z. Kiss, C.E. Rolfs, E. Somorjai, H.P. Trautvetter, ATOMKI Ann. Rep. 1992, p. 9.

Level scheme of ^{114}Sb from $(p, n\gamma)$ reaction

Z. Gácsi and Zs. Dombrádi

The results we obtained in the study of ^{114}Sb nucleus and reported earlier [1] have been extended and are briefly summarized below.

Measurement of γ , $\gamma\gamma$ -coincidence, internal conversion electron and γ -ray angular distribution spectra for the $^{114}\text{Sn}(p, n\gamma)^{114}\text{Sb}$ reaction were made at 7.8 and 8.0 MeV bombarding proton energies with Ge γ -ray and superconducting magnetic lens-plus-Si(Li) electron spectrometers. The energies and relative intensities of 74 ^{114}Sb γ rays, as well as the internal conversion coefficients of 31 ^{114}Sb transitions have been determined and new angular distribution data have been obtained for 30 γ rays. From this information, a more complete and consistent level scheme has been deduced. Spin and parity values have been determined from the internal conversion coefficients, a Hauser-Feshbach analysis of the (p, n) reaction cross sections, and the γ -ray angular distributions. The low lying levels were grouped into proton-neutron multiplets and the energy splitting of these multiplets have been interpreted in terms of the parabolic rule.

This work has been supported by the National Scientific Research Foundation (OTKA).

Reference

- [1] Z. Gácsi, ATOMKI Annual Report 1991, p. 19.

Levels in ^{116}Sn from decays of ^{116}Sb isomers

Z. Gácsi

The excited states of ^{116}Sn were studied [1] by means of the decays of the 15.8-min, 3^+ ^{116}Sb ground state, and the 60.3-min, 8^- ^{116}Sb isomer. Proton and α beams of the Debrecen cyclotron were utilized for the production of the ^{116}Sb activities. Singles- γ and $\gamma\gamma$ -coincidence spectra were measured. More than 50 γ rays were observed and incorporated into a level scheme consisting of 32 excited states. A new level is proposed at 3986 keV. Except for this level, the current study fully supports an exhaustive study of levels in ^{116}Sn reported earlier [2]. The previous study was an attempt to develop a nearly complete level scheme of ^{116}Sn up to an excitation energy of 4.3 MeV.

The reported part of the current study benefited from discussions with S. Raman. This work has been supported partly by the National Scientific Research Foundation (OTKA) under Contract No. T4428.

References

- [1] Z. Gácsi and S. Raman, Phys. Rev. C, accepted for publication.
- [2] S. Raman, T. A. Walkiewicz, S. Kahane, E. T. Journey, J. Sa, Z. Gácsi, J.L. Weil, K. Allart, G. Bonsignori, and J. F. Shriner, Jr., Phys. Rev. C **43**, 521 (1991).

Identification and in-beam spectroscopy of the neutron deficient $^{108,110}\text{Te}$ nuclei

Zs. Dombrádi, M. Józsa, B. M. Nyakó, G. E. Perez,
C. Fahlander^a, D. Seweryniak^a, J. Nyberg^a, A. Atac^a,
B. Cederwall^b, A. Johnson^b, A. Kerek^b, J. Kownacki^c,
L-O. Norlin^b, R. Wyss^b, E. Adamides^d, E. Ideguchi^e, R. Julin^f,
S. Juutinen^f, W., Karczmarczyk^c, S. Mitrai^e, M. Piiparinen^f,
R. Schubart^g, G. Sletten^h, S. Törmänen^f and A. Virtanen^f

^a The Svedberg Laboratory, Uppsala, Sweden, ^b The Royal Institute of Technology, Physics Dept/Frescati-Stockholm, Sweden, ^c Institute of Experimental Physics, Warsaw, Poland, ^d National Centre for Scientific Research, Attiki, Grece, ^e Kyushu University, Fukuoka, Japan, ^f University of Jyväskylä, Jyväskylä, Finland, ^g Hahn-Meitner Institute, Berlin, Germany, ^h The Niels Bohr Institute, Copenhagen, Denmark

Neutron deficient nuclei close to the doubly magic ^{100}Sn were investigated by in-beam gamma spectroscopic methods in an experiment performed at the Tandem Accelerator Laboratory of the Niels Bohr Institute in Risø, Denmark. Here we present results for the light ^{108}Te and ^{110}Te isotopes.

In the experiment a 10 mg/cm² thick ^{54}Fe target, isotopically enriched to 99.8%, was bombarded with a beam of 270 MeV ^{58}Ni . The emitted γ rays, neutrons, and charged particles were detected in the NORDBALL detector system [1], configured with 15 BGO-shielded Ge detectors and an array of 11 liquid scintillator neutron detectors covering about 1π solid angle in the forward direction [2]. Inside the ball a 4π charged particle detector array of 21 ΔE type Si detectors [3] and a 30-element γ -ray calorimeter of BaF₂ crystals covering the backward 2π hemisphere were placed.

A total of 420 million $\gamma\gamma$ -charged particle-neutron coincidence events were collected and off-line sorted into $E_\gamma-E_\gamma$ matrices by setting different conditions on the number of detected protons, α particles and neutrons. This procedure enabled to select γ rays belonging to a given final nucleus. In order to reduce the contamination in the channels of interest, caused by γ rays coming from other nuclei, a successive matrix subtraction technique was applied. For data reduction standard gating technique was used on the cleaned matrices. The projected spectra of the cleaned matrices for ^{108}Te and ^{110}Te are shown in Fig.1. All the γ rays labelled by their energy are new, and belong to the given nucleus.

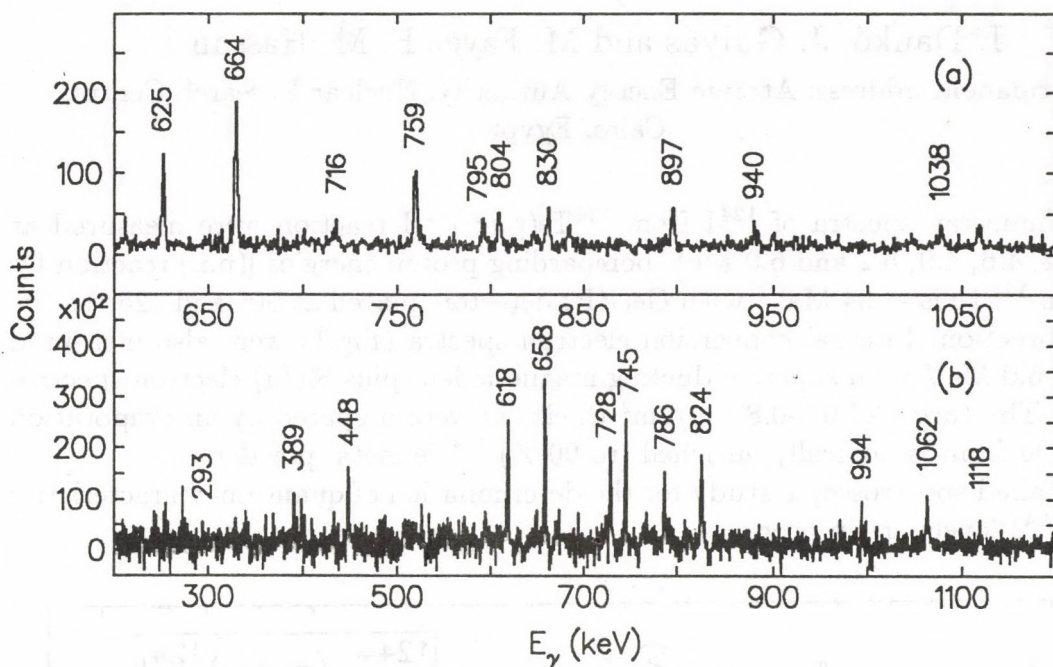


Fig. 1. Total projection spectra of the cleaned matrices for ^{108}Te (a) and ^{110}Te (b). The assigned transitions are labelled by their energy.

The level scheme of both nuclei was constructed mainly on the basis of the coincidence relations, but the energy balance, the intensity balance deduced from γ -ray intensities in the total projection spectrum and in the gated spectra, and expectation from the systematics were also considered. Spin and parity assignments were taken from the measured DCO ratios and the systematics of heavier Te nuclei.

In the ^{108}Te nucleus we could identify the first few members of the ground state vibrational band. In the ^{110}Te nucleus, in addition to this band, we found a quasi rotational band based on the $\nu g_{7/2} h_{11/2} 9^-$ configuration, as well as several side bands.

The experimental results are discussed on the basis of the cranked shell model.

This work was partially supported by the Hungarian Science Foundation (OTKA) contract No:T007481, and by the Swedish Natural Science Research Council.

References

1. B. Herskind et al., Nucl. Phys. **A447**, 395 (1985).
2. S. E. Arnell et al., Nucl. Instr. Meth. **A300**, 303 (1991).
3. T. Kuroyanagi et al., Nucl. Instr. Meth. **A316**, 289 (1992).

Spectroscopic study of the $^{124}\text{Te}(p,n\gamma)^{124}\text{I}$ reaction

I. Dankó, J. Gulyás and M. Fayez F. M. Hassan †

†Permanent address: Atomic Energy Authority, Nuclear Research Centre, Cairo, Egypt

Gamma-ray spectra of ^{124}I from $^{124}\text{Te}(p,n\gamma)^{124}\text{I}$ reaction were measured at $E_p = 4.4, 4.6, 4.9, 5.2$ and 6.0 MeV bombarding proton energies [(p,n) reaction Q-value on ^{124}Te is -3.94 MeV] with Ge(HP) detectors placed at 90° and 125° to the beam direction. Internal conversion electron spectra (Fig.1) were also measured at $E_p = 6.0$ MeV with superconducting magnetic lens plus Si(Li) electron spectrometers. The target of $0.3\text{-}0.8$ mg/cm² thickness were prepared by an evaporation technique from isotopically enriched (to 90 %) ^{124}Te metal powder.

Detailed spectroscopic study for the determination of quantum-characteristics of the ^{124}I levels are in progress.

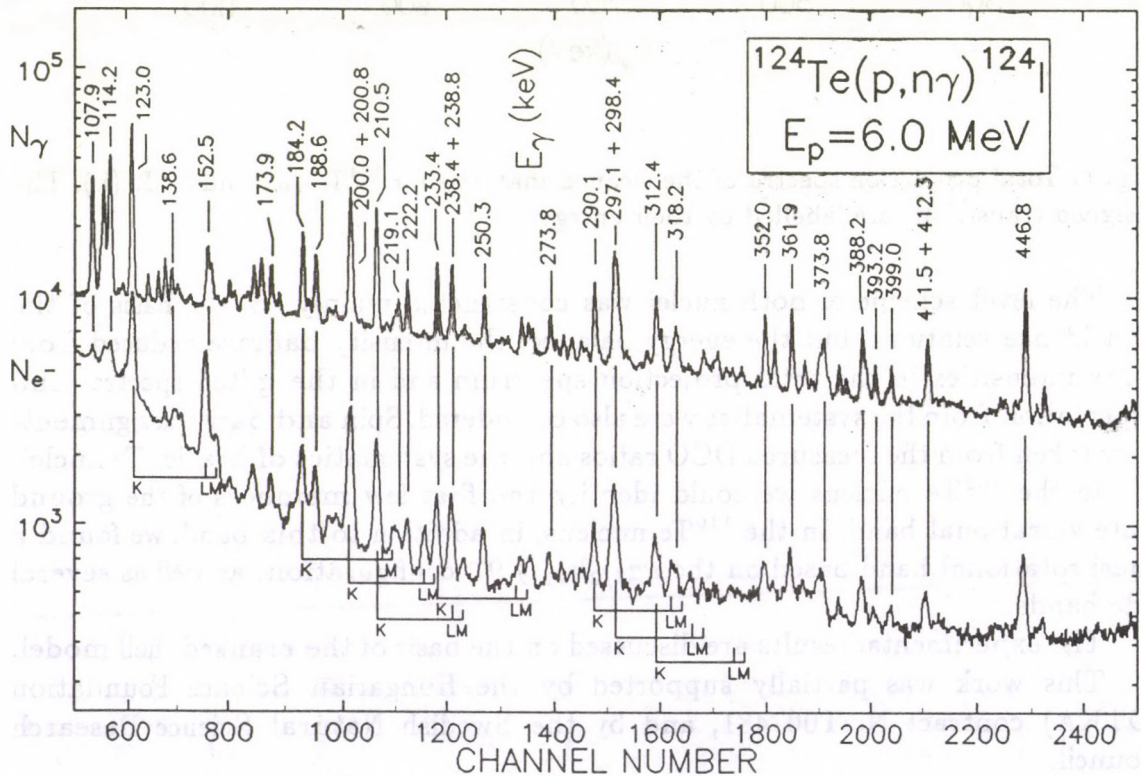


Fig. 1. Typical γ -ray and internal conversion electron spectra.

1. T. Tamura, K. Miyano and S. Ohya, Nucl. Data Sheets **41** (1984) 413.
2. J. Burde, V. Richter, J. Tsaliah and I. Labaton, Nucl. Phys. A**385** (1982) 29.

Study of ^{126}I from $(p,n\gamma)$ reaction

M. Fayez F. M. Hassan [†], J. Gulyás and I. Dankó

[†]Permanent address: Atomic Energy Authority, Nuclear Research Center, Cairo, Egypt

As an extension of the spectroscopic study of the odd-odd nuclei in $Z\sim 50$ region, the γ -ray and internal conversion electron spectra of the $^{126}\text{Te}(p,n\gamma)^{126}\text{I}$ reaction were measured at different proton energies between 3.9 and 6.0 MeV with Ge(HP) γ -ray and superconducting magnetic transporter plus Si(Li) electron spectrometers (Fig. 1). The targets were prepared by an evaporation technique from isotopically enriched (to 98.5 %) ^{126}Te . Internal conversion electron lines were detected for many lines in the γ -spectra, making it possible to determine internal conversion coefficients for the observed transitions.

This is the first step in a more detailed spectroscopic study of the ^{126}I nucleus, with the aim of getting more complete information on the structure of low-spin excited states of this nucleus. Previous data on ^{126}I were summarized in [1,2].

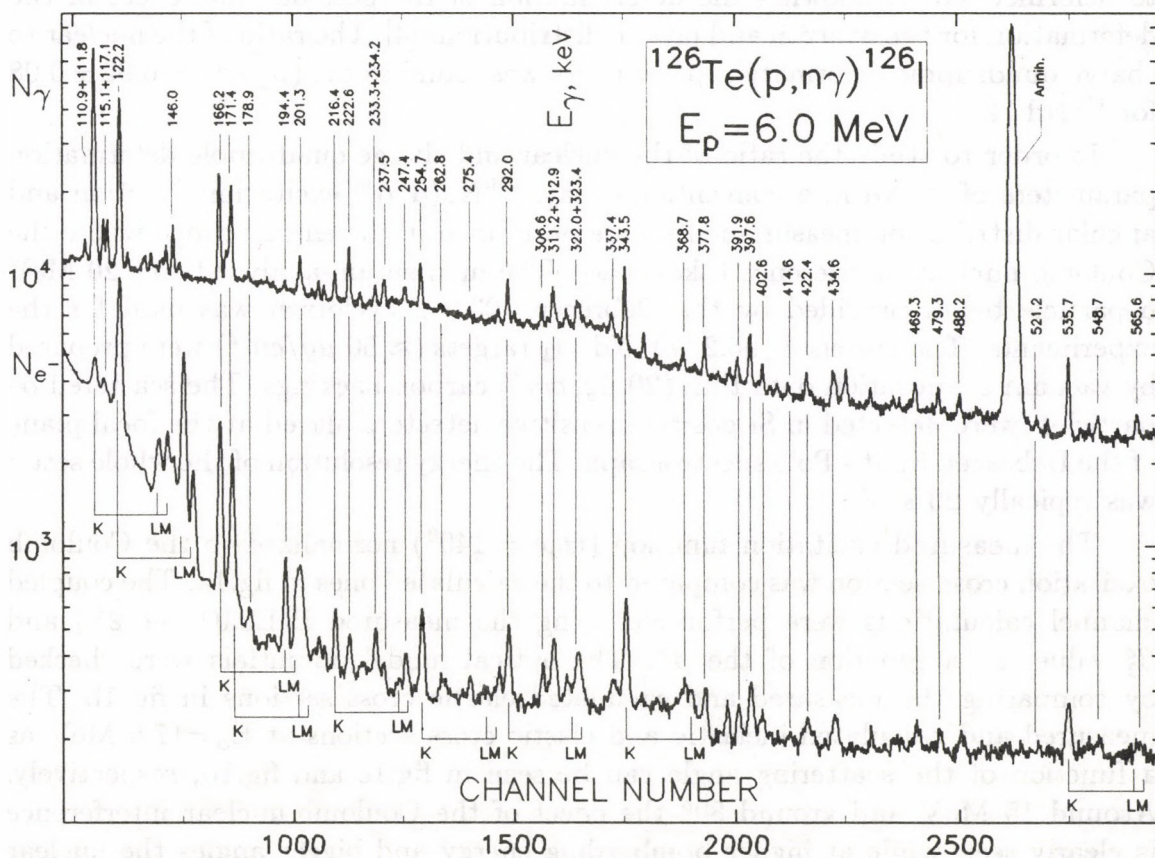


Fig. 1. Part of typical γ -ray and internal conversion electron spectra.

1. T. Tamura, K. Miyano and S. Ohya, Nucl. Data Sheets **36** (1982) 227.
2. J. Burde, V. Richter and I. Labaton, Nucl. Phys. **A402** (1983) 205.

Nuclear and charge quadrupole deformation parameters of ^{150}Nd

A. Krasznahorkay, M. Csatlós, Z. Máté and A.T. Kruppa

A long-standing question in nuclear physics is whether the collective model properly describes the relative isoscalar and isovector ground state deformations of nuclei [1]. The charge-density deformation parameters ($\beta_2^c, \beta_4^c \dots$) are usually obtained with high accuracy on basis of the Bohr-Mottelson model which relates them to the transition probability from the ground state to the rotational level with angular momentum L . In contrast, the nuclear-density deformation parameters ($\beta_2^n, \beta_4^n \dots$) investigated with strongly interacting probes usually have much larger uncertainties so that the ratio of the two is badly known, although it would pose new challenges to models of nuclear structure and reaction mechanisms [2].

In our recent work a novel method was developed in Gronigen to investigate the neutron skin thickness of spherical nuclei [3]. The method was generalized also to deformed nuclei allowing the determination of the possible differences in the deformation for the neutron and proton distributions [4]. The ratio of the nuclear to charge quadrupole deformation parameters was found to be: ($\beta_2^n / \beta_2^c = 0.92 \pm 0.08$ for ^{150}Nd [4].

In order to study the ratio of the nuclear and charge quadrupole deformation parameters of ^{150}Nd in a conventional way, $^{150}\text{Nd}(\alpha, \alpha')$ excitation function and angular distribution measurements were performed in the energy range where the Coulomb-nuclear interference takes place. The momentum-analyzed 14 - 20 MeV α -particle beam provided by the Debrecen 103 cm cyclotron was used for the experiments. The enriched (95.2 %) Nd_2O_3 targets ($\approx 50 \mu\text{g}/\text{cm}^2$) were prepared by vacuum evaporation onto thin ($20 \mu\text{g}/\text{cm}^2$) carbon backings. The scattered α -particles were detected in Si position sensitive detectors placed at the focal plane of the Debrecen Split - Pole spectrograph. The energy resolution of the whole setup was typically 20 keV.

The measured excitation function ($\theta_{\alpha'} = 140^\circ$) normalized to the Coulomb excitation cross-section was compared to the calculated ones in fig.1a. The coupled channel calculations were performed using the measured $B(E2, 0^+ \rightarrow 2^+)$ and β_2^c values as a function of the β_2^n . The optical model potentials were checked by comparing the measured and calculated elastic cross sections in fig 1b. The measured and calculated inelastic and elastic cross sections at $E_\alpha = 17.6$ MeV as a function of the scattering angle can be seen in fig.1c and fig.1d, respectively. Around 15 MeV and around 80° the effect of the Coulomb-nuclear interference is clearly seen while at higher bombarding energy and bigger angles the nuclear excitation dominates, giving data for the β_2^n .

As a result of a preliminary analysis, the nuclear deformation parameter was found to be $\beta_2^n = 0.23 \pm 0.02$ giving a ratio of $\beta_2^n / \beta_2^c = 0.80 \pm 0.10$ in good agreement with our previous results.

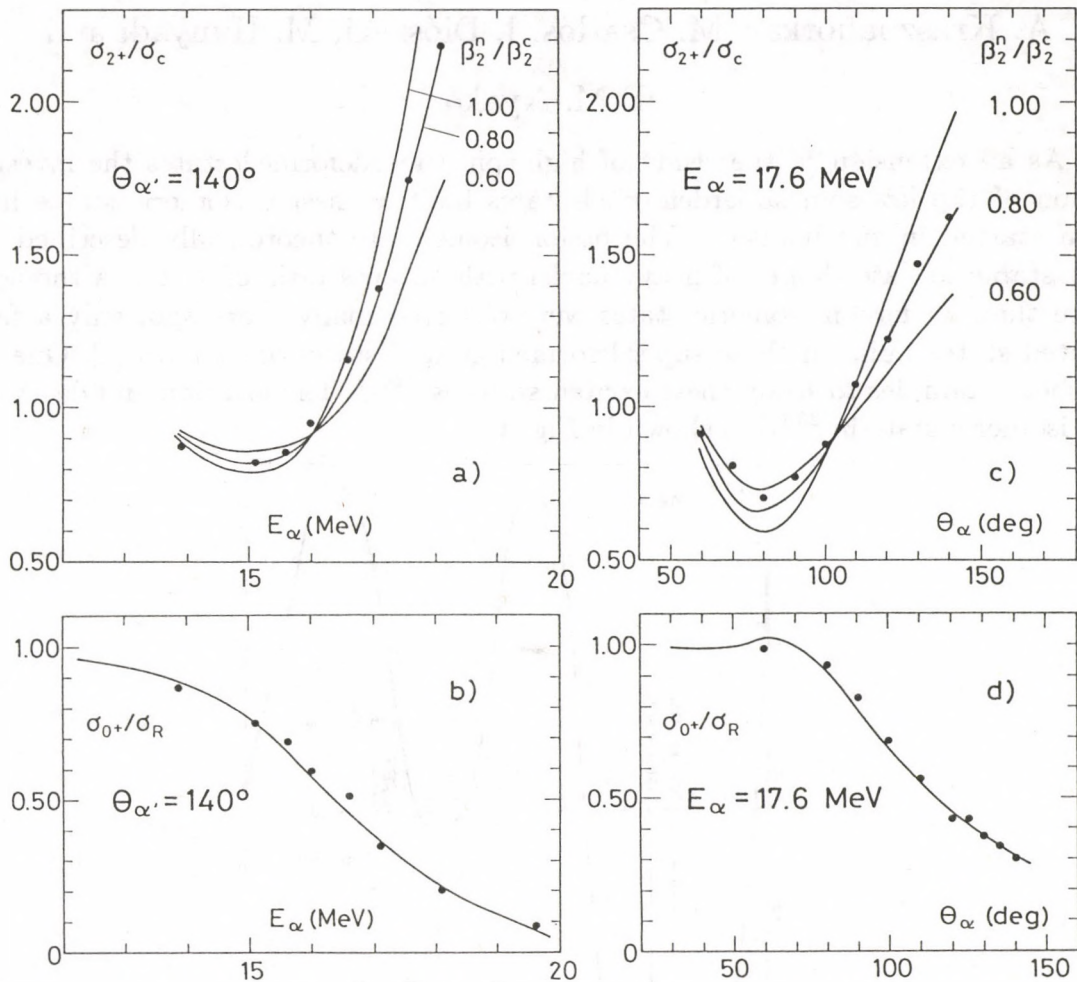


Fig. 1. Measured (full dots) and calculated (solid lines) inelastic a), c) and elastic b), d) scattering cross-sections of $^{150}\text{Nd}(\alpha, \alpha')$. The inelastic cross sections were normalized to the pure Coulomb-excitation theory, while the elastic ones to the cross-sections of the Rutherford scattering. The coupled channel calculations were performed for different ratios of nuclear/Coulomb quadrupole deformation parameters.

This work was supported by the National Scientific Research Foundation (OTKA No: 7486 and 3010)

References

- [1] R.C. Barrett and D.F. Jackson, Nuclear Sizes and Structure, Clarendon Press, Oxford (1977)
- [2] J.M. Knudson et al., Phys. Rev. Lett **66** (1991) 1026
- [3] A. Krasznahorkay et al., Phys. Rev. Lett. **66** (1991) 1287
- [4] A. Krasznahorkay et al., Nucl. Phys. **A567** (1994) 521

Search for superdeformed states in ^{236}U

A. Krasznahorkay, M. Csatlós, I. Diószegi, M. Hunyadi and
B.M. Nyakó

As an extension to the study of high-spin superdeformed states the investigation of the low-spin superdeformed states built on fission isomeric states has been started in our Institute. The fission isomers are theoretically described as metastable prolate shapes of heavy nuclei with an axes ratio of $\approx 2:1$. Although, more than 30 fission isomeric states were observed many years ago, only a few excited states built on these superdeformed ground states are known [1]. One of the best examples to study these excited states is ^{236}U . The location and decay of the isomeric state in ^{236}U is shown in Fig. 1.

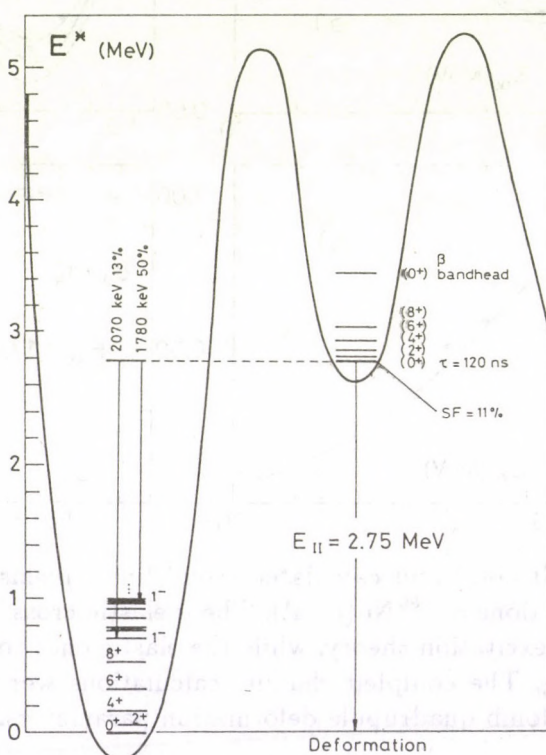


Fig. 1. Location and decay of the low-spin superdeformed states in ^{236}U

The superdeformed (Class II) ground state is located 2.75 MeV above the normal (class I) ground state. In contrary to the class I states which decay only by γ emission in the energy region of $E^* = 2.8 - 3.8$ MeV, the γ decay of the fission isomeric state to the class I states is highly hindered, therefore the fission becomes also a non-negligible (11 %) decay channel characterizing this state. As the lifetime of the (mostly rotational) excited states built on the fission isomeric state is very short ($\tau \ll 1$ ns) and they decay back to the class II ground state, these states can be identified by delayed coincidence measurements with the fission products.

The class II states of ^{236}U were excited by $^{235}\text{U}(d, pf)$ reaction. This reaction has a reasonably high ($\approx 1\mu\text{b}$) cross section. The proton spectra were measured with the Debrecen Split-Pole spectrometer, while the fission fragments were detected by Si surface barrier detectors. An energy spectrum detected by a Si position sensitive detector at the focal plane of the spectrograph can be seen in Fig. 2. In the magnetic spectrograph with the same $B\rho$ value different particles can reach the focal plane, but according to their energy, position and time-of-flight, they can be well identified. The coincidence rate between the spectrograph and the fission detectors was very low. During the 2 days preliminary experiment there was not enough statistics to see peaks in the coincidence spectrum. We are going to increase the efficiency of the setup in two ways:

- i.) Using large area parallel plate avalanche counters (PPAC) instead of Si detectors [2].
- ii.) Increasing the solid angle of the spectrograph from 2 msr to 10 msr. As it was shown in reference [3] the solid angle of the spectrometer can be increased without losing the energy resolution. In this case one has to use a specially designed focal plane detector which is capable to measure not only the position, but the angle of incidence of the detected particles [4].

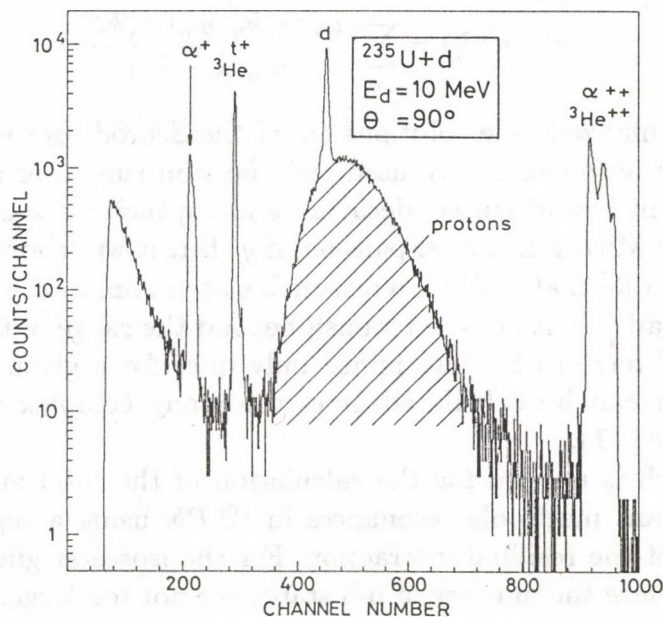


Fig. 2. Energy (energy loss for protons) spectra of the particles detected at the focal plane of the spectrograph

This work has been supported by the OTKA Foundation, No: 7486.

- [1] C. Wagemans: The Nuclear Fission Process, CRC Press (1991)
- [2] H. Stelzer, Nucl. Instr. and Meth. **133** (1976) 409
- [3] R.M. DeVries, D. Shapira and M.R. Clover, Nucl. Instr. and Meth. **140** (1977) 479
- [4] J.M. Schippers et al., Nucl. Instr. Meth. Phys. Res. **A247** (1986) 467

Description of the continuum in calculating partial decay widths of giant resonances in ^{208}Pb

P. Lind¹, E. Maglione², R. J. Liotta³, T. Vertse

Since giant resonances are collective excitations, lying, in general, above the threshold of the particle emission one has to take into account the possibility of the nucleon escape in the theoretical description. The usual treatment is in the frame of the continuum random phase approximation[1] (CRPA), in which the effect of the continuum is taken into account exactly. For heavy nuclei CRPA calculations are time consuming since large number of p-h configurations form the giant multipole resonance. Dealing with a realistic single particle potential one has to integrate the Schrödinger equation numerically in order to get the solutions which determine the Green's function. Therefore, the major part of the computation time in the CRPA is spent on calculating the Green's function at different energies. In order to speed up the CRPA calculations we introduced[2] a pole expansion of the Green's function:

$$g(r, r'; k) = \sum_n \frac{w_n(r, k_n) w_n(r', k_n)}{2k_n(k - k_n)}, \quad (1)$$

in which the normalized pole solutions w_n of the Schrödinger equation belonging to complex wave numbers k_n are used and the sum runs over all classes of poles i.e. bound and antibound states, decaying and capturing resonances. This form is also given by the Mittag-Leffler expansion of g . But it was shown only recently by Berggren and Lind[3] that eq.(1) is a reasonable approximation even if the potential has a Coulomb tail (i.e. it does not vanish beyond the range of the nuclear forces). The w_n "states" have to be determined only once for a given potential and the Green's function can be calculated quickly for any complex value of the wave number k using eq.(1).

Our approach is applied for the calculation of the total and partial neutron widths of the giant multipole resonances in ^{208}Pb , using a separable multipole-multipole form of the residual interaction. For the isoscalar giant monopole resonance (GMR) where the number of p-h states are not too large, we carried out an exact CRPA calculation as well and used its result for checking the accuracy of our method. We found that the correlated energies agreed with the CRPA results up to 3-4 decimal places and the values of the partial widths were also reproduced up to an accuracy of 5-15% using a basis which consisted of 5-7 resonant states besides the bound and antibound states in each partial wave[2].

We calculated the giant multipole resonances also for $J = 1, 2, 3, 4, 5$ and found that all the $J \neq 2$ giant resonances were considerably fragmented.

In order to understand the structure of the giant resonances we used the resonant RPA[4,5] (RRPA). In the RRPA the basis is composed of a subset of the pole functions used above. The truncated form of the Berggren's completeness

relation[6] is used, which includes only bound states and decaying resonances. The wave functions of the correlated states are expanded in terms of p-h configurations with complex energies. For a separable interaction, the RRPA gives the forward amplitudes as

$$X(k, i; n) = N_n \frac{\langle k || f || i \rangle}{\omega_n - (\mathcal{E}_k - \mathcal{E}_i)}, \quad (2)$$

where ω_n , \mathcal{E}_k and \mathcal{E}_i are the energies of the correlated, the particle and the hole states, respectively. N_n is the normalization factor and $\langle k || f || i \rangle$ is the matrix element of the separable interaction. A common property of the giant resonances is that the wave function is dominated by those p-h configurations in which the particle is in bound or quasi-bound states. Therefore, the escape width of these resonances is small.

The attractive feature of our approach is that our code runs 2-3 orders of magnitude faster than the CRPA and this is promising indeed for the calculation of the spreading width where the number of configurations is excessive.

This work was supported by the OTKA Foundation Hungary (contract numbers 3017 and 3010).

References

- 1.- S. Shlomo and G. Bertsch, Nucl. Phys. **A 243** (1975)507.
- 2.- P. Lind, R.J. Liotta, E. Maglione, T. Vertse, Resonant state expansion of the continuum, submitted to Z. Phys. **A**
- 3.- T. Berggren and P. Lind, Phys. Rev. **C 47**(1993)768.
- 4.- T. Vertse, P. Curutchet, O. Civitarese, L. S. Ferreira and R. J. Liotta, Phys. Rev. **C 37**(1988)876.
- 5.- P. Curutchet, T. Vertse and R. J. Liotta, Phys. Rev. **C 39** (1989) 1020.
- 6.- T. Berggren, Nucl. Phys. **A109** (1968) 265.

¹Department of Mathematical Physics, Lund Institute of Technology,
P.O. Box 118, S-221 00 Lund, Sweden

²Dipartimento di Fisica "Galileo Galilei", Via Marzolo 8, Padova, Italy,

³Royal Institute of Tecnology, Physics Department Frescati, Frescativ 24,
S-104 05 Stockholm, Sweden

Multicluster description of the neutron-rich helium isotopes

K. Varga and Y. Suzuki[†]

[†]Physics Department, Niigata University, Niigata 950-21, Japan

In a previous paper [1], we presented a microscopic multicluster approach to the ground state of ${}^6\text{He}$ and ${}^8\text{He}$ in a model comprising an alpha cluster and single neutron clusters. In this model the intercluster wave function is a superposition of terms of different relative coordinate arrangements, and each term is a product of nodeless harmonic oscillator functions with different width parameters. To determine the combination coefficients we used the "stochastic variational method".

The aim of this paper is to demonstrate that our model produces realistic wave functions, that is, the physical properties extracted using our wave functions are close to the experimental results.

We have calculated the matter, proton and neutron density distributions of the ${}^6\text{He}$ and ${}^8\text{He}$ nuclei. By using these distributions we calculated the proton and neutron radii of these nuclei and the results agree with experiment within a few percent.

An other characteristic property of the halo nuclei is the very narrow transverse momentum distribution. The momentum distributions of the ${}^4\text{He}$ and the ${}^6\text{He}$ fragments in the (${}^4\text{He}, {}^6\text{He}$) and the (${}^6\text{He}, {}^8\text{He}$) reactions respectively, calculated using our two-neutron removal spectroscopic amplitude perfectly follow the experimental distributions.

We have also calculated the β decay transition probability per time and energy units and compared it to the experimental data. From the good agreement we concluded that asymptotic part of the wave function in our model is approximated satisfactorily.

The application of this model to other nuclei is planned in the near future.

References

1. K. Varga, Y. Suzuki and R. G. Lovas Nucl. Phys. A, in press

Multicluster model of neutron-halo nuclei with a stochastic variational method

K. Varga, R. G. Lovas and Y. Suzuki[†]

[†]Department of Physics, Niigata University, Niigata, Japan

Neutron-halo nuclei are currently in the focus of intense interest [1]. Their description requires a unified approach with very flexible neutron orbits and a correct treatment of the centre-of-mass motion and of the Pauli principle. In last year's Annual Report we reported on two approaches: on a full-fledged three-cluster approach [2] and on a simplified one, which is applicable to more than three clusters as well [3]. In this contribution we report on the first applications of the latter. Some even more recent developments are included in another contribution [4].

The model is based on a linear variational method, and it is made feasible by stochastic sampling in setting up the basis. We used the three-cluster system ${}^6\text{He}=\alpha+n+n$ as a testing ground, and present results for the five-cluster system ${}^8\text{He}=\alpha+n+n+n+n$ as well.

Our model employs a trial function, which is a sum over various cluster arrangements μ , each associated with a particular set of intercluster Jacobi coordinates. For $\alpha+n+n$, there are two non-trivially different arrangements, viz. $\mu=(\alpha n)n$ and $\alpha(nn)$, while for $\alpha+n+n+n+n$ there are nine. Each arrangement, together with a particular set of angular momenta, defines a subspace of the full state space. The coupling of the nucleon spins to S , and of the orbital angular momenta l_i ($i = 1, \dots, n$) to L follow the pattern of the n Jacobi coordinates. The product of the relative-motion functions is expanded in terms of products of n zero-node oscillator wave functions of a range of size parameters, with the expansion coefficients being the only variational parameters.

We chose the central effective interaction of Ref. [5].

For ${}^6\text{He}$ the energies obtained in the individual subspaces are very close to each other, and yet, when they are combined, the binding gets stronger moderately. This behaviour is typical of strongly overlapping subspaces, in which case the united basis is likely to be largely redundant. To reduce the redundancy of the basis, we selected the basis elements by stochastic sampling. We enlarged the basis step by step by selected random elements. They were qualified for admittance if their contribution was either the best among 10 randomly chosen candidates ("preselected basis") or was larger than 0.005 MeV ("utility-tested basis").

Whichever selection prescription was used, the energies as well as radii calculated with random bases were always found to converge to the "exact" energy, and, at the expense of ~ 20 keV loss of binding, it was possible to reduce the basis dimension with respect to systematically constructed bases by a factor of 3–6.

This enabled us to make reliable calculations for the five-cluster system as well. A summary of the calculations for ${}^8\text{He}$ is given in Table 1. The configuration $\{[\alpha(nn)]n\}n + [\alpha(nn)](nn) + \{[(\alpha n)n]n\}n$ seems to be adequate; not even the inclu-

sion of configuration $\{[(\alpha n)n]n\}n'$, which is the best by itself, could deepen the binding appreciably.

Table 1. Energies and rms radii of ${}^8\text{He}$ in different model spaces. All l_i are zero except in $\{[(\alpha n)n]n\}n'$, where $l_1 = l_2 = 1$

Subspace	N	E (MeV)	r (fm)
$\{[(\alpha n)n]n\}n$	153	-2.509	2.341
$\{[(\alpha n)n]n\}n'$	130	-3.033	2.322
$\{[\alpha(nn)]n\}n$	161	-2.961	2.305
$[\alpha(nn)](nn)$	163	-2.676	2.278
$\alpha[(nn)(nn)]$	176	-1.167	2.188
$(\alpha n)[(nn)n]$	220	> 0	
$\alpha\{[(nn)n]n\}$	157	-1.368	2.196
$\{[\alpha(nn)]n\}n + [\alpha(nn)](nn)$	211	-3.292	2.306
$\{[\alpha(nn)]n\}n + \alpha\{[(nn)n]n\}$	223	-3.027	2.225
$\{[\alpha(nn)]n\}n + [\alpha(nn)](nn)$ + $\{[(\alpha n)n]n\}n$	303	-3.395	2.271
$\{[\alpha(nn)]n\}n + [\alpha(nn)](nn)$ + $\alpha\{[(nn)n]n\}$	311	-3.321	2.317
Experiment		-3.112	2.50

We managed to reproduce the g.s. energies of ${}^6\text{He}$ and ${}^8\text{He}$ simultaneously with an accuracy of 100 keV. The calculated matter radii would be slightly larger with a force that reproduces the empirical α -particle radius.

For ${}^6\text{He}$ we have calculated a discretized 1^- continuum as well. We have found that the distribution of the strength $B(E1)$ of the electromagnetic transition to the ground state peaks below the excitation energy of 3 MeV, which is a clear indication for the existence of the soft dipole mode predicted earlier [6].

References

1. Ikeda, K., Suzuki, Y. (eds.): Proc. Int. Symp. on Structure and reactions of unstable nuclei (Niigata, 1991) (World Scientific, Singapore, 1991)
2. A. Csóto, K. Varga and R. G. Lovas, ATOMKI Annual Report (1992) p. 32; A. Csóto, Phys. Rev. **A48** (1993) 165; A. Csóto, Phys. Lett. **B 315** (1993) 24
3. K. Varga, Y. Suzuki, A. Csóto and R. G. Lovas, ATOMKI Annual Report (1992) p. 34
4. K. Varga and Y. Suzuki: Multicluster description of the neutron-rich helium isotopes, contribution to this volume
5. D. R. Thompson, M. LeMere and Y. C. Tang, Nucl. Phys. **A286** (1977) 53
6. Y. Suzuki, Nucl. Phys. **A528** (1991) 395

Semimicroscopic algebraic cluster model of light nuclei

J. Cseh and G. Lévai

We have discussed the relation of the phenomenological algebraic cluster model (i.e. of the vibron model and its extensions), to the microscopic description. Based on this connection we have formulated [1] a semimicroscopic approach, in which the internal cluster degrees of freedom are treated in terms of the $SU(3)$ shell model, and the relative motion is described by the vibron model. For a two-cluster system this model has a group structure of $U_{C_1}^{ST}(4) \otimes U_{C_1}(3) \otimes U_R(4) \otimes U_{C_2}(3) \otimes U_{C_2}^{ST}(4)$, and the phenomenological interactions are obtained in terms of the group generators. The model space is constructed to be free from the Pauli forbidden states and spurious center of mass motion, similar to that of the $SU(3)$ cluster model.

We have given detailed formulation of the model for three special types of two-cluster systems [1], where the spin-isospin degrees of freedom do not appear explicitly: i) One of the clusters is a closed-shell nucleus and the other is an even-even one with $N = Z$, ($U_C(3) \otimes U_R(4)$ model). ii) Both clusters are even-even nuclei with $N = Z$, ($U_{C_1}(3) \otimes U_{C_2}(3) \otimes U_R(4)$ model). iii) One of the clusters is a closed-shell nucleus and the other one has $N = Z \pm 2t = \text{even}$, (the restricted $U_C^{ST}(4) \otimes U_C(3) \otimes U_R(4)$ model). We have presented three examples, the $^{12}C + \alpha$, the $^{12}C + ^{12}C$ and the $^{14}C + \alpha$ systems to demonstrate various aspects of the semimicroscopic algebraic cluster model and its special subcases.

The model can be developed further along several lines. These possibilities are also discussed in Ref. [1].

References

1. J. Cseh and G. Lévai: "Semimicroscopic algebraic cluster model of light nuclei: I. Two-cluster-systems with spin-isospin-free interactions", Ann. Phys. (N. Y.), in press.

Semimicroscopic $^{34}\text{S} + \alpha$ cluster model of the ^{38}Ar nucleus

G. Lévai and J. Cseh

The first applications of the semimicroscopic algebraic cluster model [1] to the $^{14}\text{C} + \alpha$ and $^{12}\text{C} + ^{12}\text{C}$ cluster systems have shown that this model is able to reproduce many important characteristics of the ^{18}O and ^{24}Mg nuclei [2,3]. The α -cluster states of the ^{38}Ar nucleus offer another interesting application of the model for several reasons. i) The model can be tested near the sd -shell closure, where α -clustering is known to be relevant to several nuclei. ii) Experimental information on the energy spectrum and electromagnetic transitions of the ^{38}Ar nucleus is relatively rich. iii) New experimental results on $^{34}\text{S}(\alpha, \gamma)^{38}\text{Ar}$ resonances are directly available from our laboratory [4].

We have used the $\text{SU}(3)$ dynamical symmetry limit of the model [1], which was found to be a realistic approximation in the previous studies [2,3]. This assumption simplified calculations to a considerable extent by allowing the utilization of the $\text{SU}(3) \supset \text{O}(3)$ tensorial character of the semimicroscopic basis states and the phenomenological operators. In this case the experimental states can be assigned to bands labeled by $\text{SU}(3)$ quantum numbers (λ, μ) , which also determine selection rules for the electromagnetic transitions. We have used this information to calculate the energy spectrum of approximately 100 states by fitting the 8 parameters of a phenomenological Hamiltonian. The results for positive-parity states are displayed in Fig. 1.

Although the model was not able to reproduce the properties of some individual bands, it gave a reasonable account of some global characteristics of the energy spectrum and electromagnetic transitions. An example for this was, that the model predicted very few E2 and E1 transitions to the ground-state region, which we found to be in good agreement with the experimental data. E2 transitions were reproduced reasonably well (especially for negative-parity states), while the model was somewhat less successful in describing M1 transitions. Selection rules for E1 transitions were found to be too restrictive. Resonance states in the $E_x \simeq 10$ –11 MeV region [4] are expected to contain significant components from $\text{SU}(3)$ multiplets with low values of λ and μ , which may explain why, in contrast with lower-lying states, many of these resonances prefer decaying to the ground state.

In conclusion, our $^{34}\text{S} + \alpha$ cluster model was able to account for some global properties of the ^{38}Ar nucleus, nevertheless, the $\text{SU}(3)$ dynamical symmetry approximation turned out to be less realistic here, than for other nuclei in the lower half of the sd -shell. We expect that the results can be improved by breaking the $\text{SU}(3)$ dynamical symmetry by introducing additional interaction terms in the Hamiltonian, which could result a more realistic energy spectrum, and would also relax the occasionally too strict selection rules implied by the $\text{SU}(3)$ dynamical symmetry.

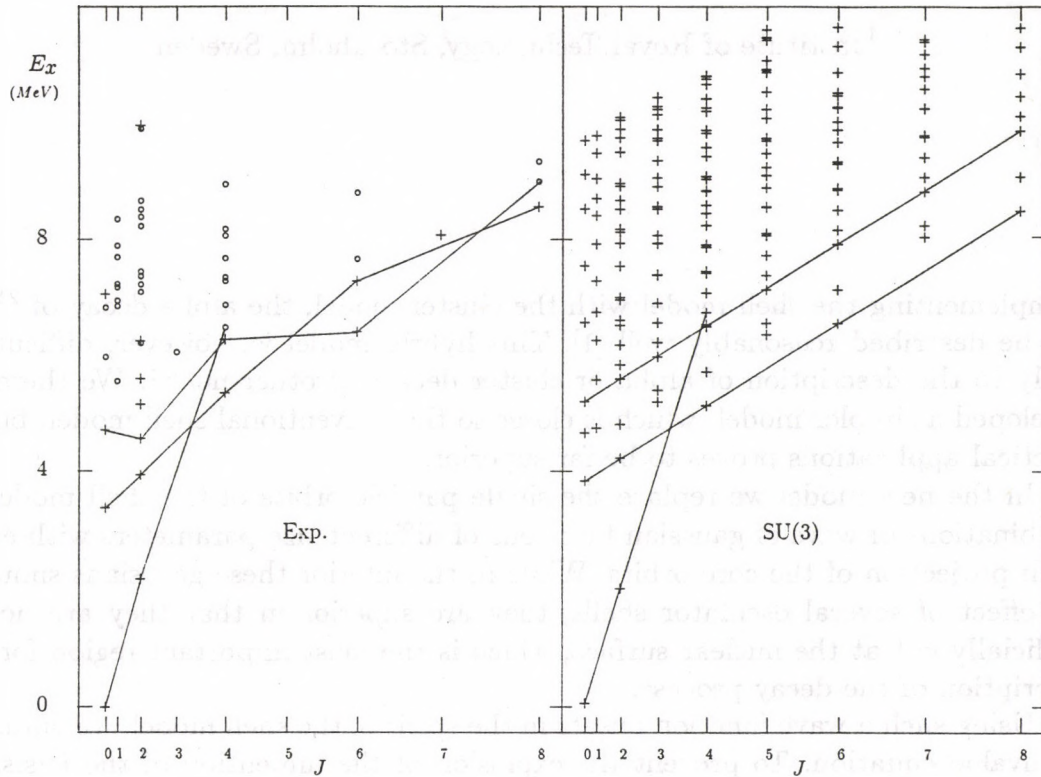


Fig. 1. Positive-parity $T = 1$ energy levels of the ^{38}Ar nucleus, displayed in rotational diagram form. Circles (o) stand for states with uncertain J^π assignment in the experimental energy spectrum. The members of possible rotational bands are connected by solid lines.

References

1. J. Cseh and G. Lévai: "Semimicroscopic algebraic cluster model of light nuclei: I. Two-cluster-systems with spin-isospin-free interactions", Ann. Phys. (N. Y.), in press.
2. G. Lévai, J. Cseh and W. Scheid: Phys. Rev. C **46** (1992) 548.
3. J. Cseh, G. Lévai and W. Scheid: Phys. Rev. C **48** (1993) 1724.
4. Zs. Fülöp, Á. Z. Kiss, E. Koltay, E. Somorjai, J. Keinonen and P. Tikkanen: ATOMKI Annual Report (1991) p. 4; (1992) p. 11.

Shell model on random gaussian basis: Description of ^{212}Po

K. Varga and R. J. Liotta[†]

[†]Institute of Royal Technology, Stockholm, Sweden

Complementing the shell model with the cluster model, the alpha decay of ^{212}Po can be described reasonably well [1]. This hybrid model is, however, difficult to apply to the description of alpha or cluster decays of other nuclei. We therefore developed a simpler model, which is closer to the conventional shell model, but in practical applications proves to be far superior.

In the new model we replace the single particle orbits of the shell model by combinations of wave of gaussian functions of different size parameters with exact Pauli projection of the core orbits. While in the interior these gaussians simulate the effect of several oscillator shells, they are superior in that they are not so artificially cut at the nuclear surface, which is the most important region for the description of the decay process.

Using such a wave function ansatz in the spirit of the shell model, we obtain an eigenvalue equation. To prevent the explosion of the dimension of the basis, we employ the "stochastic or Monte Carlo diagonalisation" technique [2]. With this method the important states are selected from randomly chosen basis state sets according to their contribution to the ground state energy.

To test the performance of this model, we compare it with our previously used hybrid description. We found that this technically simpler model is as good as the hybrid model. The predicted alpha decay width is about one third of the experimental value, the alpha cluster formation probability is somewhat less (15%) than in the previous calculation. These results encourage us to apply this model to the alpha decays of other nuclei and to exotic cluster decays.

References

1. K. Varga, R. G. Lovas and R. J. Liotta, Phys. Rev. Lett. **69** (1992) 37
K. Varga, R. G. Lovas and R. J. Liotta, Nucl. Phys. **A550** (1992) 421
2. H. De Raedt and M. Frick, Physics Reports **231** (1993) 109

ATOMIC PHYSICS

Observation of Enhanced ECC Cusp Yield at Impact of Metastable Neutral He Projectile

M. Kuzel †, L. Sarkadi, J. Pálinkás, P. A. Závodszy,
R. Maier †, D. Berényi and K. O. Groeneveld †

The cusp peak associated with the ionization of the target (known as electron capture into the continuum, ECC) is well understood theoretically as a singularity caused by the long-range Coulomb interaction between the projectile and the ejected electron. Such a singularity is not expected for bombardment by neutral atoms because of the short range of the completely screened Coulomb potential. Surprisingly, a sharp cusp was observed in an experiment using He^0 projectiles [1]. (The ECC reaction channel was identified detecting the electrons in coincidence with the outgoing He^0 atoms.) To give a theoretical explanation of this unexpected experimental result Barrachina [2] suggested that a modified electron-neutral atom interaction due to the presence of a low-lying virtual resonance state in the electron-projectile system can be responsible for the observation. According to Barrachina a suitable virtual state can be found in the e-He system, when the He core is in a metastable 2^1S excited state. Since a considerable part (25–35%) of the He atoms in the incoming neutral beam is in metastable 2S state, the formation of the above virtual state is very probable.

In the present experiment [3] we investigated the contribution of the metastable fraction of the beam to the ECC cusp in 400 keV He^0 on Ar collisions. The experimental arrangement was similar to those used in our previous investigations [4,5] except that an additional gas cell was applied to change the metastable fraction of the beam by collisional quenching [6]. Detecting coincidences between the electrons and the outgoing He^0 , He^+ , and He^{2+} particles, cross sections for the capture (ECC), the single loss (ELC), and the double loss (DELIC) processes have been determined as a function of the pressure of the quenching gas. For a given reaction channel (labelled by i) the dependence of the effective (i.e., the measured) singly differential cross section on the thickness of the quenching gas (μ) is given by

$$\left(\frac{d\sigma}{d\Omega}\right)_i^{(\text{eff})} = \left(\frac{d\sigma}{d\Omega}\right)_i^0 \frac{1 + R_i \rho \exp[-\mu(\sigma_L^* - \sigma_L^0)]}{1 + \rho \exp[-\mu(\sigma_L^* - \sigma_L^0)]}. \quad (1)$$

Here ρ is the ratio of the number of the metastable and ground-state atoms in the beam entering into the quenching cell. $R_i = \left(\frac{d\sigma}{d\Omega}\right)_i^* / \left(\frac{d\sigma}{d\Omega}\right)_i^0$, where $\left(\frac{d\sigma}{d\Omega}\right)_i^*$ and $\left(\frac{d\sigma}{d\Omega}\right)_i^0$ are cross sections for the cusp production in channel i corresponding to the impact of pure metastable and pure ground-state He atoms, respectively. σ_L^* and σ_L^0 are the corresponding total electron loss cross sections [6]. Fitting the function (1) to the measured cross sections (see Fig. 1) we have got the following values for the metastable-to-ground state cross section ratio (R_i): 3.15, 10.2, and 1.45

for ELC, ECC, and DELC, respectively. The order-of-magnitude enhancement obtained for ECC strongly supports the formation of an intermediate virtual state of the $e\text{-He}(2^1S)$ system.

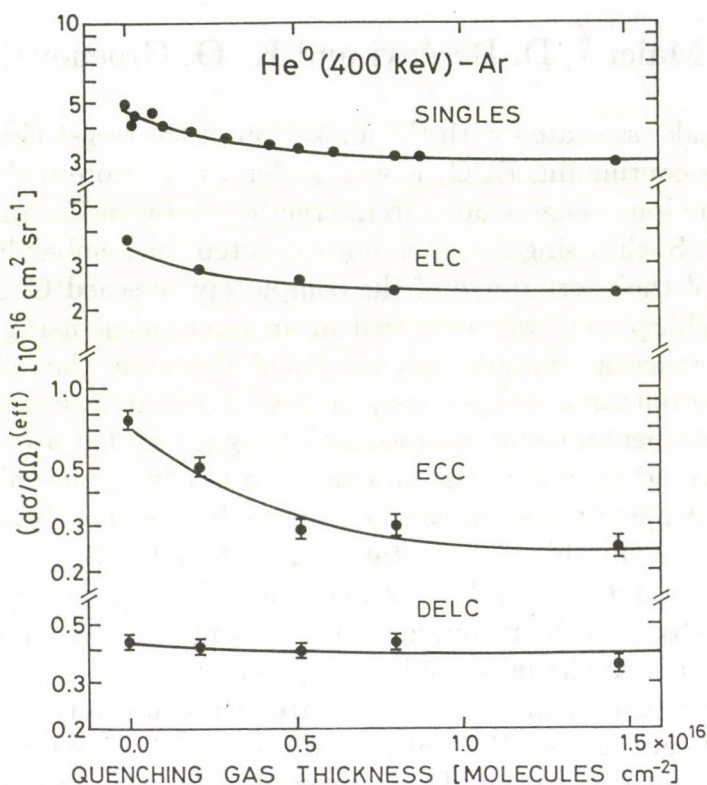


Fig. 1. Singly differential cross sections as functions of the thickness of the quenching gas.

References

- † Institut für Kernphysik der J.W. Goethe-Universität, D-60486 Frankfurt/M, Germany
1. L. Sarkadi, J. Pálinkás, Á. Kövér, D. Berényi, T. Vajnai: *Phys. Rev. Lett.* **62** 527 (1989)
 2. R. O. Barrachina: *J. Phys. B* **23** 2321 (1990)
 3. M. Kuzel, L. Sarkadi, J. Pálinkás, P. A. Závodszy, R. Maier, D. Berényi, K. O. Groeneveld: *Phys. Rev. A* **48** R1745 (1993)
 4. Á. Kövér, L. Sarkadi, J. Pálinkás, D. Berényi, Gy. Szabó, T. Vajnai, O. Heil, K. O. Groeneveld, J. Gibbons, I. A. Sellin: *J. Phys. B* **22** 1595 (1989)
 5. H. Trabold, G. M. Sigaud, D. H. Jakubassa-Amundsen, M. Kuzel, O. Heil, K. O. Groeneveld: *Phys. Rev. A* **46** 1270 (1992)
 6. E. Horsdal Pedersen, J. Heinemeier, L. Larsen, J. V. Mikkelsen: *J. Phys. B* **13** 1167 (1980)

Observation of Collisionally Induced (1s2p2p') $^4P^e$ Shape Resonance of He^-

P. A. Závodszy, L. Sarkadi, L. Víkor[†] and J. Pálinkás

It is well known that He^- exists only in the (1s2s2p) $^4P^o$ state, which is metastable against both autodetachment of electrons and radiative decay. This is a typical example of a long-lived Feshbach resonance (electron bound to an excited state) and has received considerable attention in the past [1] as a strong evidence of correlation between the active electrons.

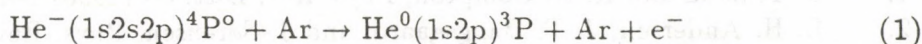
The electron detachment from the simplest negative ion H^- (2s2p) $^1P^o$ was studied using different experimental methods, e.g., e-H scattering, photodetachment, collisions between H^- and rare gases. With the advent of high resolution 0° electron spectroscopy it became possible to measure directly [2] the excitation and decay of the 1P shape resonance of H^- , which lies only 17 meV above the H^0 ($n = 2$) state.

Similar shape resonance exists also in the case of He^- , but until now this was investigated only by photodetachment. The theoretical calculations [3] agree well with the experiments [4] and fix the resonance position at ≈ 10 meV above the He^0 (1s2p) 3P state, with a resonance width of ≈ 7 meV. However, the experimental value of the resonance position depends strongly on the precise determination of the threshold in the photodetachment.

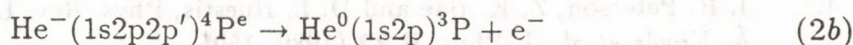
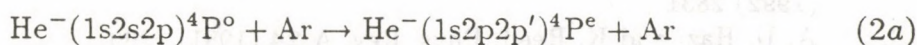
We report here the investigation of single and double electron loss to the continuum (ELC and DELC) processes in He^- on Ar collisions. The He^- ions in the energy range between 25 and 87.5 keV/u were obtained by charge changing collisions from He^+ ions produced with our 1.5 MV VdG accelerator. The experimental setup was similar to that used in our previous investigations [5]. The cusp electrons were measured at 0° in coincidence with the outgoing charge-state selected particles. The relative energy resolution of the electron spectrometer was 0.3%, and the angular acceptance combined with the beam divergence was $\pm 0.8^\circ$. The target pressure was kept low enough to avoid double collisions.

Fig. 1 shows typical electron spectra obtained at 75 keV/u projectile energy. In the ELC spectrum a resonance appears which can be seen on both sides of the cusp (due to the peak-doubling kinematic effect).

The shape of this autodetaching line is generally asymmetric due to the interference between the direct non-resonant detachment process



and that via the resonant $^4P^e$ state



The process

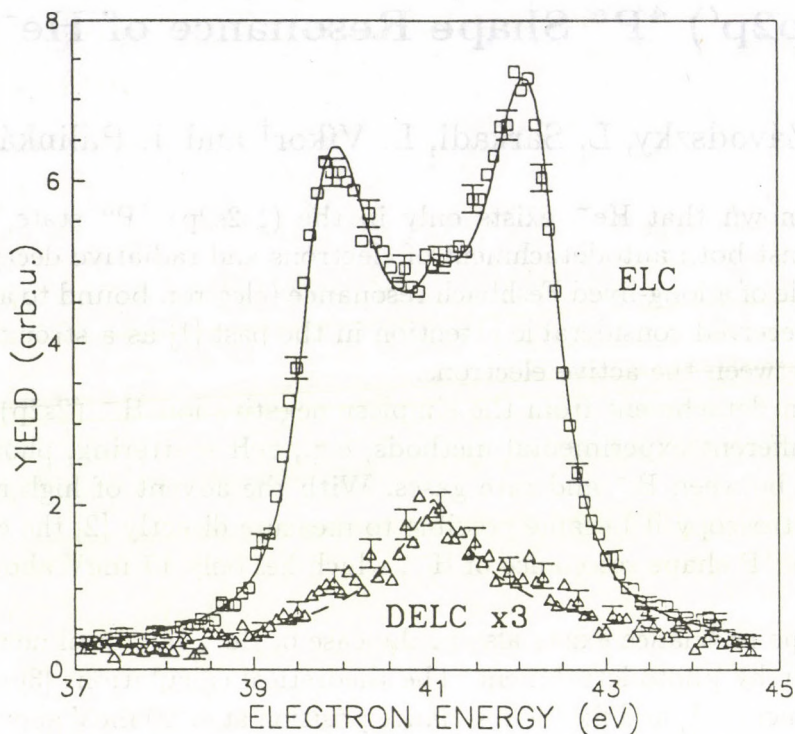


Fig. 1. Energy spectra of cusp electrons for 75.3 keV/u He⁻ impact on Ar. Symbols: □ - ELC, △ - DELC multiplied with factor 3, - - - results of fitting.



contributes also to the non-resonant part of the ELC. The simultaneous loss of two electrons produces the DELC spectrum also seen in Fig. 1. and do not show any structure on the wings of the cusp.

From a fitting of the spectra using a method presented in [6] we obtained the resonance energy and width in the projectile reference frame. This experimental values are in reasonable agreement with the results of the photodetachment measurements [4].

References

- † Permanent address: Institute of Physics, Belgrade, Yugoslavia
1. H. P. Saha and R. N. Compton, *Phys. Rev. Lett.* **64** (1990) 1510
 2. L. H. Andersen, J. P. Bangsgaard, and J. Sørensen, *Phys. Rev. Lett.* **57** (1986) 1558; M. M. Duncan and M. G. Menendez, *Phys. Rev. A* **39** (1989) 1534; F. Penent, J. P. Grouard, J. L. Montmagnon and R. I. Hall *J Phys. B* **24** (1991) 173 and **25** (1992) 2831
 3. A. U. Hazi and K. Reed, *Phys. Rev. A* **24** (1981) 2269
 4. J. R. Peterson, Z. K. Bae and D. L. Huestis, *Phys. Rev. Lett.* **55** (1985) 692
 5. Á. Kövér *et al.*, *J. Phys. B* **22** (1989) 1595
 6. P. A. Závodszy, L. Sarkadi, L. Víkor and J. Pálinkás, submitted to *Phys. Rev. Lett.* (January 1994)

Correlation Effects Observed in Collisional Population and Subsequent Decay of He^{0**} ($2l, 2l'$)

P. A. Závodszy, L. Sarkadi, L. Víkor[†] and J. Pálinkás

The study of electron correlation in high-energy ion-atom collision received considerable interest during the past decade [1]. The advent of high-resolution 0° projectile Auger-electron spectroscopy [2] made possible state-selective studies for a variety of different collision systems. Among the possible applications we shall restrict ourself to present some preliminary results on the study of double electron capture and resonant transfer excitation in $\text{He}^{2+,1+} \rightarrow \text{Ar}$ collisions.

Zouros *et al.* [3] studied the double electron capture in the $\text{He}^{2+} \rightarrow (1s^2)^1\text{S He}^0$ collisions. Their results cannot be explained in the framework of the independent particle model. At the same time the coupled channel calculations of Jain *et al.* [4] including electron correlation effects produce cross sections in agreement with the experimental data [3]. Zouros *et al.* [3] explained the appearance of the $(2s2p)^3\text{P He}^{0**}$ state by double collisions, arguing that spin flip cannot take place in low- Z targets where the spin-orbit interaction is small. Contrary to their results, we found in $\text{He}^{2+} \rightarrow \text{Ar}$ collisions a non-zero probability for the population of the $(2s2p)^3\text{P He}^{0**}$ state even extrapolating to $P = 0$ target pressure. In the Fig. 1 we compare the relative intensity of the $(2s2p)^3\text{P}$ line for excitation, single electron capture + excitation and double electron capture in collisions of He^0 , He^+ and He^{2+} on Ar. The spectra were normalized to equal $(2s^2)^1\text{S}$ line intensity.

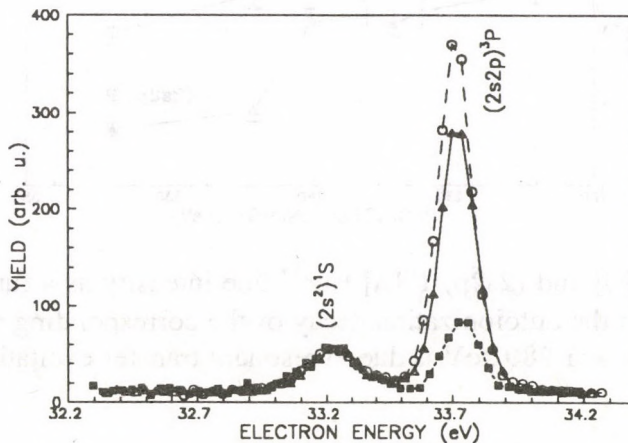


Fig. 1. Electron yield resulted from the autoionization decay of the $(2s^2)^1\text{S}$ and $(2s2p)^3\text{P}$ states of He^{0**} in collision of $\text{He}^{0,1+2+} \rightarrow \text{Ar}$ at 75 keV/u bombarding energy. Symbols: o - He^0 , \blacktriangle - He^+ , \blacksquare - He^{2+} projectile. The spectra are normalized for the $(2s^2)^1\text{S}$ line after background subtraction and transformation in the projectile system.

The highest $(2s2p)^3\text{P}/(2s^2)^1\text{S}$ ratio in the case of He^0 projectile can be understood having in mind that the He^0 beam contains 20-25% $(1s2s)^3\text{S He}^{0*}$ atoms [5] which can be excited easily to the $(2s2p)^3\text{P}$ state. This state can be populated in double electron capture for He^{2+} impact without spin flip if the electrons come from different subshell

of the Ar target. However, the $(2s2p)^3P/(2s^2)^1S$ ratio in the case of He^{2+} projectile is much smaller than in the case of He^+ projectile. A possible explanation of this fact is the repulsion of the two electrons with parallel spin when they are captured in the same time during the population of the $(2s2p)^3P$ state.

Transfer excitation (TE) is a two-electron process involving the transfer of a target electron to the projectile with the simultaneous excitation of a projectile electron, giving rise to a doubly excited state. This state may decay by x-ray emission or autoionization. If the TE is correlated, it is a resonant process (RTE). Formerly the RTE was investigated by detecting the x-rays or Auger electrons [6] for asymmetric ($Z_p > Z_T$, e.g., $\text{O}^{6+} \rightarrow \text{He}$) and symmetric collisions ($\text{He}^+ \rightarrow \text{He}, \text{H}_2$). Here Z_p and Z_T are the projectile and the target nuclear charge, respectively. In Fig. 2. we presented our results for the RTE process in $\text{He}^+ \rightarrow \text{Ar}$ collisions. This case is also asymmetric, but now $Z_p < Z_T$. The resonant character is well pronounced in the case of $(2p^2)^1D$ line and less pronounced in the case of $(2s2p)^1P$ line. The resonance location (≈ 280 keV) is higher than the 261 keV value expected without taking into account the binding energy of the target electron which is transferred during the process.

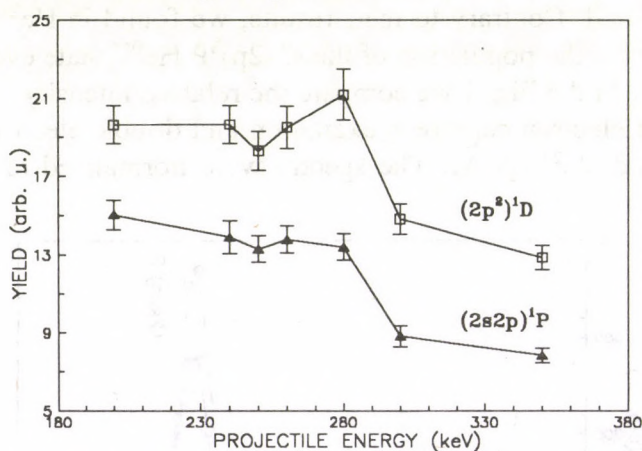


Fig. 2. The $(2p^2)^1D$ [□] and $(2s2p)^1P$ [▲] He^{0**} line intensity as a function of projectile energy resulting from the autoionization decay of the corresponding states in $\text{He}^+ \rightarrow \text{Ar}$ collisions. The hump near 280 keV is due to resonant transfer excitation.

References

- † permanent adress: Institute of Physics, Belgrade, Yugoslavia.
1. N. Stolterfoht, *Spectroscopy and Collisions of Few-Electron Ions*, Bucharest, eds. M. Ivascu, V. Florescu and V. Zoran (World Scientific Singapore 1989) 342
 2. N. Stolterfoht, *Phys. Rep.* **146** (1987) 315
 3. T. J. M. Zouros, D. Schneider and N. Stolterfoht, *Phys. Rev. A* **35** (1987) 1963
 4. A. Jain, C. D. Lin and W. Fritsch, *Phys. Rev. A* **39** (1989) 1741
 5. M. Kuzel, L. Sarkadi, J. Pálinkás, P. A. Závodszky, R. Maier, D. Berényi and K. O. Groeneveld, *Phys. Rev. A* **48** (1993) R1745-R1748
 6. A. Itoh *et al.*, *J. Phys. B* **18** (1985) 4581; J. K. Swenson *et al.*, *Phys. Rev. Lett.* **57** (1986) 3042; T. J. M. Zouros, D. Schneider and N. Stolterfoht, *J. Phys. B* **21** (1988) L671; and *Nucl. Instr. Meth. B* **31** (1988) 349

Production of Low-Energy Electrons by 80 keV O^{8+} Ions

V. L. Plano⁽¹⁾, R. R. Haar⁽¹⁾, J. A. Tanis⁽¹⁾,

L. Sarkadi, P. A. Závodszky, J. Pálinkás, D. Berényi,

M. H. Prior⁽²⁾, H. Khemliche^{(2)*} and D. Schneider⁽³⁾

We have measured the production of low-energy ($\approx 0 - 10$ eV lab) electrons in slow (≈ 4.5 keV/amu) collisions of O^{8+} ions with H_2 , He and Ar targets. This work follows recent related studies [1-3] and has been motivated, in part, by the continuing discussion of the role of electron correlation in multiple electron transfer processes. The measurements were made using the Electron Cyclotron Resonance ion source and associated atomic physics facilities at the Lawrence Berkeley Laboratory 88-inch cyclotron.

Electrons emitted in the forward direction from a biased gas cell were energy analysed by a McPherson spherical sector electron spectrometer equipped with a microchannel plate position-sensitive detector at the exit. Projectile product ions leaving the target region were separated into charge-state components using an electrostatic deflector. The component of interest was detected by a high-rate microchannel plate multiplier, while the O^{8+} beam was collected in a Faraday cup. (In runs searching for electrons in coincidence with no projectile charge change, the attenuated O^{8+} beam was detected with the high-rate multiplier.) Position coordinates of electrons at the spectrometer exit and the arrival times of the selected projectile product ions at the particle multiplier were recorded in event mode by a data collection computer system. Coincident events appeared as a peak in the time (TAC) spectrum. Data were collected for several target gas pressures to ensure that single-collision conditions prevailed.

Total cross sections were measured for single and double capture to bound states by O^{8+} ions in collisions with the H_2 , He and Ar targets. These are of general interest and are needed in the analysis of the coincidence data. By using these targets, cross sections can be compared for different ionization potentials (Ar, $H_2 \approx 15$ eV, He ≈ 24 eV) and varying number of outer shell electrons (Ar = 6, He, $H_2 = 2$).

In related works [2,4], it was found that continuum-electron emission occurs only when accompanied by bound-state capture to the projectile, i.e. no electrons are observed coincident with the O^{8+} projectile charge state. The present measurements for the H_2 and incident He targets confirm these earlier observations as shown in Fig. 1. For the Ar target however the results are more involved. Here, the fraction of electrons coincident with the $O^{8,7,6,5+}$ final projectile states are approximately 0, 30, 20 and 1%, respectively. That is, while essentially no electrons were seen coincident with projectiles which did not undergo bound-state capture, the contributions from the two- and three-electron processes resulting in outgoing O^{7+}

and O^{6+} states are nearly equal. Furthermore, there is a measurable contribution from a four-electron mechanism resulting in the O^{5+} final state.

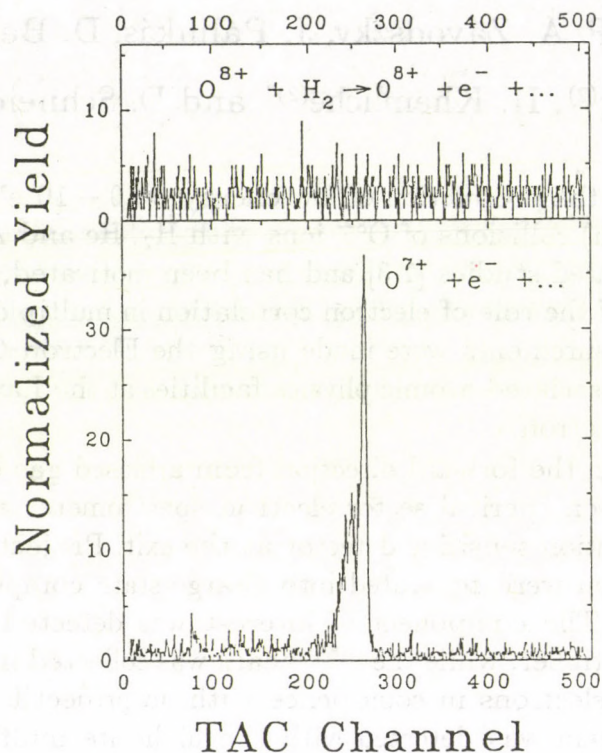


Fig. 1. Time spectra for coincidences between outgoing projectiles and detected continuum electrons for (a) $O^{8+} + H_2 \rightarrow O^{8+} + e^-$ and (b) $O^{8+} + H_2 \rightarrow O^{7+} + e^-$ showing that continuum-electron emission occurs only when accompanied by bound-state capture.

References

- (1) Western Michigan University, Kalamazoo, Michigan, 49008, USA
 - (2) Lawrence Berkeley Laboratory, Berkeley, California 94720, USA
 - (3) Lawrence Livermore National Laboratory, Livermore, California 94550, USA
- * On leave from the Université de Pierre et Marie Curie, Paris, France
1. See, for example, N. Stolterfoht, K. Sommer, J. K. Swenson, C. C. Havener and F. W. Meyer, *Phys. Rev. A* **42** (1990) 5396
 2. J. A. Tanis, D. Schneider, S. Chantrenne, M. H. Prior, R. Herrmann, R. Hutton and G. Schiwietz, *Phys. Rev. A* **42** (1990) 5776
 3. P. A. Závodszky, L. Sarkadi, J. A. Tanis, D. Berényi, J. Pálinkás, V. L. Plano, L. Gulyás, E. Takács, and L. Tóth, *Nucl. Instr. and Meth. B* **79** (1993) 67
 4. J. A. Tanis, R. R. Haar, D. Schneider, M. W. Clark, M. H. Prior, R. D. DuBois and K. Randall, *AIP Conference Proceedings* **274**, (American Institute of Physics, New-York, 1993).

The polarization of the Al $K_{\alpha'}$ x-ray satellite in metal and in sapphire (Al_2O_3)

I. Török, V. P. Petukhov ¹, P. A. Závodszy, J. Pálinkás, and
L. Sarkadi

¹Moscow State University, Institute of Nuclear Physics, 119899 Moscow,
Russian Federation

Although the K x-ray lines are not polarized, some of the KL satellites, where the non-spherical L_3 subshell is involved in the transitions can show significant polarization. (See e. g. [1] and references therein.) This effect, in principle, can depend on chemical environment, and therefore the polarization can be different in pure metals and in their compounds. We started measurements of the polarization of the $K_{\alpha'}$ satellite line of Al in metal and in oxide (sapphire, $\alpha-Al_2O_3$).

We used 3.2 MeV He^+ -ions and 1 MeV proton projectiles at the Van de Graaff accelerator in ATOMKI [2-4]. A Soller-type (flat crystal) x-ray polarimeter [5] was used for taking spectra. The evaluation of all spectra was performed by using the EWA code [6]. The peak shapes were approximated by Gaussians with independent left and right exponential tails. The nominal energies of the distinct satellite features ($K_{\alpha'}$, K_{α_3} , K_{α_4} , ...) were used in the fitting, taking into account also the chemical shifts [7,8].

For both target materials, and for both measuring positions (i. e. parallel and perpendicular relative to the incoming ion beam) the intensities of the satellite features were determined relative to the K_{α_1} peak, which is assumed to be unpolarized.

The degree of polarization (P) was calculated from these relative intensities. The obtained linear polarization values are listed in Table 1.

projectile		P	
particle	energy	for the metal	for the oxide
He^+	3.2 MeV	0.52 ± 0.15	0.22 ± 0.12
p	1.0 MeV	0.41 ± 0.10	0.39 ± 0.10

Table 1. The polarization fractions (P) obtained from present measurements.

A new evaluation of our He⁺-ion induced x-ray spectra gave similar results, as the one described in [3]. The polarization fraction of the x-rays obtained from oxide is about half of that from the metal. The spectra induced by 1 MeV protons - although they are taken at about the same projectile velocity as the He⁺-ion induced ones - does not show this large difference in the polarization fractions, obtained from spectra of metal and oxide. The reason may be the higher multiple ionization in the case of the heavier projectile.

This work was supported by OTKA (Hungarian National Scientific Research Foundation), Grant: No. 3011.

References

1. B. Cleff, Acta Phys. Pol. **A61** (1982) 285.
2. V. P. Petukhov, I Török, P. Závodszky, J. Pálinkás, L. Sarkadi, ATOMKI Ann. Rep. 1991 (1992) 71.
3. V. P. Petukhov, I. Török, P. Závodszky, J. Pálinkás, L. Sarkadi, S. M. Blokhin, Nucl. Instrum. Meth. **B75** (1993) 17.
4. V. P. Petukhov, I. Török, P. Závodszky, J. Pálinkás, L. Sarkadi, S. M. Blokhin, ATOMKI Ann. Rep. 1992(1993) 55.
5. V. P. Petukhov: Prib. Tech. Expt., No.1, p. 195 (1990) (*in Russian*)
6. J. Végh: Thesis, 1990, ATOMKI, Debrecen.
7. Y. Cauchois, C. Senemaud: *Wavelengths of X-ray emission lines and absorption edges*, Pergamon Press, Oxford, etc., 1978.
8. M. O. Krause, J. G. Ferreira, J. Phys. B: Atom. Molec. Phys. **8** (1975) 2007.

Projectile	Energy	for the metal	for the oxide
He ⁺	2.3 MeV	0.8210	0.2830
p	1.0 MeV	0.4100	0.2830

Table I. The polarization fraction (P) obtained from present measurements.

The manganese $KL_{2,3}L_{2,3}$ Auger spectrum excited by bremsstrahlung

A. Némethy, L. Kövér, I. Cserny and D. Varga and P.B. Barna[†]

[†]Research Institute for Technical Physics of the Hungarian Academy of Sciences, Budapest

In a previous study the manganese K-Auger spectra from ^{55}Fe decay were examined by Kovalik et al¹. Following the electron capture decay of ^{55}Fe , a K-shell vacancy is produced and an outer electron finds itself excited to an unoccupied state, while the atom remains neutral. Photoionization, however, yields a final state of a positive ion with a core hole, the creation of which is accompanied with similar electronic rearrangement processes. The differences concerning the ionization/excitation processes in the two cases can be reflected in the respective Auger spectra as well, e.g. in different transition energy values or in appearance of various satellite lines.

In the present study the Mn $KL_{2,3}L_{2,3}$ Auger transitions were excited by using Mo bremsstrahlung. Manganese films of 10 nm thickness were evaporated onto Si wafer substrates in vacuum and were cleaned and thinned in situ prior measurements by argon ion sputtering. The Auger spectra were measured by a high luminosity electron spectrometer^{2,3} using an energy resolution of $3 \cdot 10^{-4}$. Evaluating the spectra, peaks were fitted by Voigtians with inelastic tails⁴ applying a Tougaard type⁵ inelastic background. For estimating the respective total shake probabilities, relativistic Dirac-Fock-Slater wavefunctions and sudden approximation were used⁶.

An overall agreement can be seen between the respective relative energy values from the different experiments^{7,8}. In spite of the better resolution used, no satellite line can be identified at the low energy side of the Mn KL_2L_3 (1D_2) peak in the present measurement (Fig. 1) opposing to the result of A. Kovalik et al¹. This difference in the result of the two experiments cannot be attributed to the different atomic excitation probabilities on the basis of the calculated values presented in the Table 1. It can be due, however, to chemical effects because the measured energy value of the Mn KL_2L_3 (1D_2) line in MnO is in agreement with that obtained from the previous measurement¹ (Table 2). This assumption is supported also by the fact that in the MnO spectrum mentioned an extra peak can be identified at the low energy side of the main line in a distant of 7.9 eV (Table 2).

Table 1 Total shake probabilities(%) for 1s photoionization of Mn and 1s electron capture of ^{55}Fe

Process	Present work	Ref. 9	Ref. 10
Photoionization: $(1s)^1 \dots (3d)^5$	26.64	33.10	-
Electron capture: $(1s)^1 \dots (3d)^6$	0.51	0.68	0.38

Table 2 Mn KL_{2,3} (¹D₂) Auger energies

	Experiment					Theory			
	Present work			Ref. 1		Pres. work [†]	Ref. 11 [†]	Ref. 12 [†]	Ref. 13 [†]
	Metallic Mn	MnO	Extra Peak in MnO	"Metallic" Mn	Extra Peak				
Energy (eV)	5208.2 (8)	5203.3 (10)	5195.4 (10)	5202.5 (25)*	5194.3 (25)* 5195.5 (25)*	5192.41 5212.1*	5202.8*	5191.7	5195.71

[†]Calculations for free atoms

*Auger transition following electron capture

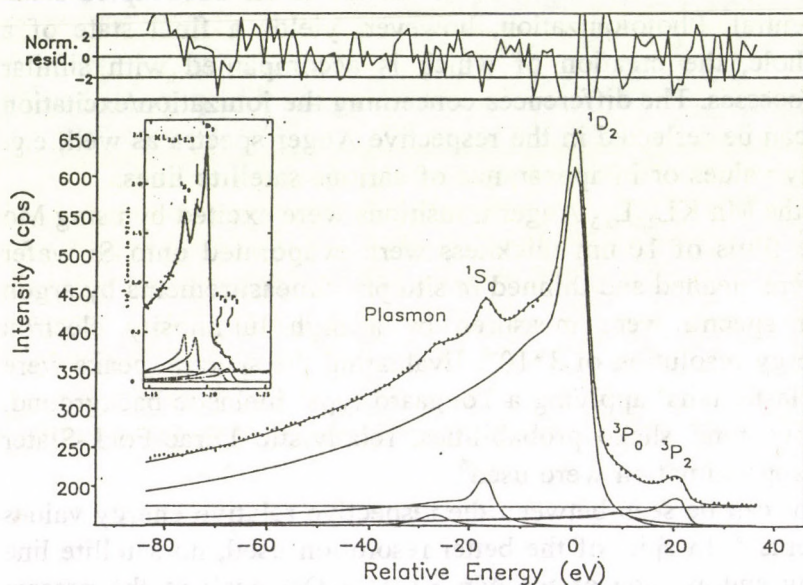


Figure 1

Photoexcited Mn KL_{2,3}L_{2,3} Auger spectrum from the present work with a resolution of 1.3 eV, compared to the measured spectrum¹ following electron capture (insert) with a resolution of 2.2 eV.

References

- 1 A. Kovalik, V. Brabec, J. Novák, O. Dragoun, V. M. Gorozhankin, A. F. Novgorodov and Ts. Vylov, *J. Electron Spectrosc. and Rel. Phenom.*, **50** (1990) 89
- 2 L. Kövér, D. Varga, I. Cserny, J. Tóth and K. Tőkési, *Surface and Interface Anal.* **19** (1992) 9
- 3 L. Kövér, D. Varga, I. Cserny, J. Tóth and K. Tőkési, to be published
- 4 J. Végh, PhD. Thesis (1990) Kossuth University of Debrecen
- 5 S. Tougaard, *Surface and Interface Anal.* **11** (1988) 453
- 6 T. Mukoyama and K. Taniguchi, *Bull. Inst. Chem. Res., Kyoto Univ.*, **70** (1992) 1
- 7 A. Némethy, L. Kövér, I. Cserny, D. Varga and P. B. Barna, X'93 Conference. Debrecen 1993, Book of Abstracts, 340 (1993)
- 8 A. Némethy, L. Kövér, I. Cserny, D. Varga and P. B. Barna, to be published
- 9 E. Arndt, G. Brunner and E. Hartmann, *J. Phys. B* **15** (1982) L887
- 10 B. Crasemann, M. H. Chen, J. P. Briand, P. Chevallier, A. Chetioui and M. Tavernier, *Phys. Rev. C* **19** (1979) 1042
- 11 L. Bandurina, O. Zatsarinny, A. Lengyel, E. Yu Remeta, X'93 Conference. Debrecen 1993, Book of Abstracts, 286 (1993)
- 12 F. P. Larkins, *Atomic Data and Nucl. Data Tables* **20** (1977) 311
- 13 S. T. Perkins, D. E. Cullen, M. H. Chen, J. H. Hubbel, J. Rathkopf, J. Scofield, *Tables and Graphs of Atomic Subshells and Relaxation Data Derived from the LLNL Evaluated Atomic Data Library (EADL), Z=1-100*, Lawrence Livermore National Laboratory, Livermore, CA, UCRL-50400, Vol. 30 (1991)

Local electronic structures reflected in the P K-Auger spectra of phosphorus oxyanions

L. Kövér, A. Némethy, I. Cserny, and H. Adachi*

*Dept. of Metallurgy, Kyoto University, Yoshida-honmachi, Kyoto 606, Japan

Core-valence X-ray and Auger spectra are containing unique information on the local electronic structure surrounding the core-ionized atom. Site specific local density of valence electron states (LDOS) can be obtained from the lineshapes of the respective Auger transitions involving valence band holes in the final state¹. Correlation of final state vacancies and core hole screening can influence strongly the core-valence Auger lineshapes².

The structure of the K_{β} and $L_{2,3}$ X-ray-, as well as the LVV Auger and XPS spectra of P in different phosphorus oxyanions, having a common tetrahedral (T_d) symmetry, were studied previously^{3,4,5} and a relatively small interaction was suggested between the phosphate anion and the respective cation, as a consequence of the strong group localization of valence states over the tetrahedron cluster.

High energy Mo X-ray excited Auger spectra of Na_3PO_4 , Li_3PO_4 and $(NaPO_3)_n$ polycrystalline powder samples were obtained by using a high energy electron spectrometer^{6,7} (with an energy resolution of $2.6 \cdot 10^{-4}$). The vacuum was $5 \cdot 10^{-7}$ Pa during measurements. Energy calibration of the electron spectra was performed in the XPS region with the aid of polycrystalline Cu and Ag samples⁸ applying a linear extrapolation for higher energies. Corrections for charging effect were made by using the C 1s line from the surface hydrocarbon¹⁰. Metal samples and single crystal GaP were cleaned before measurement by argon ion sputtering. For calculating the LDOS for PO_4^{3-} , a DV- $X\alpha$ cluster⁹ molecular orbital model was applied, taking into account of the presence of a final state core hole, using a T_d symmetry¹⁰. The core-core valence Auger intensity distributions were calculated using the "final state rule"¹¹ and the respective atomic matrix elements¹⁰, applying an additional broadening to the theoretical spectra when comparing to the experimental ones.

The measured P KLL Auger spectra of the phosphates are rather similar, while in the case of the metaphosphate besides a larger chemical shift the 1D_2 line is narrower. The general features of the experimental P KLV spectra reflect the dominance of the effect of the common T_d symmetry, similarly to the previous results^{3,4,5}. In Fig 1 the Li_3PO_4 Mo X-ray excited KLV Auger spectra is compared to the result of our calculation, based on the semiempirical approximation described above. For the $KL_1V/KL_{2,3}V$ Auger intensity ratio, the theoretical value¹² from Table 1 was used. The relatively good agreement between the experimental and theoretical spectra demonstrates, that by using a simple model including LDOS obtained from MO cluster calculations and atomic Auger transition probabilities, the main structure of the KLV Auger spectra of phosphates can be explained.

In most cases the measured molecular KLV Auger intensity ratios (Table 1) agree well with those for free atoms obtained from the theory¹² (except for the $KL_1V(S)/KL_{2,3}V(P)$ ratio. The measured $KL_{2,3}V(S)/KL_{2,3}V(P)$ ratios are sensitive to

cations or superstructure, showing an order of magnitude drop, for the GaP. Large chemical effects and disagreement with atomic theory can be observed in the case of the KL_2L_3/KL_2L_2 ratios. Concerning the P K-Auger transition energies (Table 2) the atomic theory fails to give a good approximation for the measured KLM energies, while these show a strong dependence on the chemistry.

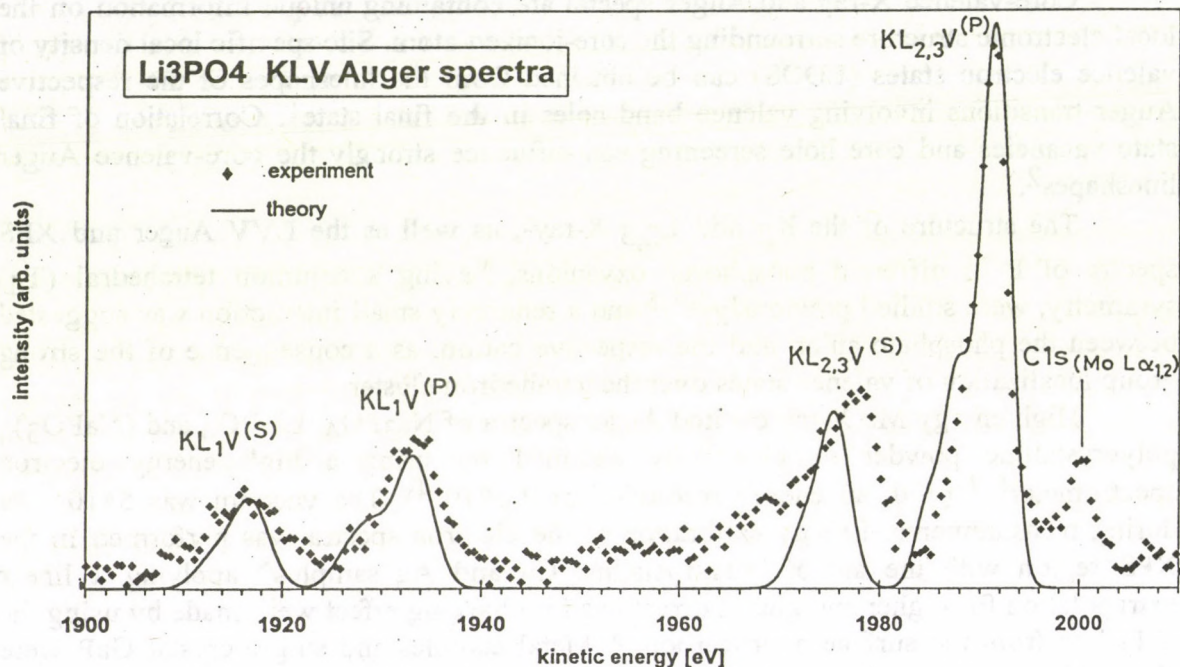


Figure 1 Calculated P KLV Auger spectra of Li_3PO_4 (solid line) in comparison with the respective experimental results (diamonds).

Table 1: P K-Auger intensity ratios

	KL_2L_3/KL_2L_2	KL_1V/KL_2L_3	$KL_{2,3}V/KL_2L_3$	$KL_1V/KL_{2,3}V$	$KL_1V^{(S)}/KL_1V^{(P)}$	$KL_{2,3}V^{(S)}/KL_{2,3}V^{(P)}$
Li_3PO_4	14.13	0.064	0.203	0.315	0.769	0.636
Na_3PO_4	15.28	0.072	0.214	0.336	0.790	0.468
$(NaPO_3)_n$	5.88	0.056	0.192	0.292	0.718	0.532
GaP	5.90	0.051	0.298	0.172	0.616	0.077
Red P ¹³	9.09	-	-	-	-	-
P ¹⁴ (theory) [*]	25.29	0.068	0.176	0.385	1.570	0.502

$KL_1V^{(S)}=KL_1M_1$; $KL_1V^{(P)}=KL_1M_{2,3}$; $KL_{2,3}V^{(S)}=KL_{2,3}M_1$; $KL_{2,3}V^{(P)}=KL_{2,3}M_{2,3}$
^{*}for isolated, neutral atom

Table 2: P K-Auger transition energies (eV)

	KL ₂ L ₂ (¹ S ₀)	KL ₂ L ₂ (¹ D ₂)	KL ₁ M ₁	KL ₁ M _{2,3}	KL _{2,3} M ₁	KL _{2,3} M _{2,3}
Li ₃ PO ₄	1843.2 (0.5)	1850.4 (0.2)	1925.3 (0.5)	1941.7 (0.2)	1983.8 (0.3)	1999.0 (0.2)
Na ₃ PO ₄	1844.0 (0.4)	1851.0 (0.2)	1924.5 (0.8)	1941.9 (0.7)	1983.6 (0.5)	1999.6 (0.2)
(NaPO ₃) _n	1841.9 (0.4)	1849.2 (0.2)	1926.5 (0.5)	1940.9 (0.5)	1982.6 (0.3)	1998.1 (0.2)
Red P ¹³	1849.6 (0.4)	1857.3 (0.2)	1938.0 (3.0)	1949.0 (3.0)	1996.0 (3.0)	2006.0 (1.0)
P ¹⁴ (theory)*	1852.1	1853.1	1926.0	1934.9	1974.1 1975.0	1982.9 1983.9
P ¹⁵ (theory)*	1839.4	1845.1	-	-	-	-

*for isolated, neutral atom

References

1. D.E. Ramaker, Crit. Rev. in Solid State and Mater Sci., **17**, 211 (1991).
2. Yu.N. Kucherenko, J. Electron Spectrosc. Relat. Phenom., **53**, 39 (1990).
3. K. Taniguchi, Bull. Chem. Soc. Japan, **57**, 909 and 915 (1984).
4. M.K. Bernett, J.S. Murday and N.H. Turner, J. Electron Spectrosc. Relat. Phenom., **12**, 375 (1977)
5. H. Adachi and K. Taniguchi, J. Phys. Soc. of Japan **49**, 1944 (1980).
6. L. Kövér, D. Varga, I. Cserny, J. Tóth and K. Tőkési, Surf. Interface Anal. **19**, 9 (1992)
7. D. Varga, L. Kövér, I. Cserny, J. Tóth and K. Tőkési, to be published
8. M.P. Seah, G.C. Smith and M.T. Anthony, Surf. Interface Anal. **15**, 293 (1990)
9. H. Adachi, M. Tsukada and C. Satoko, J. Phys. Soc. Jpn. **42**, 875 (1978).
10. L. Kövér, A. Némethy, I. Cserny, A. Nisawa, Y. Ito and H. Adachi (accepted for publication in the Surface and Interface Anal.)
11. E. Tillmanns and W.H. Baur, Acta Cryst. **827**, 2124 (1971).
12. D.E. Ramaker, F.L. Hutson, N.H. Turner and W.N. Mei, Phys. Rev. B **33**, 2574 (1986)
13. M. Schärly and J. Brunner, Z. Phys. B-Condensed Matter **42**, 285 (1981).
14. S.T. Perkins, D.E. Cullen, M.H. Chen, J.H. Hubbel, J. Rathkopf and Scofield, Tables and Graphs of Atomic Subshells and Relaxation Data Derived from the LLNL Evaluated Atomic Data Library (EADL), Z=1-100, Lawrence Livermore National Laboratory, Livermore, CA, UCRL-50400, Vol. **30** (1991).
15. F. P. Larkins, At. Data and Nucl. Data Tables **20**, 311 (1977)

Observation of K-shell Compton effect in silicon with Si(Li) detector as a live-target

G. Kalinka

As Compton effect takes place primarily on loosely bound outer valence and conduction electrons, it is applicable to investigation of materials' structure as a method called Compton profile determination [1-3]. The contribution of inner shell electrons [4], though relatively weak, may adversely influence the accuracy of such measurements, but can be advantageous as well, for example providing a complemter means of XANES and/or EXAFS for low binding energy K and L shells, where they are difficult to implement. Knowledge of inner shell effects is important also from the point of view of X-ray absorption of and transport in materials.

The energy resolution ΔE of semiconductor detectors scales as $\propto \sqrt{E}$, whereas the Compton shift as $\propto E_i$, this is one of the reasons why Compton profile measurements are usually made with high energy γ rays. In practice the lowest energy used in conjunction with semiconductor detectors is $E_i \approx 60$ keV (γ from ^{241}Am , or $\text{WK}_{\alpha 1}$ X-ray [5]). In this case the scattered photon energy fall in the $E_f \approx \{49, 60\}$ keV range, where a Si(Li) detector has a typical resolution of ≈ 400 eV. Correspondingly, the recoiled electrons are distributed in the $\varepsilon \approx \{0, 11\}$ keV range, with an expected jump at $E_{\text{SiK}ab} = 1.838$ keV due to the onset of K-shell Compton scattering, i.e. the process when the energy transferred to a K-shell electron exceeds its binding energy. Since a small sized Si(Li) detector is to large extent transparent to scattered photons and the energy resolution is ≈ 100 eV in this energy range, the effect can be nicely observed with the detector itself as a live-target as shown in Fig. 1.

The measured (single) Compton recoil electron spectrum $C(\varepsilon)$, can be described with the formalism developed by Seltzer [6] in the following modified form:

$$C(\varepsilon) = \int_0^\pi n(\varepsilon, \Theta) \left[\frac{d\sigma}{d\Omega}(\Theta) \right]_{KN} G(r, w, \Theta) 2\pi \sin \Theta d\Theta, \quad (1)$$

where $[d\sigma/d\Omega]_{KN}$ indicates the Klein-Nishina cross section, G is a geometrical escape factor depending on detector radius r , thickness w and scattering direction Θ , n is the available, effective scattering electron density :

$$n(\varepsilon, \Theta) = \frac{\rho N_A}{A} \frac{dp_z}{d\varepsilon}(\varepsilon, \Theta) \sum_i^{\varepsilon > E_{iab}} n_i J_i(p_z(\varepsilon, \Theta)), \quad (2)$$

where ρ , N_A and A are the density, Avogadro's number and atomic mass respectively, p_z is the projection of the initial electron momentum \mathbf{p} parallel to the scattering vector, n_i is the number of electrons in the i th shell, E_{iab} is the binding energy, and J_i is the corresponding Compton profile :

$$J_i(p_z) = \int_0^\infty \int_0^\infty n_i(\mathbf{p}) dp_x dp_y. \quad (3)$$

References

1. B.G. Williams, ed.: Compton Scattering, McGraw-Hill, 1977
2. M.J. Cooper, Adv. Phys. **20**(1971)453
3. M.J. Cooper, Rep. Prog. Phys. **48**(1985)415
4. P.P. Kane, Phys. Rep. **218**(1992)67
5. S. Manninen, V. Honkimäki and P. Suortti, J. Appl. Cryst. **25**(1992)268
6. S.M. Seltzer, Nucl. Instr. Meth. **188**(1981)133

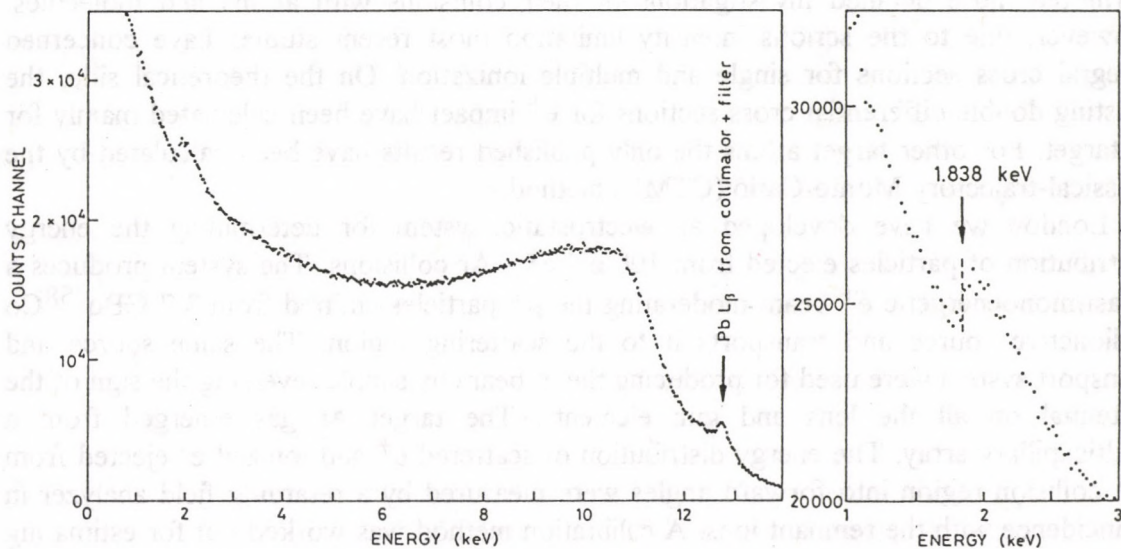


Fig. 1. Compton recoiled electron spectrum of 59.536 keV γ rays from ^{241}Am measured with a Si(Li) detector.

Doubly Differential Cross-Sections For Particles Ejected From Ar by Positron and Electron Impact

Á. Kövér, G. Laricchia† and M. Charlton †

† Department of Physics and Astronomy, University College London, UK

Comparing scattering processes at positron (e^+) and electron (e^-) impact allows us to separate the effects of varying the sign of the projectile charge while keeping other collision parameters (e.g. projectile mass) constant. Furthermore e^+ - atom collisions can provide valuable insights into the dynamics of the process since, unlike the situation for e^- impact, the projectile and the ionized electron are distinguishable.

In the last decades progress in producing low energy quasi-monoenergetic e^+ beams has permitted more detailed investigations of their collisions with atoms and molecules. However, due to the serious intensity limitation most recent studies have concerned integral cross sections for single and multiple ionization. On the theoretical side, the existing double differential cross sections for e^+ impact have been calculated mainly for H target. For other target atoms the only published results have been calculated by the classical-trajectory-Monte-Carlo (CTMC) method.

In London we have developed an electrostatic system for determining the energy distribution of particles ejected from 100 eV e^\pm - Ar collisions. The system produces a quasi-monoenergetic e^+ beam moderating the β^+ particles emitted from 3.7 GBq ^{58}Co radioactive source and transports it to the scattering region. The same source and transport system were used for producing the e^- beam by simple reversing the sign of the potential on all the lens and gun elements. The target Ar gas emerged from a multicapillary array. The energy distribution of scattered e^+ and ionized e^- ejected from the collision region into forward angles were measured by a retarding field analyzer in coincidence with the remnant ions. A calibration method was worked out for estimating the absolute double differential cross sections.

At 30° and 45° the energy distributions of both outgoing particles (e^+ and e^-) were determined for 100 eV e^+ impact on Ar [1]. Furthermore the secondary e^- distribution were also recorded at 100 eV e^- impact and found to be in agreement with the data of DuBois and Rudd [2]. Figure 1 shows the scattered e^+ and ejected e^- spectra at 100 eV e^+ impact at 30° . The results of the CTMC calculation [3] are also indicated. The agreement between experimental and theoretical data for the ejected e^- is good. The shape of the experimental scattered e^+ spectrum, however, does not follow the theoretical prediction.

Recently Schmitt *et al* [4] compared the angular distribution of secondary e^- emitted at the specific energy of 15 eV for both e^+ and e^- projectiles at 100 eV impact and have found significant differences at the forward angles for the two projectiles, with cross sections for e^+ exceeding those for e^- . Our data, however, suggest a ratio much less than that found by Schmitt *et al* [4], although the large uncertainties on the ratios inhibit a definitive conclusion.

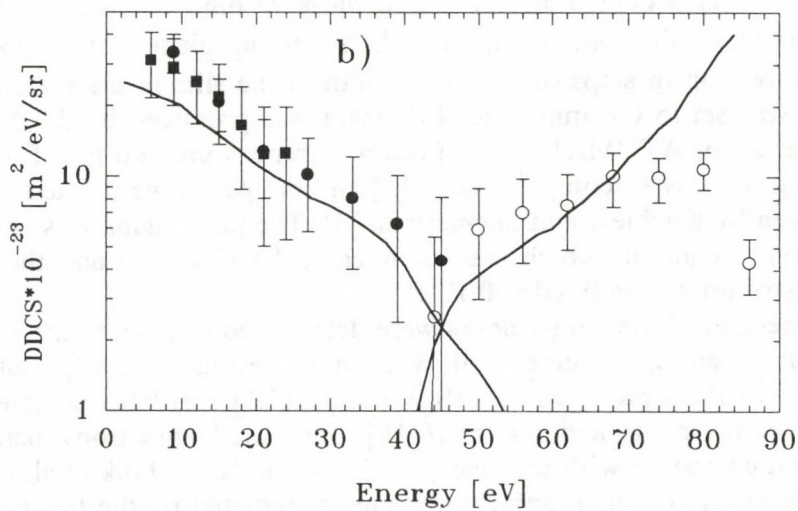
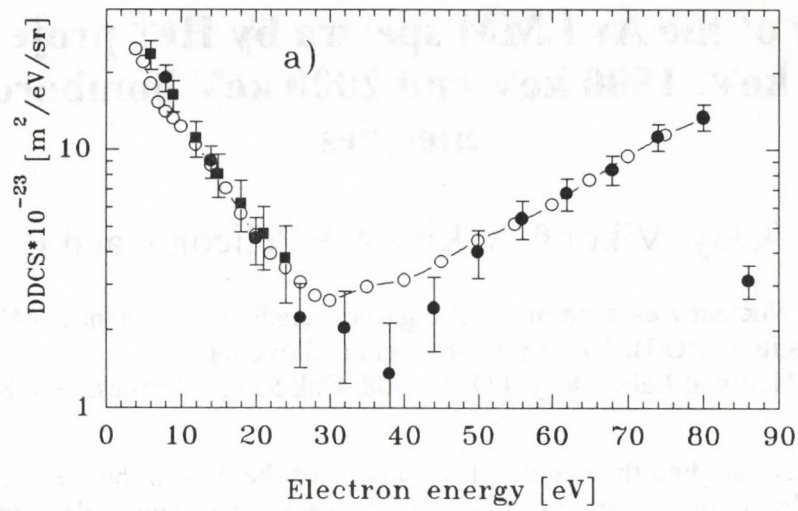


Figure 1. Double differential cross section of ejected e^- and scattered projectile as a function of the energy at 30° for 100 eV e^- (a) and e^+ (b) impact. Symbols:(a) \blacksquare, \bullet : measured DDCS of e^- particles in coincidence with Ar^+ ions; \circ : DDCS data of Dubois and Rudd [2], (b) \blacksquare, \bullet : measured DDCS of ejected e^- particles in coincidence with Ar^+ ions; \circ : measured DDCS of scattered e^+ particles in coincidence with Ar^+ ions. -- :CTMC calculation by Sparrow and Olson [3]

References:

- [1] Á. Kövér, G. Laricchia and M. Charlton, submitted to J.Phys. B. At. Mol.Opt.Phys.
- [2] R. D. DuBois and M.E. Rudd, Phys. Rev. A17 (1978) 843.
- [3] R. A. Sparrow and R. E. Olson 1993 private communication and to be published
- [4] A. Schmitt, U.Cerny, H.Möller, W.Raith and M. Weber submitted to Phys. Rev. Lett.

Study of the Ar LMM spectra by He⁺ projectile at 1250 keV, 1500 keV and 2000 keV bombardment energies

L. Tóth ^a, Gy. Víkor ^a, S. Ricz ^a, P. Pelicon ^b and R. Miller ^c

^a Institute of Nuclear Research of the Hungarian Academy of Sciences (ATOMKI)

^b J. Stefan Institute, P.O.B. 100, Ljubljana 61111, Slovenia

^c Oak Ridge National Laboratory, P.O.B. 2008, Oak Ridge, Tennessee 37831, USA

We have studied the angular distributions of the PCI in the He⁺-argon collision, where the velocity of projectile was close to the velocity of Auger-electron.

The measurements were performed on the ESA-21 triple stage electrostatic spectrometer [1]. This device allows one to measure high resolution electron spectra simultaneously at 13 observation angles in the scattering plane from 0° to 180° relative to the beam direction in steps of 15°. The width of the slits in the second stage of the spectrometer was set to 0.6 mm. The He⁺ beam was produced by the 5 MeV Van de Graaff accelerator of ATOMKI. Typical beam currents were 200 nA. The spectra were analyzed using the EWA computer code [2] and the peaks were fitted an asymmetric line shape given by Kuchiew and Sheinerman [3]. The peak shape was convoluted with the spectrometer function, which was assumed to be Gaussian and the width of the Lorentzian distribution was fixed at 0.12 eV.

The energies of the Auger peaks were determined relative to the L₃M^{2,3}(¹D₂) line and relative energies agree well with other results [4-6,10], but the relative intensities of five isotropic L₂M^{2,3}(¹S₀), (¹D₂), (³P_{0,1,2}) lines deviate significantly from other measurements and theory [6-10]. Evaluated anisotropy parameters were determined and compared with the theory of Sizov and Kabachnik et al. [11-13]. In the measured energy region the alignment parameter predicted by the theory of Sizov and Kabachnik [13] is close to zero. Our experiment confirm this prediction [10].

The main reason for performing the present experiment was to measure the shape of the Auger line in the region where the speed of the receding ion is close to the speed of Auger electrons. The speed of LMM Auger electron of argon corresponds to approximately 1494 keV He⁺ impact. Thus, we choose 1250 keV, 1500 keV and 2000 keV impact energies. The measured angular dependencies of the energy shifts produced by the PCI process are presented in Fig. 1. The theory of Barrachina and Macek [14] could reproduce the measured data in forward direction. In this measurement, a slight enhancement was observed in the backward direction, as it was observed by Takács et al., [15]. The measured energy shifts are higher than the calculated ones in the backward direction. One can see that the energy shift is systematically higher in the 1.25 MeV and 1.5 MeV He⁺-Ar collision compared to 2.0 MeV in backward directions. The higher energy shift can be interpreted as a post collision interaction between the Auger- and loss electron in the backward direction in both cases.

Acknowledgment

This work was supported by the Hungarian National Science Found (OTKA No. 3011) and Research Found of the Sciences (AKA No. 1-300-2-91-0-790).

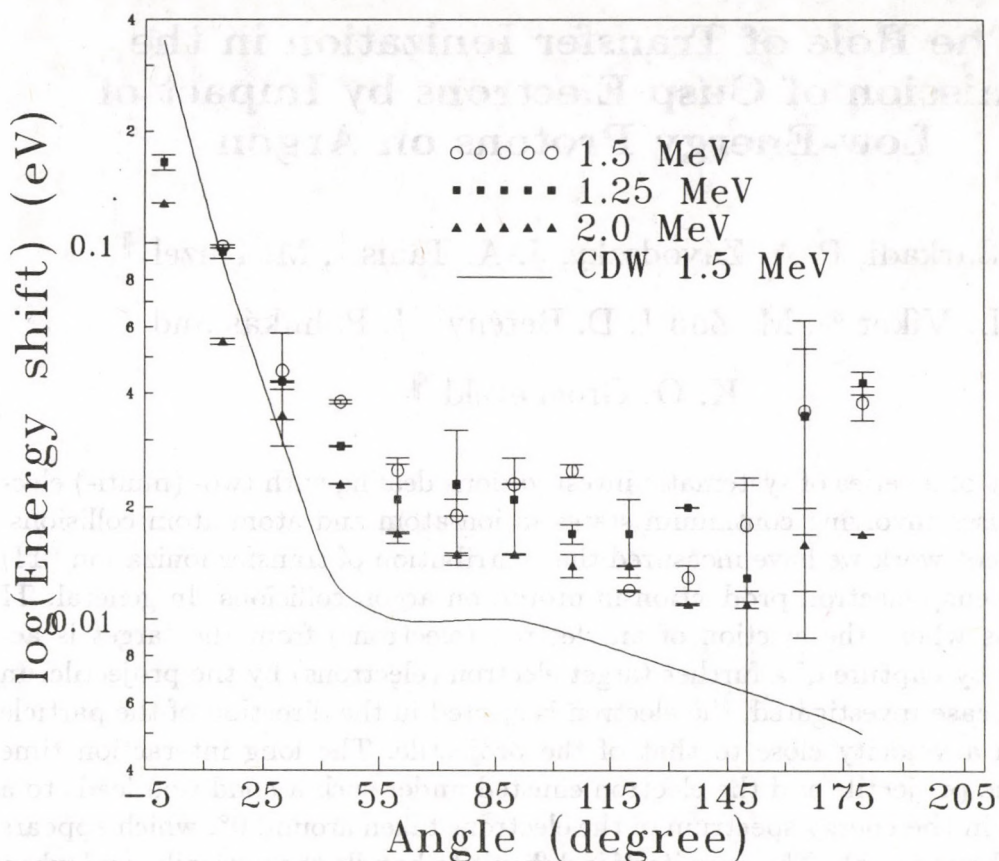


Fig. 1. The angular dependence of the energy shift produced by the PCI process. The solid line presents the theoretical results of Barrachina and Macek [14] for the case of 1500 keV ion energy.

References

- [1] A. Kövér *et al.*, J. Phys. B **16** (1983) 1017.
- [2] J. Végh, Thesis, ATOMKI (1990), *unpublished*.
- [3] M. Yu. Kuchiev and S. A. Sheinermann, Sov. Phys.-JETP **63** (1986) 986.
- [4] W. Mehlhorn, Z. Naturforsch. **23a** (1968) 287.
- [5] L. Asplund, Phys. Scripta **16** (1977) 268.
- [6] Ch. E. Moore, Atomic Energy Levels Vol. 1-3, Nat. Bureau of Standards Circular 467 (1949/52) and NSRDS-NBS 35 (1971)
- [7] D. Ridder, Thesis, Freien Universität Berlin (1977).
- [8] D. Ridder, J. Dieringer and N. Stolterfoth, J. Phys. B **9** (1976) L307
- [9] W. N. Assad and W. Mehlhorn, Z. Phys. **271** (1968) 304.
- [10] L. Tóth *et al.*, Nucl. Instr. and Meth. in Phys. Res. B **99** (1994) *in press*
- [11] N. M. Kabachnik, J. Phys. B **24** (1991) 2249.
- [12] N. M. Kabachnik, J. Phys. B **22** (1988) 267.
- [13] V. V. Sizov and N. M. Kabachnik, J. Phys. B **13** (1980) 1601
- [14] R. O. Barrachina and Macek, J. Phys. B **22** (1989) 2151.
- [15] E. Takács *et al.*, J. Phys. B **24** (1991) L381.

The Role of Transfer Ionization in the Emission of Cusp Electrons by Impact of Low-Energy Protons on Argon

L. Sarkadi, P. A. Závodszky, J. A. Tanis[†], M. Kuzel[¶],

L. Víkor[§], M. Zhu[†], D. Berényi, J. Pálinkás and

K. O. Groeneveld[¶]

As part of a series of systematic investigations dealing with two- (multi-) electron processes involving continuum states in ion-atom and atom-atom collisions, in the present work we have measured the contribution of transfer ionization (TI) to forward cusp-electron production in proton on argon collisions. In general, TI is a process where the ejection of an electron (electrons) from the target is accompanied by capture of a further target electron (electrons) by the projectile. In the special case investigated, the electron is ejected in the direction of the particle beam with a velocity close to that of the projectile. The long interaction time between the projectile and the electron emitted under such a condition leads to a singularity in the energy spectrum of the electrons taken around 0° , which appears as a cusp-shaped peak. The cusp itself is difficult to handle theoretically, and when it is accompanied with further processes like capture of an electron (electrons) by the projectile, it represents an even more serious challenge for theory. At the same time, the study of processes where two or more electrons are activated may reveal important information about the possible role of dynamical electron correlations in ion-atom collisions.

In our previous investigations on the same subject, He [1] and heavier ions [2] were used as projectiles; here we chose protons. The case of proton impact has a special importance mainly because the proton is the simplest projectile causing the smallest perturbation, and therefore measurements with protons are unavoidable for determination of the scaling properties of the studied process. Our further motivation to use protons was to decide the question [3] whether cusp electron production leading to a *neutral* projectile in the final state [4] can proceed via a direct or exchange mechanism. (For bare projectiles only the direct process is possible.)

The experiment was performed at the 1.5 MV van de Graaff accelerator of ATOMKI. The experimental setup (see, e.g., [4] and references therein) consisted of an electrostatic beam cleaner, a double-stage cylindrical mirror electron spectrometer (angular acceptance: 1.9° ; energy resolution: 0.4%), an electrostatic charge-state selector and a fast particle detector. The principle of the measurement was that the cusp electron production process via TI could be identified by detecting the electrons in coincidence with the outgoing neutralized hydrogen atoms. The yield of this two-electron process was compared to that of the one-electron ECC (electron capture to the continuum) process identified by detecting the cusp elec-

trons in coincidence with the outgoing protons. Special care was taken to avoid contributions from double-collisions of protons with the target atoms – the coincidence yields were measured as functions of the target gas pressure – and the ECC and TI yields were determined by extrapolation to zero target pressure.

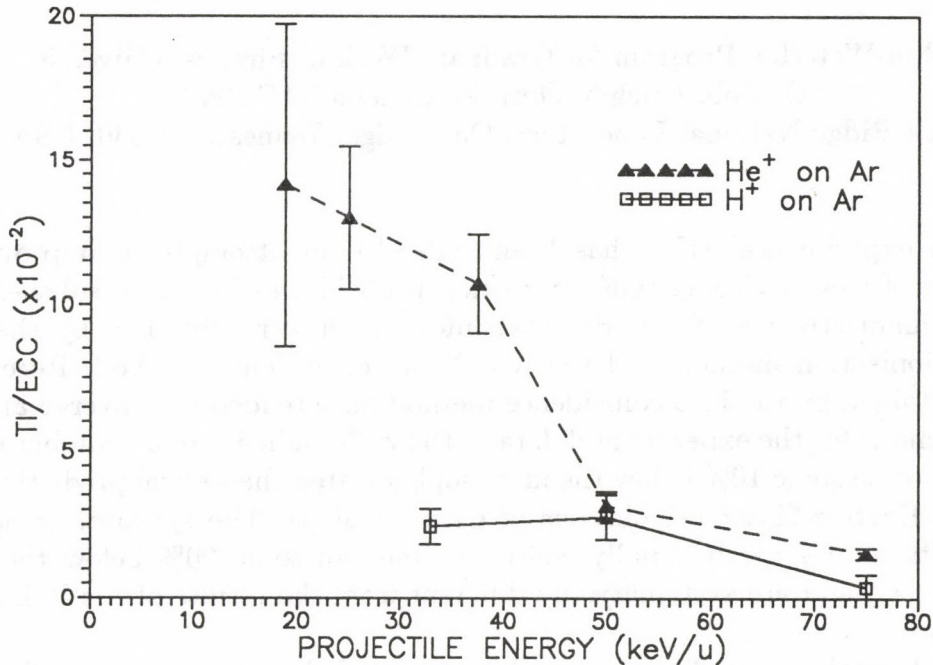


Fig. 1. TI/ECC ratios for proton and helium impact.

The obtained TI/ECC ratios together with the results of the previous experiment using He⁺ projectiles [1] are seen in Fig. 1. An interesting feature of the displayed data is that the rather large difference between the proton and helium values seen at low impact velocities diminishes with increasing velocity. This finding indicates that at high velocities TI is due to a single projectile – target-electron interaction which is followed by a secondary electron – electron interaction.

References

† Western Michigan University, Kalamazoo, Michigan 49008, USA

¶ Institut für Kernphysik der J.W. Goethe-Universität, D-60486 Frankfurt/M, Germany

§ Permanent address: Institute of Physics, Belgrade, Yugoslavia

1. P. A. Závodszky, L. Sarkadi, J. A. Tanis, D. Berényi, J. Pálinkás, V. L. Plano, L. Gulyás, E. Takács, L. Tóth: Nucl. Instr. and Meth. B **79** 67 (1993)
2. K. Khemliche, M. H. Prior, V. L. Plano, R. R. Haar, J. A. Tanis, P. A. Závodszky, L. Sarkadi, J. Pálinkás, D. Berényi, D. Schneider: Bull. Am. Phys. Soc. **38** 1160 (1993)
3. A. Salin, private communication (1992)
4. L. Sarkadi, J. Pálinkás, Á. Kövér, D. Berényi, T. Vajnai: Phys. Rev. Lett. **62** 527 (1989)

Lineshape effects on the determination of Coster-Kronig probabilities using Si(Li) X-ray detectors

T. Papp, J.L. Campbell ¹ and S. Raman ²

¹Guelph-Waterloo Program for Graduate Work in Physics, University of Guelph, Guelph, Ontario, Canada N1G 2W1

²Oak Ridge National Laboratory, Oak Ridge, Tennessee 37830, USA

Much experimental effort has been expended in attempts to improve our knowledge of Coster-Kronig (CK) transition probabilities for the L subshells [1]. The two main streams of experimental information were obtained by the synchrotron ionisation method and the K-L X-ray coincidence method. Recent f_{23} results obtained by the K-L coincidence method have tended to converge and the overall trend is for the experimental data in the well-studied atomic number region $60 < Z < 90$ to lie some 10% below the most sophisticated theoretical predictions viz the Dirac-Hartree-Slater calculations of Chen et al [2]. The synchrotron ionisation results for f_{23} are internally consistent but fall some 20% below the DHS predictions [1] and are systematically different from the results of the K-L X-ray method.

In both methods the X-rays were detected by Si(Li) spectrometers. The purpose of this paper is to examine the influence of three factors which have hitherto been ignored in the interpretation of data from these techniques; the first factor is the intrinsic Lorentzian energy distribution within a given X-ray line; the second is the satellite contribution to the X-ray spectra; and the third is the low energy tail in the detector response function. We studied these effects for uranium and gadolinium atoms using the K-L coincidence technique on radioactive sources.

The result of a C-K transition is a double vacancy state, which will de-excite through various decay channels, with the resulting X-ray spectrum containing very many satellite transitions. The peculiarity of X-ray spectra emitted after vacancies have been shifted to higher subshells by the CK process is that the main contribution arises from satellites. This differs from the case of direct vacancy creation by proton or photon beams, where only a very minor contribution is due to doubly ionised atoms. When the L_2-L_3M C-K channels are open, the spectra contain LM satellites whose energy separation from the diagram line (singly-ionised atom transition) can be as large as 50-60 eV for uranium L_3 X-rays, while the detector resolution is around 200-250 eV. This spreading out of the studied transition impacts differently upon the K-L coincidence technique and the impact ionisation technique. In the $K\alpha_2-L$ coincidence spectrum, the $L\alpha$ satellite compound is fitted by a Gaussian which may be broader than the detector resolution and can have a different centroid than the diagram line. In the case of impact ionisation the spectrum consists predominantly of the diagram line on which is superposed a

small contribution (5-10%) of satellite spectrum. Here the Gaussian width and the centroid energy will be determined predominantly by the diagram line spectrum, and the resulting values will not be precisely appropriate for the superimposed satellite contribution.

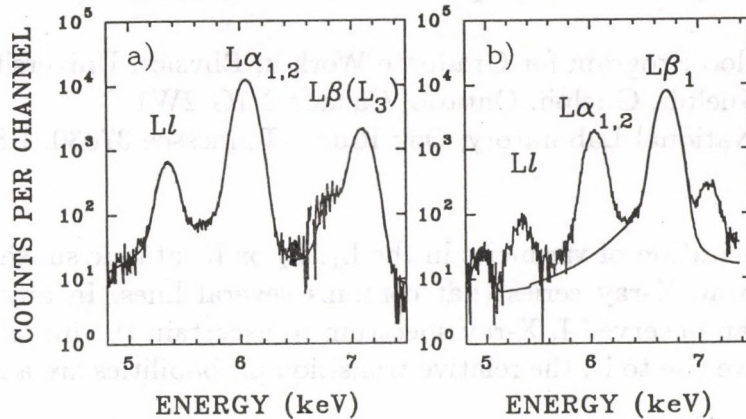


Fig. 1. The Ll - $L\alpha$ - $L\beta$ range of the gadolinium spectra in coincidence with the $K\alpha_1$ (a) and $K\alpha_2$ (b) transitions. Fig. 1b also shows the fitted lineshape of the $L\beta_1(L_2-N_4)$ transition.

In the case of gadolinium the L_3M channels are energetically forbidden. However here the peaks are closer to each other. The $L\alpha$ peak is the main peak in the $K\alpha_1$ -L spectrum (see fig. 1a), while the $K\alpha_2$ -L spectrum is dominated by the $L\beta_1(L_2-N_4)$ peak. The $L\alpha$ is positioned on the tail of the $L\beta_1$ peak. This tail is represented by the full line in fig. 1b.

We concluded for these two examples, that half of the deviation between the f_{23} parameters obtained by the K-L coincidence and synchrotron ionisation methods can be explained by the difference in the data evaluation methods, where the various lineshape effects have been approximated differently. We found that neglect of the proper lineshapes limits the accuracy of the determination of the f_{23} Coster-Kronig transition probabilities. Generally, neglecting the various lineshape components will result in an underestimate of the f_{23} Coster-Kronig transition probabilities. We found that the underestimate is larger in the case of the synchrotron ionisation method. This finding shows the same tendency as has been remarked upon in the comparison of the results of the two methods [1].

Research supported in part by the Natural Sciences and Engineering Research Council of Canada and by the USDOE under contract with Martin Marietta Energy Systems, Inc. (Oak Ridge).

References

- [1] W. Jitschin, in the Proceedings of the Fifteenth International Conference on X-ray and Inner-Shell Ionization, edited by T.A. Carlson, M.O. Krause and S.T. Manson, American Institute of Physics Conference Proceedings 215 p. 408-423 (1990).
- [2] M. H.Chen, *ibid.* 215 p. 391-407 (1990).

An experimental test of Dirac-Fock versus Dirac-Hartree-Slater L X-ray intensity ratios

T. Papp, J.L. Campbell ¹ and S. Raman ²

¹Guelph-Waterloo Program for Graduate Work in Physics, University of Guelph, Guelph, Ontario, Canada N1G 2W1

²Oak Ridge National Laboratory, Oak Ridge, Tennessee 37830, USA

Radiative de-excitation of vacancies in the L_1 , L_2 or L_3 atomic subshells gives rise in each case to an X-ray series that contains several lines. In any attempt to work back from an observed L X-ray spectrum to ascertain the initial vacancy distribution that gave rise to it, the relative transition probabilities are a necessary ingredient.

The most widely used theoretical tabulation is that of Scofield [1], based upon Dirac-Hartree-Slater (DHS) atomic wave functions. However an interpolation scheme based on the DF/DHS ratios has been employed [2] to extend the DF data [3] to all atomic numbers between 40 and 92.

Scofield [4] presented figures comparing DHS predictions for various intensity ratios to a subset of contemporary experimental measurements. While there was an overall suggestion that the data exceed the DHS theoretical values, much reduced error bars would be needed in order to effect a definitive comparison of the two theoretical treatments.

Several recent developments suggested to us that coincidence measurements could now be made and interpreted with much improved accuracy, and that individual line intensities might be extracted with confidence. K X-ray L X-ray coincidence experiments were performed using two radioactive sources. The first source was ^{233}Pa , which decays to ^{233}U , and the second source was ^{157}Tb , which decays to ^{157}Gd . The K X-ray spectra were recorded using an Aptec HpGe detector (FWHM=530 eV at 122 keV), while the L X-ray spectra were recorded with a Link Analytical plc Si(Li) detector (FWHM=133 eV at 5.9 keV).

With the ^{233}Pa source, twelve coincidence measurements were performed at 10 angles in the range 90° - 180° . With the ^{157}Tb source, a single long coincidence measurement was done, with detectors at 180° and very close to one another. In addition, singles K and L X-ray spectra were also recorded to high intensities.

The L X-ray coincidence spectra were fitted by a non-linear least squares routine. Each peak was taken to be a Gaussian distorted at the low-energy side by a quasi-exponential tailing feature whose two parameters were variables of the fit. Each combination of Gaussian and tail was convoluted with a Lorentzian distribution representing the intrinsic X-ray lineshape. Although hitherto neglected in such work, the Lorentzian is in fact the principal contributor to low-energy tailing in the uranium L X-ray case. We investigated the model-dependence of the results

by carrying out a large number of fits in which the Lorentzian widths, and the tailing intensity were varied. This enabled us to enlarge the quoted uncertainty in a manner that we believe reflects the sensitivity of the results to the model used to represent the spectrum in the fitting process. A test was made to detect any systematic error arising from the subtraction of the random coincidence spectra.

Once the relative intensities in the L_2 and L_3 series of Gd had been determined they were employed as fixed quantities in fitting a singles Gd spectrum containing 56 million counts. Given the exceptionally high counting statistics, the quality of this fit is very good. This exercise provided the relative L_1 X-ray intensities. All L X-ray intensities were corrected for source self-absorption, detector efficiency and angular correlation.

The line intensity ratios data support the predictions of the DF calculation [3] rather than those of the DHS model [1]. This preference is particularly clear for the intensity ratios L_2N_4/L_2M_4 and $L_3N_{4,5}/L_3M_{4,5}$; these are cases where the difference between the two predictions is largest compared to the experimental error estimate.

Our main conclusion then is that these careful measurements, which treat the detector lineshape in more depth than previous work and which employ very high counting statistics, support, with one minor exception (L_3M_1), the DF predictions of [3] for relative X-ray line intensities. We believe that these intensities should be used in appropriate data bases rather than the earlier DHS values or values taken from the experimental survey of [5].

This conclusion has implications for measurements of quantities such as L sub-shell ionization cross-sections by charged particles, since the interpretation of such measurements relies in part upon a data base of relative L X-ray line intensities.

Research supported in part by the Natural Sciences and Engineering Research Council of Canada and by the USDOE under contract with Martin Marietta Energy Systems, Inc. (Oak Ridge)

References

- [1] J. H. Scofield, Lawrence Livermore Laboratory Report UCRL - 51231 (1972)
- [2] Campbell J.L. and Wang J.-X., At. Data Nucl. Data Tables 43, 281 (1989)
- [3] J. H. Scofield, Phys. Rev A10, 1507 (1974)
- [4] J. H. Scofield, Atomic Inner-Shell Processes ed. B. Crasemann (Academic Press, New York) p 265 (1975)
- [5] S. I. Salem, S. L. Panossian and R. O. Krause, At. Data Nucl. Data Tables 14 91 (1974)
- [6] D. D. Cohen, Nucl. Instrum. Meth. B49 1 (1990)

Coherences in decay of autoionizing states in photoionization

I. Exchange effect between photo- and Auger electrons

L. Végh, J. H. Macek ^a

^aOak Ridge National Laboratory, Oak Ridge, Tennessee 37831-6373,
U.S.A.

In photoinduced Auger decay experiments, in which photo- and Auger electrons have approximately the same energy, an interference effect should occur in the angular correlation pattern [1]. If the spin-dependent interactions can be neglected and the two electrons participating in the Auger process are in a singlet state then the photoelectron and autoionized electron are in a singlet state, too. In this case the orbital state must be symmetric and therefore in a coincidence experiment between photo- and Auger electron one expects a strong enhancement for the electrons ejected parallelly and a vanishing or at least reduced coincidence rate for a relative angle of 180° between the electrons.

Schwarzkopf, Kämmerling and Schmidt [2] have reported preliminary results on the two-step double photoionization in xenon ($4d_{5/2}$ photoionization followed by $N_5 - O_{23}O_{23} \ ^1S_0$ Auger decay). The relative angle of the electron analysers was 180° . Due to the pure energy resolution the magnitude of the reduction can not be extracted from the spectra.

In order to make a realistic comparison with the experiment, we have calculated the angular correlation in the presence of the exchange term for the general case. To describe the amplitude of the Auger electron emission following photoionization we use the treatment of Åberg and Howat [3]. For specifying the polarization of the incident light beam we use the density matrix of the photon beam which is expressed by the three Stokes parameters. We have derived the following expression for angular correlation between electrons of momenta \mathbf{k}_1 and \mathbf{k}_2

$$\frac{d\sigma}{d\varepsilon_1 d\Omega_1 d\Omega_2} = \frac{3(2J+1)}{4\pi} C \sum_{k_1 k_2 \kappa} \left\{ \frac{B(k_1 k_2 \kappa)}{(\varepsilon_2 - \varepsilon_r)^2 + \frac{\Gamma^2}{4}} + \frac{(-1)^\kappa B(k_2 k_1 \kappa)}{(\varepsilon_1 - \varepsilon_r)^2 + \frac{\Gamma^2}{4}} \right\} \\ \times \mathcal{A}_{k_1 k_2 \kappa}(\Omega_1 \Omega_2) - 2Re \left\{ \frac{B_{int}(k_1 k_2 \kappa)}{(\varepsilon_1 - \varepsilon_r + i\frac{\Gamma}{2})(\varepsilon_2 - \varepsilon_r - i\frac{\Gamma}{2})} \mathcal{A}_{k_1 k_2 \kappa}(\Omega_1 \Omega_2) \right\}$$

The coefficients $B(k_1 k_2 \kappa)$ and $B_{int}(k_1 k_2 \kappa)$ depend upon geometrical factors and the dynamics of the double ionization process. The first two terms in with

$B(k_1 k_2 \kappa)$ give the sum of the photoelectron and Auger-electron intensities in the absence of interference. The term with B_{int} is the interference term which is the product of the direct and exchange amplitudes. $\mathcal{A}_{k_1 k_2 \kappa}(\Omega_1 \Omega_2)$ depends on the angles and the Stokes parameters of the photon beams.

The exchange effect is present even when only one electron is detected, but is strongly reduced by the averaging over the direction of the undetected electron.

References

1. L. Végh, R. L. Becker, and J. H. Macek, *Fifteenth International Conference on X-Ray and Inner-Shell Processes, Knoxville, 1990*, Book of Abstracts, D11. and L. Végh and J. H. Macek, submitted to Phys. Rev. A.
2. V. Schmidt, *Sixteenth Int. Conf. on X-Ray and Inner-Shell Processes, Debrecen, 1993* Invited talk.
3. T. Åberg and G. Howat, in *Encyclopedia of Physics*, Vol. XXXI, edited by S. Flügge and W. Mehlhorn, (Springer, Berlin, 1982), p.469;

Coherences in decays of autoionizing states in photoionization

II. Coherences of non-degenerate states

L. Végh

Coherence between states of different excitation energies have already been studied by electron impact excitation of the autoionizing states in the papers of Van den Brink et al [1]. Their method is based on the occurrence of interferences between scattered and ejected electrons resulting from the electron impact excitation and subsequent autoionization of states concerned. Very recently this group has published the observation of coherent excitation of non-degenerate levels in photoionization [2].

We present a theoretical description of the effect. In photoionization coherence occurs between the photoejected and autoionized electrons. We investigate processes which lead to indistinguishable final states of the residual doubly-ionized atom. This can be realized by the suitable choice of the synchrotron light energy $\hbar\omega$. At the proper photon energy the energy of the photoelectron from the channel with autoionizing state A_1 (channel 1) and the energy of the Auger electron from the channel with autoionizing state A_2 are equal, that is $E_{ph1} = E_{Aug2}$. At the same time it is true that $E_{ph2} = E_{Aug1}$. At the region of this photon energy the angular correlation of the two final electrons exhibits state-state interference pattern.

Under these conditions the energy dependence of the cross section exhibits interference structure due to two paths to the same final state. We present a theoretical description of the effect. The incident photon beam is described by the Stokes parameters and the amplitude of the Auger electron emission following photoionization is taken from Åberg and Howat [3]. The cross section formulae for angular distributions and angular correlations are presented in paper [4].

This phenomena is of fundamental interest as it provides a new tool for testing photoionization theories. Both the photoionization and autoionization amplitudes contain information about the coherence between the two discrete states.

References

1. J. P. van den Brink, J. van Eck, and H. G. M. Heideman, Phys. Rev. Lett. 61, 2106 (1988); J. P. van den Brink et al, J. Phys. B22, 3501 (1989); J. P. van den Brink et al, J. Phys. B23, 2349 (1990).
2. J. A. de Gouw, J. van Eck, A. C. Peters, J. van der Weg, and H. G. M. Heideman: Phys. Rev. Lett. 71, 2875 (1993).
3. T. Åberg and G. Howat, in *Encyclopedia of Physics*, Vol. XXXI, edited by S. Flügge and W. Mehlhorn, (Springer, Berlin, 1982), p. 469.
4. L. Végh, submitted to Phys. Rev. A.

Model calculation for the ECC peak at neutral projectile impact

K. Tókési, L. Sarkadi and T. Mukoyama^a

Since 1970, the first observation of the cusp-like peak [1] in the energy spectrum of electrons emitted in ion-atom collisions, the ECC (Electron Capture to the Continuum) studies have been very intensive and important to understand the collision dynamics. It was a very surprising experimental result, when Sarkadi et al. [2] have shown that ECC cusp electrons can be observed for incoming neutral projectiles.

In the present work we applied the three- and four-body classical trajectory Monte Carlo method [3-5] to calculate the DDCS for the ECC peak as a function of the ionized target electron energy at forward observation angles.

In the three-body approximation we used the "frozen" electron model of the projectile atom. Hydrogen-like wave functions were used to determine the potential around the projectile. For H(1s) we have:

$$V(H[1s]) = \frac{e^{-2R}}{R}(1 + R), \quad (1)$$

where R is the distance between the particles.

When the projectile electron is excited to the 2s state, the potential is given by

$$V(H[2s]) = \frac{e^{-R}}{R} \left(\frac{R^3}{8} + \frac{R^2}{4} + \frac{3R}{4} + 1 \right). \quad (2)$$

Using the full four-body approximation we have not found any peak in the calculated doubly differential cross section. This result indicates that the $e^- - e^-$ interaction in H+H type collisions plays a dominant role in the classical picture.

As a result of the three-body calculation using the equations (1) and (2) for model potentials of projectile, the cross section for the production of cusp electrons in the target ionization process by metastable H(2s) atom has been found to be about ten times larger than the cross section for the same process for ground-state projectiles H(1s) (in good agreement with the experimental data of Kuzel et al. [6]). Fig. 1 shows the calculated doubly differential cross section of the ionized electron of the target atom as a function of the electron energy.

Acknowledgements

This work was performed under the Japanese-Hungarian Cooperative Research Project.

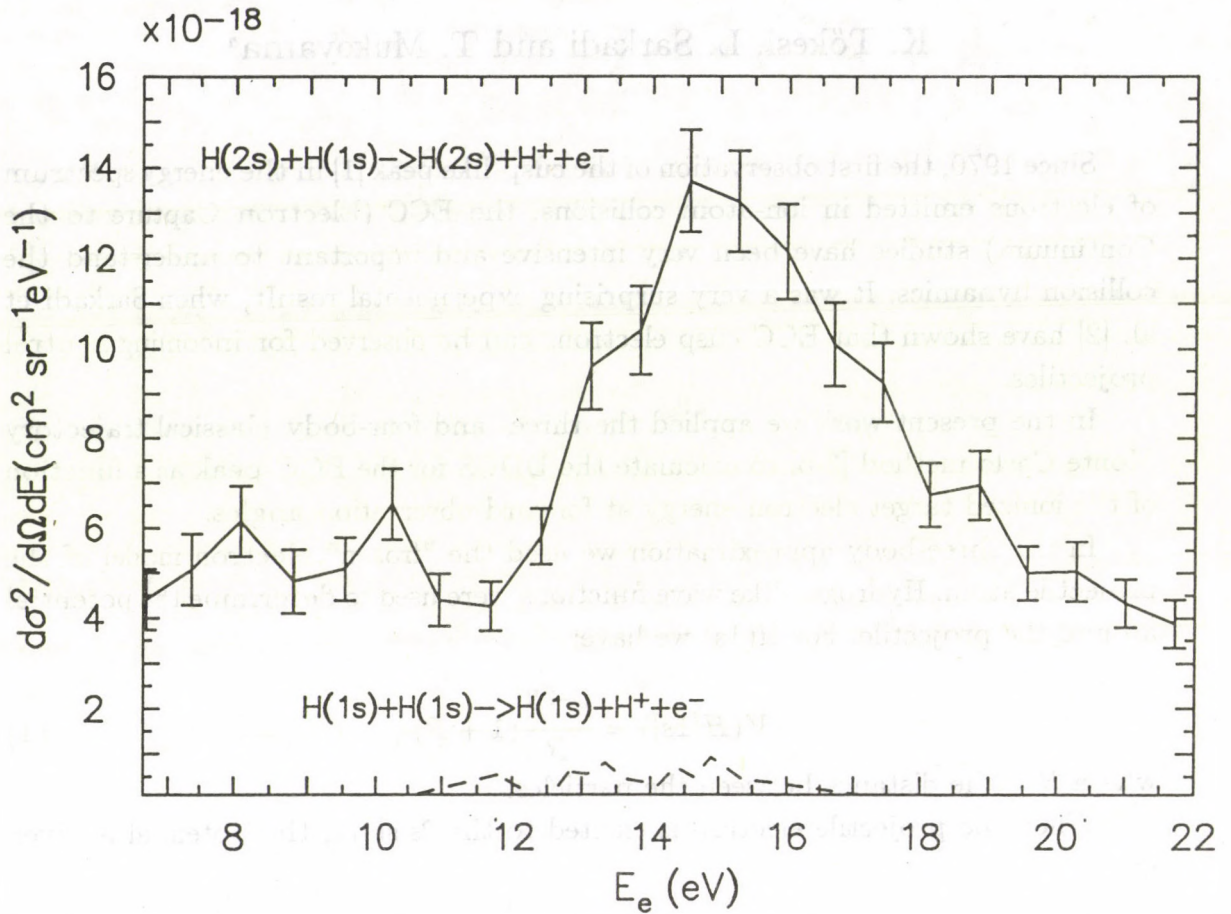


Fig. 1. Cross sections of target ionization at forward observation angle in 25 keV/amu H+H collision: - - - potential (1); — potential (2). The calculations were made assuming 0.5 eV energy resolution and $\pm 2^\circ$ angular window.

References

^a *Division of States and Structures, Institute for Chemical Research, Kyoto University, Uji, Kyoto, 611 Japan*

1. G. B. Crooks and M. E. Rudd, *Phys. Rev. Lett.* **25** (1970) 1599
2. L. Sarkadi et al., *Phys. Rev. Lett.* **62** (1989) 527
3. R. Abrines and I.C. Percival, *Proc. Phys. Soc.* **88** (1966) 861
4. R.E. Olson, and A. Salop, *Phys. Rev.* **A16** (1977) 531
5. K. Tökési and T. Mukoyama, to be published
6. M. Kuzel et al., *Phys. Rev.* **A48** (1993) R1745

Interpretation of Al KL_1V and KVV Auger spectra by the help of a cluster type MO calculation

Zs. Kovács, L. Kövér, J. Pálincás, H. Adachi*

*Dept. of Metallurgy, Kyoto University, Yoshida-honmachi, Kyoto 606, Japan

As a result of several recent studies, by now it is well established¹ that for simple metals with wide bands of s and p valence character core-valence Auger processes obeys the final state rule according to which the KL_1V and $KL_{2,3}V$ line shapes should reflect the screened DOS (density of states) local to the core hole, while the KVV line shape reflects the final state DOS in the absence of a core hole (e.g. the ground state DOS).

Al KL_1V and $KL_{2,3}V$ Auger line shapes of metallic Al were measured and the experimental Al KL_1V and $KL_{2,3}V$ Auger spectra were interpreted using a DVX- α cluster type MO calculation². In the present experiment the Al KL_1V and $KL_{2,3}V$ spectra were excited by Mo X-rays and measured by using a home built, high luminosity hemispherical electron spectrometer^{3,4}. The experiments were performed on vacuum evaporated aluminium (111) samples applying in situ Ar^+ ion sputtering for surface cleaning prior to measurements. Structures due to plasmon losses were subtracted from the spectra and corrections for the inelastic background were made by using the Shirley method⁵.

Theoretical Auger lineshapes were obtained by using the ground state DOS from DVX- α MO calculation with O_h ($Fm3m$) cluster symmetry and a cluster including 22 atoms. The core hole screening effects were accounted for by applying the formalism of the Green functions and considering an atom with a hole as a point defect in a crystal⁶.

Fig. 1-2 show the calculated KL_1V lineshapes based on the respective screened DOS distributions in comparison with the experimental Al KL_1V and $KL_{2,3}V$ spectra, indicating that the difference between the Al KL_1V and $KL_{2,3}V$ lineshapes is mainly due to the increase of the s-type partial DOS. In Figs. 3.a. and 3.b. the experimental core-valence-valence lineshapes, and the calculated KVV lineshape are presented, respectively, showing a good agreement. Fig. 4. shows the effect, due to the presence of oxygen atoms adsorbed on the surface, as it is reflected in the calculated Al KVV lineshape.

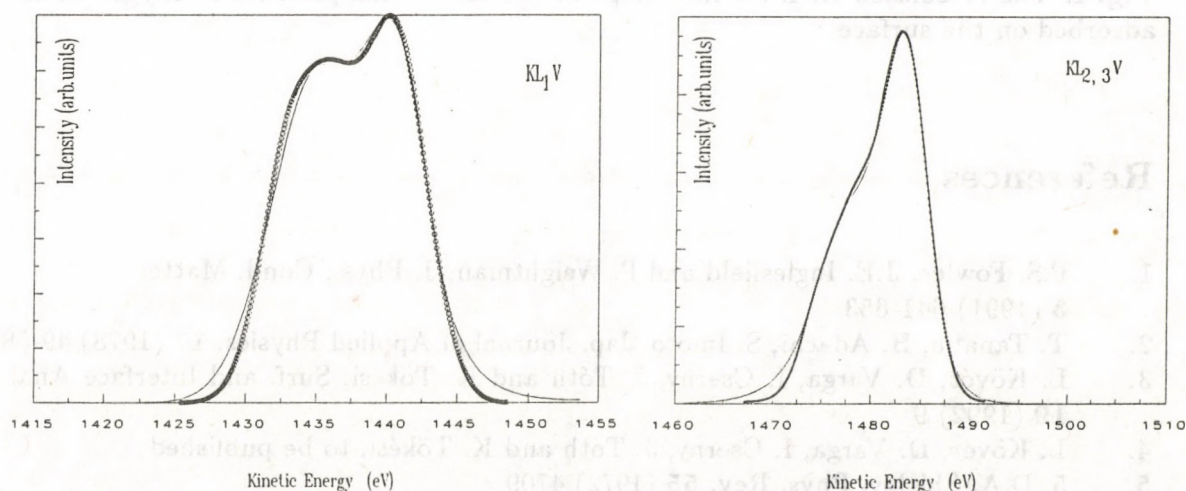


Fig. 1. The calculated Al KL_1V lineshape (dots) in comparison with the experimental KL_1V spectrum (solid line)

Fig. 2. The calculated Al $KL_{2,3}V$ lineshape (dots) in comparison with the experimental $KL_{2,3}V$ spectrum (solid line)

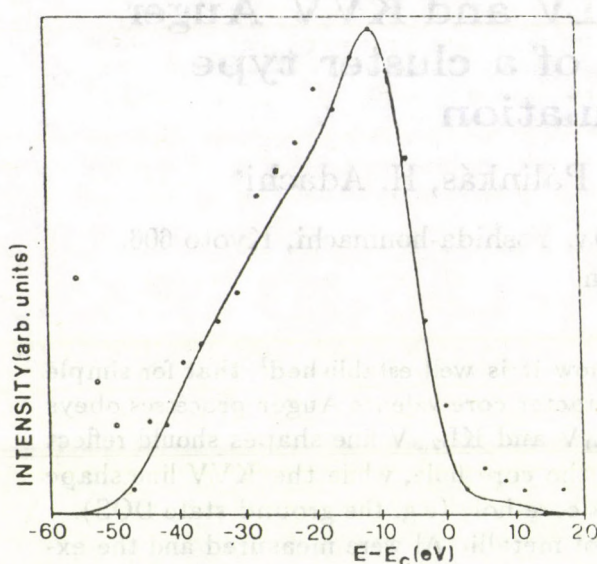


Fig. 3.a. Experimental⁶ Al KVV (dots) and LVV lineshapes (solid lines)

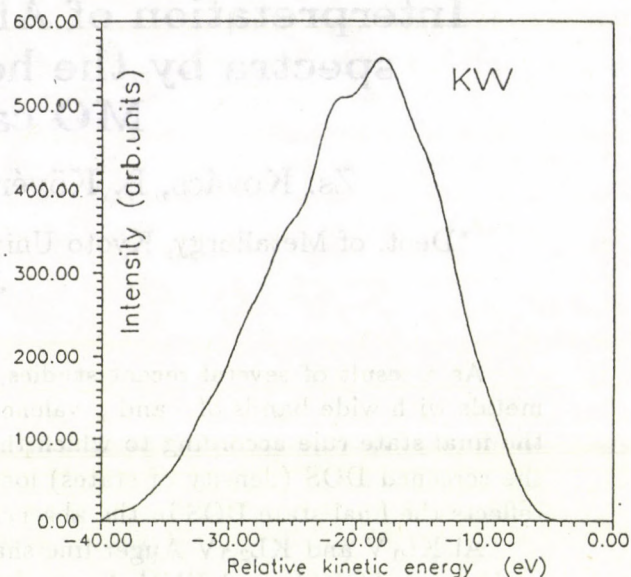


Fig. b. The Al KVV lineshapes calculated with a cluster consisting of 14 atoms

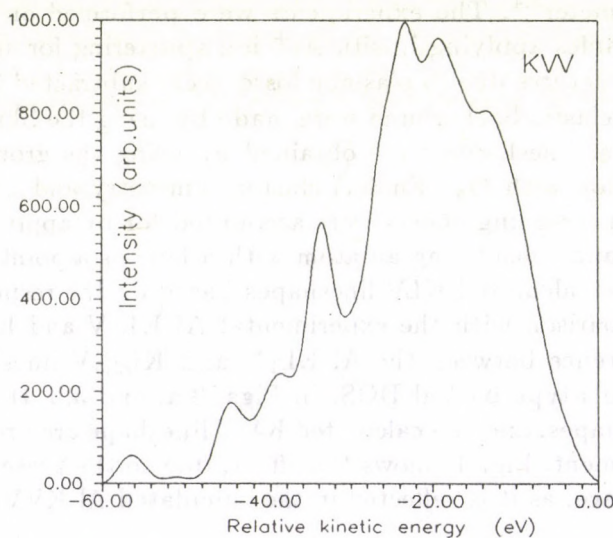


Fig. 4. The calculated Al KVV line-shape in the case of the presence of oxygen atoms adsorbed on the surface

References

1. P.S. Fowles, J.E. Inglesfield and P. Weightman, *J. Phys.: Cond. Matter* **3** (1991) 641-653
2. T. Tanabe, H. Adachi, S. Imoto, *Jap. Journal of Applied Physics*. **17** (1978) 49-58
3. L. Kövér, D. Varga, I. Cserny, J. Tóth and K. Tökési, *Surf. and Interface Anal.* **19** (1992) 9
4. L. Kövér, D. Varga, I. Cserny, J. Tóth and K. Tökési, to be published
5. D.A. Shirley, *Phys. Rev.* **55** (1972) 4709
6. D.E. Ramaker, F.L. Hutson, N.H. Turner, W.N. Mei, *Phys. Rev.* **B33** (1986) 2574
7. V. Contini, C. Presilla and F. Sacchetti, *Solid State Comm.* **70** (1989) 851-853

Generalized Description of the Electron Emission by Autodetachment in Fast Ion-Atom Collisions

P. A. Závodszy, L. Sarkadi and J. Pálinkás

During high-energy ion-atom collisions different processes can contribute to the electron emission. Electrons produced in a direct process and that via resonances cannot be distinguished in the final state. This can result in interferences in the cross section, producing asymmetric line shapes.

A convenient parametrization of the double differential cross section (DDCS) was originally introduced by Shore, further developed by Balashov *et al.*, and generalized by Tweed [1]. According to this parametrization the DDCS in the projectile reference frame can be written as,

$$\left(\frac{d^2\sigma}{dE'_e d\Omega'_e} \right)_p = \left(\frac{d^2\sigma}{dE'_e d\Omega'_e} \right)_p^{\text{NR}}(\mathbf{k}'_e) + \sum_{\mu} \frac{\alpha_{\mu}(\mathbf{k}'_e)\varepsilon_{\mu} + \beta_{\mu}(\mathbf{k}'_e)}{1 + \varepsilon_{\mu}^2}, \quad (1)$$

where $\left(\frac{d^2\sigma}{dE'_e d\Omega'_e} \right)_p^{\text{NR}}$ is the non-resonant cross section which characterizes the direct electron detachment process, $\mu = LMS$ specifies the autodetaching state with total angular momentum and spin quantum numbers L , M and S , $d\Omega'_e$ defines the solid angle of detection for the ejected electron, $\varepsilon_{\mu} = 2(E'_e - E_{\mu})/\Gamma_{\mu}$, E'_e and \mathbf{k}'_e are the energy and the momentum of the ejected electron in the projectile reference frame, E_{μ} and Γ_{μ} are the energy and the width of the resonance depending primarily on the properties of the state, α_{μ} and β_{μ} are the so-called Shore parameters that describe the shape of the resonance, reflecting the mode of its formation and decay.

The direct electron detachment (electron loss) alone produces a cusplike peak in the energy spectrum of the electrons emitted in the forward direction. This peak is centered at an electron velocity equal to the projectile velocity. Meckbach *et al.* [2] introduced a series expansion method of the transition amplitude of the cusp-producing process, obtaining a set of series expansion coefficients free of instrumental effects that can be compared directly with values obtained in different theoretical models.

Generalizing the above method for the Shore parameters, we obtain:

$$\alpha_{\mu}(\mathbf{k}'_e) = \sum_{n,l=0}^{\infty} a_{\mu}^{nl}(v_p) \left(\frac{v'_e}{v_p} \right)^n P_l(\cos \vartheta'_e), \quad \beta_{\mu}(\mathbf{k}'_e) = \sum_{n,l=0}^{\infty} b_{\mu}^{nl}(v_p) \left(\frac{v'_e}{v_p} \right)^n P_l(\cos \vartheta'_e), \quad (2)$$

where $a^{nl}(v_p)$ and $b^{nl}(v_p)$ are the series expansion coefficients, v'_e and ϑ'_e are the velocity and the emission angle of the ejected electron, v_p is the velocity of the projectile, and P_l are the Legendre polynomials.

For the measured electron yield Y (omitting the μ index) we get:

$$Y(v_e, v_p, \vartheta_a) = \sum_{n,l=0}^{\infty} [a^{nl} W_{nl}(v_e, v_p, \vartheta_a) + b^{nl} V_{nl}(v_e, v_p, \vartheta_a) + c^{nl} U_{nl}(v_e, v_p, \vartheta_a)], \quad (3)$$

where v_e and ϑ_e are the velocity and the emission angle of the ejected electron in the laboratory reference frame, the U_{nl} functions are similar to that deduced in [2], the W_{nl} and V_{nl} functions can be expressed with:

$$W_{nl}(v_e, v_p, \vartheta_a) = \frac{4\pi R v_e^3}{v_p} \int_0^{\vartheta_a} \frac{\varepsilon}{1+\varepsilon^2} \left(\frac{v'_e}{v_p}\right)^{n-1} P_l(\cos \vartheta'_e) \sin \vartheta_e d\vartheta_e, \quad (4)$$

$$V_{nl}(v_e, v_p, \vartheta_a) = \frac{4\pi R v_e^3}{v_p} \int_0^{\vartheta_a} \frac{1}{1+\varepsilon^2} \left(\frac{v'_e}{v_p}\right)^{n-1} P_l(\cos \vartheta'_e) \sin \vartheta_e d\vartheta_e. \quad (5)$$

Here $R = \Delta v_e / v_e$ and ϑ_a are the relative velocity resolution and the acceptance angle of the spectrometer.

In Fig. 1 are represented the W_{nl} and V_{nl} functions for $n, l = 0, 1$ for the detached electron spectrum in $\text{He}^- \rightarrow \text{Ar}$ collisions [3]. In previous works the Shore parameters were considered as constants in the resonance region. With the above generalization we are able to take into account the angular and velocity dependence of the electron emission during the decay by autodetachment of a negative ion resonant state.

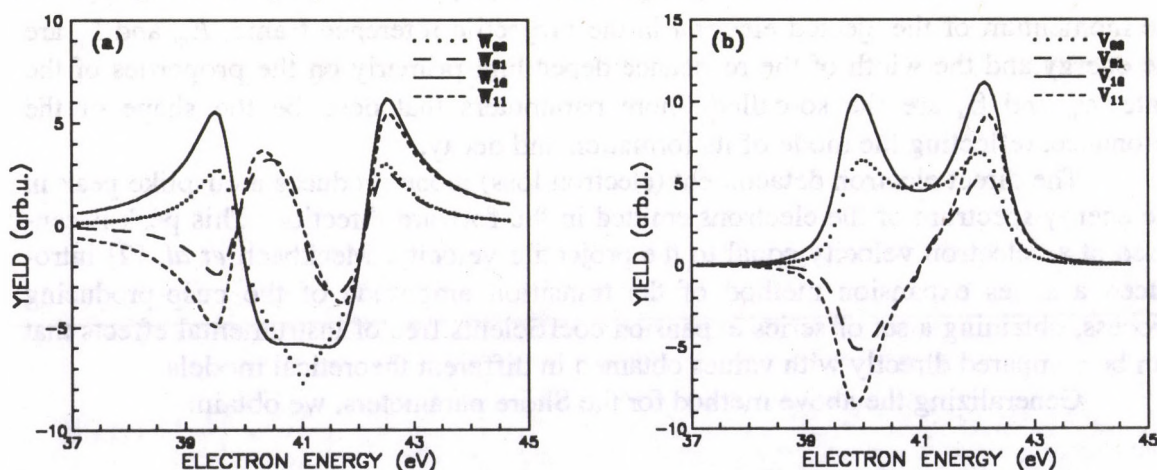


Figure 1. a, b. The functions W_{nl} and V_{nl} as defined in eqs.(4-5) for $n, l=0, 1$, $E_{\text{He}^-}=75.3$ keV/u, $R=0.125\%$, $\vartheta_a=0.8^\circ$, $E_r=11.5$ meV and $\Gamma=10$ meV.

References

1. B. W. Shore, Rev. Mod. Phys. **39** (1967) 439; V. V. Balashov *et al.*, Zh. Eksp. Theor. Fiz., **63** (1972) 1622; R. J. Tweed, J. Phys. B **9** (1976) 1725
2. W. Meckbach, I. B. Nemirowski and C. Garibotti, Phys. Rev. A **24** (1981) 1793
3. P. A. Závodszy, L. Sarkadi, L. Víkor and J. Pálinkás, present volume and submitted to Phys. Rev. Lett. (January 1994)

Quantitative Two-Center Effects in Single Ionisation

P.D. Fainstein[†], L. Gulyás and A. Salin[‡]

[†] Laboratoire de Chimie Physique, Université Pierre Curie, 75231 Paris, France and
Centro Atómico, 8400 san Carlos de Bariloche, Argentina

[‡] Laboratoire des Collision Atomiques, Université de Bordeaux I, 33405 Talence,
France

Ionisation of atoms by high energy charged particles has been the subject of many theoretical and experimental studies over the last decade (see the recent review by Fainstein et al. [1]).

From the theoretical point of view the main difficulty lies in the representation of the electronic state in the Coulomb field of both the moving projectile and target ion. Only the asymptotic solution to this problem is known exactly [2,3].

The first Born approximation (FBA), which neglects the interaction with the Coulomb field of the projectile in both the initial and final channel (no distortion of the wave function) is in good agreement with the measured total cross section. However this model shows important discrepancies with the details of electron emission especially at small and large emission angles. Different approaches were proposed to explain these discrepancies. The Born approximation does not satisfy the correct asymptotic condition, since the final state of the ejected electron is described by a plane wave. It was found that the main discrepancies at small ejection angles were due to the neglected projectile-ejected-electron interaction [3]. On the other hand, Manson et al [4] have shown within the FBA the importance of using orthogonal wave functions and a Hartree-Fock-Slater potential to describe the initial and final state of the 'active' electron. The results obtained with this approach improve significantly the agreement with experiments whenever the interaction of the electron with the projectile in the final state can be neglected.

To improve the agreement with the more detailed experimental data Crothers and McCann [5] have developed the continuum distorted wave-eikonal initial state model (CDW-EIS). In this model the initial state is represented as a bound state distorted by a projectile eikonal phase, while the final continuum wavefunction is a 'two center' function accounting for the Coulomb interaction with both the projectile and target nuclei. This model satisfies the correct asymptotic conditions. Fainstein et al [6] used this approach within the independent electron approximation to calculate the transition amplitude for ionisation from arbitrary initial states of an atom. The bound states and energies of the 'active' electron are represented by a Roothaan-Hartree-Fock approximations, while the interaction between the ejected electron and residual target ion was modeled by a screened coulomb potential.

In the present work we have generalized the CDW-EIS. Whereas the Coulomb interaction with the projectile is treated as in previous formulations of the CDW-EIS method, the interaction of the 'active' electron with the target is represented through a Hartree-Fock potential, as was done in the FBA of Manson et al [3]. In this way we

have built a theory including at the same time two-center effects and a realistic interaction with the target. Calculations have been performed for various noble gas targets (He, Ne, Ar) and fully stripped projectiles. We reproduce very well the experimental findings for proton impact as illustrated in the figure showing on results in comparison with the FBA and experiments for 350 keV H^+ -Ar collisions.

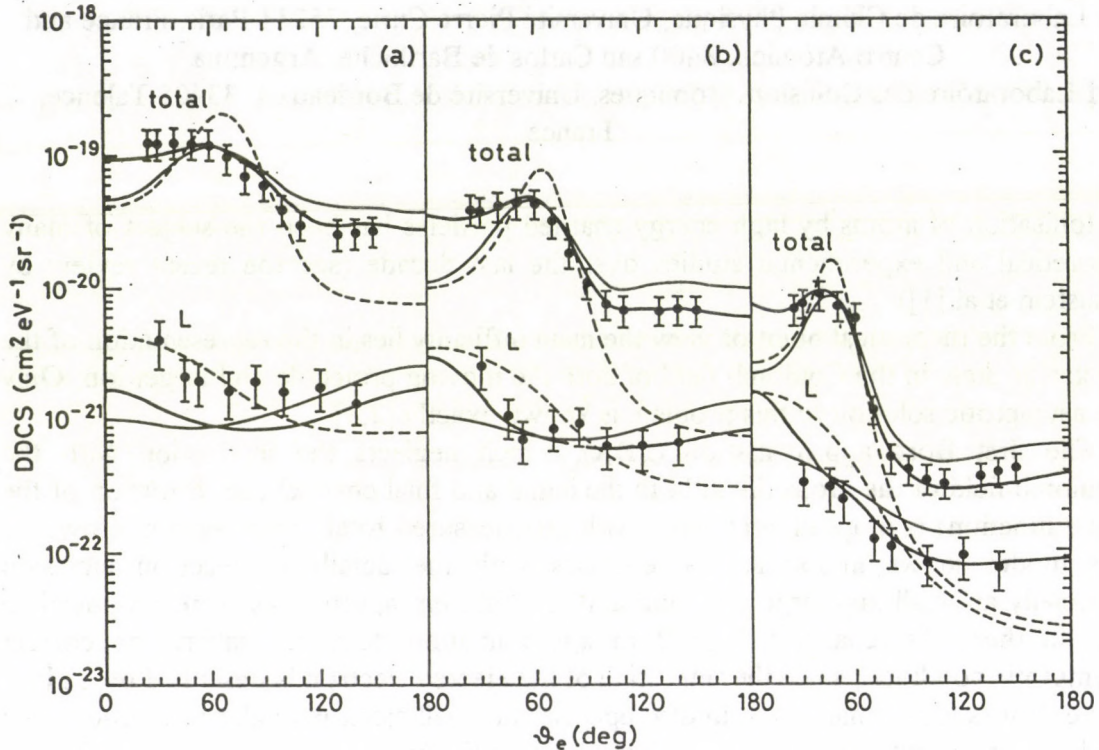


Figure: Absolute double-differential cross section for electron emission at electron energies of (a) 46 eV, (b) 100 eV, (c) 308 eV. Full thin curves, PWBA calculations using Hartree-Fock-Slater wavefunctions [4]; broken curves, PWBA calculations using screened hydrogen-like wavefunctions; full thick curves, present CDW-EIS calculations. Experimental points are from Ref. 7.

References

1. Fainstein P.D., Ponce V.H. and Rivarola R.D.: J. Phys. B24 3091 (1992)
2. Belkić Dž.: J. Phys. B11 3529 (1978)
3. Salin A.: J. Phys. B2 631 (1969)
4. Manson S.T., Tuboren L.H., Madison D.H. and Stolterfoht N.: Phys. Rev A12 60 (1975)
5. Crothers D.S.F and McCann J.F.: J. Phys. B16 3229 (1983)
6. Fainstein P.D., Ponce V.H. and Rivarola R.D.: J. Phys. B23 1481 (1990)
7. Sarkadi L., Bossler J., Hippler R. and Lutz O.D.: J. Phys. B16 71 (1983)

MATERIALS SCIENCE
AND
ANALYSIS



Surface structure of Al-Sn layered systems codeposited in the presence of oxygen

L. Kövér, A. Némethy, P.B. Barna* and M. Adamik*

*Research Institute for Technical Physics of the Hungarian Academy of Sciences,
Budapest

Recent experiments¹ revealed that codeposition of Sn decreases the sensitivity of microstructural evolution of Al films to oxygen. The aim of the present work is to determine the phases developing in this system.

Al films with 20 wt % Sn and with thicknesses of 1.8-2 μm were prepared in vacuum, evaporating Al and Sn simultaneously onto oxidized Si wafers. The deposition rates were 2 nm/s for Al and 0.07 nm/s for Sn, respectively, at a deposition temperature of 470-480 K and at a residual pressure of $(2-4) \cdot 10^{-4}$ Pa. O_2 was introduced through a needle valve increasing the partial pressure to $5 \cdot 10^{-3}$ Pa and $1.3 \cdot 10^{-2}$ Pa, respectively. The structure of the films was studied by cross sectional (XTEM) electron microscopy on samples prepared by ion milling. XPS measurements were performed by a home built electron spectrometer², with an instrumental resolution of $3 \cdot 10^{-4}$. Depth profilings were made² by an argon ion gun using a beam energy of 4.5 keV and a current between 6 and 23 μA , respectively (in all cases the sputtered area was 1.0 cm^2).

During the codeposition of Al and Sn, the Sn species, insoluble in the Al crystal lattice, are segregated together with oxygen. Due to the influence of Sn, the self-surface diffusion of Al as well as the coalescence of Al crystals are promoted, resulting in the increase in the grain size. At an oxygen partial pressure of $\sim 5 \cdot 10^{-3}$ Pa a solid phase develops covering the surface of the growing Al crystals (Fig.1) and blocks their growth at critical grain sizes (the condensation of Al and Sn proceeds by repeated nucleation). Increasing the O_2 pressure to 10^{-2} Pa during the codeposition, the enhancement of the formation of this phase and the development of a cermet-like structure³ is observed (Fig.2). This can be explained by the more intensive formation¹ of the surface covering solid phase due to the stronger interaction between the segregated Sn and oxygen species and Al adatoms.

The results of the XPS depth profile analysis⁴ reveal that this phase consists of mainly metallic-like Sn⁵ (small particles segregated during codeposition, with a surface layer consisting of SnO_2), Al metal and Al_2O_3 (Fig.3). In the surface region of films codeposited at an O_2 partial pressure of $\sim 10^{-2}$ Pa, SnO_2 (due to the surface oxidized segregates) can be found throughout the region investigated (Fig.4).

References

1. P.B. Barna, G. Barcza, L. Tóth, G. Vincze, A. Bergauer and H. Bangert, *Surface and Coatings Technol.* **57**, 7 (1993).
2. L. Kövér, D. Varga, I. Cserny, J. Tóth and K. Tőkési, *Surf. Interface Anal.* **19**, 9 (1992).
3. P.B. Barna, in J.L. de Segovia (ed.), *Proc. 9th Int. Vacuum Congr.*, Madrid, 1983, p.382.
4. L. Kövér, A. Némethy, P. B. Barna and M. Adamik (accepted for publication in the *Surface and Interface Anal.*)
5. J.M. Themlin, M. Chtaib, L. Henrard, P. Lambin, J. Darville and J.-M. Gilles, *Phys. Rev. B* **46**, 2460 (1992).

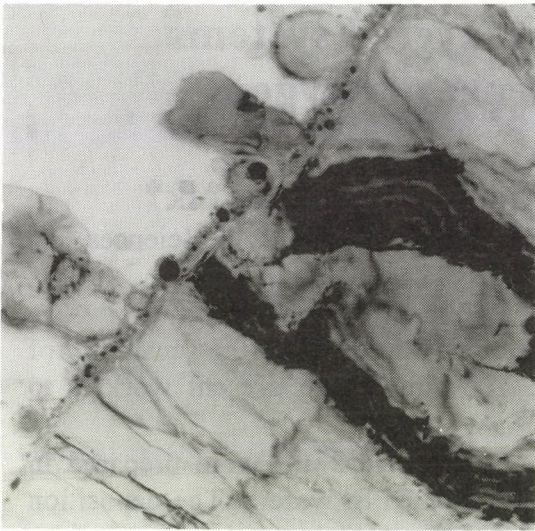


Figure 1 Cross sectional (XTEM) image of the film prepared by Al and Sn codeposition at 470 K substrate temperature and $5 \cdot 10^{-3}$ Pa oxygen partial pressure.

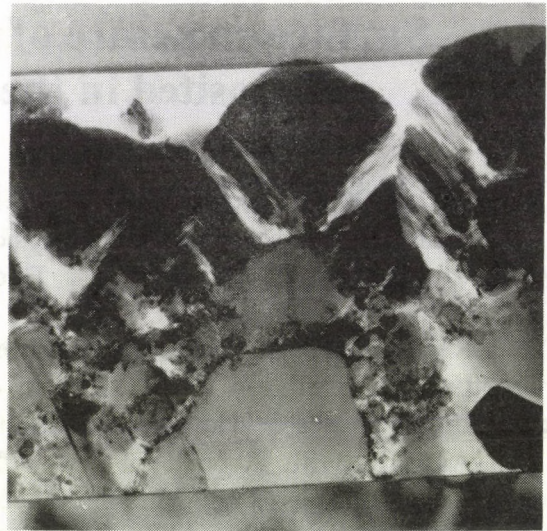


Figure 2 Cross sectional (XTEM) image of the Al film prepared by Al and Sn codeposition on oxidized Si substrate at 470 K substrate temperature and 10^{-2} Pa oxygen partial pressure.

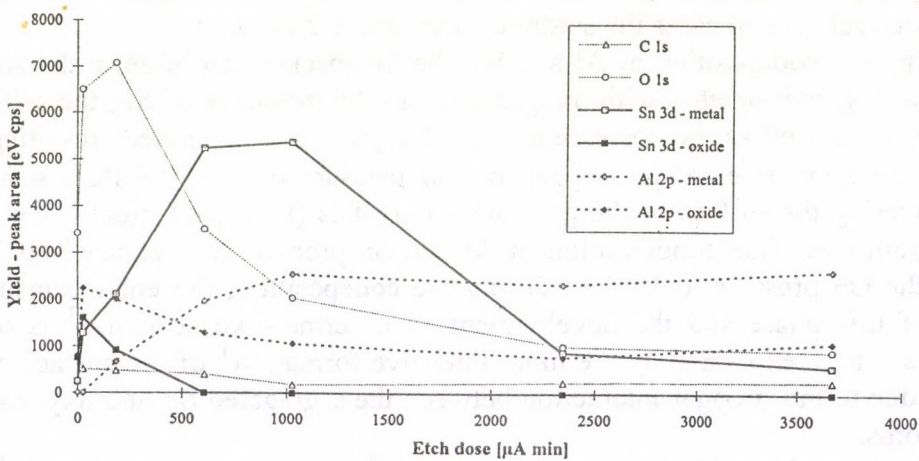


Figure 3 XPS depth profile of sample 1 (prepared at $P_{O_2} \sim 5 \cdot 10^{-3}$ Pa).

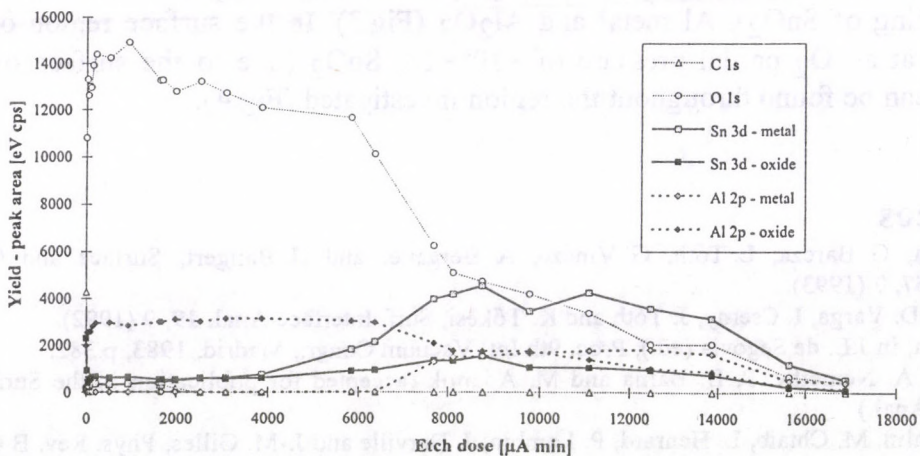


Figure 4 XPS depth profile of sample 2 (prepared at $P_{O_2} \sim 1.3 \cdot 10^{-2}$ Pa).

Measurement of excitation function of $^{nat}\text{B}(p, x)^7\text{Be}$ nuclear reaction for application in wear measurements

F. Ditrói, A. Fenyvesi, S. Takács, F. Tárkányi, J. Bergman*, S.-J. Heselius*, O. Solin*

* Åbo Akademi Accelerator Laboratory, Porthansg. 3-5, SF 20500 Turku 50, Finland

Boron of natural composition was irradiated to measure the cross section function of the $^{nat}\text{B}(p, x)^7\text{Be}$ nuclear reaction. The reaction is very important from the point of view of Thin Layer Activation (TLA) technique to monitor the wear of boron containing superhard materials (e.g. BN)[1]. The aim was to determine the cross sections of the above reaction in the energy region used in wear measurements because practically there are no cross section data available below 10 MeV for these reactions.

The irradiations were performed by using stacked foil technique. The targets were prepared from Ni-B-Si (78.0 %, 14.0 % and 8 % respectively) metallic glass foils (manufactured by Goodfellow) with a thickness of 25 μm . The composition of the foil was checked by using PIXE and REA analysis. Aluminium foils of 50 μm thickness were inserted into the stack for separation the target foils and for covering the whole energy range. Copper foils of 10 μm thickness were used to monitor the beam current and energy in different depths of the stack.

The irradiations were performed at 18.0, 14.5 and 12.0 MeV incident proton-energies on an MGC-20 type isochronous cyclotron. The irradiation times took about two hours at 200 nA beam current.

Standard high resolution gamma spectrometry was used to measure the activity of ^7Be produced in the target foils. The correct impact energies at each foil were calculated, and the cross section at a given energy was derived from the activity of the given foil. A smooth curve was fitted on the measured data, and the results were compared with the available cross section data and tick target yield published in literature.

1. F.Ditrói, S.Takács, L.Vasváry, I.Mahunka, under publication in NIMB

Remeasurement and Compilation of Excitation Function of Proton Induced Reactions on Iron for Activation Techniques

S. Takács, L. Vasváry and F. Tárkányi

The knowledge of the quantity of the produced radioisotopes and secondary particles is very important for various practical applications of the charged particle accelerators: thin layer activation technique (TLA) for monitoring and measuring wear and corrosion, nuclear safety, charged particle activation analysis, flux and energy monitoring of bombarding beams, production of radioisotopes for medical and other applications, production of radioactive particle beams. These applications require the use of special standards, or knowledge of relative distribution of the produced activity. However, in several applications (e.g. monitoring of the flux of charged particle beams, radioisotope production, radiation safety work) absolute values are necessary.

Excitation functions of proton induced reactions on $^{nat}\text{Fe}(p,n)^{56}\text{Co}$ have been remeasured in the energy region up to 18.0 MeV using stacked foil technique and standard high resolution gamma-ray spectrometry at the Debrecen MGC-20E cyclotron. Compilation of the available data measured between 1959 and 1993 has been made. The corresponding excitation functions have been reviewed, critical comparison of all the available data was done to obtain the most accurate data set.

The feasibility of the evaluated data set was checked by reproducing experimental calibration curves for TLA by calculation (Fig. 1).

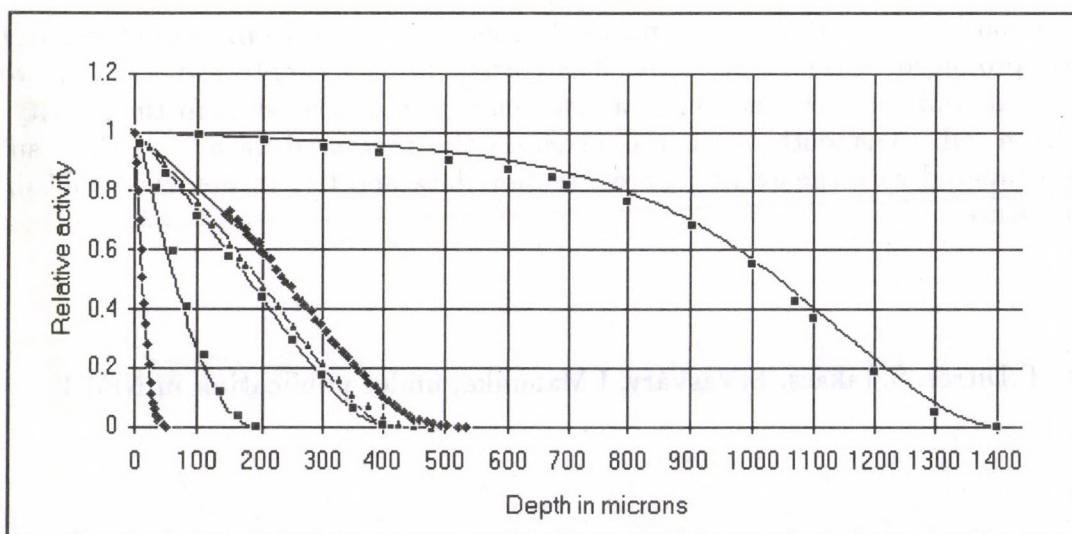


Figure 1. Measured calibration curves for iron at different incident proton energies and calculated curves (solid) based on the recommended values of the excitation function of the $^{nat}\text{Fe}(p,n)^{56}\text{Co}$ reaction.

Study of Static and Dynamic Effects in Gas Targets

F. Tárkányi, S. Takács, S-J. Heselius*, O. Solin*
and J. Bergman*

* Accelerator Laboratory, Åbo Akademi, Porthansgatan 3-5, SF-20500 Turku, Finland

Beam shape in equilibrium state

Several experimental methods have been developed to study the interaction of charged particles with gaseous material on the basis of measurement of the activity of the produced radioisotopes, secondary neutrons, heat, charge, emitted light and change of density, temperature, refractory indexes, etc. The video technique and charge distribution measurement used allowed us to study both the transient effects and the equilibrium state of the penetrating beam in gaseous targets at horizontal and vertical arrangements.

In the present work a target chamber equipped with plexiglass window for optical study and with an isolated electrode for charge collection was used to study the emitted

light and the charge distribution along the beam axes simultaneously. The charge was integrated at a given position along the chamber at different angles in a plane perpendicular to the beam direction to confirm the asymmetry of the horizontal beam observed earlier. The measured charge distribution was found to be asymmetric in good agreement with the optical studies (see Fig.1).

The symmetric distribution of the emitted light at vertical irradiation position is clearly seen in Figure 2. in accordance with the expectation, i.e. due to symmetric upward mass transport and symmetric density reduction in vertical irradiation position.

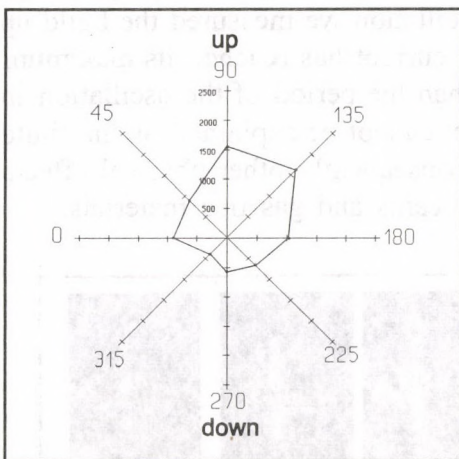


Figure 1. Angular distribution of the collected charge in a plane perpendicular to the beam axes at horizontal irradiation arrangement.

Investigation of dynamic effects

The transient effect of the first period of the interaction of charged particle beams with the target gas was investigated both at horizontal and vertical irradiation arrangements. The process was investigated by recording the emitted light with a videocamera. The recorded pictures were digitized and evaluated with commercial image processing programs. The penetration of the beam was followed continuously from the very first impact after opening the beamstop. The beam current and the target pressure were recorded simultaneously. Figures 2 and 3 present the views of light emission for the first 1 sec period of time at horizontal and vertical beam arrangements respectively. From the detailed analysis of the records the following conclusions can be drawn.

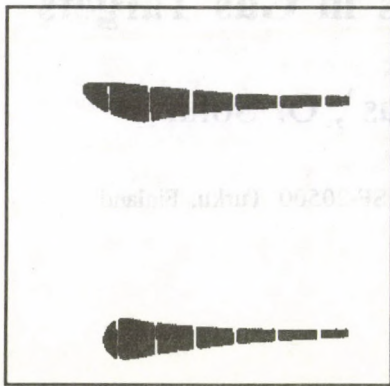


Figure 2. The shape of proton beam at horizontal and vertical irradiation arrangements ($E_p=8$ MeV, $I_p=5.8$ μ A, target=Ar, initial pressure=7 bar).

In vertical irradiation geometry the early round shape changes to an arrow form and then takes up a round shape again.

With measuring the pressure no oscillation was found. The time scale of the oscillations of the range was in seconds and the used pressure transducer was linear up to 3 kHz.

The optically observed range oscillation was verified and reproduced by charge measurement. Searching the reason of the observed oscillation we measured the build up of the beam current on solid target in time. The beam current has reached its maximum during a much shorter period of time on solid target than the period of the oscillation in gaseous target, therefore, the observed oscillation effect cannot be explained by the finite speed of the beamstop, opening the way of the beam, consequently other physical effects may participate in the interaction of charged particle beams and gaseous materials.

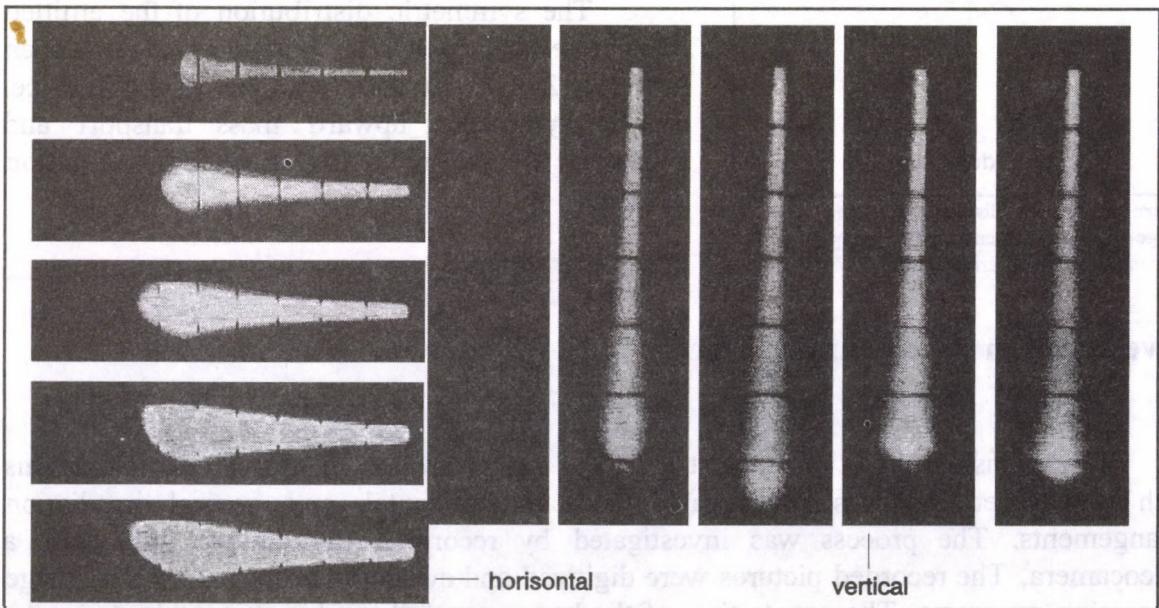


Figure 3. Change of the beam shape during the first few seconds time period at horizontal (left) and at vertical (right) beam arrangement (1, 5, 15, 30, 60 frames $\Delta t=1/24$ sec/frame).

Progress Report on Nuclear Data for Application

F. Tárkányi, S. Takács, F. Szelecsényi, Z. Kovács, Z. Szűcs,
T. Molnár, A. Fenyvesi and F. Ditrói

During 1993 significant progress has been made in the development of new experimental facilities, in measurement of new nuclear data and in the collection and analysis of the published data related to practical application.

Development of methods and instruments

Development of an automatic sample changer has been started for automatic measurement of gamma spectra of series of targets irradiated at the cyclotron. The aim of the work is to assure more economic use of the cyclotron, the measuring equipment and the manpower.

A new beam line and a new monoenergetic neutron source has been installed, in collaboration with Kossuth L. Univ., which gives new and upgraded possibilities for measurements of nuclear data of neutron induced reactions.

New experimental results

Investigation of proton and deuteron induced reactions on natural Te and ^{122}Te have been started for production of ^{123}I and ^{124}I .

Excitation functions of proton induced reactions on enriched ^{124}Te have been measured for optimisation of production of ^{124}I in collaboration with the Institute of Nuclearchemie, Forschungszentrum Jülich GmbH, Jülich, FRG.

Measurement for determination of cross sections of $^{121}\text{Sb}(\alpha, n)^{124}\text{I}$ nuclear reaction has been performed to investigate it as an alternative production route of ^{124}I .

To monitor the wear of boron containing materials the cross section of the $^{10}\text{B}(p, x)^7\text{Be}$ nuclear reaction has been studied in collaboration with the Accelerator Laboratory of the Abo Akademi, Turku, Finland.

Dynamic effects of the interaction of high intensity charged particle beam with thick gas targets was studied in collaboration with the Accelerator Laboratory of the Abo Akademi, Turku, Finland.

To complete the data-base and to resolve the contradictions in the cross-section/yield data, measurement of the excitation functions has been started for $^{66}\text{Zn}(p,n)^{66}\text{Ga}$, $^{67}\text{Zn}(p,2n)^{66}\text{Ga}$, $^{68}\text{Zn}(p,3n)^{66}\text{Ga}$ and $^{68}\text{Zn}(p,2n)^{67}\text{Ga}$ nuclear reactions in collaboration with the cyclotron Laboratory of the Mount Sinai Medical Center, Miami Beach, USA.

Data compilation and evaluation

In collaboration with the IAEA Nuclear Data Group the evaluation of cross sections of the charged particle induced reactions in the EXFOR format has been continued.

Compilation and evaluations of the total cross sections of proton induced nuclear reactions on ^{66}Zn , ^{67}Zn , ^{68}Zn and on natural Zn targets have been performed to provide a consistent and well documented set of cross section data for routine isotope production, nuclear analytical and wear measurements in collaboration with the Cyclotron Laboratory of Mount Sinai Medical Center, Miami Beach, USA.

Compilation and evaluations of the cross sections and thick target yields data for production of medically important cyclotron produced ^{111}In radioisotope via light charged particle induced nuclear reactions were performed in collaboration with the Cyclotron Laboratory of Mount Sinai Medical Center, Miami Beach, USA.

Wear measurement with implantation of radioactive nuclei into plastic and ceramic materials

F. Ditrói, I. Mahunka

It is possible to measure and follow the wear of different materials containing such elements in major or trace constitution, which can be easily activated by using the available accelerators [1]. In this case the tracing radioactive nucleus is generated from the sample material itself. Depending on the constitution of the sample with a relative short irradiation time and low beam intensity a very long measuring period can be produced.

In other cases, when the material of the sample can not be so easily activated, the method of implantation of radioactive nuclei can be used. These materials are the plastics and some types of ceramics, which are nowadays widely used in machinery and as structural material. Their wear, corrosion and erosion must be also measured and tested in different circumstances.

The implantation can be so performed, that a thin foil is placed in front of the sample, containing the suitable element for producing the chosen radioactive nucleus. The type and energy of the bombarding particle must be chosen so, that the reaction, producing the radioactive nucleus could be performed at an appropriate yield, and because of the kinematic effect of the collision an appropriate part of the produced radioactive nuclei could be hit out from the foil and reach the surface of the sample with a proper impact velocity. To avoid the direct beam-impinge on the sample surface a beam-stop must be used in zero degree direction. Only the projectiles scattered in an angle larger than the angle determined by the beam-stop geometry can hit the sample-surface. The whole implantation must be performed in high-vacuum because of the short range and big stopping power of the heavy projectiles. The produced activated area because of the beam-stop will be a ring, the radius of that depends on the sizes of the beam-stop and the distances between the sample, the implantation foil and the beam-stop.

The produced activity in the sample generally lower than that with direct activation, but because of the nature of the implantation it contains no disturbing radiation.

1. F.Ditrói, S.Takács, L.Vasváry, I.Mahunka, under publication in NIMB

Investigation of Silicon with (p,p') resonance scattering in $\langle 110 \rangle$ direction

F. Ditrói¹, J.D. Meyer*, R. Michelmann*, D. Kislat*, K. Bethge*

*Institut für Kernphysik der Universität Frankfurt

Crystalline Silicon samples were investigated both in channeling and random directions by using the (p,p') resonance scattering at 2.3 MeV bombarding energy. The samples were positioned in the scattering chamber of VdG accelerator after 2 m collimating path. The channeling direction was adjusted using 1.4 MeV ⁴He particles. The backscattering spectra were measured in 156° direction with surface barrier semiconductor detector. The peaks due to the resonance at 2.1 MeV were measured at different angles in the vicinity of the channeling and random directions.

A peak shift and broadening was seen at the channeling and near channeling directions compared with the random one. The spectra were also simulated using our modified Monte-Carlo calculation method for stopping, range and energy distribution in highly ordered materials. The capability of the method was tested on single range and distribution calculation at the MeV energy range. The experimental spectra were simulated using this method, and the energy shift and the broadening between the random and the channeling spectra were compared and explained.

It was determined that the resonance-peak moves downwards by reaching the perpendicular impact (0° impact angle = channeling direction) and it becomes wider at the same time. This phenomenon can be explained by using our theory for the channeling energy loss of charged particles in crystals [1, 2, 3]. The dependence of the energy distribution after a given path in the material from the impact angle has been proved with these experiments and simulations. The plot of the calculated spectra is seen in Fig. 1., the angles between 0°-1° are inside of the channeling dip, the 8° considered as random direction.

¹This work was partly supported by the Alexander von Humboldt Foundation

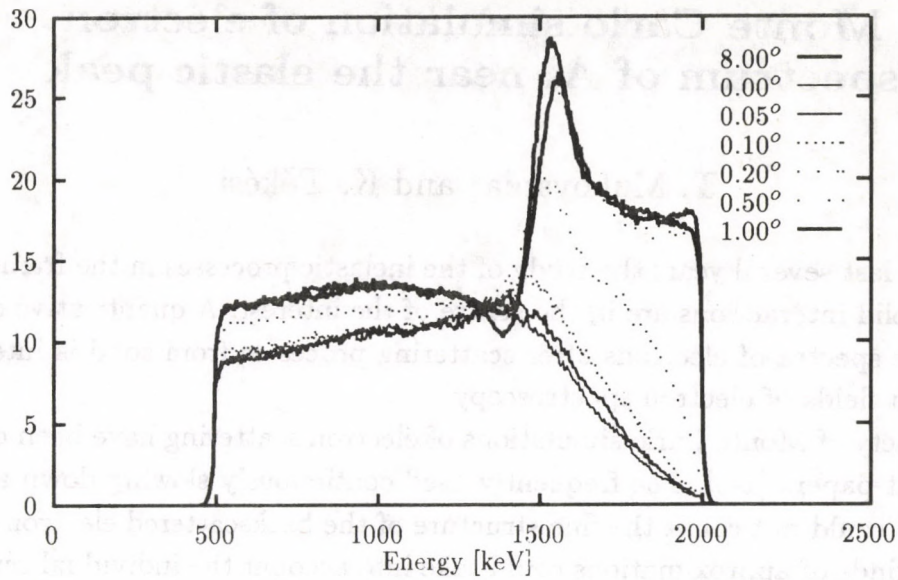


Fig. 1 Calculated resonance backscattering spectra from 2.3 MeV proton Bombardment of Si crystals in different near-channeling and random directions (0° - 8°).

1. F.Ditrói, J.D.Meyer, R.W.Michelmann, D.Kislat, K.Bethge, ATOMKI Annual Report, 1992. p. 78.
2. F.Ditrói, J.D.Meyer, R.Michelmann, D.Kislat, K.Bethge, under publication in NIMB
3. J.D.Meyer, R.W.Michelmann, F.Ditrói, K. Bethge, under publication in NIMB

Monte Carlo simulation of electron spectrum of Al near the elastic peak

T. Mukoyama^a and K. Tókési

In the last several years the study of the inelastic processes in the frame of the electron solid interactions are in the centre of the interest. A quantitative description of the spectra of electrons after scattering processes from solid is interesting in different fields of electron spectroscopy.

A variety of Monte Carlo simulations of electron scattering have been describe in different papers [1-8]. The frequently used continuously slowing down approximation [6] could not count the fine structure of the backscattered electrons. Many different kinds of approximations could take into account the individual scattering processes, for example Shimizu et al. [1] described one way which was used in our study [9].

Our goal is to define the complete inelastic processes which can describe the magnitudes and the shapes of the inelastic peaks near the elastic peak. Our investigation goes up to cc. 100 eV from the elastic peak. In this region the results of the calculation are very sensitive to the computation methods used. The calculation was made at 5000 eV primary electron energy in amorphous aluminium sample.

Fig. 1 shows the calculated and the measured electron spectra. It is clear from the figure that the present model can well reproduce the magnitude and the shape of the experimental electron peaks. The small discrepancy between the calculated and the measured position of the plasmon peaks is ascribed to the difference between the calculated and measured plasmon energies.

Acknowledgements

This work was performed under the Japanese-Hungarian Cooperative Research Project.

References

^a *Division of States and Structures, Institute for Chemical Research, Kyoto University, Uji, Kyoto, 611 Japan*

1. R. Shimizu, Y. Kataoka, T. Ikuta, T. Koshikawa and H. Hashimoto; *J. Phys. D: Appl. Phys.*, Vol.9 (1976) 101
2. F. Salvat, J.D. Martinez, R. Mayol and J. Parellada; *J. Phys. D: Appl. Phys.* 18.(1985) 299
3. J.D. Martinez, R. Mayol, and F. Salvat; *J. Appl. Phys.* 67 (6), (1990) 2955
4. A. Desalvo, A. Parisini and R. Rosa; *J. Phys. D: Appl. Phys.* 17(1984) 2455
5. A. Desalvo and R. Rosa; *J. Phys. D: Appl. Phys.* 20 (1987) 790
6. M. Kotera, K. Murata, and K. Nagami; *J. Appl. Phys.* 52(2) (1981) 997

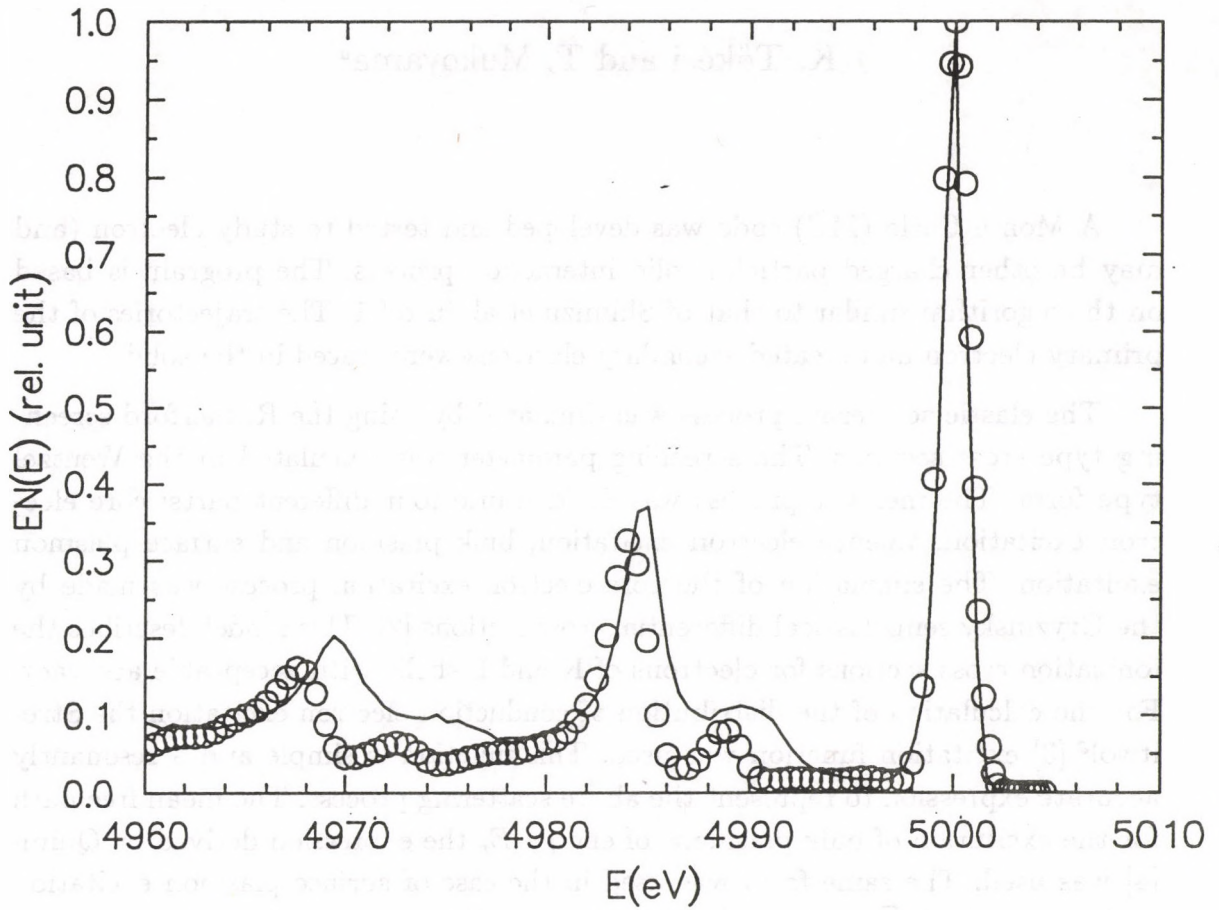


Fig. 1. EN(E) spectra of the amorphous aluminium sample near the elastic peak. — measured by Némethy with ESA-31 electrospectrometer [10] ; ○ calculated (The spectrum was convoluted for finite relative energy resolution: $E_p=5$ keV and $\Delta E/E=0.035$ %.)

7. Z. J. Ding and R. Shimizu; Surf. Sci. 222(1989) 313
8. Z.J. Ding, and R. Shimizu; Surf. Sci. 197(1988) 539
9. K. Tókési and T. Mukoyama, Present volume
10. A. Némethy, private communications

Monte Carlo code for the study of charged particle-solid interaction

K. Tőkési and T. Mukoyama^a

A Monte Carlo (MC) code was developed and tested to study electron (and may be other charged particle) solid interaction process. The program is based on the algorithm similar to that of Shimizu et al. in ref 1. The trajectories of the primary electron and created secondary electrons were traced in the solid.

The elastic scattering process was simulated by using the Rutherford screening type cross sections. The screening parameter was calculated in the Wentzel type form. The inelastic process was divided into four different parts: core electron excitation, valence electron excitation, bulk plasmon and surface plasmon excitation. The simulation of the core electron excitation process was made by the Gryzinsky semiclassical differential cross sections [2]. This model describes the ionization cross sections for electrons of K and L shells with acceptable accuracy. For the calculation of the distribution of conduction electron excitation the Streitwolf [3] excitation function was used. This function is simple and a resonantly accurate expression to represent the above scattering process. The mean free path for the excitation of bulk plasmons of energy E_p the expression derived by Quinn [4] was used. The same form was used in the case of surface plasmon excitation with energy $E_p/\sqrt{2}$ as in a bulk plasmon excitation.

The angular deflection of the particle track in each scattering event is specified by the polar and azimuthal scattering angle, θ and ϕ , defined as usual, i.e. as seen in the reference frame with the polar axis parallel to the velocity of the particle before the interaction. Each collision in the specimen is determined by 5 random number. By the help of these random numbers the following parameters were described: 1. the point of interaction, 2. the collision type, 3. the azimuthal angle, 4. the spherical angle, 5. the energy loss (if the observed collision is inelastic). The Fig. 1 shows the flow diagram of the calculation.

Acknowledgements

This work was performed under the Japanese-Hungarian Cooperative Research Project.

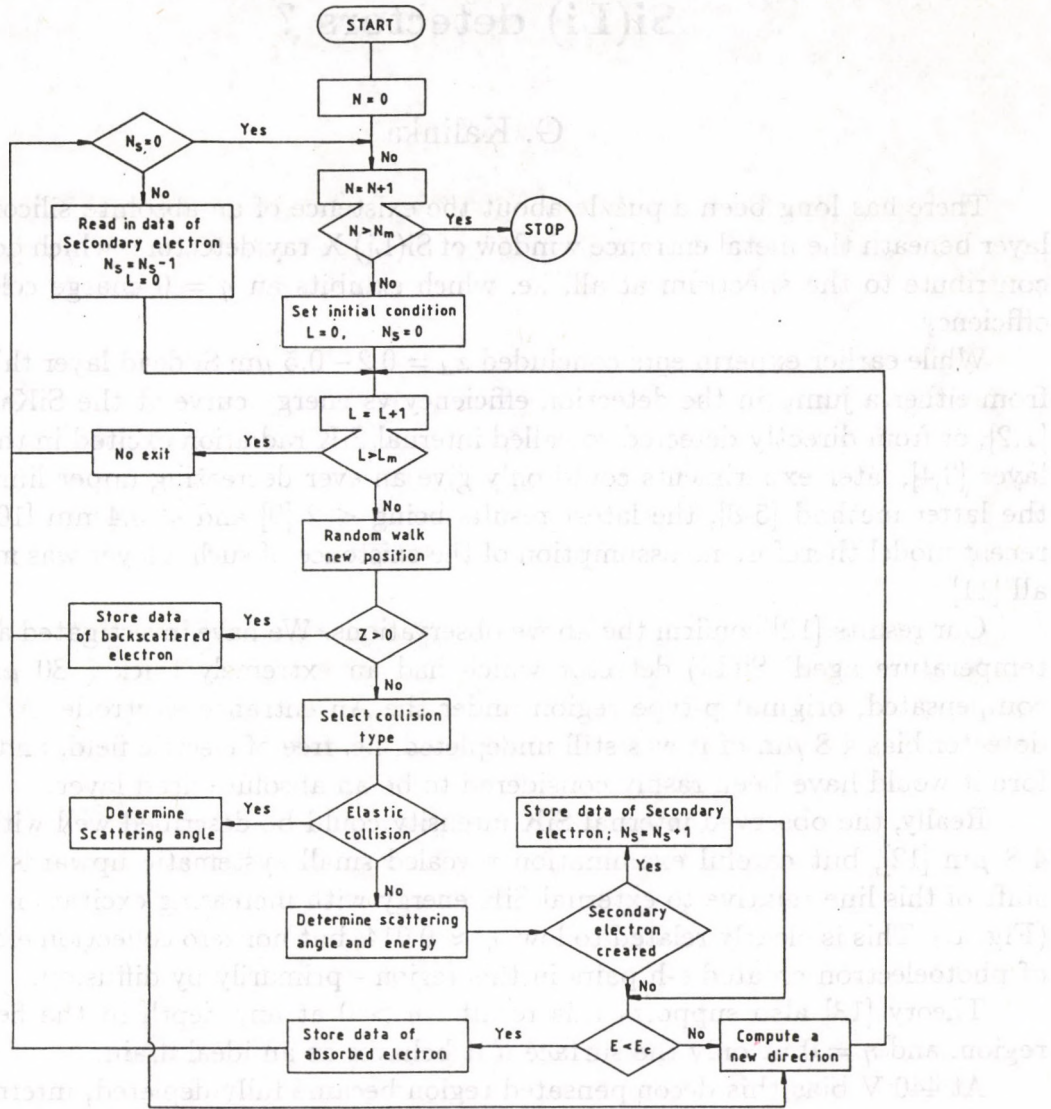


Fig. 1. Flow diagram of the Monte Carlo program which simulate the primary electron and secondary electron trajectories. N and L denote the number of histories and the number of steps of the tracing electron, respectively, N_m and L_m are their maximum values. N_s is the number of secondary electrons. z is the depth of the tracing electron, E is the kinetic energy of the electron and E_c is the cut-off energy.

References

^a Division of States and Structures, Institute for Chemical Research, Kyoto University, Uji, Kyoto, 611 Japan

1. R. Shimizu, Y. Kataoka, T. Ikuta, T. Koshikawa and H. Hashimoto; J. Phys. D: Appl. Phys. 9 (1976) 101
2. M. Gryzinski; Phys. Rev. 138 (1965) A336
3. H.W. Streitwolf; Ann. Phys. Leipzig 3 (1959) 183
4. J.J. Quinn; Phys. Rev. 126 (1962) 1453

Does really exist absolute dead layer in Si(Li) detectors ?

G. Kalinka

There has long been a puzzle about the existence of an absolute silicon dead layer beneath the metal entrance window of Si(Li) X-ray detectors, which does not contribute to the spectrum at all, i.e. which exhibits an $\eta = 0$ charge collection efficiency.

While earlier experiments concluded $x_d = 0.2 - 0.5 \mu\text{m}$ Si dead layer thickness from either a jump in the detection efficiency vs energy curve at the SiK α edge [1,2], or from directly detected so called internal SiK radiation excited in the dead layer [3,4], later experiments could only give an ever decreasing upper limit with the latter method [5-8], the latest results being < 2 [9] and $< 0.4 \text{ nm}$ [10]. In a recent model therefore no assumption of the existence of such a layer was made at all [11].

Our results [12] confirm the above observations. We have investigated a 'room temperature aged' Si(Li) detector which had an extremely thick ($80 \mu\text{m}$) decompensated, original p-type region under the Au entrance electrode. At 300 V detector bias $4.8 \mu\text{m}$ of it was still undepleted, i.e. free of electric field, and therefore it would have been rashly considered to be an absolute dead layer.

Really, the observed internal SiK intensity could be described well with $x_d = 4.8 \mu\text{m}$ [12], but careful examination revealed small systematic upwards energy shift of this line relative to external SiK energy with increasing excitation energy (Fig. 1.). This is clearly related to low, $\eta \approx 0.014$, but nonzero collection efficiency of photoelectron created e-h pairs in this region - primarily by diffusion.

Theory [13] also supports this result : $\eta > 0$ at any depth in the field free region, and $\eta = 0$ at only the surface if it behaves as an ideal drain.

At 440 V bias this decompensated region became fully depleted, internal SiK intensity reduced to zero, and its energy tended to reach primary excitation energy, i.e. η approached its bulk value. At even higher voltages, a situation typical of a good quality detector, no field free region, consequently no absolute dead layer exists any more !

References

1. J.M. Jaklevic and F.S. Goulding, IEEE Trans. Nucl. Sci. **NS-18**,No.1(1971)187
2. R.G. Musket and W. Bauer, Nucl. Instrum. Meth. **109** (1973)593
3. P.J. Statham, PhD Thesis, University of Cambridge, 1975
4. P.J. Statham, J. Phys. E.: Sci. Instrum. **9**(1976)1023
5. W. Maenhaut and H. Raemdonck, Nucl. Instrum. Meth. **B1**(1984)534
6. A.J. Craven, P.F. Adam and R. Howe, Proc. EMAG '85, Inst. Phys. Conf. Ser. No.78, Adam Hilger, 1985, p.189.
7. J.L. Campbell and P.L. McGhee, Nucl. Instrum. Meth. **A248** (1986)393

8. M. Geretschläger, Nucl. Instrum. Meth. **B28**(1987)289
9. J.L. Campbell and J.-X. Wang, X-Ray Spectrom. **20**(1991)191
10. S.M. Brodskiy, Atomn. Energ. **72**(1992)575
11. S. Goto, Nucl. Instrum. Meth. **A333**(1993)452
12. G. Kalinka, submitted to Nucl. Instrum. Meth. **B**
13. G.R. Hopkinson, Nucl. Instrum. Meth. **216**(1983)423

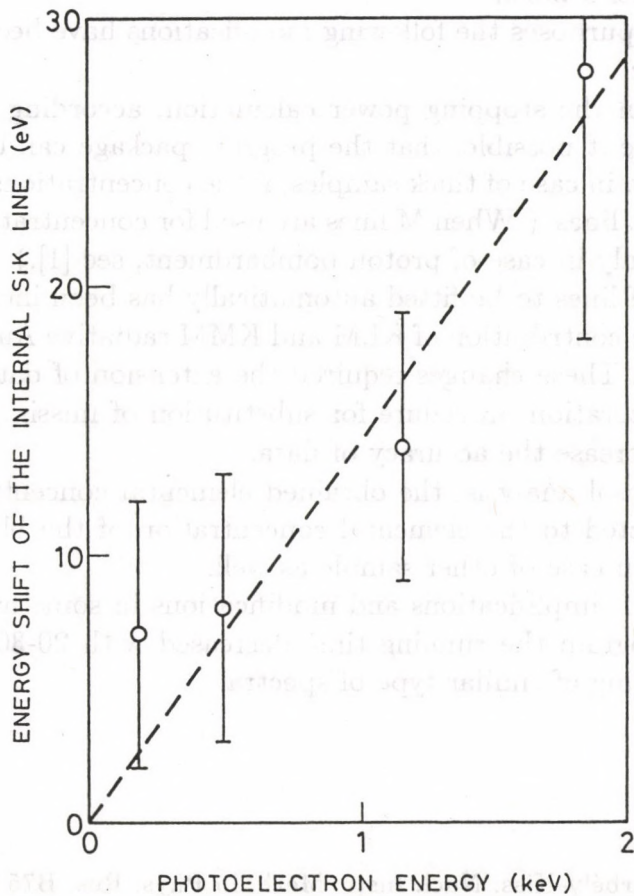


Fig. 1. Shift of the internal SiK energy versus created photoelectron energy in the case of 4.8 μm thick undepleted region underneath the Au entrance electrode of a Si(Li) detector.

Modifications in PIXYKLM Program Package

Gy. Szabó, I. Borbély-Kiss

The PIXYKLM program package, described in [1] and [2] has been improved on the bases of our experience obtained during the analyses of high number of samples last year. Changes were done to extend the applicability of the program, to increase the authenticity of concentration data and "goodness" of the fit, moreover to make easier the user's work.

To achieve these purposes the following modifications have been performed in the program package:

1. The changes in the stopping power calculation, according to the method described in [3], made it possible, that the program package can be used for any kind of projectile even in case of thick samples, if the concentrations are calculated on the bases of K or L lines. (When M lines are used for concentration calculation, the program works only in case of proton bombardment, see [1].)

2. The number of lines to be fitted automatically has been increased for both K and L lines and the contribution of KLM and KMM radiative Auger process has been considered, too. These changes required the extension of data base and the modification of the iteration procedure for substitution of missing data (in some cases), in order to increase the accuracy of data.

3. In case of aerosol analysis, the obtained elemental concentrations can automatically be corrected to the elemental concentration of the blank filter. This process can be used in case of other sample as well.

In consequence of simplifications and modifications in some numeric process, performed in the program the running time decreased with 20-30%, specially in case of successive fitting of similar type of spectra.

References

1. Gy. Szabó, I. Borbély-Kiss: Nucl. Instr. Meth. in Phys. Res. B75 (1993) 123.
2. Gy. Szabó, I. Borbély-Kiss: ATOMKI Annual Report (1992) 84.
3. I.F. Ziegler, I.P. Biersack, U.Littmark, The Stopping and Range of Ions in Solids, in Stopping and Ranges of Ions in Matter (Ed.: I.F. Ziegler) Vol.1. Pergamon Press, 1985.

Production and Magnetic Properties of Nanocrystalline Fe and Ni

L. Daróczy *, D.L. Beke *, G. Posgay * and M. Kis-Varga

*Department of Solid State Physics, L. Kossuth University, 4010 Debrecen, P.O. Box 2., Hungary

The nanostructured materials and their properties are widely studied in the last years. Different methods of their synthesis result in materials with promising features. These are manifested in magnetic behaviour too, and their study is one of the most important topics of recent investigations [1-8].

The magnetic properties of pure nanocrystalline iron [9] and nickel, produced by ball milling and by heavy cold deformation was investigated by magnetization measurements at low temperatures and by Barkhausen-noise technique at room temperature as well.

Powders with different grain size were produced in a vibratory ball mill under vacuum. The average grain size (D) was measured by X-ray diffractometry with CuK_{α} radiation using a double peak Warren-Averbach analysis [10], and with MoK_{α} radiation using Voigt functions for profile fitting [11].

The bulk samples were prepared by combining cold rolling (using a profile roll) and torsional deformation of the pure element wires.

The magnetization measurements of powdered samples showed that the saturation magnetization is independent of the grain size and the temperature, which is in contrast to the results described in [1].

The results of the Barkhausen-noise experiments on powders are shown in Fig. 1 and Fig. 2. The coercitive force (H_c) of Fe and Ni shows different behaviour as the grain size decreases but their saturation values are close to each other. The sharp decrease of H_c for Ni at small D values is in agreement with the random anisotropy model [12] according to which the magnetic softening starts where D is comparable with the domain wall thickness d ($d_{Ni} > d_{Fe}$). The saturation values of the Barkhausen-noise (MBN) have a maximum in the grain size region of 10-100 nm. In case of Fe however, a saturation-like curve is also possible, because the high MBN values may be caused by texture.

In case of cold rolled samples the change of H_c with the grain size is much more less, and the MBN shows an inverse and more moderate change with the grain size as compared to the ball milled powders. This behaviour is probably related to the texture produced by rolling.

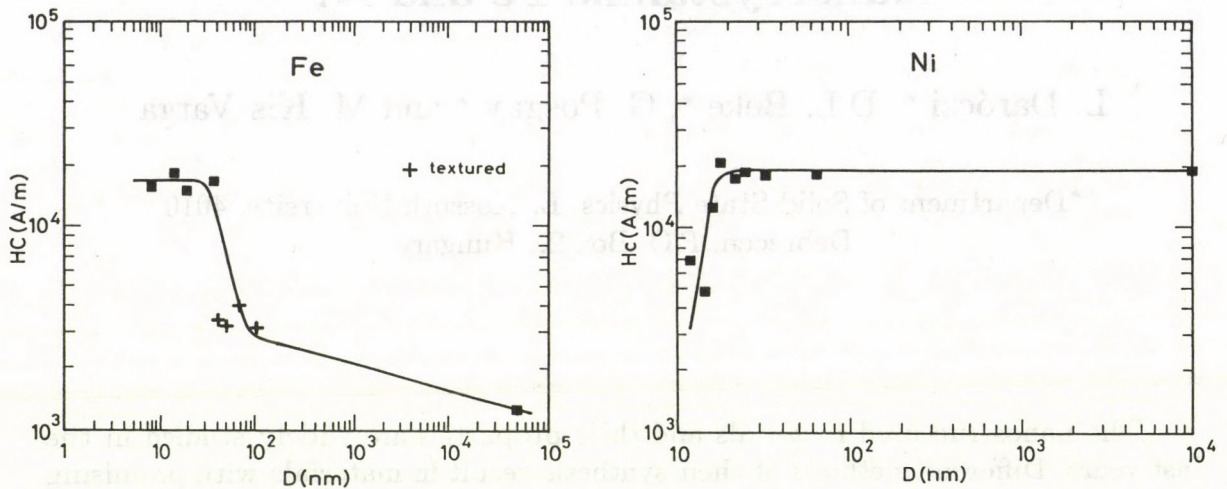


Fig. 1. The coercive forces of Fe and Ni as a function of the grain size.

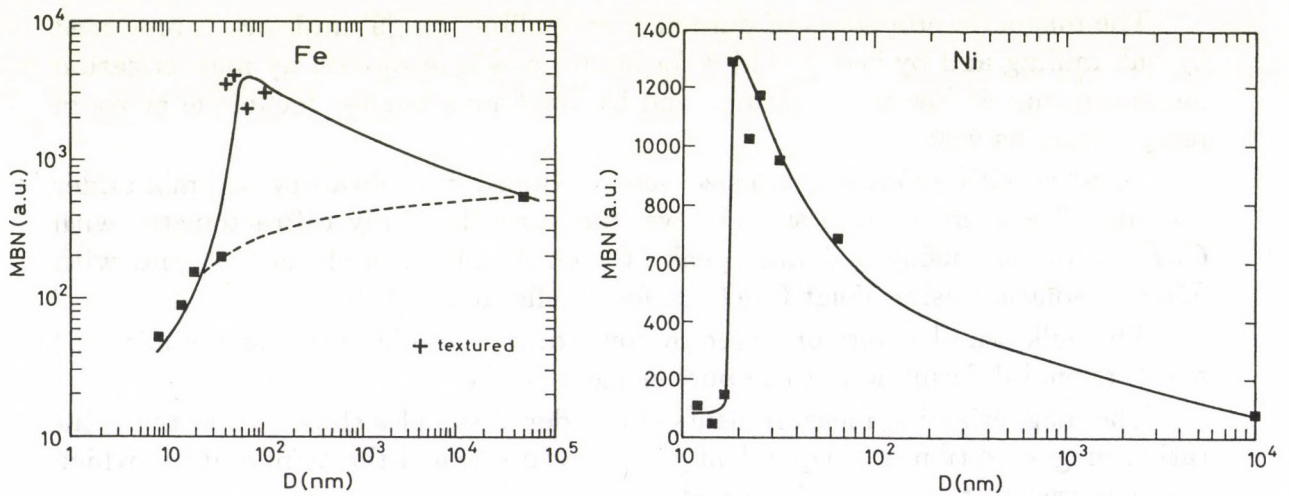


Fig. 2. The saturation values of Barkhausen-noise as a function of the grain size.

References

1. H. Gleiter, *Nanostructured Materials* **1** (1992) 1
2. H.-E. Schaefer et al., *Nanostructured Materials* **1** (1992) 523
3. S. Gangopadhyay et al., *J. Appl. Phys.* **70**(10) (1991) 15
4. S. Gangopadhyay et al., *Nanostructured Materials* **1** (1992) 449
5. Huang Ying Kai, PhD Thesis, University of Amsterdam
6. C.R. Albedo and P.W. Selwood, *J. Appl. Phys.* **32** (1961) 229S
7. G. Herzer, *Journal of Magnetic Materials* **112** (1992) 258
8. V.A. Pavlov, *Phys. of Met. and Metall.* **59**(4) (1985) 1
9. L. Daróczy et al., *Nanostructured Mat.* **2** (1993) 515
10. H.P. Klug and L.E. Alexander, *X-Ray Diffraction Procedures*, John Wiley, New York (1974)
11. J. Végh, Thesis, Debrecen (1990)
12. G. Herzer, *Mat. Sci. and Engin.* **A133** (1991) 1

Electromagnetic response of Bi(Pb)SrCaCuO superconducting granular films

S. Mészáros, K. Vad, N. Hegman and G. Halász

Magnetic flux dynamics of vortex lattice in granular superconducting systems poses interesting questions of vortex lattice structure, order-disorder transition in the structure, chaotic dynamics, dynamical symmetry breaking, etc. HTSC thick films are good candidates to observe these phenomena. In our study screen-printed *Bi(Pb)SrCaCuO* HTSC films of film thickness of $30\ \mu\text{m}$ were used. Average grain size was $10\ \mu\text{m}$, so the film could be regarded as randomly arranged quasi-2D Josephson junction array. The superconducting phase was the 2232 with $T_c \sim 100\ \text{K}$. Static electric field generated in the superconducting film was systematically studied as a function of temperature, DC transport current density, external static magnetic field and external radiofrequency field. The DC magnetic field was changed from 0 to 5 T and the temperature from 4.2 K to 120 K. The external Rf field frequency ranged from 5 MHz to 500 MHz, its amplitude from zero up to $1\ \mu\text{T}$. The spatial average of electric field was determined from voltages measured in longitudinal and transversal directions relative to the DC transport current. The main features of electric field generation are:

Three different regimes can be distinguished on the current-voltage characteristics: the coherent state with zero longitudinal and transversal voltage, the paracoherent state with linear dependence of longitudinal voltage on excess current (displaced linear branch) and the resistive state. In the latter case excess fluctuation of longitudinal voltage at fixed external conditions was observed and interpreted as the chaotic flux dynamics in the biased Josephson junction network.

The voltage transversal to the transport current was observed (see fig 1.) and its sign change behaviour was established not only in the temperature range near T_c but at much lower temperatures, too. It was experimentally proved that the sign change is a universal feature of the transversal voltage in HTSC films.

Longitudinal DC voltage was observed if the sample was exposed to RF field. The basic effect of RF field was the modification of the static current-voltage characteristics. This modification is typically the increment of the DC voltage compared to values measured without RF irradiation. The most exciting feature however was that static DC voltage appears even in the absence of DC transport current as shown in fig 2. The explanation of this 'rectification effect' can be based on the inverse AC Josephson effect. The comparison of excitation frequencies and measured voltages point to a high degree of synchronization of individual Josephson oscillators in the granular system.

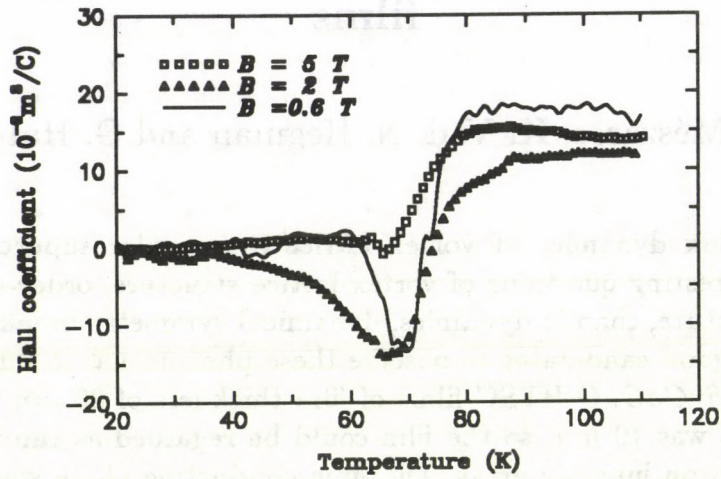


Fig. 1. Magnetic field and temperature dependence of the Hall coefficient of a screen-printed Bi(Pb)SrCaCuO film

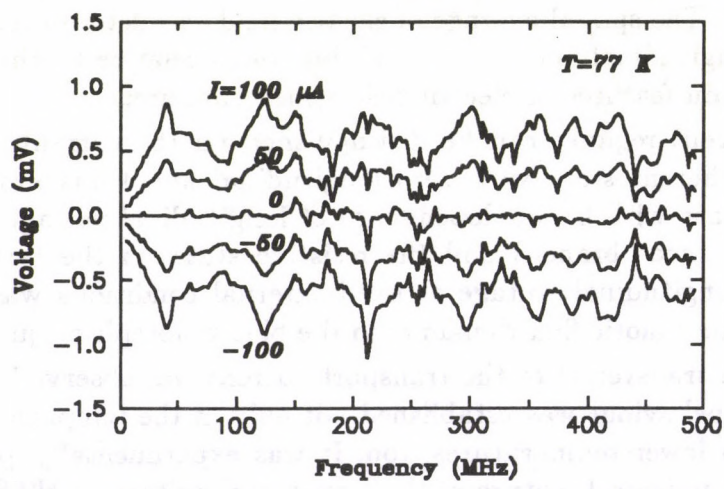


Fig. 2. Dependence of the DC voltage generated under RF irradiation on the excitation frequency at different (including zero) DC transport currents

References

1. S. Mészáros, K. Vad and N. Hegman, *Physica C* **218** (1993) 471.

EARTH AND COSMIC SCIENCES,
ENVIRONMENTAL RESEARCH

Mass spectrometric method for monitoring ecophysiological responses of reed

S.Bohátka, Gy. Lakatos*, M. Makádi* and M. Simon

*Department of Ecology, L. Kossuth University, Debrecen

The reed [*Phragmites Australis* (Cav.) Trin ex Steudel] is considered as a common species all the world over. In Hungary the reed stands of large extension can be found in the shorelines of the shallow lakes. These most important plant communities (*Scirpo-Phragmitetum*) in the littoral zone of shallow lakes play multifold role in the preservation of nature and environmental protection. The effectivity of reed belt in improvement of water quality and management is enhanced by the periphyton formed on the under-water parts of reed [1, 2].

Although it was already more than 20 years ago when reed decline was first observed in Hungary, serious damages have been reported since the early 80's and mostly on large lakes [3].

As the accelerated and large-scale reed decline is a great problem of environmental protection and nature reservation, many research institutes and scientists make efforts in this field [4, 5]. Since the main reasons of reed decline have not been revealed in details, simulation laboratory experiments are going on for the better understanding of the ecophysiological responses of reed species to different environmental conditions, and to search the most effective means in prevention of the deterioration processes in reed communities of our lakes.

An experimental method and instrumentation have been created in ATOMKI for the mass spectrometric measurement of gases in living plants [6, 7], and the method is applied for reed. The individuals are bred in perlite substrate in plastic boxes (45*20*15cm) placed in a phyto-chamber. Only water and Hutner nutrient are added. Optimizing propagation and breeding conditions as well as the adequate sampling process have been established. A quadrupole mass spectrometer is used to measure the gases in the living plants.

The analyser system is based on the equipment described earlier [8]. The mass spectrometer has been changed for a computer controlled quadrupole MS (type PCQ-300, ATOMKI). Mass scans in a preset range and single ion monitoring are available. Oxygen and CO₂ are the key components but N₂ and Ar are also monitored. The latter ones are used as normalizing factors in long measurements (several weeks or months), when signals are inevitably subjected to changes because of temperature variations and the usual drift of such systems.

Culms and rhizomes of the reed samples are drilled and the small probes (diameter 2mm) are introduced into the holes. Wounds are sealed with plaster to block gas exchange and water penetration through the holes. Probes are also located in the substrate. Intensive gas exchange is suspected between the plant and substrate. Intensive changes in O₂ and CO₂ are detected in the culms during light and dark periods due to photosynthesis and respiration (Fig.1 a and b). The

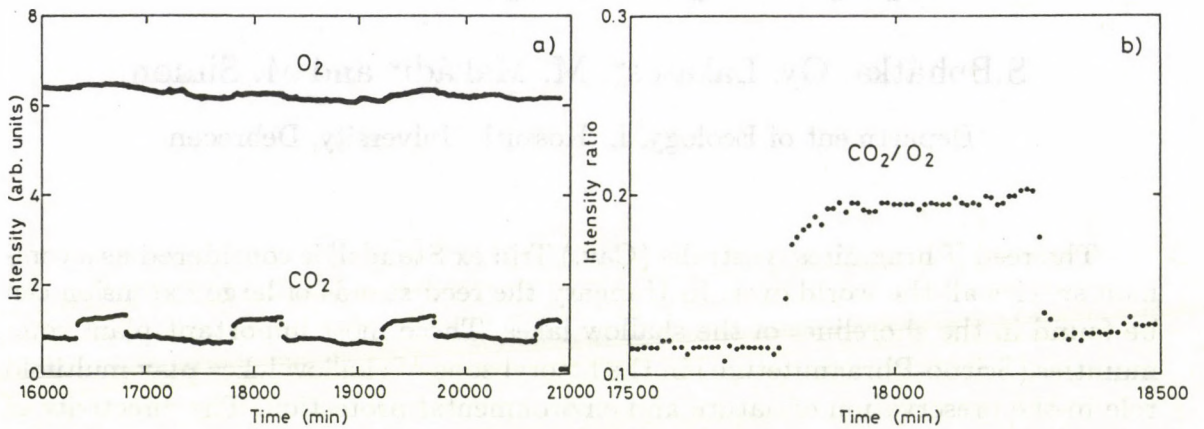


Fig. 1. Change of O₂ and CO₂ in the rhizome of the reed in successive light and dark periods (a), and calculated CO₂/O₂ ratio in a short time interval (b).

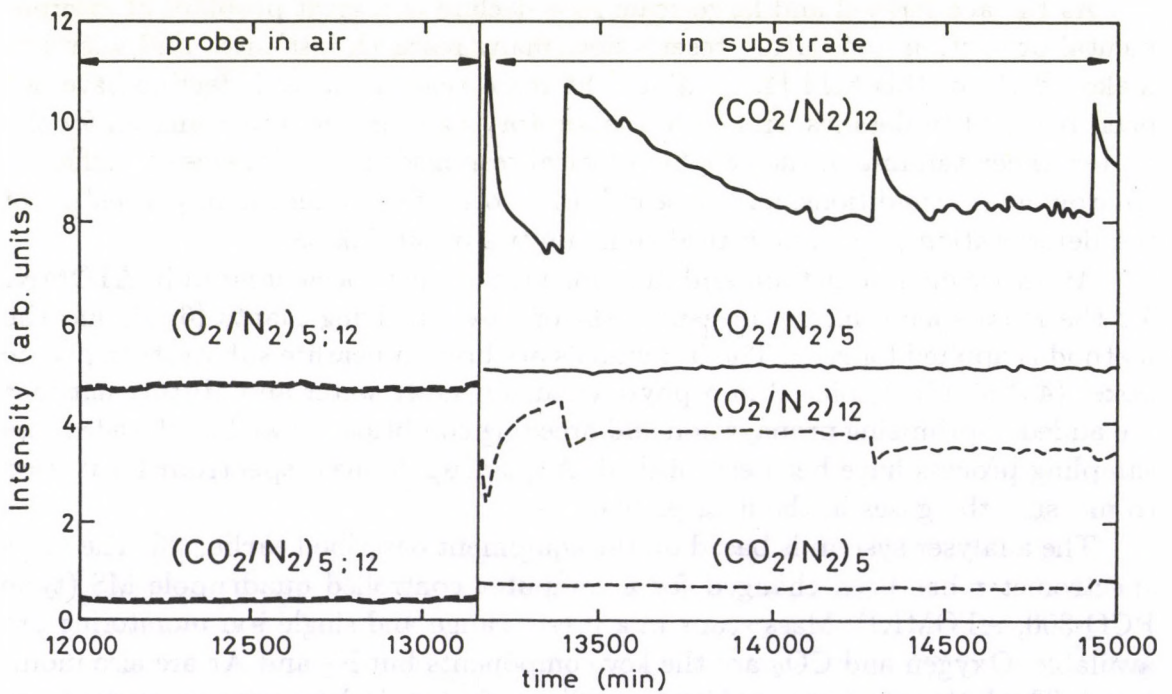


Fig. 2. Change of O₂ and CO₂ when the probes are put from ambient air into the substrate to a depth of 12cm and 5cm, respectively. Sudden peaks on the CO₂ curve coincide with watering.

amplitude is increasing in the lower internodes. CO₂ concentration is remarkably high in the rhizomes and consequently in the substrate (Fig.2).

Physiological responses to physical, chemical and other simulated environmental effects are recorded as changes in O₂ and CO₂ concentration. The measure of this change and the slope of the curves (response time) are characteristic to the effects.

This work was supported by the Hungarian Scientific Research Foundation, OTKA, contract no. T 006234.

References

1. Gy. Lakatos and p. Bíró, BFB-Bericht 77, 1991, 157-164.
2. Gy. Lakatos, Environ. Contam. 5, 1992, 97-99.
3. M. Kovács, G. Turcsányi et al., Symp. Biol. Hung. 38, 1989, 461-471.
4. Gy Lakatos, Studies in Environ. Science 55, 1993, 365-372.
5. W. Ostendorp, Aquat. Bot. 35, 1989, 5-26.
6. G. Langer, S. Bohátka et al., Proc. 9th Intern. Vacuum Congr., Sep 26-30, 1983, Madrid, p.101.
7. S. Bohátka, in Gas Enzymology (edited by H. Degn et al.), 1985, D. Reidel P. Co., pp 1-16.
8. G. Langer, S. Bohátka et al., ATOMKI Annual Report, 1990, 97-98.

Geochronological studies with the K/Ar method in 1993

K. Balogh, E. Árva-Sós, Z. Pécskay

Lower and Middle Miocene ages were measured on Tertiary tuffs from the Mecsek Mts., this is an evidence against the existence of Paleogene volcanic rocks in that region (1). In the Baia Mare region the Sarmatian volcanic activity is restricted to the SW and SE parts of the region, while the Pannonian andesitic volcanites cover greater area. Pannonian age (9 Ma) was measured on the youngest volcanic rock in the Baia Mare Region, thus, the Pontian and Pliocene ages supposed earlier were not confirmed (2). Badenian age (~ 14 Ma) was measured on basalts from borehole Balatonmária-1 (3).

In cooperation with Tanta Univ., Egypt (M. F. Ghoneim) and JATE, Szeged (T. Szederkényi) upper Proterozoic ages of 656 to 562 Ma were measured on biotites from Nubian granites. Results from the Sopron Mts. suggest, that the Sopron Micaschist Formation was in an elevated position when the Austro-Alpine Nappe System was formed (Coop.: MTA GKL, Budapest, I. Dunkl). Continued the chronologic study of Mesozoic magmatic rocks in Hungary and adjacent areas: in the Mecsek Mts. (Coop.: ELTE, Budapest, I. Bilik), the Transdanubian Central Mts. (Coop.: ELTE, Budapest, S. Józsa, Gy. Szakmány), in the Great Hungarian Plain (Coop.: MOL Rt, Budapest, A. Nusszer), and in the Moravian-Silesian Beskides (Coop.: ELTE, Budapest, I. Kubovics, Sz Harangi. Cretaceous and Jurassic ages were measured in all of these areas, a part of the younger corresponds to tectonic events. Upper Cretaceous, Oligocene-Miocene and Badenian ages were measured on igneous rocks from NE Croatia (Coop.: Inst. Geol., Zagreb, J. Pamic). Alpine magmatites from Poiana Rusca Mts. (Southern Carpathians, Romania) resulted ages from 110 Ma (gabbro) to 68 Ma (monzodiorite) (Coop.: Univ. Bucharest, G. Cioflica). 14.8 ± 0.3 Ma was measured on biotite from Badenian tuffs in the Borsod region (Coop.: Hung. Geol. Inst., Budapest, M. Bohn-Havas). 5.37 Ma age was obtained by isochron method on the basalt of Kissalgó, Nógrád, this proves that volcanic activity started here earlier and lasted for longer time than it was believed up to now (Coop.: ELTE, Budapest, Cs. Szabó).

References

1. E. Árva-Sós., Z. Máthé (1992): Acta Geol. Hung. **35/2** pp. 177-192
2. O. Edelstein, A. Bernad, M. Kovács, M. Crihan, Z. Pécskay (1992): Rev. Roum. de Géol. **36** pp. 45-60
3. S. Józsa, E. Árva-Sós, Gy. Majoros (1993): Abstracts of MAEGS-8 Congress, Budapest, p. 89

Daily and home external exposure in the Bryansk region

I. Uray

As a consequence of the Chernobyl catastrophe there are large territories, where the population has to learn to live together with a high level of contamination. Nowadays the presence of the radiocesium results in a higher internal and external exposure for the population living in those territories. These two dose components show however quite different characters. For an incorporation of the activity one has to eat contaminated meal, consequently the internal exposure is avoidable by consuming clean food. More serious is the external exposure: it is a direct consequence of the contamination level of the environment, and one cannot "cut off" the external radiation. Therefore all knowledge by which the external exposure can be decreased is very important. The external dose is predestinated by the contamination level of the environment, practically without any extremities. Different local, social and other factors can only modify the level of the external burden. However their role is important, because the external exposure may reach a high level, and now it is the main component of the collective dose as well.

A conventional personal dosimetry is able to quite accurately determine the mean value of the external dose from place to place, but, because of the high inaccuracy in the single measurements one has difficulties in realising finer regularities. To arrange a possibly high volume and accurate, multiparametric view about the feature of the external exposure it was necessary to elaborate a precise measuring technics [1] and to adapt it for the routine work. For this purpose commercial LiF detectors, but a special TLD evaluation technique was used, by which the accurate measurement of the extremely low dose values was possible. According to the permanent quality control the standard deviation achieved is about 20% at $10\mu\text{Sv}$, 10% at $20\mu\text{Sv}$ and 5% at $100\mu\text{Sv}$.

As a suitable territory for the investigation the western part of the Bryansk region was chosen, about 100-300 km's away from Chernobyl in north, north-east direction. It is very probable, that most of the contamination in the Bryansk region had been deposited in the first 3 to 5 days after the accident from wet deposition with different levels of precipitation, which resulted in the spotty character of the area's contamination.

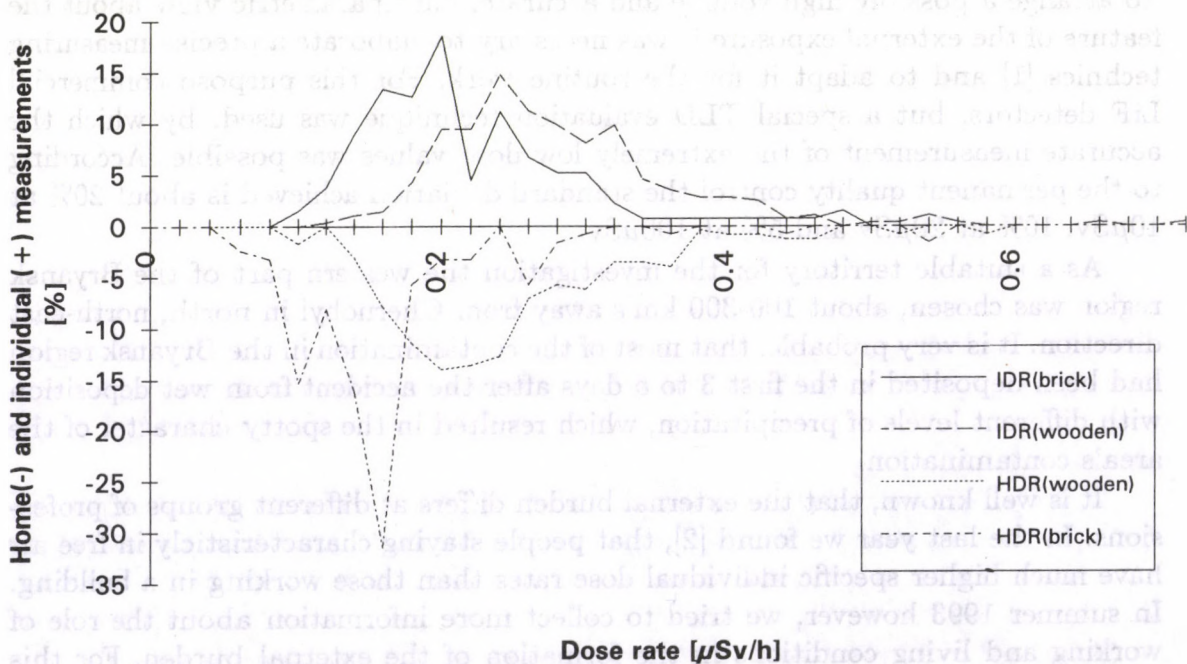
It is well known, that the external burden differs at different groups of professions. In the last year we found [2], that people staying characteristicly in free air have much higher specific individual dose rates than those working in a building. In summer 1993 however, we tried to collect more information about the role of working and living conditions in the formation of the external burden. For this purpose everybody received two dosimeters for the control. One of them was the individual dosimeter (like in the last year) to control the "individual dose rate" (IDR), and a second one, the "home dosemeter" to measure the "home dose rate" (HDR) in the flat. The first one to wear during the whole exposition period (in

general one week) and the second one to place it near the bed for this period. By this way we wanted to survey the living conditions of different types and the working conditions as well.

The results show, that the individual dose rates are only about 15% higher in average than the home dose rates. The ratio is nearly 1 for the small villages, and 1.3-1.4 for the towns. However, the difference between the individual and home dose rate is insignificant. It is possible, when the shielding power of the buildings is very poor, or if the flats are quite hard contaminated. It means, that in the contaminated regions not even buildings provide a perfect protection against external radiation.

The small difference between the individual and home dose rates may be connected also with the rainy weather of this summer. The dose rate in the environment has decreased by the shielding effect of the water content of the soil. At the same time the radiation conditions of buildings were unaltered.

A typical example is the village Novye Bobovitsi, having a mixed character. The inhabitants are working partly in the agriculture, partly in the industry, and the number of pensioner is also considerable. About two third of the people are living in wooden houses, the village has typical Russian provincial character. The contamination around it is nearly homogenous and quite high, it takes now 0.87MBq/m^2 .



The dose rate distributions from Novye Bobovitsi (see Figure) are similar to those, when summarizing over more villages. The two distributions seem like pictures of a slightly distorting mirror: the similarity is very well recognizable. The composition of the distributions is interesting as well: the low-lying curves repre-

sent the individual (positive part) and home (negative part) dose rate distributions of people are living in brick buildings, while the upper-lying distributions are of people living in wooden houses. The first group is practically identical with the people working in bureaus, spending only a short time in open air. Therefore their individual and home exposure are low alike. In summer 1993 about 1800 persons were controlled altogether from about 30 localities.

References

- [1] I. Uray, A background elimination treatment for TLDs, Radiation Protection Dosimetry, Vol. 40 No. 4 pp. 275-278 (1992)
- [2] I. Uray, R. Hille, Meßprogramm der Bundesrepublik Deutschland, Externe Strahlenbelastung der Bevölkerung in den Bezirken Brjansk und Gomel der Republiken Rußland und Weißrußland im Sommer 1992, Jül-2729, Februar 1993

Measurement of Trapped Proton Mission Fluence on LDEF Satellite*

N. Nefedov¹, I. Csige, E. V. Benton¹, R. P. Henke¹ and E. R. Benton¹

¹Physics Research Laboratory, University of San Francisco, 2130 Fulton St. San Francisco, CA 94117-1080, USA

The Long Duration Exposure Facility (LDEF) was flown in space for almost six years at low Earth orbit and low inclination. Pre-recovery estimate shows that 95 % of the charged particle exposure on LDEF orbit proves to be from trapped protons. Almost all proton fluence encountered in the South Atlantic Anomaly (SAA).

In an experiment (named P0006) on the LDEF satellite we have measured the trapped proton mission fluences at two different energies using Plastic Nuclear Track Detectors (PNTDs). LDEF was three axes stabilized, its orientation and moving direction in the SAA is shown on figure 2. Our detector stack was located on the second row of the satellite. In the experiment, volume density of stopping particles was measured at two different shielding depths in the PNTD stack. Separation of proton particle tracks from short range recoil particles and polar and azimuthal angle determination were based on measurements of etched track sizes. Arriving directions of trapped protons show very high anisotropy with most protons arriving from the west direction (see figure 1.). Selecting these particles the Eastward directed mission fluence of trapped protons was determined taking into account the extinction of protons because of interaction with nuclei of the stack. Result are presented in figure 2 in comparison with model calculations of Armstrong and Colborn [1].

References

1. T. W. Armstrong and B. L. Colborn. Second Post-Retrieval Symposium, NASA Conference Publication 3194, Part 1, (1992) 207-220.

* Work partially supported by NASA Grant No. NAG8-168 NASA Marshall Space Flight Center, AL 35812

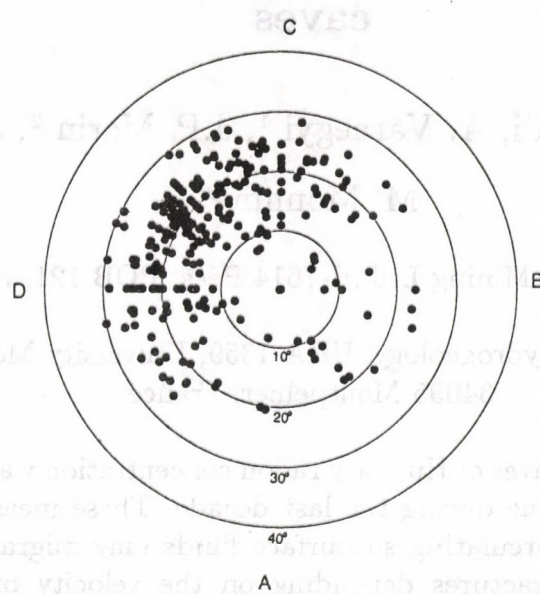


Fig. 1. Directional distribution of trapped protons in the LDEF P0006 experiment. The polar angle is measured from the normal of the surface of the LDEF satellite. The West direction was between the C and D side at about 30 degree polar angle at the time when the satellite was in the SAA.

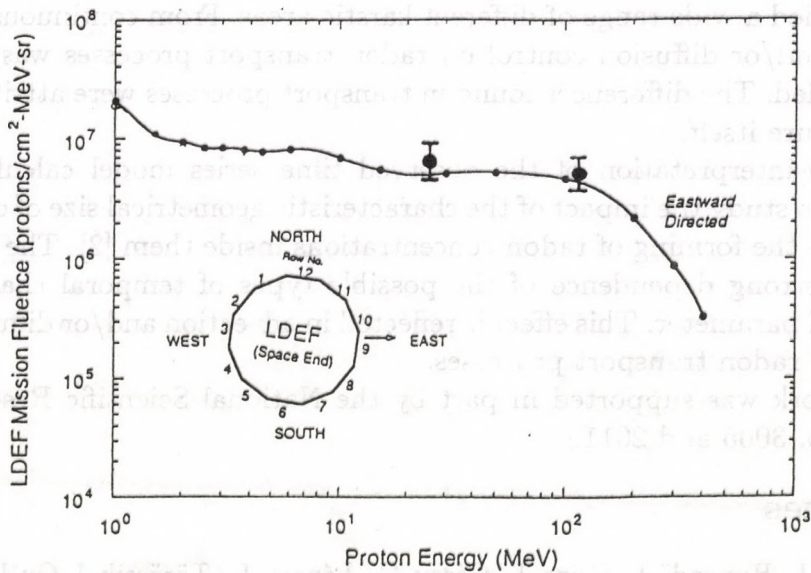


Fig. 2. Mission fluence of Eastward directed trapped protons. The solid line was calculated by Armstrong and Colborn [1], experimental points were measured on the second row of the satellite in this work.

Experimental and theoretical studies on radon transport based on monitoring in caves

J. Hakl, I. Hunyadi, A. Várhegyi ¹, J.P. Morin ², J.L. Seidel ²,
M. Monnin ²

¹ Mecsek Ore Mining Ltd., H-7614 Pécs, POB 121, Hungary

² Laboratory of Hydrogeology, URA-1359, University Montpellier II,
34095 Montpellier, France

In different karstic caves of Hungary radon concentration was monitored in situ using track etch technique during the last decade. These measurements showed, that radon carried by circulating subsurface fluids may migrate over longer distances along caverns, fractures depending on the velocity of the transporting medium [1].

The growing interest for better time resolution initiated the development of a special low consumption automatic field radon monitor (Dataqua Ltd, Hungary), which are applied since 1991. Using Dataqua radon monitors the Institute of Nuclear Research of the Hungarian Academy of Sciences in collaboration with the Mecsek Ore Mining Ltd. and Laboratory of Hydrogeology, University Montpellier, France studied a wide range of different karstic areas. From continuous time series advection and/or diffusion control on radon transport processes was experimentally identified. The differences found in transport processes were attributed to the karst structure itself.

For the interpretation of the observed time series model calculations were performed to study the impact of the characteristic geometrical size of conduits and fractures on the forming of radon concentrations inside them [2]. The calculations justified a strong dependence of the possible types of temporal changes on the investigated parameter. This effect is reflected in advection and/or diffusion control of emerging radon transport processes.

This work was supported in part by the National Scientific Research Funds contract No. 3005 and 2011.

References

1. Hakl, J., Hunyadi, I., Csige, I., Géczy, G., Lénárt, L., Töröcsik, I. Outline of natural radon occurrences on karstic terrains of Hungary. Rad. Prot. Dos.45, pp. 183-186 (1992)
2. Hakl, J. Radon transport studies, (PhD thesis), Debrecen, 1993.

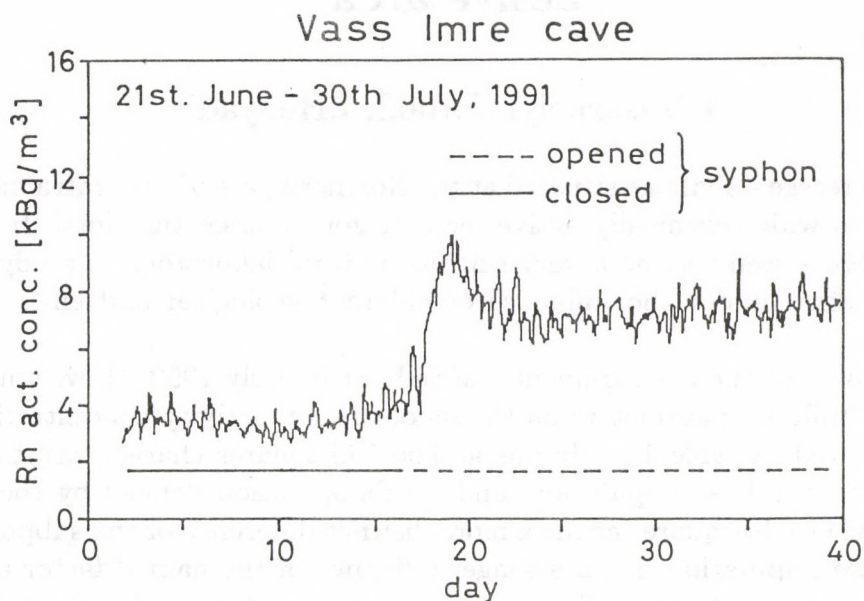


Fig. 1. Radon transient induced by syphon opening at 300 m from the entrance of the Vass Imre cave, Hungary. The transient is characterized by a time constant approximately equal to radon decay constant, so the whole process is predominantly controlled by diffusion in spite of the observed daily air flow fluctuations.

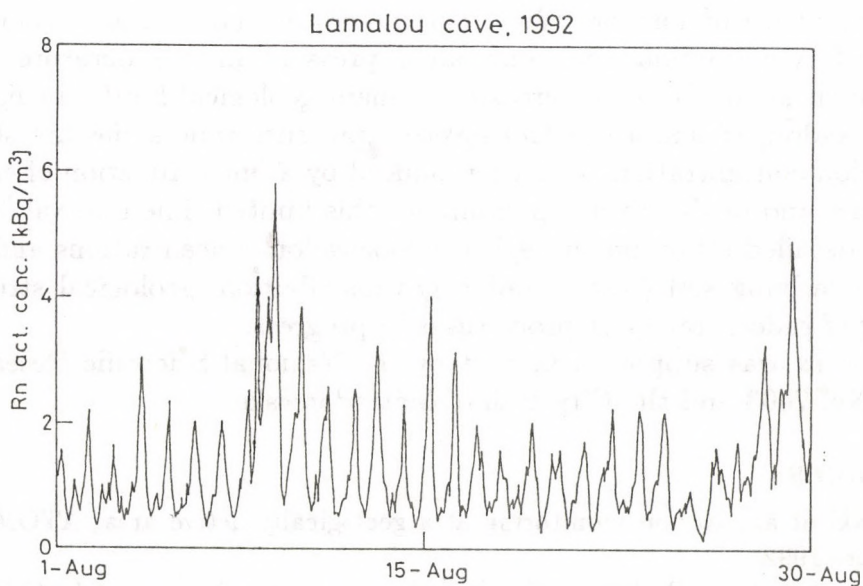


Fig. 2. Strong daily fluctuations of radon activity concentrations observed at the Lamalou (France) test site. Main controlling process is advection, which can be more dominant in highly fractured regions.

Radon monitoring experiences learned in a Hungarian village, located at a geologically active area

A.Vásárhelyi, J.Hakl, I.Hunyadi

Mátraderecske - a village situated at the Northern part of the Mátra mountain, where few km wide seismically active tectonic zone crosses the North Hungarian Central Range - seems to be a very suitable natural laboratory to study the behaviour of radon under the influence of different geological and environmental parameters.

On the base of the measurements carried out in early 1992 [1], we studied the influence of building parameters on the indoor radon activity concentration. The results are listed in table 1., columns a. The Chi-squares characterize the differences between the base population, and a subpopulation defined by the studied factor. A higher Chi-square means a more distinct difference of the subpopulation from the base population, i.e. a stronger influence of the named factor upon the radon activity concentration. The results are not so relevant, due to several perturbing factors. We developed a method [3], the normalization of indoor radon by underlying soil radon gas concentration, to eliminate the influence attributed to the spatial fluctuation of the soil radon gas concentration. The results for the normalized data are shown in columns b. of table 1. The higher Chi-squares indicate stronger influence of the studied factors.

The influence of meteorological parameters on indoor radon concentrations was studied by continuous real time radon, pressure and temperature monitoring in a house situated above the crossing of main geological faults. In figure 1. the smoothed radon, temperature and inverted pressure time series are shown. The indoor radon concentration is well reproduced by a linear function of the outdoor temperature and of the inverse pressure for this limited time interval [2].

More detailed study on surveying indoor radon concentrations and the influence of underlying soil (water) radon gas distribution, geological structure and modelling of radon transport processes is in progress.

This work was supported in part by the National Scientific Research Fund, contract No. 7603 and the City Hall of Mátraderecske.

References

1. J.Hakl et al., Radon monitoring at a geologically active area, ATOMKI Annual report 1992
2. I.Hunyadi et al., Radon monitoring experiences and important facts that may affect dose estimation, Austrian-Italian-Hungarian Radiation Protection Symposium 1993, 28-30 April, Obergurgl, Austria
3. A.Vásárhelyi et al., Soil gas and indoor radon mapping in a Hungarian village located at a geologically active area, Austrian-Italian-Hungarian Radiation Protection Symposium 1993, 28-30 April, Obergurgl, Austria

Table 1. Dependence of radon activity concentration on house parameters, and the Chi-squares for the original and normalized data. The Chi-square test in each case is referred to the distribution of the base sample.

studied factor		Rn* [Bq/m ³]		Chi-square	
		a	b	a	b
cellar existence	with cellar	211	15.14	0.1882	0.2464
	without cellar	225	9.70	0.0472	0.0874
floor	1. floor	259	13.60	0.0181	0.0262
	2. floor	53	2.22	1.5561	1.9884
heating condition	coal	175	17.34	0.2298	0.5800
	central	100	4.30	0.5874	1.1811
	gas	244	14.00	0.1040	0.0877
building material	brick	265	16.70	0.0483	0.5140
	sundried brick	266	9.30	0.0425	0.1620
	brick & sundried brick	233	12.30	0.5226	0.6599
floor material	stone	132	7.00	0.5813	0.7352
	wood	258	11.50	0.2022	0.5226
	concrete	264	13.00	0.0120	0.0395

a -original data
 b -normalized data
 * -mean radon activity concentration

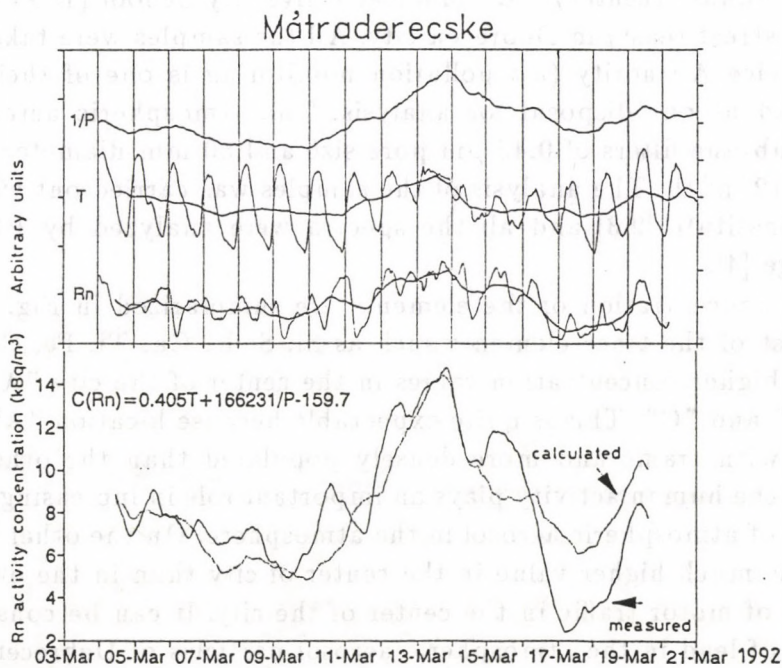


Fig. 1. Indoor radon concentration (one day moving average of hourly readings) can be related to atmospheric pressure and temperature by a linear formula.

Trace Element Concentrations in Atmospheric Aerosol Particles at Three Different Sites of Debrecen City

A. Ali¹, I. Borbély-Kiss, F. Medve², Gy. Szabó, E. Koltay and
J. Bacsó

¹Nuclear Physics Department, College of Science, Minia University, Egypt

²Health Service Authority, Debrecen

The concentration and composition of atmospheric aerosols are important factors in understanding the effects of anthropogenic pollutants on the environment. Since atmospheric aerosols interact with solar radiation and affect micro-meteorological processes, they may affect not only the Earth's energy balance, but also the climate. The concentrations and composition of aerosols near the surface of the earth are often controlled by local particulate sources [1]. The aim of our measurements has been to determine the variation of elemental concentrations of the atmospheric aerosols throughout a longer period of time at given urban sites.

Atmospheric aerosol samples were collected weekly at three different locations: "A" Dosa Nádor square (center), "B" Medical University School (DOTE, north) and "C" Dobozi street (east) in Debrecen city. All the samples were taken by the local Health Service Authority (air pollution monitoring is one of their regular tasks) and passed at our disposal for analysis. The atmospheric aerosols were collected on membrane filters of 0.45 μm pore size and 50 mm diameter, with air volume of 10 to 12 m^3/h . The analysis of the samples was carried out with PIXE method at our institute [2,3] and all the spectra were analyzed by PIXYKLM computer package [4].

The average concentration of the elements are summarized in Fig. 1. It can be seen that most of the trace elements such as Si, S, K, Ca, Ti, Fe, Co, Zn, V, Br and Pb have higher concentration values in the center of the city "A" than in the outskirts "B" and "C". This is quite expectable because location "A" is much more congested with traffic and more densely populated than the other places. This means that the human activity plays an important role in increasing the total particulate mass of atmospheric aerosol in the atmosphere. On the other hand, Pb concentration has much higher value in the center of city than in the other sites, showing the role of motor traffic in the center of the city. It can be considered as the main source of lead in the atmospheric aerosol particles of Debrecen city [5]. Seasonal variation of the trace elements and other relevant details will be discussed elsewhere.

References

1. M.J. Willison et. al., Atmos. Environ. **19**, 1081, 1985.
2. E. Koltay, in X-ray Spectroscopy in Atomic and Solid State Physics, eds. J.G. Ferreira and M.T. Ramos (Plenum 1988) p. 301.
3. I. Borbély-Kiss et. al., Nucl. Inst. and Meth. in Phys. Res. **B12**, 496, 1985.
4. Gy. Szabó et. al., Nucl. Inst. and Meth. in Phys. Res. **B75**, 123, 1993.
5. A. Ali et. al., Journal of Radioanal. and Nucl. Chem., In press.

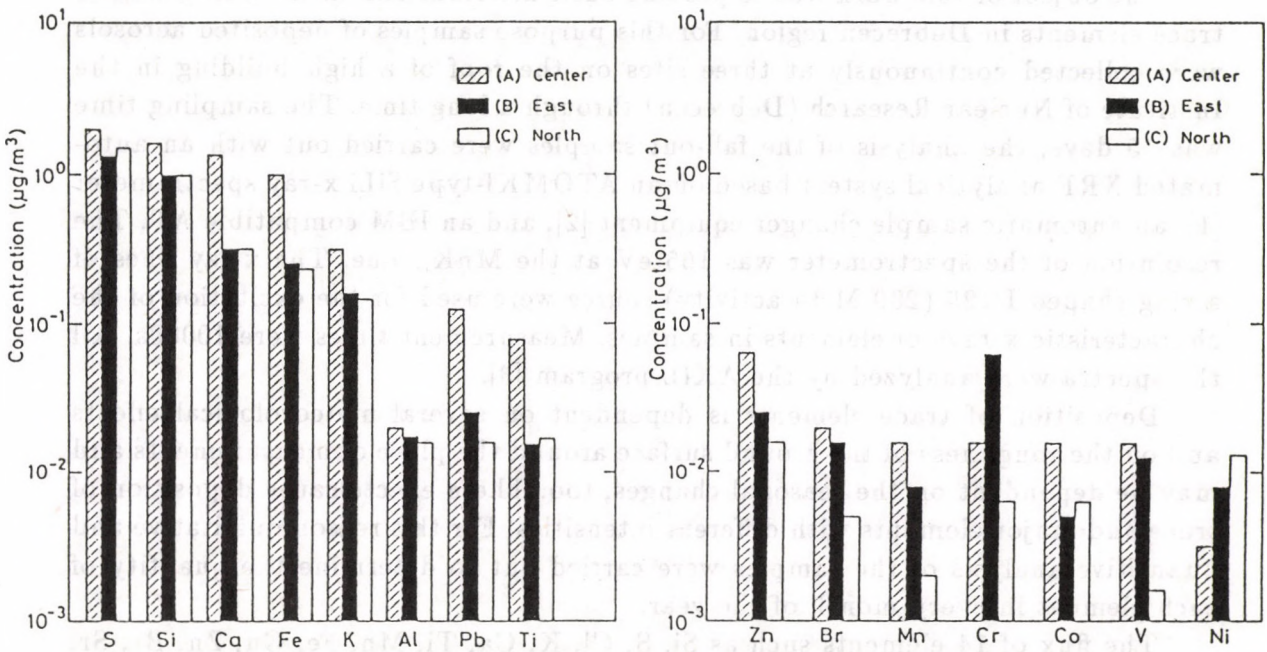


Fig. 1. The average concentration of trace elements at the three sampling sites.

Seasonal variation of trace and major elements in atmospheric deposition in Debrecen region

A. Ali *, J. Bacsó and I. Uzonyi

*Nuclear Physics Department, College of Science, Minia University, Egypt

Deposition of trace elements from the atmosphere to the ground surface is of a major importance in the study of the composition of atmospheric aerosols and it provides informations on the effects of a pollution source on the surrounding region. When assessing the input of materials into natural water and land, the sources and composition of atmospheric deposition need to be determined.

The object of this work was to provide basic informations on the deposition of trace elements in Debrecen region. For this purpose samples of deposited aerosols were collected continuously at three sites on the roof of a high building in the Institute of Nuclear Research (Debrecen) through a long time. The sampling time was 15 days, the analysis of the fall-out samples were carried out with an automated XRF analytical system based on an ATOMKI-type SiLi x-ray spectrometer [1], an automatic sample changer equipment [2], and an IBM compatible AT. The resolution of the spectrometer was 165 eV at the MnK_{α} line. The x-ray lines of a ring shaped I-125 (200 MBq activity) source were used for the excitation of the characteristic x-rays of elements in samples. Measurement times were 10000s. All the spectra were analyzed by the AXIL program [3].

Deposition of trace elements is dependent on several meteorological effects and on the roughness of the ground surface around the place of measurements and may be dependent on the seasonal changes, too. These effects cause deposition of trace and major elements with different intensities. For this reason qualitative and quantitative analysis of the samples were carried out to determine the quantity of each element in every month of the year.

The flux of 14 elements such as Si, S, Cl, K, Ca, Ti, Mn, Fe, Cu, Zn, Br, Sr, Zr and Pb have been determined and the results are shown in Fig. 1.

It can be seen that, Ca element has the greatest flux in most of the months of the year reaching $14.4 \mu\text{gcm}^{-2}\text{day}^{-1}$ in May and $0.25 \mu\text{gcm}^{-2}\text{day}^{-1}$ in October. The average flux of Ca element was $4.00 \mu\text{gcm}^{-2}\text{day}^{-1}$, which equal to 41% of the total flux of the 14 elements detected. Si flux is also relatively high and has the same fluctuation as that of Ca element: $9.4 \mu\text{gcm}^{-2}\text{day}^{-1}$ in May and $0.77 \mu\text{gcm}^{-2}\text{day}^{-1}$ in October. The average flux of Si is $3.53 \mu\text{gcm}^{-2}\text{day}^{-1}$, which is equal to 36% of the total flux amount. The flux of S comes at the third place after Ca and Si elements and has a yearly average flux of $0.64 \mu\text{gcm}^{-2}\text{day}^{-1}$.

It can also be seen that the elements Cu, Br, Zr and Pb have the lowest yearly average flux amongst elements detected, having 0.006, 0.004, 0.004 and $0.006 \mu\text{gcm}^{-2}\text{day}^{-1}$ values, respectively.

Finally, we can establish that the flux of most of the trace elements have higher values in summer than in winter season. On the other hand, comparing the results with other published data, it is found that the flux of most of the trace elements have generally lower values in Debrecen region than in other cities, e.g. Gibraltar, Seville and Almeria (Spain) [3] and Minia (Egypt) [4].

References

1. J. Bacsó et. al., ATOMKI Report, **24** (1982) 133.
2. J. Bacsó and I. Uzonyi: Istopenpraxis, **24** (1988) 72.
3. P. Van Espen et. al., NIM **145** (1977) 579.
4. A. Ali: M. Sc. Thesis, Minia University, Egypt, 1987.

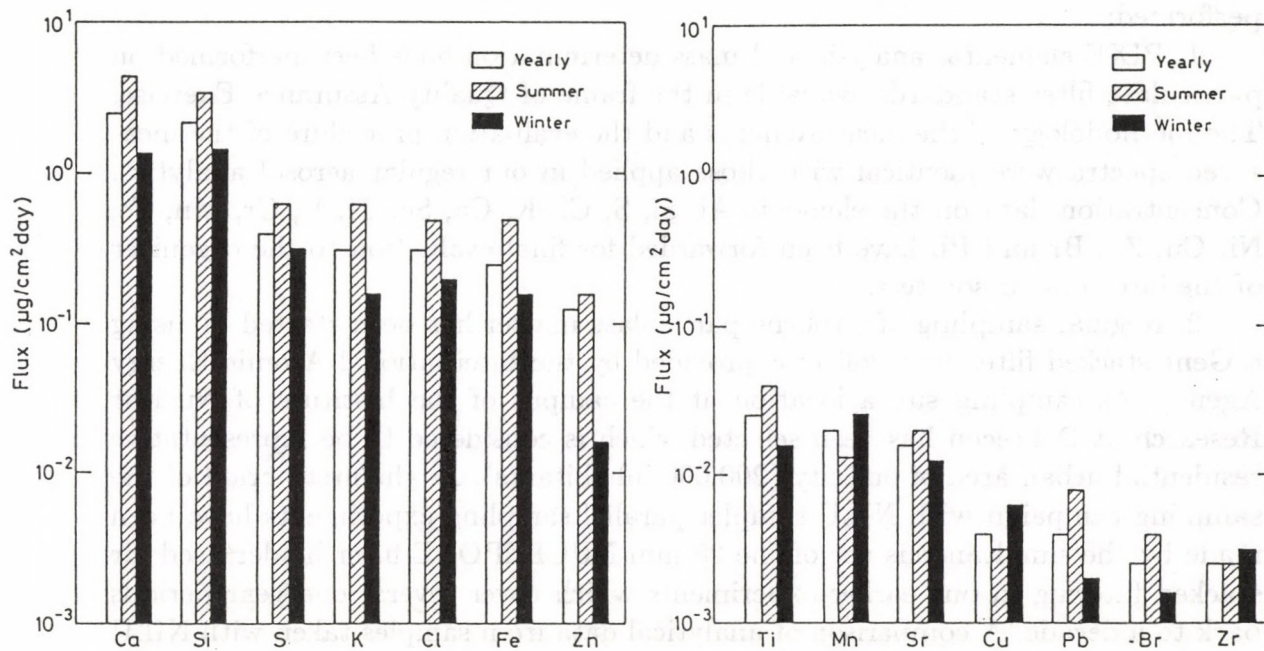


Fig. 1. Yearly, winter and summer average flux of the trace elements for long period of time.

Characterization of Regional Atmospheric Aerosol over Hungary by PIXE Elemental Analysis

E. Koltay, Gy. Szabó, I. Borbély-Kiss, E. Somorjai,

Á. Z. Kiss, E. Mészáros¹, Á. Molnár¹, L. Bozó²

¹Department of Analytical Chemistry, University of Veszprém, H-8201
Veszprém, P.O.Box 158, Hungary

²Institute for Atmospheric Physics, H-1675 Budapest, P.O.Box 39
Hungary

As part of the Co-ordinated Research Programme organized by the International Atomic Energy Agency under the title "Applied Research on Air Pollution Using Nuclear-Related Analytical Techniques" the following activities have been performed:

1. PIXE elemental analysis and mass determination have been performed on particulate filter standards available in the frame of Quality Assurance Exercise. The methodology of the measurements and the evaluation procedure of the measured spectra were identical with those applied in our regular aerosol analytics. Concentration data on the elements Al, Si, S, Cl, K, Ca, Sc, Ti, V, Cr, Mn, Fe, Ni, Cu, Zn, Br and Pb have been forwarded for final evaluation to the organizer of the intercomparison test.

2. Regular sampling of airborne particulate matter has been started by using a Gent stacked filter unit collector provided by the International Atomic Energy Agency. As sampling site a location at the campus of the Institute of Nuclear Research at Debrecen has been selected which is considered to be representative residential urban area of our city (200.000 inhabitants). At the first period of the sampling campaign with NILU sampler parallel sampling experiments have been made by the simultaneous use of the 25 mm NUCLEPORE filter holder used for stacked filtering in our earlier experiments which cover several one year periods back to a decade. A comparison of analytical data from samples taken with NILU sampler to those obtained with the earlier sampling units will be made in order to check the consistency of new data with the data sets deduced from our earlier PIXE measurements.

3. A survey paper summarizing our analytical activities in the field of air pollution studies in Hungary has been published [1]. PIXE and PIGE results obtained in the frame of our programme have been evaluated in different terms: regional signatures and their dependence on wind sector distribution reflected the influence of regional emission sources; short-range transport model contributed to the estimation of environmental impact of a separated point source; long range transport modelling which combines emission survey and air mass trajectories with a mass-balance equation gave estimation on the relative contributions of local sources

and those in the neighboring countries to the observed elemental concentrations; source profiles and scores have been determined for factors clearly appearing in target transformation factor analysis.

4. Results of our elemental analysis performed on samples of atmospheric aerosol from urban, suburban and rural air gave comparative data for air quality in downtown Budapest, in suburban Budapest and in a rural location in Hungary have been presented in paper [2]. Taking the fact into consideration, that the suburban and rural sites are located on a straight line from the center of Budapest along the direction of the prevailing wind, we substituted urban and rural data into a source-receptor model of Jaarsveld proposed for transport simulation on a regional scale. In such a way average dry deposition velocities were calculated for elements V, Cr, Co, Ni, Cu, Zn, As, Pb for days without precipitation and with a constant air mass flow observed between the source and receptor points.

5. A set of aerosol samples collected in rural sampling sites Farkasfa, K-Pusztá and Napkor situated in Western, Central and Eastern Hungary, respectively, have been analyzed by PIXE technique. The evaluation will be made in the frame of transport models.

6. Elemental concentration data obtained from our PIXE measurements performed on one hundred aerosol samples collected in Debrecen in time interval October 29 1991-October 26 1992 were subjected to wind sector analysis. The result of the analysis is described in an other contribution to this Annual Report.

7. Preparations have been made for the building-up of a microbeam channel on our 5 MV Van de Graaff accelerator. The new facility is planned to contribute to the topic of present Co-ordinated Research Programme through characterization of individual aerosol particulates.

This work has been partly supported by the International Atomic Energy Agency (CRP 7257/RB) and by the National Foundation for Scientific Research (OTKA, No 345).

References

1. E. Koltay, Nucl. Instr. Meth. B (1993) in press
2. Á. Molnár, E. Mészáros, L. Bozó, I. Borbély-Kiss, E. Koltay, Gy. Szabó, Atmospheric Environment 27A (1993) 2457.

Aerosol Sampling and Analysis by PIXE

I. Borbély-Kiss, E. Koltay, Gy. Szabó,

A regular aerosol sampling has been continued in collaboration with Central Institute of Atmospheric Physics and University of Veszprém.

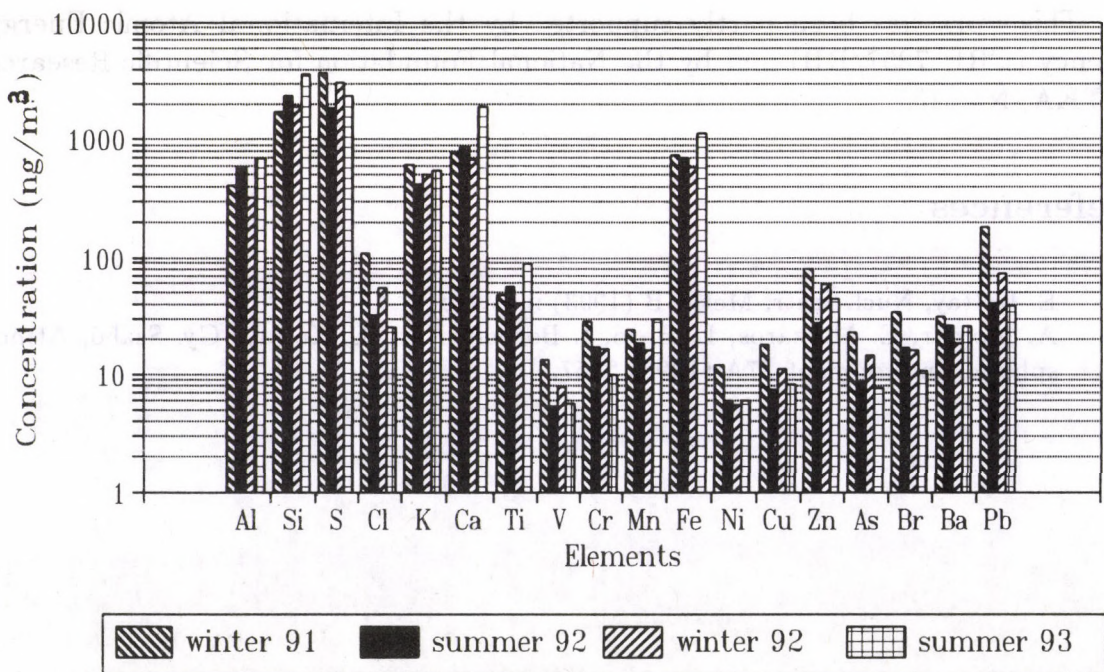
Further 225 aerosol samples collected in Debrecen (in ATOMKI) and in K-pusztá has been analysed by PIXE. Elemental concentration of Al, Si, S, Cl, K, Ca, Ti, V, Cr, Mn, Fe, Ni, Cu, Zn, As, Br, Ba, Pb has been calculated for each samples.

Yearly, winter, summer and monthly averages of the concentrations for the above mentioned elements has been calculated together with the enrichment factors for samples collected in Debrecen.

Further statistical evaluation (factor analyses) of the concentration data is in progress.

One of the results, the comparison of the winter and summer averages of the last two years is shown on the figure. Differences between the summer and winter averages of elemental concentrations are clearly seen.

Average concentrations winter and summer



A Search for Saharan Dust Intrusion in Atmospheric Aerosol over Hungary

I. Borbély-Kiss, L. Bozó¹, E. Koltay, E. Mészáros²,
Á. Molnár², Gy. Szabó,

¹Institute for Atmospheric Physics, H-1675 Budapest, P.O.Box 39
Hungary

²Department of Analytical Chemistry, University of Veszprém, H-8201
Veszprém, P.O.Box 158, Hungary

An important source of soil-derived atmospheric aerosol component worldwide is wind erosion from desert regions, its annual average contribution to the global aerosol budget is considerable. Wind blown dust from arid regions is transported over long distances: Saharan dust can be advected into the Arctic, too. The intrusion of this component into areas touched by actual air trajectories can result in continuous or sudden deposition of the dust burden. The contribution of mobilization, transport and deposition of Saharan dust is reflected by the fact, that the number of sand storm events in Sahara amounts to around 250 per year followed by dust fall events in Europe in more than 100 cases.

Mineralogical and elemental analyses have been used in some papers to point out events of Saharan origin in the Mediterranean and Central Europe. Relatively little composition data are available which may be used to characterize desert-derived component. Obviously, it contains crustal material which has not been significantly enriched in noncrustal elements. The systematic investigation of Chester et al. [1] performed in the Mediterranean area pointed out elements like Al, Fe, Mn, Cr and Ni characterizing samples of Saharan origin; concentration ratios Fe/Al, Mn/Al, Cr/Al can be used as elemental signatures. However, a direct comparison with actual elemental ratios for the parent crust cannot be made easily. Bulk crust does not adequately predict atmospheric elemental ratios due to a well-defined crust-air fractionation resulting for example in a decrease of 35-50% for Si/Al in the aerosol with respect to the elemental ratio in average crust. In a recent work of Marcazzan et al. [2] the elemental ratio Ti/Ca as well as well-defined correlations in absolute concentrations of Al, Si, Ca, Ti, Cr, Mn and Fe were found to indicate deposition of Saharan dust in a remote site of Northern Italy.

A search has been made for evidences of the contribution of Saharan source to the composition of atmospheric aerosol over Hungary by the evaluation of a suburban data set measured on samples taken in the ATOMKI's area and covering the sampling period 29 October 1991-26 October 1992 [3]. Kinematic backward trajectories of 96 h duration have been calculated for the 850 hPa level on the basis of meteorological data supplied by European radiosonde balloon flights for each sample. Including sampling site five points have been determined on each

trajectory for the times 0, 24, 48, 72 and 96 h before sampling. The total number of trajectories, i.e. samples, falling into the West-Mediterranean area denoted as wind sector 4 in Fig.1. amounted to 24. Eleven trajectories which were considered as representing air masses of North-African origin are shown in Fig.1, the corresponding values of elemental ratio Ti/Ca are indicated by full dots in Fig.2. Empty circles indicate the other cases in the sector. The number of the trajectories and dots in the respective figures are serial numbers of the samples within wind sector 4. In Fig.2 the sampling dates are indicated on the horizontal axis. Average of the concentration ratios found in wind sector 4 is shown with dot-dashed line. For a comparison, Italian data assigned to Saharan events and average value corresponding to a period of one month around Saharan intrusions are shown with dashed lines. Increased values of ratio around our sample/trajectory numbers of 3-5, 8, 11, 18, 20, 22 are considered as fair evidences of Saharan events.

Elemental ratio Ti/Ca amounting to 0.10 measured in a recent dust sample obviously assignable to a red rain of Saharan origin at 17. 10, 1993 in Debrecen also supports the conclusion for Saharan contribution in the named cases.

Strongly correlated variations observed in concentrations of elements Al, Si, Ca, Ti, Cr, Mn and Fe also indicate increased effect of a crustal source around the above serial numbers, i.e. sampling days. A comparison with the behavior of the absolute values and spreads of the measured data in the wind sectors 1, 2, 3 and 5 points out that the arguments found are not very strong. The Saharan contribution was present around the sampling dates, but we did not observe a sudden deposition of the dust burden e.g. in the form of a red rain. New data also covering the red rain event at 17. 10. 1993 are being evaluated.

From the above observations we came to the conclusion, that for more sensitive detection of normal Saharan effect in this geographic latitude the observation and evaluation should simultaneously cover a number of elemental ratios properly selected as a set of regional signatures to be considered as tracers of adequate selectivity for Saharan contribution.

This work has been partly supported by the National Foundation for Scientific Research (OTKA, No 345) and by the International Atomic Energy Agency (CRP 7257/RB).

References

1. R. Chester, E.J. Sharples, G.S. Sanders and A.C. Saydam, *Atmos. Environ.* 18(1984) 929.
2. G.M. Bragga Marcazzan, P. Bonelli, E. Della Bella, A. Fumagalli, R. Ricci and U. Pellegrini, *Nucl. Instr. Meth. in Phys. Res. B75* (1993) 312.
3. E. Koltay, *Nucl. Instr. Meth. B* (1993) in press

A Search for Saharan Dust Intrusion in Atmospheric Aerosol over Hungary



Fig. 1.

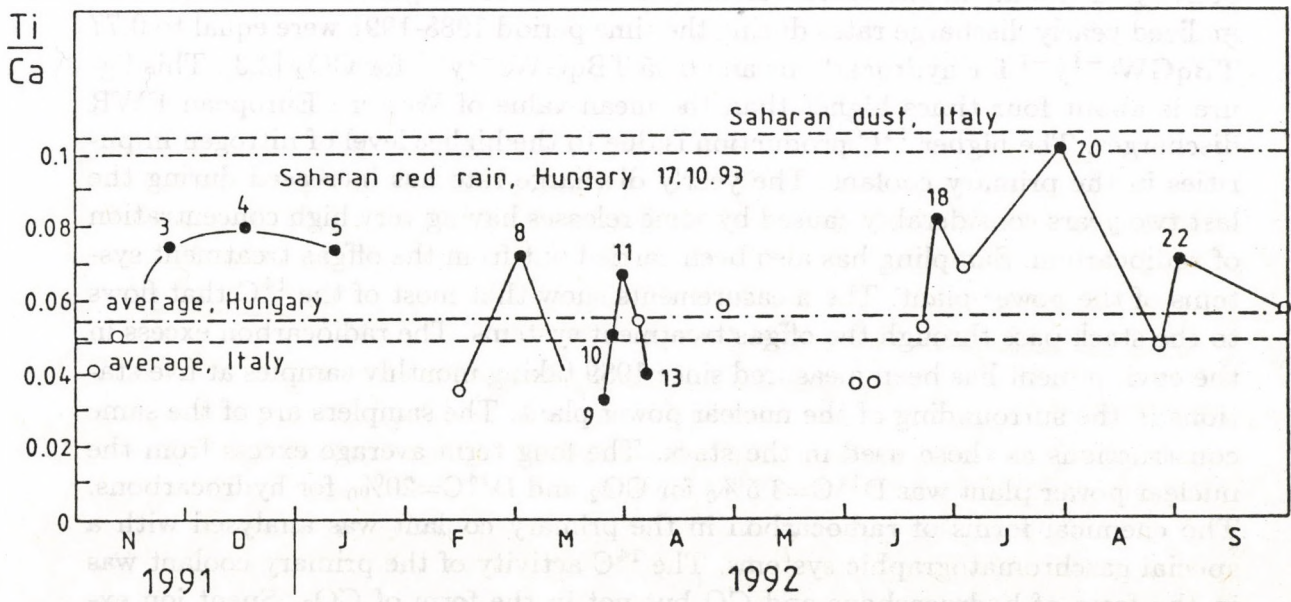


Fig. 2.

Concentration of radiocarbon and its chemical forms in primary water, gaseous effluents, environmental air and nuclear waste of a pressurized water reactor power plant in Hungary

E. Hertelendi, M. Veres, Gy. Uchrin¹, E. Csaba¹,
I. Barnabás², P. Ormai², G. Volent²

Airborne releases of ^{14}C from the Paks Nuclear Power Plant have been measured. Two continuous stack samplers have been in operation since 1988. The samplers collect radiocarbon in various chemical forms like $^{14}\text{CO}_2$ and $^{14}\text{C}_n\text{H}_m$. The radiocarbon activities were measured using two different techniques. Samples of lower activities were analyzed using the proportional counting method. The carbon dioxide extraction was carried out by adding concentrated sulphuric acid to the NaOH solution in which the ^{14}C is absorbed in the samplers. The liberated CO_2 was purified and measured in a low level counting equipment [1]. Most of the samples were measured by liquid scintillation counter after precipitating CO_2 in the form of BaCO_3 . The carbonate samples were mixed with Cab-O-Sil and toluol-based-liquid scintillation cocktail. The typical sensitivity of liquid scintillation method was $10\text{mBq}/\text{m}^3$, while the proportional counting method had a sensitivity of $0.5\text{ mBq}/\text{m}^3$. Therefore only proportional counting techniques were used for the measurement of environmental air samples. The specific radiocarbon activity of the air in the stack varies between $140\text{-}160\text{ Bq}/\text{m}^3$. The average normalized yearly discharge rates during the time period 1988-1991 were equal to $0.77\text{ TBqGWe}^{-1}\text{y}^{-1}$ for hydrocarbons and $0.05\text{ TBqGWe}^{-1}\text{y}^{-1}$ for CO_2 [2,3]. This figure is about four times higher than the mean value of Western European PWR discharges. The higher ^{14}C production is due to the higher level of nitrogen impurities in the primary coolant. The yearly discharge rate has increased during the last two years considerably caused by some releases having very high concentration of radiocarbon. Sampling has also been carried out from the offgas treatment systems of the power plant. The measurements show that most of the ^{14}C that flows to the stack pass through the offgas treatment systems. The radiocarbon excess in the environment has been measured since 1989 taking monthly samples at five stations in the surrounding of the nuclear power plant. The samplers are of the same constructions as those used in the stack. The long term average excess from the nuclear power plant was $\text{D}^{14}\text{C}=3.5\text{‰}$ for CO_2 and $\text{D}^{14}\text{C}=20\text{‰}$ for hydrocarbons. The chemical forms of radiocarbon in the primary coolant was analysed with a special gaschromatographic systems. The ^{14}C activity of the primary coolant was in the form of hydrocarbons and CO but not in the form of CO_2 . Spent ion exchange resins and evaporation concentrates have been analysed for radiocarbon.

The activities of spent mixed bed exchange resins vary between 1.2-5.3 MBq/kg of dry weight.

Reference

1. E. Hertelendi, E. Csongor, L. Záborszky, J. Molnár, J. Gál, M. Györffi, S. Nagy: Counters System for High Precision ^{14}C Dating, Radiocarbon 31 No.3 (1989) p.399
2. E. Hertelendi, G. Uchrin, P. Ormai: ^{14}C Release in Various Chemical Forms with Gaseous Effluents from the Paks Nuclear Power Plant, Radiocarbon 31 No.3 (1989) p.754
3. G. Uchrin, E. Csaba, E. Hertelendi, P. Ormai, I. Barnabás: ^{14}C Release from a Soviet-Designed Pressurized Water Reactor Nuclear Power Plant, Health Physics 63 No.6 (1992) p.651

¹ Institute of Isotopes of the HAS, Budapest

² Paks Nuclear Power Plant, Paks

Reevaluation of the Hungarian Neolithic based on calibrated radiocarbon data

E. Hertelendi, P. Raczky ¹, F. Horváth ² M. Veres,
A. Figler ³, L. Bartosiewicz ⁴

The internal chronology of the Neolithic in Hungary has been established by the late 1960's. The outline of this framework was devised by I. Bognár-Kutzián in 1969. [1] This chronological system was purely based on the traditional stratigraphic and comparative typological methods. Absolute chronological boundaries were appraised using archaeological analogies. The Neolithic cultures were fit within apparently logical chronological charts which reflected a predominantly diachronic sequence. This system fell in line with the main trend of European research at the time as was summarized by Milošević (1949, 1967) [2,3]. However, the first radiocarbon dates relevant to the area, determined by the Berlin Laboratory showed the discrepancies of this chronological system. The ever growing number of increasingly precise radiocarbon dates and the introduction of the calibration method, therefore, made its reevaluation indispensable. As a result of this process, "the traditional framework collapsed" as was convincingly summarized by C. Renfrew in 1976 [4]. The appearance of calibrated radiocarbon data had two dramatic consequences in Hungarian Neolithic research: a/ The beginnings of food producing economy in Hungary shifted back by approximately 1.5 millennia and, logically, the time span encompassed by Neolithic cultures expanded. b/ The second surprising phenomenon was that the previously diachronic sequence of Neolithic cultures was upset by overlaps. A great deal of contemporaneity occurred among the cultures. From these facts, the obvious necessity of defining new absolute chronological boundaries emerged. In archaeological terms reevaluation became a prerequisite for rethinking intercultural relationships. All relevant radiocarbon dates were collected from the literature and series of new measurements were made in the Institute of Nuclear Research of the Hungarian Academy of Sciences [5]. All dates were calibrated using the computer program developed by Stuiver and Reimer [6]. The calibrated dates were tabulated both by individual sites and cultural entities. The dispersion function and time span of each culture were analysed as well. As a result, the earliest calibrated Körös-Starcevo dates range between 6300 and 5100 cal BC. At the same time, the Tisza-Herpály-Csőszhalom complex and the Lengyel culture end at the time between 4600 to 4400 cal BC. These temporal fix-points show that the total time span of the Hungarian Neolithic was approximately 1700 years. The new upper limit of the Neolithic fits well with the recently obtained radiocarbon dates marking the subsequent Copper Age in Hungary. This newly developed chronological system, therefore, may be expanded into later prehistoric periods in the area.

Reference

1. Bognár-Kutzián: Probleme der mittleren Kupferzeit im Kapatzenbecken, in: Symposium Lengyel- Komplex (1969), 31-60.
2. V. Miložčić: Chronologie der jüngeren Steinzeit Mittel- und Südost-Europas (Berlin 1949)
3. V. Miložčić: Die absolute Chronologie der Jungsteinzeit in Südosteuropa und die Ergebnisse der Radiocarbon- ^{14}C Methode, in: Jahrb. RGZM 14, 1967, 9-37.
4. C. Renfrew: Before Civilization: The Radiocarbon Revolution and Prehistoric Europe, Harmondsworth 1976
5. E. Hertelendi, E. Csongor, L. Záborszky, J. Molnár, J. Gál, M. Györffi, S. Nagy: Counter System for High Precision Radiocarbon Dating, Radiocarbon 31 No.3 (1989) p.399
6. M. Stuiver and P. Reimer: Extended ^{14}C Data Base and Revised CALIB 3.0 ^{14}C Age Calibration Program, Radiocarbon 35 No.1 p.215

¹ Eötvös Loróránd Univ., Dep. of Archaeology, Budapest

² Móra Ferenc Museum, Szeged

³ Directorate of Museums in Győr-Moson-Sopron Counties, Győr,

⁴ Archaeological Institute of the HAS, Budapest

Radiocarbon concentration and origin of thermal karst waters in the surroundings of the Bükk Mountains, Hungary

E. Hertelendi, M. Veres, L. Mikó¹, L. Lénárt², J. Deák³,

M. Süveges³

¹ Regional Geological Service, Hungarian Geological Survey, Debrecen

² Univ. of Miskolc Dep. of Hydrogeology and Engineering Geology, Miskolc

³ Research Institute for Water Resources, Budapest

According to the theory the precipitation on the SW part of the Bükk Mountains percolates in the karstified layers down to the impervious base. In the limestone the water continues dipping towards the Great Hungarian Plains to successively greater depths assuming gradually the higher temperatures prevailing there. The karst water heated in this way emerges along faultlines to the surface and forms warm springs [1]. The karst water of 30°C temperature and 30 m³/min yield emerging to the surface in the warm springs around Eger corresponds to a thermal output of 4x10⁷W. To absorb this huge amount of heat an area over 400 km² would be needed even if the entire terrestrial heat flux would be used for heating this amount of water. In view of the fact that the warm springs are situated 5-10 km distant from the surface outcrops of the karst in the SW part of the Bükk Mountains, direct percolation starting therefrom and heated gradually to 30°C cannot be accepted as the only source of the warm water yield. This assumption is apparently in conflict with the isochronous map based on ¹⁴C data. The radiocarbon age of the water grows successively from the surface karst towards the warm springs and the more distant thermal waters. The water temperature increase follows the same pattern. However, the piezometric heads of the warm springs in the Eger area with a ¹⁴C age 6-7 thousand years, at a distance of about 7 km from the karst outcrops are lower than the heads in both the young cold karst water nearer to the karst outcrops and the oldest thermal waters at a distance between 10-15 km. The water in the springs in the Eger area is of a mixed character and the radiocarbon age is indicative of the mix proportion alone. The composition of stable isotopes in the karst waters is an additional proof of mixing. The $\delta^{13}\text{C}$ value is -13 to -14‰ typical for fresh water and -3 to -4‰ at a distance more than 10 km, while intermediary values have been measured in the Eger area. The deuterium concentrations show similar patterns. The δD values in the warm water are situated between -67‰ typical of the cold karst and groundwaters in Hungary and the -75.5‰ of the 13-15 thousand years old thermal karst waters. The δD values around -75‰ implies at the same time that the 13-15 thousand years old water originates from precipitation fallen under climate conditions colder than the present one.

This work was supported by the PHARE-ACCORD Contract No. H9112-0170.

1. Z. Schréter: The warm springs at Eger (in Hungarian.) A m.kir.Földtani Intézet Évkönyve, Vol.XXV, No.4, 1923

BIOLOGICAL
AND
MEDICAL RESEARCH



The Use of the Hair Calcium Concentration as a Noninvasive Diagnostique Technique for Coronary Heart Disease

J. Bacsó, A. MacPherson¹, B. M. Groden²

¹Scottish Agricultural College, Auchincruive, Ayr, Scotland,

²Crosshause Hospital, Kilmarnock, Scotland

Early Diagnosis of persons at risk from Coronary Heart Disease (CHD) would afford greater opportunity for preventive or corrective regimes to achieve success. Particular emphasis is currently being placed on the development of non-invasive techniques (EC Biomedical & Health Research Programme, 1991-94). This study evaluates the use of hair Ca for this purpose.

Populations normally exhibit a two-peaked log-normal distribution with the mean concentration of the low and high groups significantly ($P < 0.001$) different at 350 and 1500 mg kg⁻¹, respectively[1]. Patients suffering from CHD have considerably lower hair Ca²⁺ levels than comparable healthy controls[2]. Hair and aorta Ca²⁺ are inversely correlated so that when hair Ca²⁺ is high aorta Ca²⁺ is low and vice versa. High aorta Ca²⁺ is associated with severe alterations in the vessel walls. This, however, never co-exists with hair Ca²⁺ concentrations above 700 mg kg⁻¹[3]. In different studies conducted in Hungary it was found that 88% of acute (AMI) and 98% and 90% of two different post myocardial infarction (PMI) patient groups belonged to the low hair Ca²⁺ group[2].

Methods

Samples of scalp hair were collected from 494 apparently healthy male volunteers in 5 districts of Scotland which ranged from high to low risk of CHD as determined by their Standard Mortality Ratios (SMR's). These were in descending order: Cumnock & Doon Valley, Kyle & Carrick, Aberdeen, Edinburg and Bearsden & Milngavie.

Hair samples were cut near to the scalp on the occipital site of head. Hair Ca²⁺ concentrations were measured by XRF analysis and the distributions plotted and compared with those determined previously for other countries. In addition the ratios of the means of the low and high groups within each population were calculated and regressed against their SMR values.

Results

In Scotland similar to other countries bi-modal distributions have been observed, in general, but the ratio of the high Ca²⁺ level group to the low Ca²⁺ level group is 15-10% to 85-

90%. This is very similar to that of the Hungarian AMI and PMI groups, except Kyle & Carrick, where practically all of the persons (98%) investigated belonged to the low Ca^{2+} level group with a mean value of 352 mg kg^{-1} . Figure shows the correlation between the SMR and mean Ca value for the groups investigated.

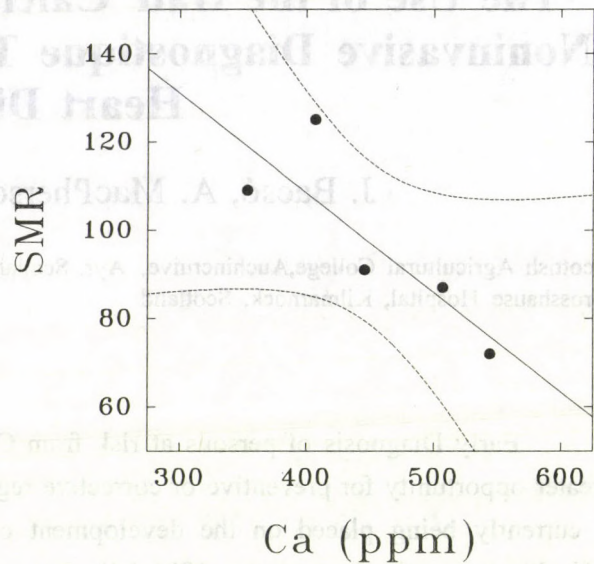
Discussion

It is evident from the markedly different distributions of hair Ca^{2+} and mean values found for Scottish population compared to those of other countries that should be some unique parameter influencing its Ca-metabolism. The strong similarity between the distributions for normal Scottish males and Hungarian MI patients is striking. This fact taken in conjunction with the finding that within Scotland hair Ca^{2+} concentration tended to be negatively correlated with SMR (see Fig., $\text{SMR} = -0.2254\text{Ca}(\text{ppm}) + 198.54$, $r=0.84$, $P=0.05$) suggest that it may well prove to be a useful screening test for CHD (and might be for others, too). Possible explanations of this effect on Ca metabolism may relate to low UV light intensity compared to the other countries sampled or to low dietary antioxidant intakes some evidence of which we have from other studies.

A wider study is required to confirm the putative relationship between hair Ca^{2+} and SMR and intervention studies should explore the possibility of moving a subject from a low to high group and hence reducing their risk of CHD. Such studies are in progress.

References

1. J. Bacso: ATOMKI Report C/2 pp.416-430 (1985)
2. J. Bacso, M. Horvath, S. Horvath, Mrs Baliczky, Mrs Mahunka, and M. Szücs: Magyar Belorvosi Archivum, 35 pp 245-250 (1982)
3. J. Bacso, G. Lusztig, A. Pal and I. Uzonyi: Exp. Pathol. 29 pp119-125 (1986)



Determination of Pt Concentration in Cervical Tumor Tissues Using EDXRF Method

K.L. Szluha ¹, I. Uzonyi, J. Bacsó, L. Lampé ², I. Czifra ², M.

Péter ¹, C. Villena ³, W. Schmidt ³

¹ Radiological Department, University Medical School of Debrecen,
H-4012 Debrecen, Pf. 37. Hungary

² Dept. of Obstetrics and Gynecology, University Medical School of
Debrecen, H-4012 Debrecen, Pf. 37. Hungary

³ Universitats Frauenklinik, 6650 Homburg-Saar, Germany

Nowadays, the overall incidence of invasive cervical neoplasia is relatively low as a consequence of effective cytologic screening programs. In spite of this fact, carcinoma of the uterine cervix remains the second leading cause of death from gynecologic cancers. The five year survival of patents treated with radiotherapy with or without surgery is approximately 50% for stage IIb, 30% for stage III, and only 7% for stage IV [1]. Forty to fifty percent of patients treated with conventional radiotherapy in stages IIa-IVa relapse within two years [2]. In cervical cancer patients chemotherapy is used mainly for palliative treatment [3], nevertheless, chemosensitivity of this tumor was also indicated [4]. The aim of a neoadjuvant chemotherapy is the reduction of bulky tumor in order to enhance the efficacy of subsequent radiotherapy and possible surgery. Currently, Cisplatin is considered the most active single drug [5]. Two ways of chemotherapy administration can be used in patients with cervical cancer: the intravenous (iv) and loco-regional intra-arterial (ia) one. Theoretically, the latter is the more advantageous assuring increased drug concentration at the tumor level and bypassing of an immediate first pass effect before reaching other organs [6].

The aim of our study was to compare the effect of intravenous and loco-regional intra-arterial Cisplatin administration in the treatment of advanced cervical cancer (stages IIb-IVa) with respect to pharmacokinetics and toxicity to determine optimal drug administration for local disease control. Measurements were initiated to test the hypotheses: loco-regional ia treatment using the same dosage of Cisplatin will result in a higher tissue concentrations in the tumor comparing to iv treatment, with comparable or lower systemic toxicity.

Determination of Pt concentration in biopsy tissues was carried out with Energy Dispersive X-Ray Fluorescence (EDXRF) method using a Kristalloflex 710H

(Siemens) x-ray generator with Mo-anode x-ray tube combined with a home-made general purpose three-axis secondary-target excitation system [7]. Samples were collected from ten patients administered with Cisplatin. Altogether, 70 biopsy and post-operative samples were analyzed.

Analytical results support the hypotheses that intra-arterial administration of Cisplatin comparing to the intravenous one produces significantly higher Pt concentration in tumorous tissues. It is worth mentioning that - except one case - intravenous chemotherapy resulted in undetectable Pt concentration values in tumorous tissues. Pt concentration seems to correlate with the vascularisation (positive correlation) and necrotic ratio of the tumor (negative correlation). Definite statement for the depth profile of Pt in tumor can't be concluded currently because little cases were analyzed. Nevertheless, there seems to exist a positive correlation between deepness and Pt concentration. Comparing cervix, corpus and the ovaries, there were no significant differences in Pt concentration. As it was expectable, Pt level in the parailiacal lymphnodes was lower with an order of magnitude than that of in the tumor. It is interesting to note that similar observations were reported for selectively administered citostatic agents yielding 15 times higher tissue concentration in the tumors than in the peripheral organs [6].

References

1. Richter, M.P. Carcinoma of the cervix: principles of management. In Principles of cancer treatment (S.K. Carter Ed.), pp. 494-503. Mc Graw Hill, New York, 1982.
2. Sasieni, P. The Lancet, **338** (1991) 818-819.
3. Wasserman, T.H.; Carter, S.K. Cancer Treat. Rev., **4** (1977) 25-46.
4. Guthrie, D.; Obstet. and Gynecol., **12** (1985) 229.
5. Alberts, D.S.; Garcia, D.; Mason Liddil, N. Seminars in Oncology, **18/1** (suppl. 3) (1991) 11-24.
6. Taguchi T.; Nakamura, H. Arterial Infusion Chemotherapy. In Arterial Infusion Chemotherapy, pp. 11-21. Jpn. J. Cancer and Chemother. Pub. Inc., Tokyo, 1989.
7. Kiss-Varga, M. Thesis, Debrecen, 1993.

New Cross Section Data for $^{66,67,68}\text{Zn}+p$ Reaction up to 25 MeV

F. Szelecsényi*, T.E. Boothe*, Y. Feijoo*, M.E. Plitnikas*,
E. Tavano* S. Takács, F. Tárkányi and Z. Szűcs

* Cyclotron Facility, Division of Nuclear Medicine, Mount Sinai Medical Center, 4300 Alton Road, Miami Beach, FL 33140 USA.

A critical overview of the nuclear data relevant for production of $^{66,67,68}\text{Ga}$ via proton induced nuclear reaction on zinc showed that for some reactions the cross sections/thick target yield data in the middle energy range [up to 40 MeV] are insufficient and/or contradictory [1]. The aim of the present study was to complete the existing data base to obtain reliable data sets and to perform an evaluation to get recommended sets of cross sections/thick target yield values for routine radioisotope production and different analytical applications.

Excitation functions have been measured for $^{66}\text{Zn}(p,n)^{66}\text{Ga}$ [from 5 to 25 MeV], $^{67}\text{Zn}(p,2n)^{66}\text{Ga}$ [from 14 to 25 MeV], $^{68}\text{Zn}(p,3n)^{66}\text{Ga}$ [from 24 to 25 MeV] and $^{68}\text{Zn}(p,2n)^{67}\text{Ga}$ [from 21 to 25 MeV] nuclear reactions. Targets were prepared via electrolytic deposition of isotopically enriched zinc [$^{66}\text{Zn}(99\%)$, $^{67}\text{Zn}(93\%)$ and $^{68}\text{Zn}(98\%)$] on commercially available Ni foils. The target samples and the copper monitor foils were activated in the form of a stack. Irradiations were carried out at the external beam of the CS-30 cyclotron of Mount Sinai [25 MeV incident energy] using a beam current of apr. 100nA. The total integrated charge was detected by Faraday cup measurements and was cross-checked via monitor reactions induced in the Ni backings and in thin Cu foils inserted separately into the stacks [2]. The activity of each foil was measured via high resolution gamma-ray spectroscopy without chemical separation. Special attention was paid to the necessary corrections to obtain absolute activities. The energy degradation of incident proton beam, data evaluation and error calculation were similar as described in more detailed in [3]. The total estimated error of the cross sections varied from 10 to 15 %.

On the basis of these completed data sets, new evaluated values were calculated for the above mentioned reactions. Comparison between yields calculated on the basis of the new evaluated excitation functions and the experimental yield values shows acceptable agreement.

References

- [1] Szelecsényi et al., Appl. Radiat. Isot., (in print)
- [2] Tárkányi et al., Acta Radiologica, Supl., 376(1991)72
- [3] Tárkányi et al., Appl. Radiat. Isot., (in print)

Compilation and Evaluation of Cross Sections/Thick Target Yields for ^{111}In Production

F. Szelecsényi*, T.E. Boothe*, E. Tavano*, Y. Feijoo*,
M.E. Plitnikas*, S. Takács, T. Molnár and F. Tárkányi

*Cyclotron Facility, Division of Nuclear Medicine, Mount Sinai Medical Center, 4300 Alton Road, Miami Beach, FL 33140 USA.

The radioisotope ^{111}In is one of the most important cyclotron produced isotopes and is widely used in diagnostic nuclear medicine. The possible production routes have been investigated by many authors. Detailed excitation functions for its production have been measured both in terms of nuclear theory and routine production. In one of our earlier work, to check and supplement the data available in literature, we have studied the excitation functions of proton induced reactions on ^{111}Cd and ^{112}Cd [1]. In the present work as a continuation of our study we have compiled and evaluated all the cross sections and thick target yield data $[\sigma/Y]$ for the light charged particle induced reactions appearing in the literature through 1993. The studied direct production routes were proton and deuteron induced reactions on Cd with natural and enriched isotopic composition and ^3He and alpha particle induced processes on Ag. Due to practical production purposes the $[\sigma/Y]$ values of the most important competing reactions leading to major contaminants were also investigated.

During the evaluation we have tried to resolve the most obvious discrepancies found in the presented values. The published data have been corrected on the basis of the most recent values of accepted standard nuclear data. First, after the necessary correction the individual data sets were fitted separately and then values were calculated from the same energy points from fitted data sets. The error of these fitted values in a given energy points was estimated by summing up the error of the nearest experimental value and the deviation of the fitted value in the energy point in question from the interpolated value calculated from the two nearest experimental data points. In the second step weighted average values and their corresponding uncertainties were computed from the fitted ones at each grid point. Finally, to eliminate the significant discontinuities arising from the fact that different energy ranges were investigated by different groups, the weighted averages were fitted once again and the errors were calculated [2].

This critical review of the status of reactions used for production of ^{111}In shows that the experimental data available on cross sections and thick target yields via most common production routes are sufficient. An agreed set of cross section data could be produced for reactions of $^{111}\text{Cd}(p,n)$, $^{112}\text{Cd}(p,2n)$ and $^{109}\text{Ag}(\alpha,2n)$. There is, however, need for new measurements to complete and clear the discrepancies for the following reactions: $^{\text{nat}}\text{Cd}(p,xn)$, $^{113}\text{Cd}(p,3n)$, $^{114}\text{Cd}(p,4n)$, $^{\text{nat}}\text{Cd}(d,xn)$, $^{110}\text{Cd}(d,n)$, $^{111}\text{Cd}(d,2n)$, $^{112}\text{Cd}(d,3n)$ and $^{109}\text{Ag}(^3\text{He},n)$.

References

- [1] Tárkányi et al., Appl. Radiat. Isot., (in press)
- [2] Takács et al., NIM B, (in press)

Analysis of $^{209}\text{At}[\text{DTPA}]$ complex by thin layer chromatography

Z. Szűcs

The ^{209}At isotope is one of the latest radioisotopes produced with the MGC-20 cyclotron in Debrecen [1]. It is a useful radionuclide for the investigation of chemical property of astatine, which is the rarest element in the Earth.

The synthesis of the first chelate-complex of astatine [2] showed the new aspects in inorganic chemistry because it proved the metallic character of the fifth member of the halogen group. The $\text{At}[\text{DTPA}]$ complex was synthesised similarly to that which was described for $\text{At}[\text{EDTA}]$ preparation by Milesz et al. [2].

The identification and determination of the chemical yield was carried out by TLC-analysis with the following parameters:

thin layer: WATHMAM 1 paper, 21 cm length

mobile phase: pyridine:ethanol:water/1:2:4

evaluation time: 150 min.

R_f values: 0.1 for free At^+ and 0.85 for $\text{At}[\text{DTPA}]$

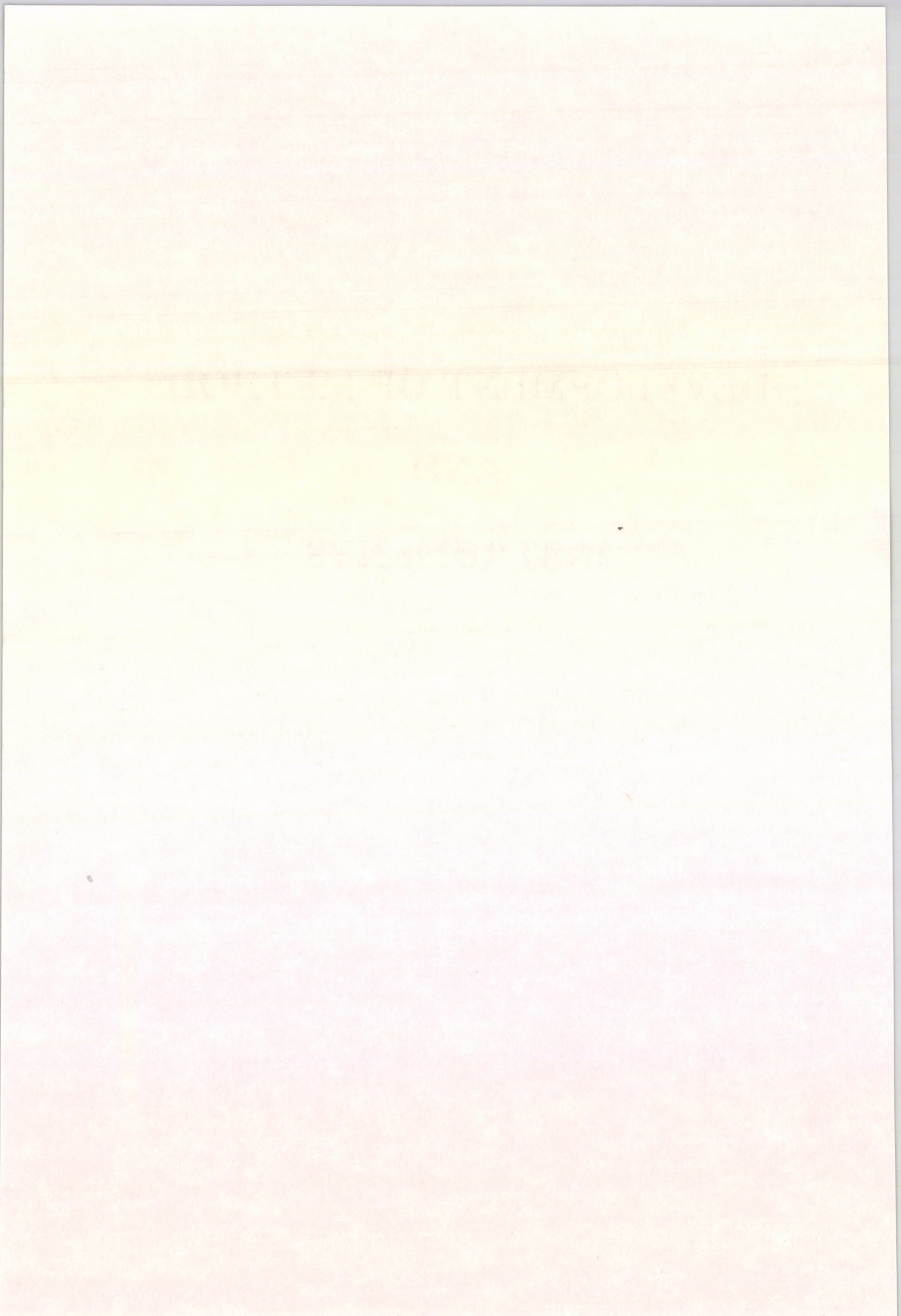
The chromatogram was detected by a plastic detector coupled with Nucleus PCA-II γ -ray measuring system. The chemical yield was found to be $70\pm 3\%$. The new astatine compound can be used for elaboration of labelling methods for $^{211}\text{At}[\text{DTPA}]$ conjugated monoclonal antibody, which is a potential agent for in vivo radiotherapy.

This work was supported by the National Research Foundation of Hungary (grant No. F-4061).

References:

- 1., Z. Szűcs, F. Szelecsényi; ATOMKI Annual Report 1991
- 2., S. Milesz et al.; JINR preprint 12-88-178, Dubna (1988)

DEVELOPMENT OF METHODS
AND
INSTRUMENTS



Preliminary experiment with a Si p-i-n photodiode for room temperature X-ray detection

G. Kalinka

Liquid nitrogen cooled Si(Li) detectors with typical resolution of ≈ 150 eV at 6 keV still have been the most popular and widely used energy dispersive X-ray detectors [1]. Operation of common Si(Li) detectors at room temperature results in serious degradation of resolution to $\gtrsim 10$ keV due primarily to increased leakage currents in the order of several hundred nanoamperes.

It is possible, however, to manufacture radiation detectors with state-of-the-art microelectronic technology on high resistivity Si wafers (the necessary high temperature steps, unfortunately, are not applicable to Si(Li) detectors) with substantially reduced leakage currents in the order of $1 \text{ nA/cm}^2/100 \text{ }\mu\text{m}$ at 20°C [2,3], and what is more to reduce (pixel type) device dimensions down to $1000 \text{ }\mu\text{m}^3$, which scales currents and capacitances even further.

A $10 \text{ mm}^2/300 \text{ }\mu\text{m}$, so called PIP (passivated ion implanted) Si detector produced with this technology really gave 1.1 keV resolution for 60 keV at room temperature [4].

Among various room temperature Si detectors [5] the best up to date results are related to CCD (135 eV) [6], drift detector (172 eV) [7] and DEPMOS (250 eV) [8].

While PIP detectors, though relatively expensive, are sold commercially, the latter devices are not even available - at least for the time being. Si p-i-n photodiodes, with dimensions of $0.1\text{-}800 \text{ mm}^2$ area and $100\text{-}500 \text{ }\mu\text{m}$ depletion layer thickness, are manufactured with similar technology and exhibits similar performance for nuclear radiation detection, but are much cheaper than PIP detectors. It is therefore not surprising that photodiodes has already found widespread application in nuclear spectroscopy primarily as photon detectors coupled to scintillators, and to less extent as direct ionisation detectors [9-11]. Due to their relatively thin sensitive region they are well suited to low energy ($\lesssim 20$ keV) X-ray detection. To test their performance a Hamamatsu S1223-01 diode ($3.7 \times 3.7 \text{ mm}^2 / 100 \text{ }\mu\text{m} \approx 14 \text{ pF}$) was chosen. The photodiode with removed glass window was mounted into a standard Si(Li) detector cryostat, together with an unselected 2N4416 JFET in its original header, forming the input of a NV-806 drain feedback preamplifier (ATOMKI). Drain feedback [12] is an excellent low noise charge reset method for cooled Si(Li) detectors [13], and as it is proved here it works equally well at elevated temperatures up to several nA detector leakages.

The response of the diode, reverse biased with 90 V, to uncollimated ^{55}Fe and ^{241}Am sources using NZ-870 X-ray signal processor (ATOMKI) [13,14] at $12 \text{ }\mu\text{s}$ peaking time is shown in Fig. 1.

Taking into account the adverse affect of the high dielectric loss borosilicate glass headers and the least favourable photodiode chip mount, remarkable energy

resolution improvement, relative to the presently achieved 860 eV noise line width (100 electron rms equivalent noise charge), is expected under optimised conditions.

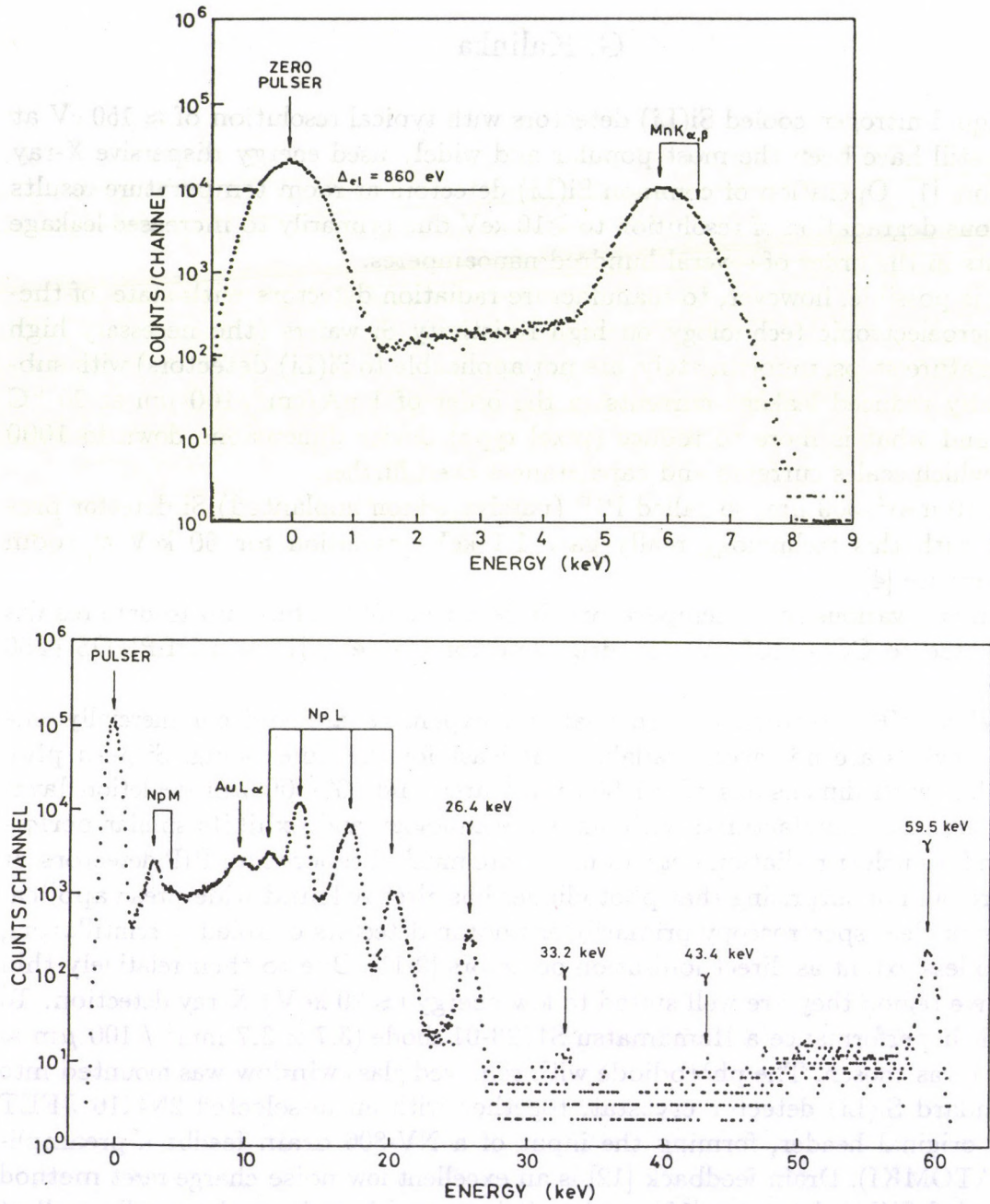


Fig. 1. ^{55}Fe and ^{241}Am spectra taken with a Hamamatsu S1223-01 photodiode in ambient air at room temperature.

References

1. G. Kalinka and K. Taniguchi, Nucl. Instr. Meth. **B75**(1993)91
2. J. Kemmer, Nucl. Instr. Meth. **169**(1980)499
3. J. Kemmer, Nucl. Instr. Meth. **226**(1984)89
4. P. Burger, M.O. Lampert, R. Henck and J. Kemmer, IEEE Trans. Nucl. Sci. **NS-31**,No.1(1984)344
5. Proc. Int. Workshop on Room Temperature Semiconductor X- and γ -Ray Detectors and Associated Electronics, September 23-28, 1991, Ravello, Italy, Nucl. Instr. Meth. **A322**(1992)
6. H. Bräuninger et al., Proc. SPIE **1344**(1990)404
7. G. Bertuccio, M. Sampietro and A. Fazzi, Nucl. Instr. Meth. **A322**(1992)538
8. J. Kemmer, G. Lutz, U. Prechtel, K. Schuster, M. Sterzik, L. Strüder and T. Ziemann, Nucl. Instr. Meth. **A288**(1990)92
9. I. Ahmad, R.R. Betts, T. Happ, D.J. Henderson, F.L.H. Wolfs and A.H. Wuosmaa, Nucl. Instr. Meth. **299**(1990)201
10. E. Gramsch, K.G. Lynn, M. Weber, B. DeChillo and J.R. Williams, Nucl. Instr. Meth. **A311**(1992)529
11. Silicon Photodiodes and Charge Sensitive Amplifiers for Scintillation Counting and High Energy Physics, Hamamatsu Cat. No. KOTH0002E01, Oct. 1992
12. E. Elad, IEEE Trans. Nucl. Sci. **NS-19**,No.1(1972)403
13. J. Bacsó, G. Kalinka, Zs. Kertész, P. Kovács and T. Lakatos, ATOMKI Közl. **24**(1982)133

Status report on the development of a 4π charged particle detector system

G. Kalinka, J. Gál, B. M. Nyakó, Z. Máté, T. Vass,
G.E. Perez, Z. Varga ^a, A. Kerek ^b and A. Johnson ^b

^aGraduate student, L. Kossuth University, Debrecen

^bThe Royal Institute of Technology, Physics Dept/Frescati-Stockholm,
Sweden

In order to obtain an insight into the details of the decay of hot compound-nuclei formed in heavy ion fusion reaction sophisticated detector systems are required with maximum particle type, energy, directional and temporal resolution, – in the whole 4π solid angle. Such detector systems should consist of charged particle, γ and neutron detector subsystems arranged in concentric shells around the target and each other consecutively.

The demand on the innermost charged particle detector shell, in addition to as high as possible resolving powers as above, are linearity, stability (including resistance against high radiation doses), and compatibility with outer detector shells, regarding size, absorption and scattering effects.

In collaboration with the Manne Siegbahn Institute Stockholm, a development of a 4π charged particle detector system comprising a large number of CsI(Tl)+photodiode detector elements with individual electronics for EUROBALL was started in 1992 [1]. Our system would rather be a cube with at least 5×5 elements on a side, than a polyhedron, allowing the use of commercial rectangular photodiodes. Until recently we have been optimising single detection element's geometry. Best results to date were obtained with $15 \times 15 \times 3$ mm³ scintillator crystals (Merck) coupled to $10 \times 10 \times 0.1$ mm³ photodiodes (S3590-03, Hamamatsu), through 5 mm plexiglass light guide glued together with optical cement. All the side surfaces are wrapped with teflon tape, while the front face is covered with aluminised 2.5 μ m Hostaphan foil. Using specially designed miniature preamplifier and signal processor [2] the noise contribution from the photodiode is 500-600 rms electron.

The resolution for 662 keV γ rays of ¹³⁷Cs is 7.1 % at the photopeak of 81 keV silicon equivalent energy, corresponding to ≈ 34000 photon/1 MeV γ energy and consequently to $\eta = 0.81$ light collection efficiency.

Best resolutions for 5.5 MeV α particles are $\approx 1.7\%$ at an Si equivalent energy of ≈ 370 keV. A resolution of 1.3 % with collimated beam, however, and a scan across the face revealed $\approx 2\%$ lateral inhomogeneity of light collection, warning for remaining insufficiencies of the construction.

One of the best detectors has also been tested for α -p discrimination up to 20 MeV at the cyclotron of ATOMKI, with the dedicated particle discrimination unit (PDU) [2]. An illustrative example of the results is displayed in fig. 1. showing a good α -p discrimination for energies $E_\alpha \geq 4$ MeV and $E_p \geq 2.5$ MeV.

References

- 1 G. Kalinka et al., EUROBALL Meeting on Auxiliary Detectors and Selective Devices, Berlin, June 1-3, 1992, Slides Report
- 2 J. Gál et al., in this report

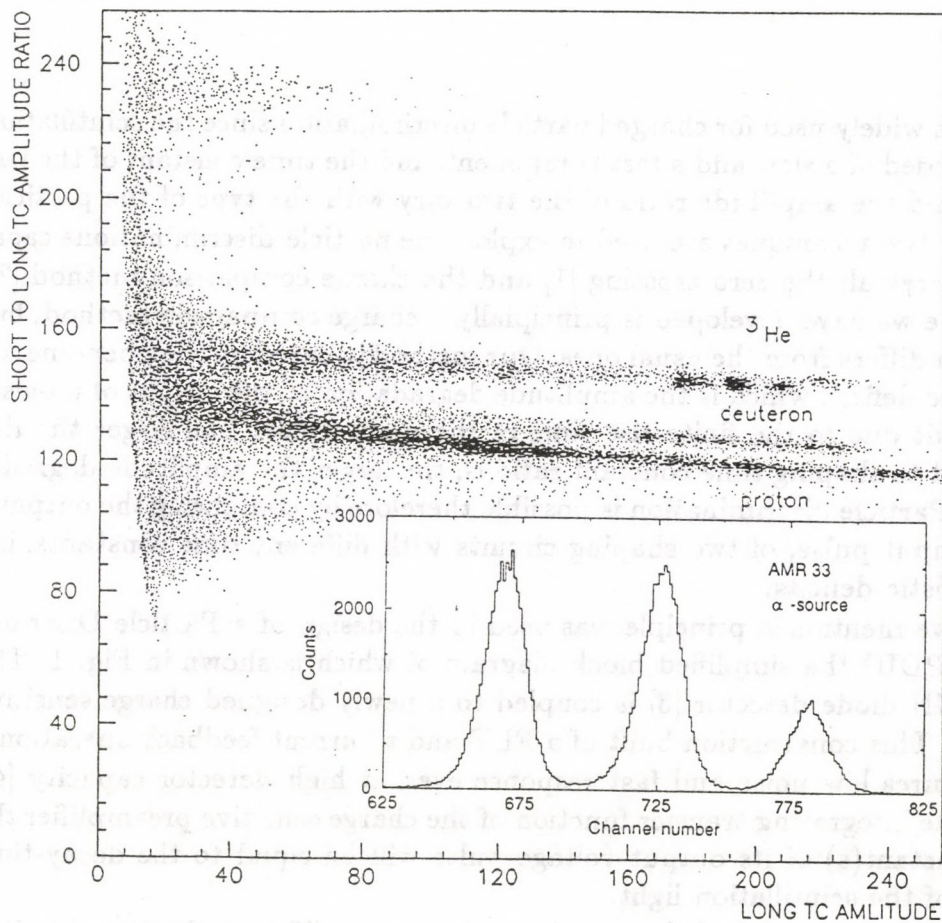


Fig. 1. Illustration of the energy (insert) and particle discrimination capability of a single channel of the 4π charged particle detection system under construction.

Method for identification of light charged particles with CsI(Tl) scintillator + Si PIN photodiode detector

J. Gál, B. M. Nyakó, G. Kalinka, Z. Máté, T. Vass,

G.E. Perez, Z. Varga ^a, A. Kerek ^b, A. Johnson ^b

^aGraduate student, L. Kossuth University, Debrecen

^bThe Royal Institute of Technology, Physics Dept/Frescati-Stockholm, Sweden

CsI(Tl) is widely used for charged particle discrimination since the scintillation light is composed of a slow and a fast component, and the time constant of the fast component and the amplitude ratio of the two vary with the type of the particle.

Basically two techniques are used to exploit the particle discriminations capability of the crystal: the zero crossing [1] and the charge comparison method [2]. The technique we have developed is principally a charge comparison method, but its realization differs from the usual ones. Our method is based on the phenomenon called ballistic deficit, which is the amplitude degradation at the output of a pulse-shaping circuit due to the finite rise time of the input pulse. The larger the rise time constant to shaping time constant ratio is, the larger the amplitude degradation will be. Particle discrimination is possible therefore by comparing the outputs, for a given input pulse, of two shaping circuits with different time constants, i.e. different ballistic deficits.

The above mentioned principle was used in the design of a Particle Discriminator Unit (PDU) the simplified block diagram of which is shown in Fig. 1. The CsI(Tl) + PIN diode detector [3] is coupled to a newly designed charge sensitive preamplifier. This construction built of a FET and a current feedback operational amplifier assures low noise and fast response even at high detector capacity [4]. Because of the integrating transfer function of the charge sensitive preamplifier the rise-time constant(s) of its output voltage pulse will be equal to the decay-time constant(s) of the scintillation light.

The PDU is composed of three main parts: an amplifier, a shaping circuitry and two ADCs. The output of the amplifier is connected simultaneously to the input of a long-time-constant unipolar shaper and to that of a short-time-constant bipolar shaper. The unipolar shaper delivers the "energy" output, since it results in no observable ballistic deficit. (This is equivalent to a total charge integration.) While, the output of the bipolar shaper corresponds to "particle-type". Its shaping time constant is chosen to be in the range of the preamplifier rise-time constant,

in order to enhance particle discrimination sensitivity, since thus practically it is only the fast component which is integrated.

For the energy measurement unipolar shaping is chosen since it offers a better signal-to-noise ratio and smaller ballistic deficit, than the bipolar shaping having the same shaping time constant. Correspondingly, for particle discrimination bipolar shaping is used because of its larger ballistic deficit, and the unnecessary of baseline restoration. The output pulses of the shapers are converted by two analog-to-digital converters. The result of the conversion can be stored in a two dimensional incrementing matrix memory. So in a plot of "particle type" output against "energy" output the different type of particles will be situated along slanting lines of different slopes. The block diagram of Fig. 1. offers a more spectacular display of the result: making the ratio of "particle type" and the "energy" signals and plotting this ratio against the "energy" output, the different types of particles will be situated along different horizontal lines. In our PDU this ratio is produced by a high precision analog divider (see Fig. 1).

The figure of merit of the separation depends on the shaping time constant. Choosing the unipolar shaping time constant large enough the optimum of the figure of merit can be found as a function of the bipolar shaping time constant. Fig. 2. displays typical results in "horizontal line" mode using pulse generator pulses, the risetime of which is adjusted to correspond to alphas and protons, respectively.

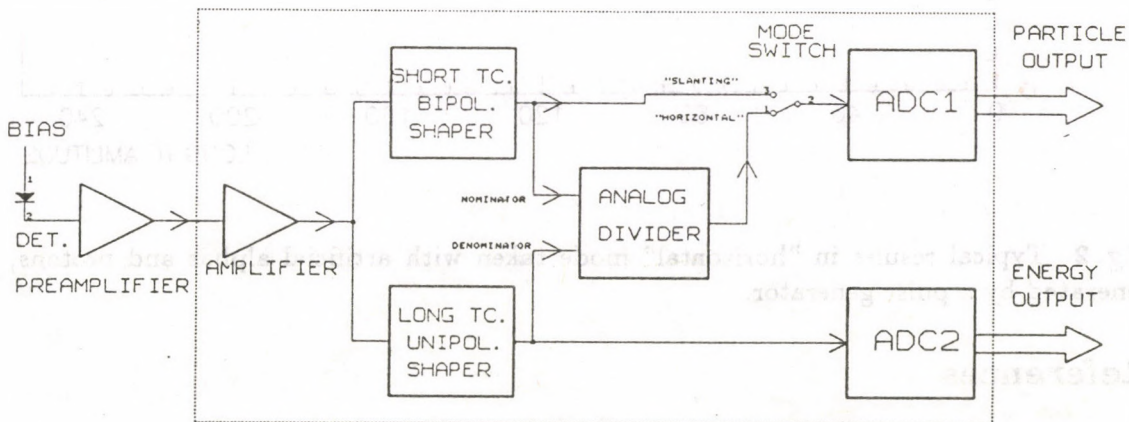


Fig. 1. Simplified block diagram of the particle discrimination unit (PDU).

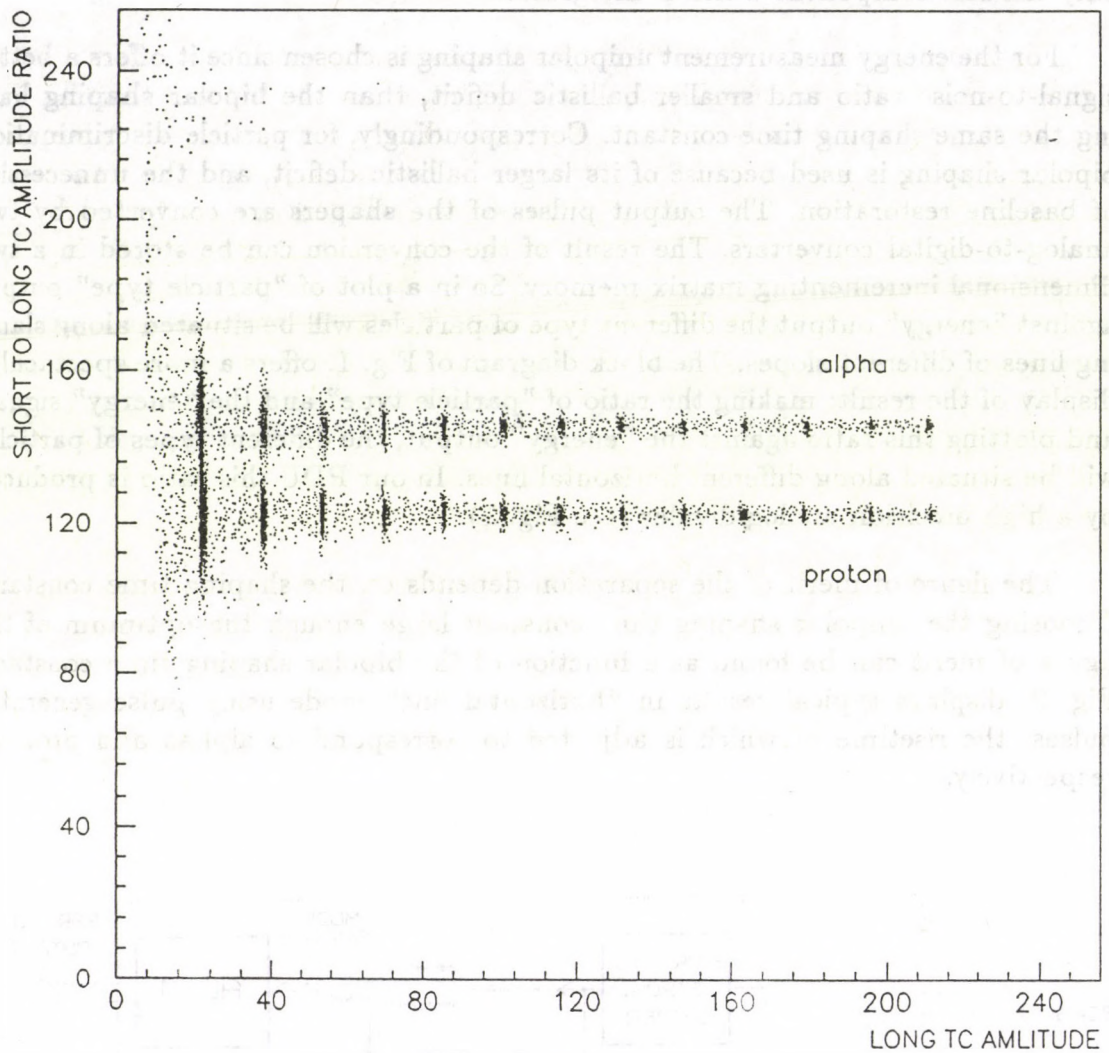


Fig. 2. Typical results in "horizontal" mode taken with artificial alphas and protons, generated by a pulse generator.

References

- [1] P. Kreutz et al., Nucl. Instr. and Meth. A260(1987)120.
- [2] F. Benrachi et al., Nucl. Instr. and Meth. A281(1989)137.
- [3] G. Kalinka et al., this Annual Report
- [4] J. Gál et al., To be submitted to Nucl. Instr. and Meth.

Building a Vertical Drift Chamber for the KVI Big-Bite Spectrometer

A. Krasznahorkay, I. Gál, A.M. van den Berg *,

M.N. Harakeh *, and J.M. Schippers *

* *Kernfysisch Versneller Instituut, 9747 AA Groningen, The Netherlands*

The superconducting $K = 600$ cyclotron AGOR, presently under construction at the IPN of Orsay, will be installed at the KVI and commissioned in 1994. The AGOR cyclotron will deliver in addition to the high quality beams of heavy ions also light ions and in this respect it distinguishes itself from other compact superconducting cyclotrons such as at MSU and at Catania. In order to take full advantage of the variety of beams that AGOR will provide a magnetic spectrometer is presently under construction and will be installed next year. This Big-Bite Spectrometer (BBS) with a maximum central rigidity of 3.1 Tm has a large solid angle to enable coincidence studies and it will be used at very small scattering angles including 0° . The combination of this new instrument with a high-energy (5-20 MeV) γ -ray spectrometer with good resolution [1], will create unique possibilities for the measurements of the neutron skin thickness of nuclei. In recent work [2] performed with the old KVI cyclotron a novel method was developed to investigate this fundamental quantity. The method is based on the fact that the giant dipole resonance (GDR) excitation cross section by inelastic α -scattering depends strongly on the neutron skin thickness of nuclei.

Using the beams of AGOR these measurements will be extended to a wider range of isotopes, including deformed nuclei, for which it is known that the GDR is split into $K = 0$ and $K = 1$ vibrational modes. For these cases it will be possible to determine the possible differences in deformation for the neutron and proton distributions. For these measurements we need good energy resolution in both the magnetic and the γ -ray spectrometer. As a first step in this project we intend to build a new focal-plane detector for the BBS re-using essential parts of the Vertical Drift Chamber (VDC) built at KVI [3].

The focal-plane detector is an essential and critical part of the spectrometer. The position resolution of the detector must be better than dictated by the focusing properties of the spectrometer. For an incoherent spot size at the target with a width of 1 mm and a height of 3 mm and using the full solid angle, the image at the centre of the BBS focal plane is 1 mm (FWHM) measured along the dispersive direction. To achieve a momentum resolution of 2×10^{-4} one needs an accurate measurement of the position and the direction of a particle at the focal plane. The accuracy needed is 0.3 mm (FWHM) for the lateral direction and 2 mrad (FWHM) for the angles in the bend and non-bend planes. In addition, the detector shall be able to give information that can be used for particle identification such as an energy-loss signal and a time-of-flight signal.

In our earlier measurements regarding to the neutron skin thickness of nuclei [2] we have successfully used a single Vertical Drift Chamber (VDC) which was built at the KVI [3] for the old Q3D spectrometer. The accuracy of this detector is 0.15 mm (FWHM) for the lateral direction and 10 mrad for the angle in the bend plane. The position resolution for the vertical direction in the focal plane is 0.2-0.3 mm (FWHM). Using the single VDC as a focal-plane detector of the BBS would result in a momentum resolution a factor of two worse (and the energy resolution a factor of four worse) than the value which can be obtained using ray-tracing. Therefore we suggest to use two parallel VDC's which are separated by a distance of 20 cm and which therefore allow to determine accurately the angle of incidence in the focal plane in both the bend and non-bend directions.

The detectors shall be positioned parallel to the focal plane, which has an inclination of 52° with respect to the beam direction. This raises a problem connected to the read out of each VDC. In the previous set-up inside the Q3D spectrograph the tilt angle of the focal-plane was 45° implying that three to maximum four wires will fire. This allowed a four-wire read-out. As a consequence of different design specifications, with the BBS three to six wires will fire. The easiest way to handle the problem is to use an eight-wire read-out instead of the four-wire one. It requires only some modification of the delay-line connections. As a consequence of the modification we have more channels to handle. For the two VDC's altogether we need 32 analog-to-digital conversion channels.

During the 0° measurements the direct beam comes very close to the edges of the detectors requiring a special design of the detector chamber. Only 66 mm will separate the edge of the detectors which are inside the chamber from the beam outside. The wall of the chamber has been designed to be parallel to the beam direction.

Using the back-side plate (with the ΔE detector) of the existing detector system a new chamber has been designed. We shall construct it from stainless steel. One of the VDC detectors shall be mounted to the back-side plate and the other VDC to the newly designed front-side plate. Both the stainless steel chamber and the Al-alloy front-side plate will be produced in ATOMKI.

References

- [1] A. Krasznahorkay, et al., Nucl. Instr. Meth. Phys. Res. **A316** (1992) 306
- [2] A. Krasznahorkay, et al., Phys. Rev. Lett. **66** (1991) 1287
- [3] J.M. Schippers, et al., Nucl. Instr. Meth. Phys. Res. **A247** (1986) 467

Remote Controlled Isotope Production System at the Vertical Beam-Line of the Debrecen Cyclotron

L. Andó, I. Dombi, A. Nagy, J. Szádai, I. Szűcs, S. Takács,
F. Tárkányi, I. Mahunka

Cyclotron Laboratory based on the MGC-20 isochronous cyclotron, established in Debrecen in 1985, partly was dedicated to biomedical research programs [1]. In connection with these programs a vertical beam-line was developed and build up for the routine production of radioisotopes [2]. At the first step of this project only the SPECT isotopes were produced because in our laboratory the PET camera has been installed only at the end of 1993. Taking into consideration the new requirement to produce PET isotopes too, it was decided to improve our single target irradiation facility and rebuild it to a four-target chamber system which is controlled by a PLC + PC based remote-control system. The main goal of this development was to improve and simplify the performance of the isotope production in different target chambers keeping the reliability and efficiency of the irradiations at high level.

Our new irradiation facility can handle four target chambers. From the storage any chamber can be chosen and transported to the irradiation position by remote-control mode. At the irradiation position the connection and the installation of the target chamber with the necessary technical circuits such as vacuum, compressed air, cooling, etc. are automatically ensured. Sensors from the technical units are connected to the PLC and their normal working parameters are controlled by the computer system. Error signals arising from the controlled circuits initiate the programmed stop of the irradiation switching off first of all the beam from the target.

In the frame of this project target chambers for the irradiation of solid-, liquid- and gas-targets have been developed too. These chambers are giving possibilities for the routine production of the most important SPECT (^{67}Ga , ^{111}In , ^{123}I) and PET (^{11}C , ^{13}N , ^{15}O , ^{18}F) isotopes.

The project partly was supported by the National Committee for Technical Development.

References:

- [1] I. Mahunka, I. Uray, ATOMKI Közl., 24(1982)63
- [2] I. Mahunka, F. Tárkányi, L. Andó, F. Szelecsényi, A Fenyvesi, F. Ditrói, S. Takács, Proc. of 4th Symp. on the Med. Appl. of Cyclotrons, Turku, Finland, 28 - 31 May 1986, Turku, (1988)137

High Yield Conical Target Construction for Production of $^{11}\text{CO}_2$

Z. Kovács, É. Sarkadi, S. Takács, F. Tárkányi and L. Andó

In our earlier work a 60 cm³ volume, 20 cm long water cooled cylindrical type alumina target was used for the production of both $^{11}\text{CH}_4$ [1] and $^{11}\text{CO}_2$ [2] intermediers for the preparation of ^{11}C - labelled compounds. The end of bombardment (EOB) yield of these products varied between 300 - 600 MBq/ μA at saturation at 1×10^6 Pa target gas pressure which could give enough activity for chemical experiments but it is low for routine production of radiopharmaceuticals used in positron emission tomography.

The conical type targets have some advantages against the cylindricals [3], one of them is the smaller volume of the chamber. This reduces the time of delivery of the irradiated target gas to the apparatus for chemical syntheses which can be important when a product of high specific activity is required. The new target chamber is shown in Fig. 1.

The 1.1 - 2.7 cm internal diameter and 14 cm long (40 cm³) chamber was made of alumina. The helium gas front cooling unit is sealed by two 25 μm titanium windows. The collimator unit and the target body, which consist of two parts and sealed by a silver ring, is cooled by water. 1.6×10^6 Pa nitrogen gas pressure is required to be filled for full absorption of 18 MeV protons. However, we tested the target with 14.5 MeV beam at 1.1×10^6 Pa. The irradiated gas is delivered to a trap cooled with liquid nitrogen and the activity collected is measured by curiemeter. After several test runs with different currents (5 - 10 μA) and irradiation time (5 - 30 min) the yield was 1.6 - 2.2 GBq/ μA at saturation ($E_p = 14.5$ MeV) which is considerably higher than it was with the old target and comparable with other values published [4, 5].

References

1. É. Sarkadi, Z. Kovács, ATOMKI Annual Report (1991) 125
2. P. Mikecz, Z. Kovács, ATOMKI Annual Report (1992) 102
3. T. Vandewalle, Inst. J. Appl. Radiat. Isot., **34** (1983) 1459
4. K. Nägren, The Åbo Akademi Accelerator Laboratory, Triennial Report, (1987 - 1989) 76
5. S. J. Heselius, Appl. Radiat. Isot., **38** (1987) 49

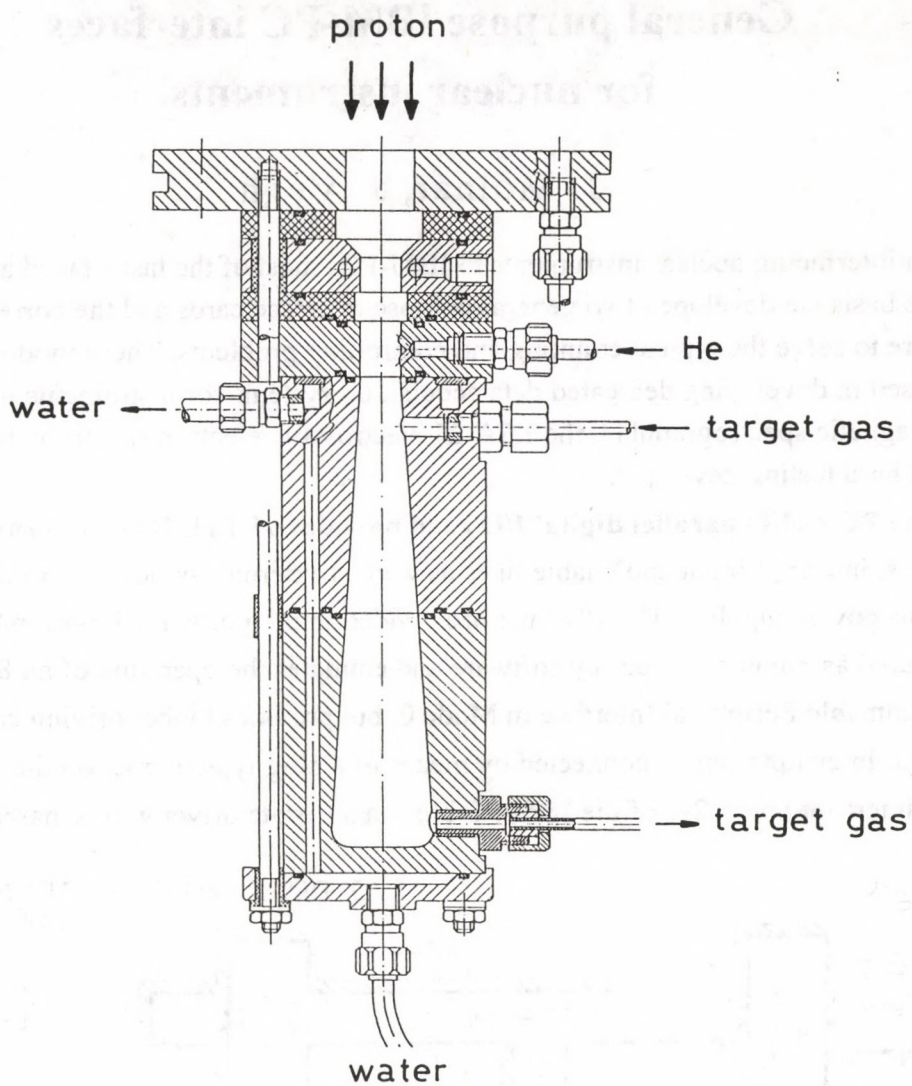


Fig. 1. Conical type target chamber for routine $^{11}\text{CO}_2$ production.

General purpose IBM-PC interfaces for nuclear instruments

J. Molnár, J. Végh

In interfacing nuclear instruments to IBM-PCs most of the tasks faced are common. On this basis we developed two general purpose interface cards and the corresponding software to solve the typical counting and controlling problems. These modules have been used in developing dedicated data acquisition systems for instruments like the split-pole magnetic spectrograph[1], the ESA-21 electrostatic electron spectrometer[2] and the rad hard testing device[3].

The **PC-64I/O parallel digital I/O card** provides 64 TTL/DTL compatible digital I/O lines, interrupt input and enable lines as well as external connections to the IBM PC's bus power supplies. The I/O lines are divided into 8 ports. Each port may be configured as input or output by software and emulates the operation of an 8255 Programmable Peripheral Interface in Mode 0, but provides higher driving capacity than an 8255. Interrupts can be connected by means of a plug type jumper on the board to any of the interrupt levels 2-7 of the IBM PC bus via a tristate driver with separate enable.

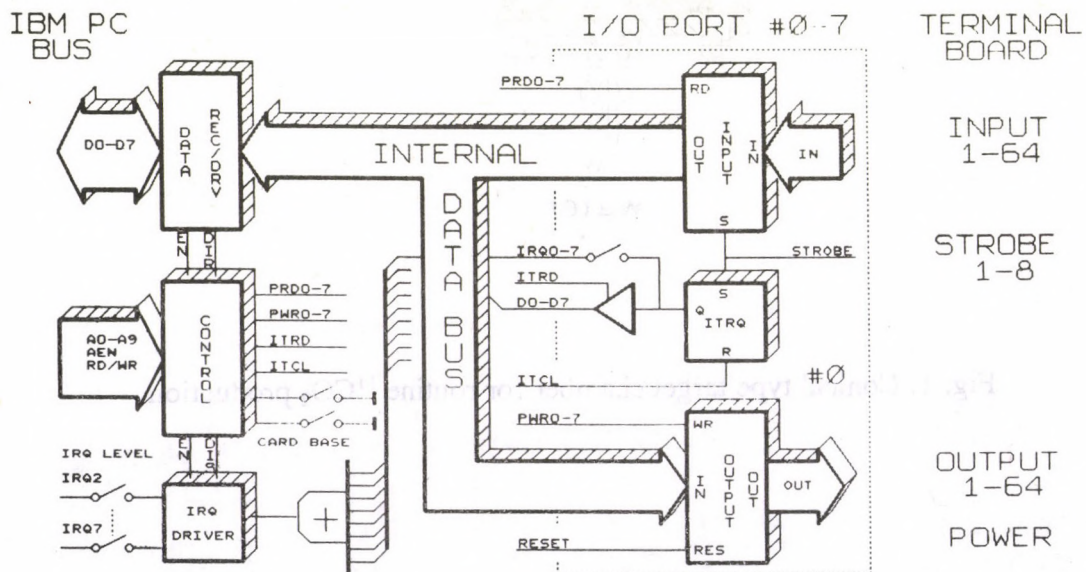


Figure 1. The scheme of the **PC-64I/O parallel digital I/O card**

The **PC-40CH general purpose counter-timer card** provides 40 channels (eight AM 9513 counter/timer chips) of 16 bit up/down counters plus frequency dividers for on board 5 MHz crystal time base. It is a widely used device with flexible and powerful function modes for many laboratory applications. A selection of various internal/

external signal sources and outputs may be chosen as inputs for the individual counters with software selectable input polarities. Each counter may be gated either in hardware or by software. The counters can be programmed to count up or count down in either binary or BCD. Counters located in one chip can be concatenated by software to form counters of effective length up to 80 bit. Each counter has an associated Load Register and a Hold Register. The Load Register is used to automatically reload the counter to any predefined value, thus controlling the effective count period. The Hold Register is used to save count values without disturbing the count process, thus permitting the IBM PC to read intermediate counts. Each counter has a single dedicated output pin. It may be configured to be off when the output is not of interest. The card has an additional 8259 interrupt controller to extend the interrupt handling capacity of PC.

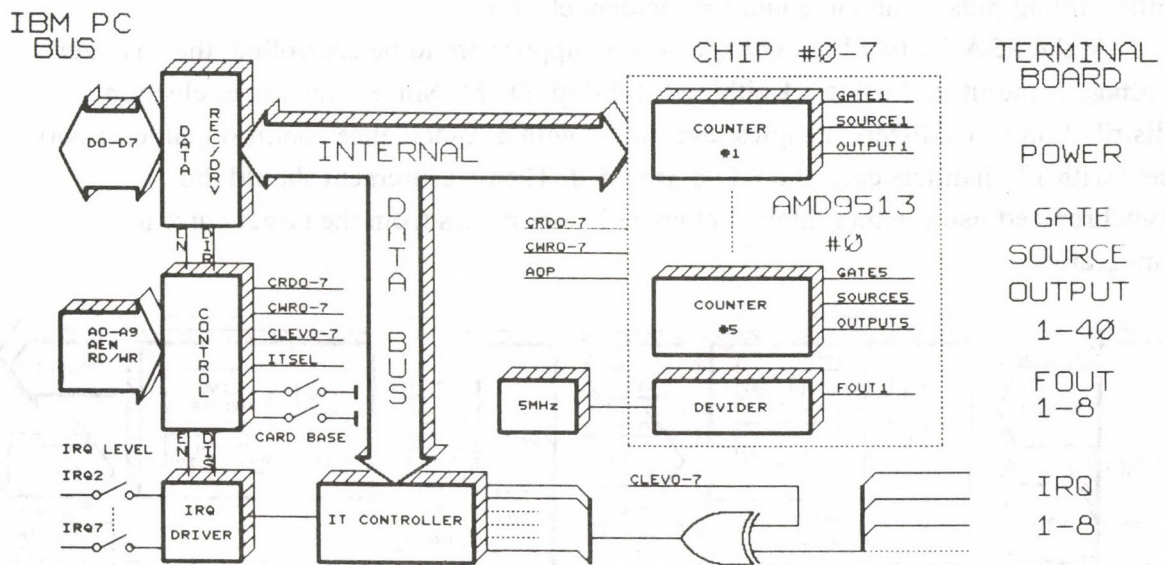


Figure 2. The scheme of the **PC-40CH counter-timer card**

Note that parts of these two cards have also been combined in one single board (the **PC-10CH+80O+16I combi card**) to provide 10 scalars and 96 I/O lines, otherwise it has the characteristics described above.

The **software** for these cards was coded mainly in Turbo Pascal and partly in assembly language. It is able to reproduce the flexibility and power of the hardware. An elemental (IC-level) and an intermediate (card-level) support is also provided. A special object oriented interrupt handler routine has been developed which enables the user to write even the interrupt service part of the measurement control program in a high-level language safely and easily while it allows to service the interrupts at the possible maximum speed.

- [1] J. Molnár, J. Végh, M. Csatlós and A. Krasznahorkai, in this volume.
- [2] J. Molnár, J. Végh, Á. Kövér, S. Ricz and B. Sulik, in this volume
- [3] J. Molnár, J. Végh, G. Dajkó, A. Fenyvesi and A. Kerék, in this volume

The voltage on the electrodes of the spectrometer can be monitored, and its measured value can be read through the input ports as a 24-bit BCD value. When a conversion is finished, the DVM provides a print signal (READY) that can cause an interrupt on the I/O board. This solution allows to use the DVM to verify only the eventual deviation/noise in the system as well as to make a feedback.

The system can be set up to work in two modes (CH/TIM) of operation. When the exciting beam is stable, the uniform data acquisition time assures that the electrons counted at different energies are excited by the same number of incident particles. In such a case the "time" mode (the synchronizing counter receives pulses generated by the internal clock) is set. The 5 MHz clock frequency is divided in such a way that the received pulses will have either 1 Hz or 1 kHz frequency, software selectable (1/1kHz). Usually, however, the "charge" mode should be used, where the pulses (TCI IN) are generated by some external hardware, usually a current integrator.

One 16-bit counter on the **PC-40CH counter-timer board** is reserved to count the synchronizing pulses (IN#40). The other counters are reserved for event counting. They can be configured in three different ways. In mode A they form 13×32-bit scalars and 13×16-bit scalars, in mode B three sets of 13×16-bit scalars, in mode C there are two sets, each of which contains 16 scalars, all but the first being 16-bit long and the first one is 32-bit long.

All the event counters are gated by the output of the synchronizing counter. This gate is opened by the first timing pulse and closed by the last pulse. In "charge" mode the system is able to provide a discharging pulse for the integrator and this pulse can also be used (jumper selectable, with adjustable delay) to open the gate. This feature can make the use of the accelerator time more effective.

Based on the software for the general purpose cards, a simple measurement control program was prepared. After the successful testing, preparation of a more refined measurement control program with data display and evaluation abilities are in course. In its final form the software will consist of a resident data acquisition and measurement control program that is interfaced to the user either with an independent data display program or the more sophisticated data evaluation and display program.

[1] D. Varga, I. Kádár, S. Ricz, J. Végh, Á. Kövér, B. Sulik and D. Berényi: Nucl. Instrum. Meth. A313(1992) 163-172.

[2] J. Molnár, J. Végh, in this volume

Development of a multiparameter data acquisition system for the split-pole magnetic spectrograph

J. Molnár, J. Végh, M. Csatlós and A. Krasznahorkay

The focal plane detector of the Split-Pole magnetic spectrograph installed in our institute [1] is constructed by using 5 silicon position sensitive detectors. Each of these detectors supplies two analog signals. One of them is proportional to the energy of the detected particles while the other one carries information about the position of the detected particles. For the investigation of the superdeformed states in the actinide region [2] we intend to measure also the time of flight of the particles travelling through the spectrograph and the time difference between the spectrograph detectors and a few fission detectors positioned close to target.

The schematical block diagram of the setup can be seen in Fig. 1. The energy and position signals of the charge sensitive preamplifiers are amplified by delay-line amplifiers. After passing the linear gates, the energy and position signals of all detectors go to two main amplifiers with additional shaping networks and base line restorers. Finally the pulses reach the ADCs. The logic pulses from the discriminators are sent to a bitbox, which generates all control signals and the identification bits for the detectors. The third ADC is used for the digitalization of the corresponding time-of-flight signals, while the fourth one is for the digitalization of the time difference between the focal plane and fission fragment detectors.

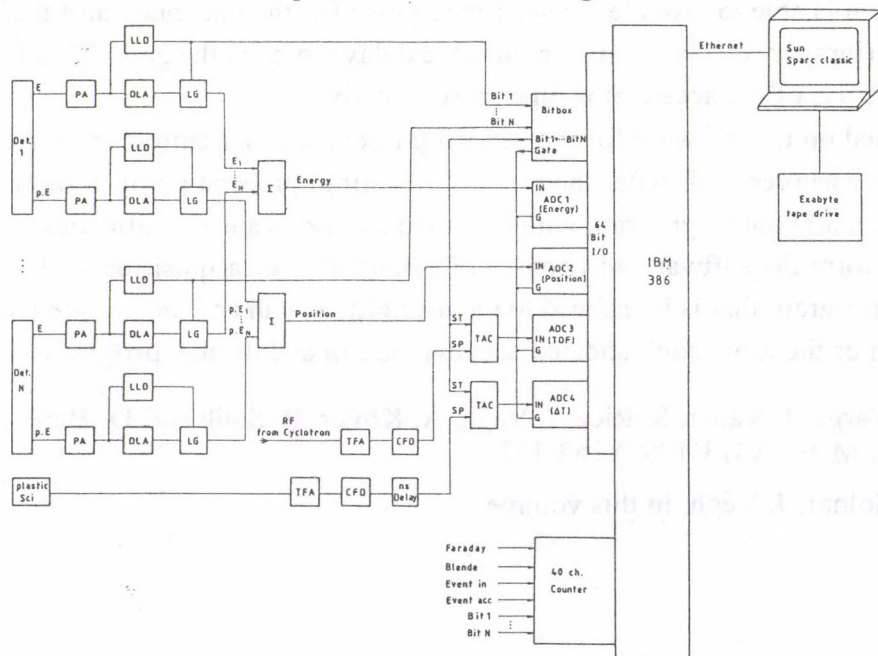


Fig. 1. Schematical block diagram of the electronics

To estimate the dead time of the detectors, to measure the charge collected by the Faraday cup and the diafragmas and to measure the count rate of the different fission fragment detectors a hardware unit based on the PC-40CH general purpose

counter/timer card[3] was constructed. To read out the signals generated by the four ADCs, the bitbox and the scalers, a multiparameter data acquisition system based on the PC-64I/O parallel digital I/O card [3], a connected IBM PC/AT and a SUN Classic computer was developed.

The incident particles trigger an interrupt signal for the computer which reads out the address(+ident) information from the ADCs, stores it temporarily in a double buffer and writes it up in blocks in a disk file - which appears already on the disk of the SUN computer via ETHERNET and PCTCP protocol. This solution allows for quasi-online analysis of the measured data by the program PAW (Physics Analysis Workstation)[4], developed at CERN, and causes no loss in the data acquisition speed.

The data acquisition program is based on the service routines of the two interface cards. For speed reasons, the interrupt service routine was coded in assembly language and only a minimum display function was implemented. The maximum readout time is $<100 \mu\text{secs}$ on a 40 MHz IBM-PC/AT.

Test measurements using Si position sensitive detectors have been carried out to demonstrate the capability of this data acquisition system. Some preliminary results can be seen in Fig. 2. The above setup was also checked in $\gamma\gamma$ -coincidence measurements using 4 HPGe detectors.

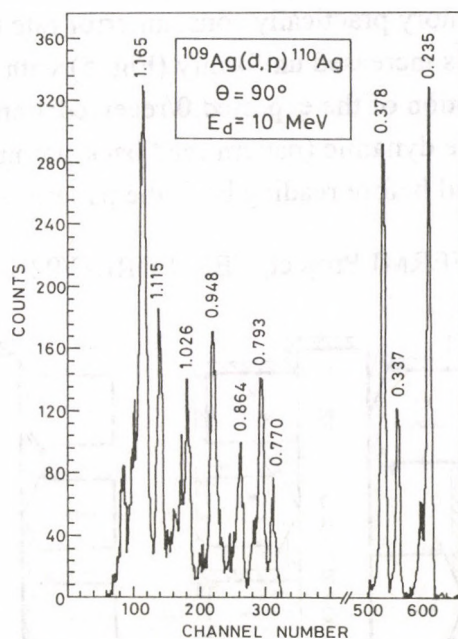


Fig. 2. A typical proton spectrum measured with the magnetic spectrograph.

This work has been supported by the OTKA Foundation, No: 7486 and 3004.

- [1] A. Krasznahorkay, S. Török and L. Félegyházi, ATOMKI Ann. Rep. (1992) 122
- [2] A. Krasznahorkay et al., ATOMKI Ann. Rep. (1993)
- [3] J. Molnár and J. Végh, ATOKI Ann. Rep. (1993)
- [4] R. Brun et al., PAW User's Guide Version 1.07, CERN, Geneva (1989)

Rad Hard tests of static RAMs

J. Molnár, J. Végh, G. Dajkó, A. Fenyvesi and A. Kerék†
 †The Royal Inst. Technol., Dept Physics/Frescati, Stockholm, Sweden

In nuclear physics experiments some electronic circuitries should operate in a severe radiation background. To improve their radiation tolerance, in the fabrication of these chips special technologies and packaging are used. In order to gain experience and prepare for the future integration of such components, in the frame of the CERN FERMI RD-16 project[1] the radiation tolerance of a standard bulk CMOS memory is compared with some radiation hardened SOS memories.

For the automatization of the rad hard measurements, an IBM-PC based test setup(Fig. 1), as well as data collection and analysis software have been developed. The RAM ICs were irradiated by gamma and neutron sources. In gamma field, both the total number of errors (Fig. 2) and especially the number of failing cells (Fig. 3) were significantly lower in the special rad hard RAM IC. In neutron field, no errors were detected in the rad hard IC, while in the standard memory practically constant error rate (Fig. 4) was experienced and the number of failing cells increased uniformly (Fig. 5) with the received flux. Note that in all cases a clear distinction of the expected:0/received:1 and its opposite type errors were observed, both in the dynamic (pattern read back promptly after writing) and static (irradiated for some period before reading back the pattern) storage tests.

[1] Status Report on the FERMI Project, CERN/DRDC/92-26, RD-16/May 1, 1992

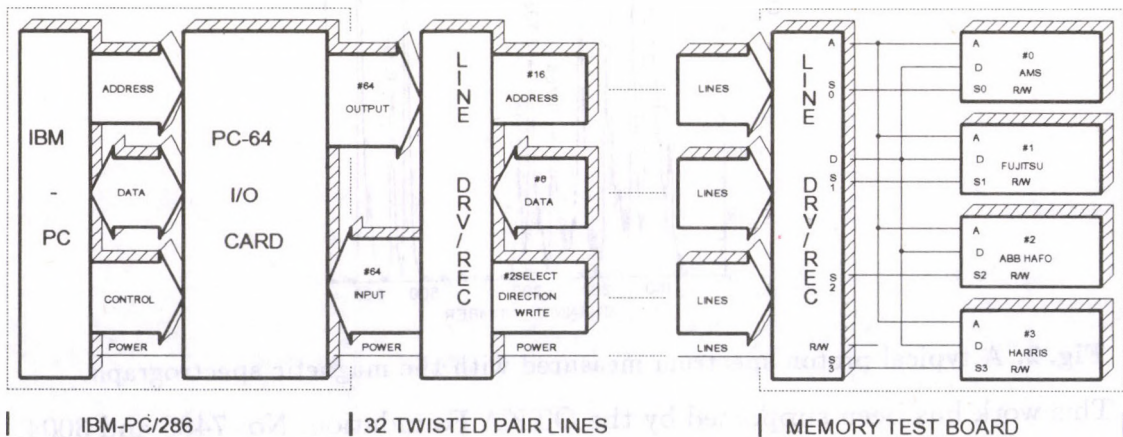


Figure 1. The test setup

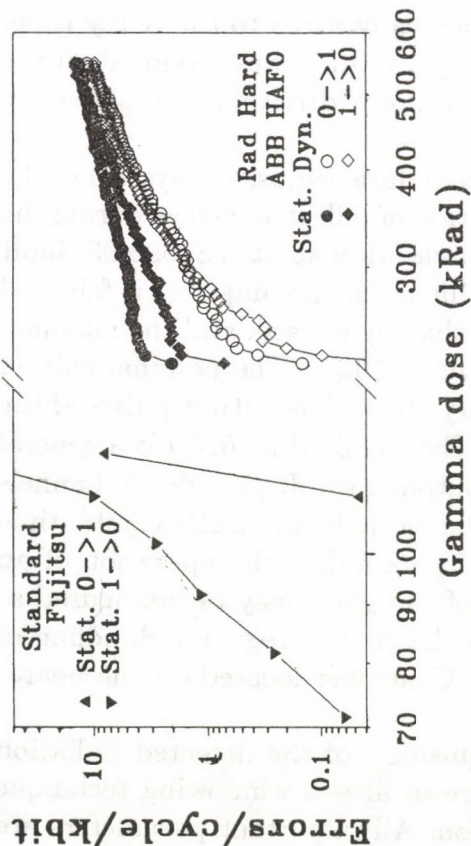


Figure 2. Total number of errors as function of gamma dose

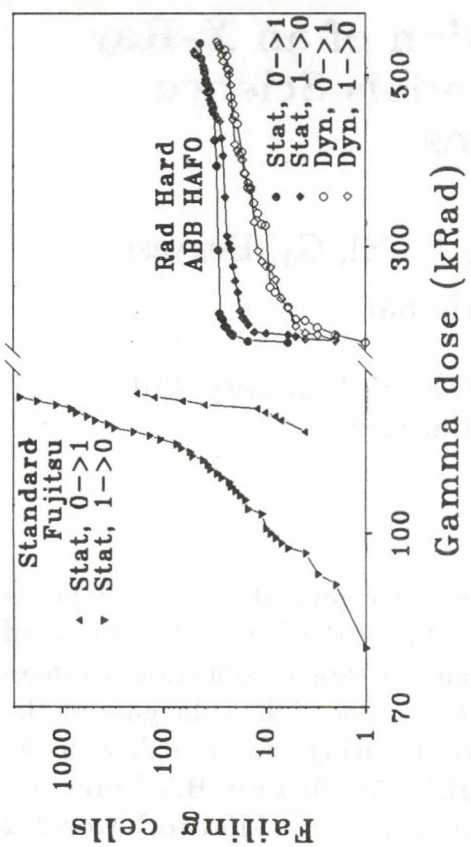


Figure 3. Total number of errors as function of neutron flux

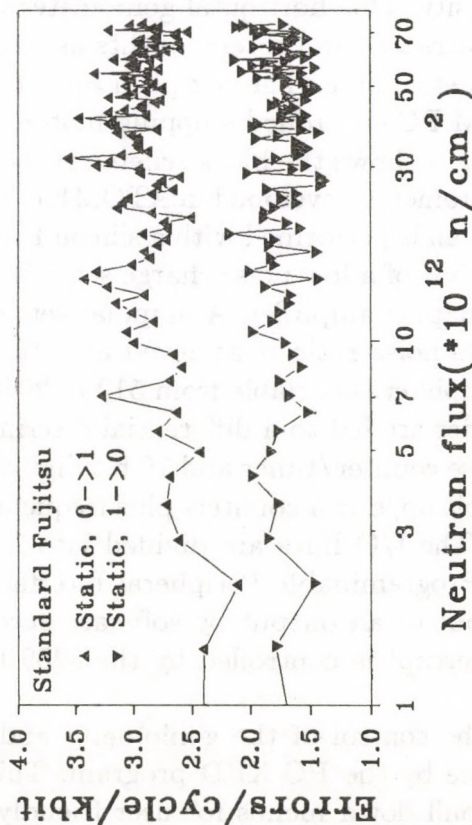


Figure 4. Number of failing cells as function of gamma dose

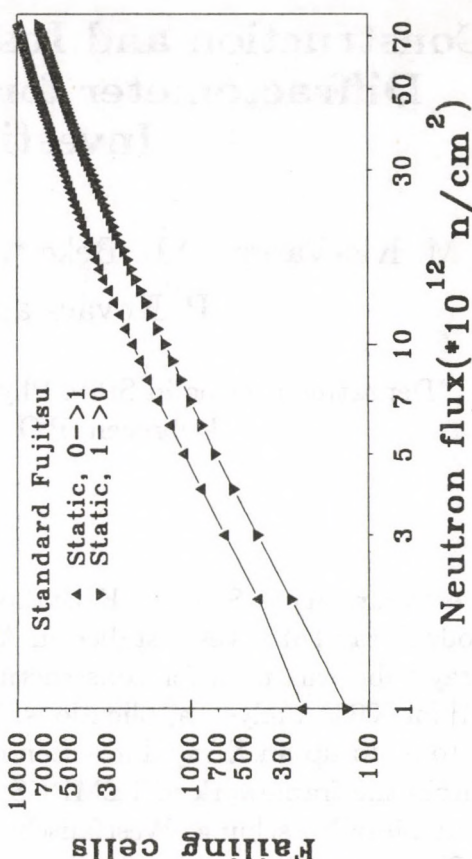


Figure 5. Number of failing cells as function of neutron flux

Construction and Installation of an X-Ray Diffractometer for Materials Science Investigations

M. Kis-Varga, D.L. Beke *, I. Gál, J. Gál, Gy. Hegyesi,
P. Kovács and M. Molnár

*Department of Solid State Physics, L. Kossuth University, 4010
Debrecen, P.O. Box 2., Hungary

A few years ago a Siemens Kristalloflex 710H X-ray generator with FK 60-04 Mo anode X-ray tube was installed in ATOMKI. One of the four exit windows of the X-ray tube was used for constructing a secondary target excitation arrangement [1] for XRF analysis applications. The line focal spot of the tube gave us the chance to build up an X-ray diffraction device, too, by using another exit window.

Within the framework of TEMPUS Project JEP 1586-91 Prof. H. Mehrer (Institut für Metallforschung, Westfälische Wilhelms-Universität Münster) provided a used Siemens goniometer to the Department of Solid State Physics of L. Kossuth University. This horizontal goniometer was mechanically fitted to the X-ray tube. New entrance- and receiving slits as well as a sample spinner was mounted on the goniometer table. The old push button controlled motor driving was replaced by an IBM PC controlled stepping motor.

Fig. 1 shows the block scheme of the control and data acquisition system of the diffractometer developed in ATOMKI. The detection of reflected X-rays during the $\theta/2\theta$ scan is performed with a silicon PIN photodiode (Hamamatsu S3590-03) built in the box of a low noise charge sensitive preamplifier. The preamplifier is followed by a shaping amplifier. A unipolar semigaussian shaping is used, and the maximal peak to noise ratio is achieved at a time constant of 10 μ s. The nominal gain of the amplifier is variable from 512 to 2048 in binary steps. The output pulses of the amplifier are led to a differential discriminator. The PC-5CH & 16I/O is a general purpose counter/timer and 16 bit digital input/output card. It provides 5 channels of 16 bit up/down counters plus frequency dividers for on board 6MHz crystal time base. The I/O lines are divided into 2 ports, which emulate the operation of an 8255 Programmable Peripheral Interface. Each of the ports may be configured as an input or an output by software according to the control register. Handling of an interrupt is controlled by the 8259 Interrupt Controller located on the board, too.

The control of the goniometer and the acquisition of the detected radiation is made by the PC-XRD program. This software utilizes a windowing technique with pull down menus for user friendly operation. All important parameters are displayed on the monitor along with the spectrum area. The analyser functions

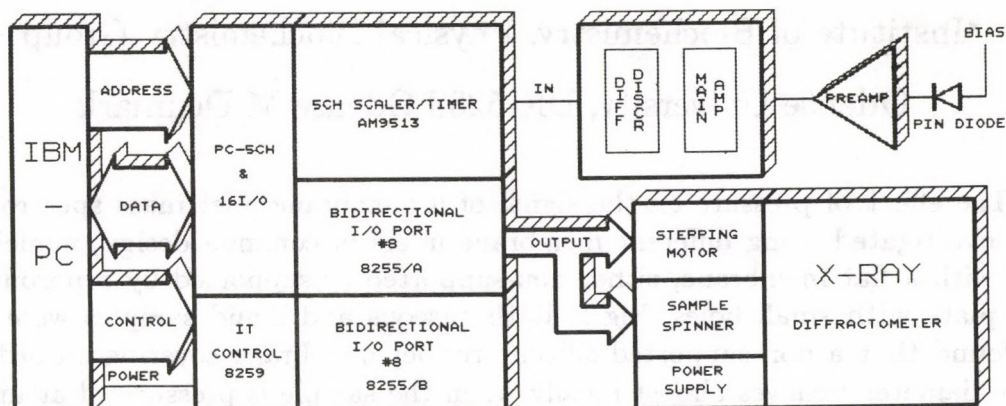


Fig. 1. The block scheme of the control and data acquisition system of the X-ray diffractometer

are as follows: erase, start/stop acquisition; set of scan parameters (step size, start angle, end angle, scan time, average mode); expand/compress spectra in horizontal or/and in vertical direction; ROI operations (set/delete ROI, background and $K_{\alpha 2}$ stripping, calculation of ROI parameters); sector operations (compare and add/subtract spectra); automatic measurement and save of maximum 10 different preprogrammed scans. The file operations are: save/load spectrum data in binary or/and ASCII form; directory of current disc; peak evaluation and save/load results; smoothing of ROI.

The diffractometer has been successfully used for study the properties of mechanically milled nanocrystalline metal powders [2]. In order to improve the angle resolution of the system a copper anode X-ray tube is planned to be installed in the near future by help of TEMPUS Project mentioned above.

References

1. M. Kis-Varga et al., ATOMKI Annual Report **1991** (1992) 99
2. L. Daróczi et al., Abstracts of International Symposium on Mechanisms of Formation of Metastable Microstructures, Cambridge, U.K., 12-16 July 1993, 56

Influence of pressure on Measurements with Membrane Inlet Mass Spectrometry

I.Futó, H.Degn*

*Institute of Biochemistry, Physical Biochemistry Group
Odense University, DK-5230 Odense M Denmark

The effect of pressure on the signal of a membrane inlet mass spectrometer was investigated using different membrane inlets of common design, namely the type with a flat membrane, either non-supported or supported by a porous disk or a plate with small holes. Fig.1. Both gaseous and liquid samples were used. We found that a non-supported silicone rubber membrane covering an orifice of 1mm diameter behaves almost ideally when the sample is pressurized at up to 1 bar above the atmospheric pressure. With a membrane of 2mm diameter there are significant deviations from ideal behaviour due to elastic deformation of the membrane. When a non-supported membrane is repeatedly pressurized up to 5 bar above atmospheric pressure the membrane properties change irreversibly and strongly non-linear effects such as hysteresis are observed. When the membrane is supported by a surface perforated small holes the signal decreases strongly with increasing pressure. The explanation is that membrane gets pressed tighter onto the supporting surface, thus reducing the space available for lateral diffusion of analyte. This effect is also seen, although to a lesser degree when membrane is supported by a porous disk. The results are pertinent to the design of membrane inlets to be used where pressure changes may occur.

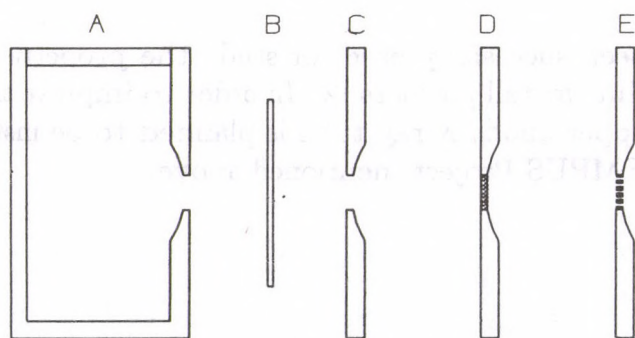


Fig. 1. Schematic drawing of tested inlets

A:measuring cell; B:membrane; C:non-supported type inlet;
D:porous support; E: support with small holes.

We found that pressure effect are insignificant with a membrane inlet with an non-supported membrane of a small diameter (1 mm). Also an inlet with the membrane supported by a porous plug is not very pressure sensitive. However, inlets where the membrane is supported by surface with small holes in it are very sensitive to changes of pressure. Also inlets with non-supported membranes of a diameter more than 1.5 mm are unfavourable with respect to changing pressure. When the signal versus pressure curves of different compounds in liquid mixtures were measured it was observed that at the higher pressures the signals due to different compound did not respond in parallel. We have done measurements with various compounds and it seems to be a rule that the signals of polar compounds increase with pressure whereas the signal of less polar compounds decrease with pressure. This phenomenon may indicate that the stretching of the membrane changes the properties of the membrane material in such a way that the diffusion of nonpolar compounds is affected in a negative direction. Fig.2. The position of the hysteresis loop also depend of the thickness of the membrane. The porous supported membrane inlet not suitable for the measuring heavy organic mass because on the big surface in the porous plug can easily stick the organic molecules increase the response. The best one among the three tested membrane inlet found the non-supported membrane with 1mm diameter.

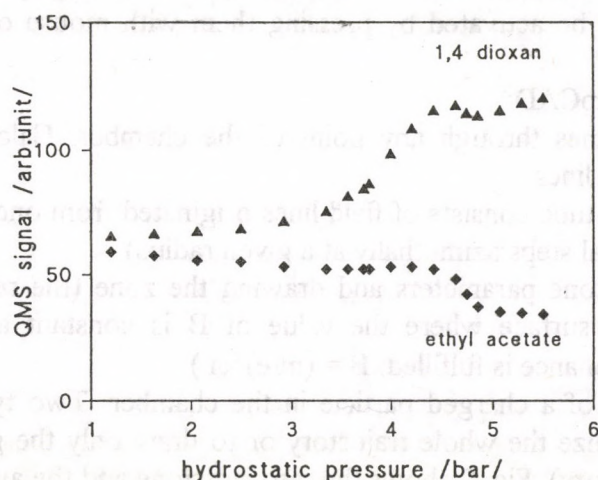


Fig. 2. QMS signal changes for polar and non-polar compounds (1,4 dioxan $m=88$ a.m.u. ethyl acetate $m=61$ a.m.u.)

References

1. I. Futó, H. Degn*
Effect of pressure on membrane inlet mass spectrometry
Annual meeting of the Center for Biotechnology Process Research, The Technical University, Copenhagen, Denmark 1993 nov.15.

Computer aided design of magnetic traps for ECR ion sources

J. Vámosi and S. Biri

The ECRIS (Electron Cyclotron Resonance Ion Source) project of the ATOMKI [1] started in January of 1993. The designing of the magnetic system has been finished by the end of 1993. To help the designing and to study the behaviour of complex charged particle traps an effective computer code (called TrapCAD) has been developed.

TrapCAD makes it possible to study the magnetic field inside the plasma chamber of ECR ion sources in three dimension. The magnetic field consists of a longitudinal component created by several solenoids of cylindrical symmetry and a transversal one created by a linear multipole (Yoffe-) type permanent magnet system. The superposition of the two components forms a 'B-minimum' geometry, where the field grows if one moves from the center of the volume to any direction.

The commercially available magnetic field calculation codes usually used for ECR-calculations (e.g. POISSON/PANDIRA) are two-dimensional applications with ASCII-type output. TrapCAD is a graphical application for IBM PC. Having loaded the contents of output data files of those 2D codes, TrapCAD switches to the graphics screen and the schematic front and the side view of the ECR chamber is displayed (Fig. 1). The pushbutton functions can be activated by pressing them with mouse or from keyboard.

The main functionalities of TrapCAD:

(1) Drawing magnetic field lines through any point of the chamber. Calculating several kinds of mirror ratios of the lines.

(2) Drawing flux tubes (a flux tube consists of field lines originated from one of the end-plates of the chamber with equal steps azimuthally at a given radius).

(3) Calculating the resonant zone parameters and drawing the zone (the resonant zone of an ECR ion source is a surface where the value of B is constant and the condition of electron cyclotron resonance is fulfilled: $B = (m/e) \cdot \omega$).

(4) Simulating the movement of a charged particle in the chamber. Two types of simulation can be chosen: to visualize the whole trajectory or to draw only the guiding center of the path (averaged trajectory). Fig. 2 shows the resonant zone and the averaged trajectory of an electron. TrapCAD produces DXF type files as output which can be displayed in AutoCAD. Using the wide-range set of tools providing by AutoCAD one can visualise the structure of the magnetic bottle in 3D.

TrapCAD is a real mode MS-DOS application coded in C/C++ language. The differential vector equation of the field lines was solved by the Runge-Kutta method. To calculate the particle path a simple but fast time-centered leapfrog scheme [2] was used.

This code was intensively used to optimize the magnetic configuration of the Debrecen-ECRIS. A detailed description of TrapCAD and its application for the ECR project can be found in [3].

References

1. S. Biri and J. Vámosi, this Annual Report.
2. T. Tajima, Computational Plasma Physics: With Applications to Fusion and Astrophysics (Addison-Wesley, Redwood City CA 1989)
3. J. Vámosi and S. Biri, submitted to the Nuclear Instruments and Methods.

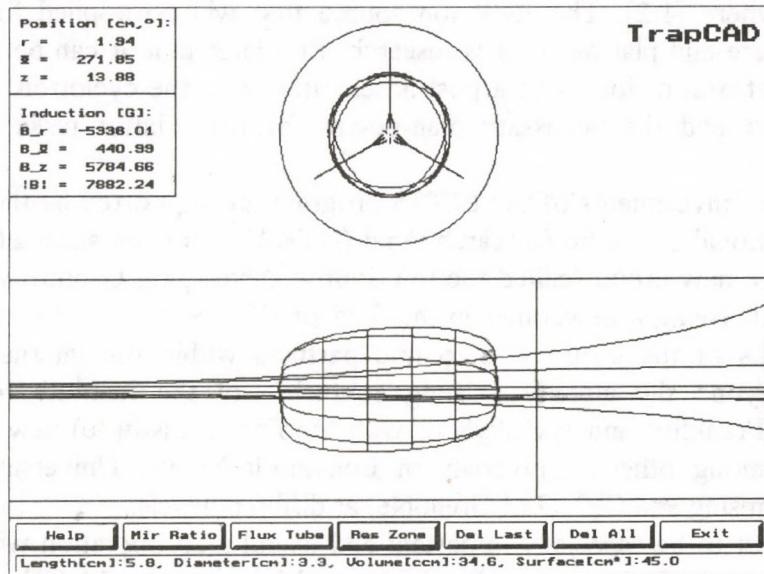


Fig. 1. Hardcopy of the VGA screen when running TrapCAD

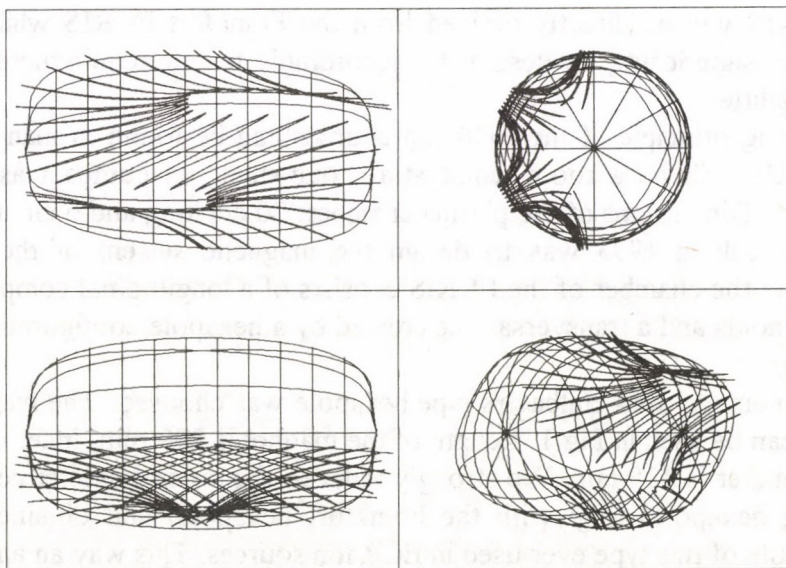


Fig. 2. The motion of the guiding center of an electron path inside the resonant zone. The figure is plotted in four different views by AutoCAD. Only the half of the whole closed trajectory is delineated for clearness.

Status of the ECRIS Project

S. Biri and J. Vámosi

After a long and uncertain preparation period of time the ECRIS (Electron Cyclotron Resonance Ion Source) program of the ATOMKI effectively started in 1993. The main goals of the program and the planned future usage of the ion source have been described elsewhere [1,2]. The ECR ion source first will be applied for low energy atomic, solid state and plasma physics research. In a later time it can be mounted on a high voltage platform or joined to a post-accelerator or to the cyclotron. However, the financial support and the necessary man-power for these latter tasks has not been ensured yet.

The costs of investments of the ECRIS program are supported by the World Bank through the National Scientific Research Fund (OTKA)¹. For the successful performing of the program a new group (called the Ion Source Developing Group) was established in the ATOMKI. Being a newcomer in the field of ECRIS, one of the most important and urgent tasks of the group was to find partners within the international ECRIS community. Beyond the already existing contacts of the institute (e.g. with the Universities of Frankfurt and Jyväskylä or with the Dubna Institute) new co-operations began (with, among others: University of Louvain-la-Neuve, University of Giessen, MSU in East Lansing and CENG of Grenoble) at different levels.

It turned out to be especially important and useful a co-operation with the Institut für Kernphysik of the University of Frankfurt am Main where a 14 GHz ECRIS and a Radio Frequency Quadrupole (RFQ) post-accelerator are being developed. After careful investigation of different possibilities and ways it was decided that to design and built our ion source first of all the Frankfurt-ECRIS, as base, will be considered. Some parts of the Debrecen-ECRIS will be directly derived from the Frankfurt-ECRIS while others (see below) must be significantly re-designed - accordingly to our requirements and limited financial possibilities.

The working principle of the ECR ion sources can be found in many papers. The Debrecen-ECRIS will be a room-temperature, one-stage, as compact as possible, 14 GHz ion source. Dimensions of the plasma chamber: 20 cm long and 6 cm in diameter.

The main task in 1993 was to design the magnetic system of the source. The magnetic field in the chamber of the ECRIS consists of a longitudinal component created by several solenoids and a transversal one created by a hexapole configuration permanent magnet system.

A 24-segments, closed Halbach's type hexapole was chosen. The magnetisation of the segments can be seen in Fig. 1. Length of the magnet is 200 mm, inner diameter is 65 mm, outer diameter is 135 mm. We strongly reduced the outer diameter comparing with other, existing hexapoles (e.g. with the Frankfurt hexapole) and obtained one of the thinnest hexapole of this type ever used in ECR ion sources. This way an approx. 40% of the magnet volume (and, consequently, of the price!) was saved while the decreasing of the magnetic field strength in the chamber is less than 20%. The magnetic calculations

¹Contract number: A077.

were performed using the PANDIRA code. The hexapole was ordered from Outokumpu (Finland).

Another important consequence of choosing a thinner hexapole was that we could decrease the inner and outer diameter of the solenoid coils as well. Furthermore, a relatively thick (5 cm) iron yoke around the two coils and also iron rings at the ends of the hexapole were carefully designed. This way the electrical power consumption, necessary for the magnetic system, could be reduced from the initially calculated 120 kW down to around 80 kW. This also significantly decreased the price of the power supplies and the future power consumption of the ion source. In Fig. 2. the schematic view of the magnetic system can be seen (half of the elements are drawn in a cylindrical co-ordinate system). The 2 iron rings at the ends of the hexapole are optional and their final shape (especially at the extraction side) will be different from those in the picture. Four coils (consisted of 5, 2, 2 and 5 double pancakes) will be formed, however, three 55 V/500 A DC power supplies is enough to feed them (the middle two thin coils will be electrically connected). This way one can set any required magnetic profile along the axes of the system. The inner diameter of the pancakes is 17.5 cm, the outer diameter: 50 cm. The highest closed magnetic surface inside the plasma chamber is expected slight above 1 Tesla (the resonant field is 0.5 Tesla for 14 GHz) that is still quite enough for highly charged ions. The magnetic calculations were performed using the POISSON and our newly developed TrapCAD [3] codes.

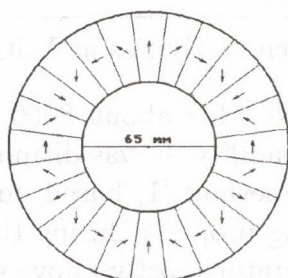


Fig. 1. Arrangement of the hexapole segments. Arrows show the directions of the magnetisation.

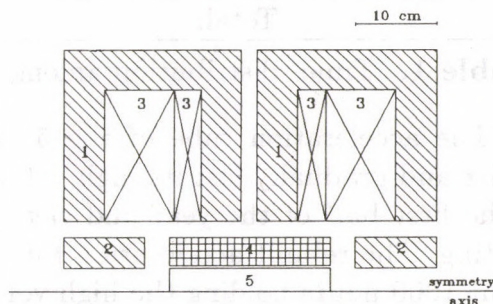


Fig. 2. Schematic view of the magnetic system. 1,2: iron, 3: coil, 4: hexapole magnet, 5: plasma chamber.

The pancakes and the power supplies have been recently ordered. Some more details about the magnetic system can be found in [3].

In 1993 the 14 GHz VARIAN transmitter and some computer hardware and software tools (for designing and for future operation and control) were also bought.

References

1. The heavy ion physics program of the ATOMKI, Institute of Nuclear Research, 1991. Compiled by S.Biri. Non-published.
2. S.Biri and J.Vámosi, In Proc. 11. Int. Workshop on Electron Cyclotron Resonance Ion Sources, Groningen, 1993, KVI-Report 996, p. 128.
3. J.Vámosi and S.Biri, this Annual Report.

Activities at the Van de Graaff Accelerator Laboratory

L. Bartha, Á.Z. Kiss, E. Koltay, Gy. Mórik,

E. Somorjai and Gy. Szabó

During 1993 the beam time of the VdG-1 machine amounted to 839 hours. The accelerator delivered proton and helium beams for atomic physics, as long as 791 hours, and it produced carbon beam in 48 hours for applications in surface science. The new beam line of VdG-1 has been completed in this year.

The 5 MeV Van de Graaff machine was operating for 1260 hours during this period, protons (65 %) and $^4\text{He}^+$ ions (35 %) were accelerated (Table 1).

Field	Hours	%
Atomic physics:	660	52
Analytical studies:	519	41
Machine tests:	81	7
Total:	1260	100

Table 1. Time distribution among different research activities at VdG-5

The acceleration tube of the 5 MV machine worked for about 8000 hours earlier and gradually lost its high voltage insulating capability. It was dismantled in the first half of the year and cleaned by a special method [1] based on sand blasting. The rebuilt acceleration tube has been working properly during the last about 1000 hours holding the high voltage of the accelerator mostly above 4 MV.

Steps have been made for the building up of a proton microbeam facility at the 5 MV Van de Graaff accelerator in the years 1994-95. Independent financial sources have been provided by the National Foundation for Scientific Research (OTKA-A-080) and by the International Atomic Energy Agency (IAEA-CRP-7257/RB) for ordering the basic electron-optical units, computer software and optical zoom microscope from Oxford Microbeam Ltd. We received these units by the end of 1993. Manufacturing of beam transport elements, vacuum system and target chamber to be done by Institute's staff is in progress.

Reference

1. L. Bartha and Gy. Mórik, to be published

Status Report on the Cyclotron

A. Valek

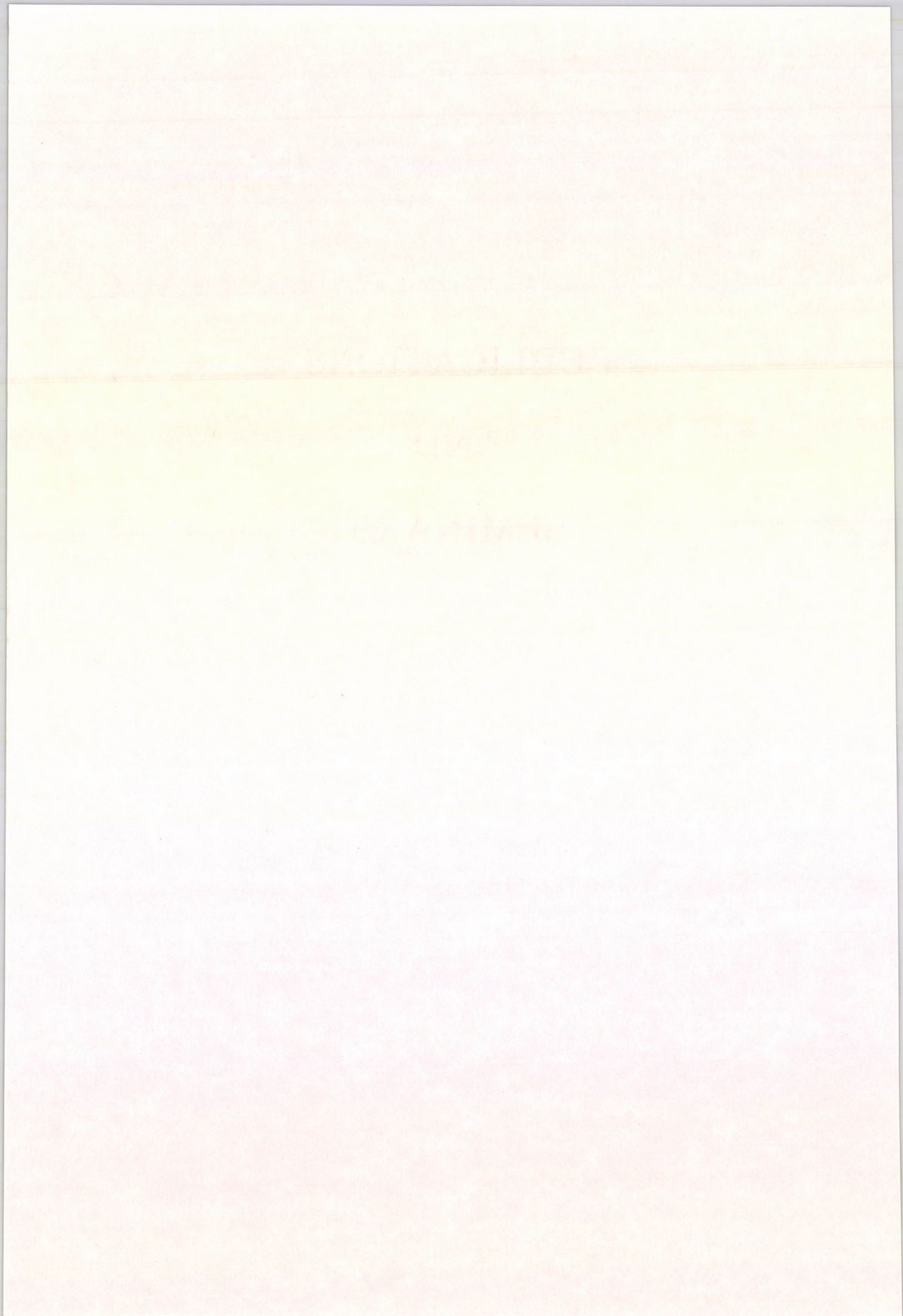
The planned operation of the cyclotron was similar to that of the previous years, though the total beam time was somewhat larger. The utilization of the machine was concentrated to 9 months; January, July and August were reserved for maintenance and holiday.

The overall working time of the cyclotron was 4560 hours and the break down periods amounted up to 318 hours. The cyclotron was available for users during 3748 hours, the effectively used beam time is summarized in Table 1. (FERMI: Front-End Readout MICROsystem, Radiation hardness measurements, CERN RD-16). Low energy protons, down to 3.3 MeV, were successfully accelerated for nuclear spectroscopy studies. In the maintenance period only the regular repairs and test runs were carried out.

Table 1. Effectively used beam time

Projects	Beam time (hours)	%
Nuclear spectroscopy	811	26
Nuclear reactions	280	9
Neutron physics	68	2
Particle spectroscopy	309	10
Nuclear astrophysics	172	5
FERMI	226	7
Detector development	68	2
Applications	1225	39
Total	3159	100

PUBLICATIONS
AND
SEMINARS



Papers published in 1993

Nuclear Physics

1. Kruppa A.T., Nagarajan, M.A., Vary, J.P., Charge exchange effects in elastic scattering with radioactive beams, *Physical Review C Nuclear Physics* **47** (1993) 451
2. 7. Csótó A., Lovas R.G., Kruppa A.T., Two-pole structure of the $3/2^+$ resonance of ^5He in a dynamical microscopic model, *Physical Review Letters* **70** (1993) 1389
3. Somorjai E., Experimental nuclear reaction studies and nuclear astrophysics, *Fizika Elementarnykh Chastits i Atomnogo Yadra* **23** (1992) 974
4. Kruppa A.T., Nagarajan, M.A., Vary, J.P., Charge exchange effects in elastic scattering with radioactive beams, *Physical Review C Nuclear Physics* **47** (1993) 451
5. Szelecsényi F., Blessing, G., Qaim, S.M., Excitation functions of proton induced nuclear reactions on enriched ^{61}Ni and ^{64}Ni : possibility of production of No-carrier-added ^{61}Cu and ^{64}Cu at a small cyclotron, *Applied Radiation and Isotopes* **44** (1993) 575
6. Cseh J., Gupta, R.K., Scheid, W., Semimicroscopic algebraic approach to clusterization in heavy nuclei. Application to the $^{210}\text{Pb}+^{14}\text{C}$ system, *Physics Letters B* **299** (1993) 205
7. Timár J., Quang, T.X., Dombrádi Zs., Fényes T., Krasznahorkay A., Brant, S., Paar, V., Šimičić, Lj., Structure of the ^{68}Ga nucleus from $(\alpha, n\gamma)$ reaction, *Nuclear Physics A* **552** (1993) 170
8. Timár J., Quang, T.X., Fényes T., Dombrádi Zs., Krasznahorkay A., Kumpulainen, J., Julin, R., Level scheme of ^{68}Ga from $(p, n\gamma)$ reaction, *Nuclear Physics A* **552** (1993) 149
9. Cseh J., $^{16}\text{O}+\alpha$ cluster states in terms of a $U_q(3)$ anharmonic oscillator model, *Journal of Physics G* **19** (1993) 63
10. Maglione, E., Liotta, R. J., Vertse T., Partial decay widths from giant resonances in ^{208}Pb , *Physics Letters B* **298** (1993) 1
11. Dombrádi Zs., Brant, S., Paar, V., Role of collectivity in the structure of $^{120,122}\text{Sb}$ and ^{124}Sb nuclei, *Physical Review C Nuclear Physics* **47** (1993) 1539
12. Kopecky, P., Szelecsényi F., Molnár T., Mikecz P., Tárkányi F., Excitation functions of (p, xn) reactions on ^{nat}Ti : Monitoring of bombarding proton beams, *Applied Radiation and Isotopes* **44** (1993) 687
13. Angulo, C., Engstler, S., Raimann, G., Rolfs, C., Schulte, W.H., Somorjai E., The effects of electron screening and resonances in (p, α) reactions on ^{10}B and ^{11}B at thermal energies, *Zeitschrift für Physik A* **345** (1993) 231
14. Leigh, J.R., Rowley, N., Lemmon, R.C., Hinde, D.J., Newton, J.O., Wei, J.X., Mein, J.C., Morton, C.R., Kuyucak, S., Kruppa A.T., Reconciling deformation parameters from fusion with those from Coulomb excitation, *Physical Review C Nuclear Physics* **47** (1993) 437
15. Gizon, J., Jerrestam, D., Gizon, A, Józsa M., Bark, R., Fogelberg, B., Ideguchi, E., Klamra, W., Lindblad, Th., Mitarai, S., Nyberg, J., Piiparinen, M., Sletten, G Alignments and band termination in $^{99,100}\text{Ru}$ *Zeitschrift für Physik A* **345** (1993) 336

16. Cseh J., On the binary fission modes of ground-state like configurations in *sd* shell nuclei, *Journal of Physics G* 19 (1993) 97
17. Beck, F.A., Fülöp Zs., Józsa M., Kiss Á.Z., Nyakó B.M., et al., The first results from EUROAM: superdeformed structures in ^{151}Tb , *Nuclear Physics A* 557 (1993) 67
18. Tárkányi F., Kovács Z., Qaim, S.M., Excitation functions of proton induced nuclear reactions on highly enriched ^{78}Kr : relevance to the production of ^{75}Br and ^{77}Br at a small cyclotron, *Applied Radiation and Isotopes* 44 (1993) 1105
19. Csótó A., Neutron halo of ^6He in a microscopic model, *Physical Review C Nuclear Physics* 48 (1993) 165
20. Kruppa A.T., Romain, P., Nagarajan, M.A., Rowley, N., Effect of multiphonon coupling on heavy-ion fusion, *Nuclear Physics A* 560 (1993) 845
21. Lévai G, Williams, B.W., The generalized Coulomb problem: an exactly solvable model *Journal of Physics A* 26 (1993) 3301
22. Varga K., Cseh J., Relation between the phenomenological interactions of the algebraic cluster model and the effective two-nucleon forces, *Physical Review C Nuclear Physics* 48 (1993) 602
23. Csótó A., Proton skin of ^8B in a microscopic model, *Physics Letters B* 315 (1993) 24
24. Lenzi, S.M., Dragún, O., Maqueda, E.E., Liotta, R. J., Vertse T., Description of alpha clustering including continuum configurations, *Physical Review C Nuclear Physics* 48 (1993) 1463
25. Curien, D., Nyakó B.M., Zolnai L., et al., Deexcitation from superdeformed bands in ^{151}Tb and neighboring $A \sim 150$ nuclei, *Physical Review Letters* 71 (1993) 2559
26. Csótó A., Localization of shadow poles by complex scaling, *Physical Review A* 48 (1993) 3390
27. Cseh J., Lévai G, Scheid, W., Algebraic $^{12}\text{C}+^{12}\text{C}$ cluster model of the ^{24}Mg nucleus, *Physical Review C Nuclear Physics* 48 (1993) 1724
28. Sudár S., Szelecsényi F., Qaim, S.M., Excitation function and isomeric cross-section ratio for the $^{61}\text{Ni}(p,\alpha)^{58}\text{Co}$ *m, g* process *Physical Review C Nuclear Physics* 48 (1993) 3115
29. Tikkanen, P., Keinonen, J., Kangasmaki, A., Fülöp Zs., Kiss Á.Z., Somorjai E., Short lifetimes in ^{28}Si , *Physical Review C Nuclear Physics* 47 (1993) 145

Atomic Physics

1. Papp T., Maxwell, J.A., Teesdale, W.J., Campbell, J.L., Inconsistent K-L x-ray angular correlations in uranium, *Physical Review A* 47 (1993) 333
2. Ricz S., Sulik B., Stolterfoht, N., Kádár I., Semiclassical treatment of two-center electron-electron interactions in energetic atomic collisions: Screening effects, *Physical Review A* 47 (1993) 1930
3. Terasawa, M., Török I., Petukhov, V.P., High resolution PIXE instrumentation survey, part I., *Nuclear Instruments and Methods in Physics Research B* 75 (1993) 105
4. Petukhov, V.P., Török I., Závodszy, P.A., Pálincás J., Sarkadi L., Blokhin, S.M., Al K alpha satellite polarization measurements in metal and in sapphire (Al_2O_3), *Nuclear Instruments and Methods in Physics Research B* 75 (1993) 17

5. Závodszky, P.A., Sarkadi L., Tanis, J.A., Berényi D., Pálincás J., Plano, V., Gulyás L., Takács E., Tóth L., Projectile energy dependence of the contributions of different mechanisms to cusp electron production in $\text{He}^+ \rightarrow \text{Ar}$ collisions, *Nuclear Instruments and Methods in Physics Research B* **79** (1993) 67
6. Jones, G.O., Charlton, M., Slevin, J., Laricchia, G., Kövér Á., Poulsen, M.R., Chormaic, S.N., Positron impact ionization of atomic hydrogen *Journal of Physics B* **26** (1993) 483
7. Kövér L., Némethy A., Cserny I., Varga D., K-shell Auger transitions induced by Mo X-rays, *Surface and Interface Analysis* **20** (1993) 659
8. Kövér Á., Laricchia, G., Charlton, M., Ionization by positrons and electrons of Ar at zero degrees, *Journal of Physics B* **26** (1993) 575
9. Kuzel, M., Sarkadi L., Pálincás J., Závodszky, P.A., Maier, R., Berényi D., Groeneveld, K.O., Observation of enhanced emission of cusp electrons at impact of excited metastable neutral He projectiles, *Physical Review A* **48** (1993) 1745
10. Wang, J., Olson, R.E., Tökési K., Quantal and classical correspondence of double scattering, *Journal of Physics B* **26** (1993) 613
11. Stolterfoht, N., Mattis, A., Schneider, D., Schiwietz, G., Skogvall, B., Sulik B., Ricz S., Time-ordering effects in K-shell excitation of 170-MeV Ne^{7+} colliding with gas atoms: Single excitation, *Physical Review A* **48** (1993) 2986
12. Papp T., Campbell, J.L., Maxwell, J.A., Deviation from the single-particle model in the angular distribution of thorium L_3 X rays in proton-impact ionization, *Physical Review A* **48** (1993) 3062
13. Papp T., Campbell, J.L., Raman, S., Experimental test of Dirac-Fock versus Dirac-Hartree-Slater L X-ray intensity ratios, *Journal of Physics B* **26** (1993) 4007
14. Szabó Gy., Wang, J., Burgdörfer, J., Ellipsoidal angular distribution of electrons emitted from Rydberg atoms, *Physical Review A* **48** (1993) 3414

Materials Science and Analysis

1. Kalinka G., Taniguchi, K., Status of solid state energy dispersive X-ray detection, *Nuclear Instruments and Methods in Physics Research B* **75** (1993) 91
2. Kis-Varga M., Végh J., Influence of in-sample scattering of fluorescent radiation on line shapes of Si(Li) detectors in XRF studies, *X-Ray Spectrometry* **22** (1993) 166
3. Török I., Bondár T., High resolution PIXE using different orders of reflection, Part II., *Nuclear Instruments and Methods in Physics Research B* **79** (1993) 413
4. Kövér L., Némethy A., Cserny I., Varga D., K-shell Auger transitions induced by Mo X-rays, *Surface and Interface Analysis* **20** (1993) 659
5. Kövér L., Cserny I., Calibration of electron spectrometers by using ^{99m}Tc internal conversion electron sources *Journal of Electron Spectroscopy and Related Phenomena* **63** (1993) 31
6. Végh J., Sloping Shirley-type inelastic line shapes, *Surface and Interface Analysis* **20** (1993) 860
7. Mészáros S., Vad K., Hegman N., Current transfer in grain-boundary junctions of Bi(Pb)SrCaCuO thick films, *Physica C* **218** (1993) 471
8. Sarkadi É., Kovács Z., Andó L., C izotóppal jelzett metionin előállítására pozitron emissziós tomográfiával végzett vizsgálatokhoz, *Izotoptechnika, Diagnosztika* **36** (1993) 18

9. Kopecky, P., Szelecsényi F., Molnár T., Mikecz P., Tárkányi F., Excitation functions of (p, xn) reactions on ^{nat}Ti : Monitoring of bombarding proton beams, *Applied Radiation and Isotopes* **44** (1993) 687

Earth and Cosmic Sciences, Environmental Research

1. Hertelendi E., Sümegi P., Szöör Gy., Geochronologic and paleoclimatic characterization of Quaternary sediments in the Great Hungarian Plain, *Radiocarbon* **34** (1992) 833
2. Árva-Sós E., Máthé Z., Mineralogical and petrographic study of some Neogene tuff layers of the Mecsek Mountains (South Hungary) and their K-Ar dating, *Acta Geologica Hungarica* **35** (1992) 177
3. Uchirin G., Csaba E., Hertelendi E., Ormai P., Barnabás I., C-14 release from a soviet design pressurised water reactor nuclear power plant, *Health Physics* **63** (1992) 651
4. Edelstein, O., Bernád, A., Kovács, M., Crihán, M., Pécskay Z., Preliminary data regarding the K/Ar ages of some eruptive rocks from the Baia Mare Neogene volcanic zone, *Revue Roumaine de Géologie* **36** (1992) 45
5. Katoh, T., Amemiya, S., Koltay E., Borbély-Kiss I., Szabó Gy., Biswas, S.K., Short-range transport of aerosols emitted by a point source of mixed character at Pálháza, Hungary, *International Journal of PIXE* **2** (1992) 645
6. Pécskay Z., Szakács S., Seghedi, I., Karátson D., Uj adatok a Kakukkhegy és szomszédsága (Dél-Hargita, Románia) geokronológiai értelmezéséhez, *Földtani Közlöny* **122** (1992) 265
7. Molnár A., Makra L., Yaning, Ch., Borbély-Kiss I., Some data on the elemental composition of atmospheric aerosol particles in Xinhiang, NW China, *Időjárás* **97** (1993) 173
8. Hakl J., Lénárt L., Hunyadi I., Radon measurement in caves and springs located in the area of the Bükk National Park, A bükki barlangok kutatásának és hasznosításának legújabb eredményei. Miskolc, 1993.nov.11-13. Szerk.:Lénárt László. Miskolc, Miskolci Egyetem (1993) 5
9. Molnár A., Mészáros E., Bozó L., Borbély-Kiss I., Koltay E., Szabó Gy., Elemental composition of atmospheric aerosol particles under different conditions in Hungary, *Atmospheric Environment* **A 27** (1993) 2457
10. Borbély-Kiss I., Koltay E., Szabó Gy., Apportionment of atmospheric aerosols collected over Hungary to sources by target transformation factor analysis, *Nuclear Instruments and Methods in Physics Research* **B 75** (1993) 287
11. Borbély-Kiss I., Koltay E., Szabó Gy., Apportionment of atmospheric aerosols collected over Hungary to sources by target transformation factor analysis, *Nuclear Instruments and Methods in Physics Research* **B 75** (1993) 287
12. Scheuer Gy., Szöör Gy., Sümegi P., Balázs E., Hertelendi E., Schweitzer F., A magyarországi quarter és neogen édesvízi mészkövek termoanalitikai és izotópgeo-kémiai elemzése facies és rétegtani értékeléssel, *Hidrologiai Közlöny* **75** (1993) 298
13. Hertelendi E., Radiocarbon age of a bone sample from the Upper-Paleolithic settlement near Jászfelsőszentgyörgy, *Tisicum* **8** (1993) 41
14. Katoh, T., Amemiya, S., Tsurita, Y., Masuda, H., Koltay E., Borbély-Kiss I., PIXE analysis of atmospheric aerosol collected over Hungary and Japan, *Nuclear Instruments and Methods in Physics Research* **B 75** (1993) 296

Biological and Medical Research

1. Deng, H., Bohátka S., Lloyd, D., Enzyme activity in organic solvent as a function of water activity determined by membrane inlet mass spectrometry, *Biotechnology Techniques* **6** (1992) 161
2. Cortes Toro, E., De Goeij, J.J.M., Bacsó J., Yuan-di Cheng, Kinova, L., Matsubara, J., Niese, S., Sato, T., Wesenberg, G.R., Muramatsu, Y., Parr, R.M., The significance of hair mineral analysis as a means for assessing internal body burdens of environmental pollutants: Results from an IAEA co-ordinated research programme, *Journal of Radioanalytical and Nuclear Chemistry, Articles* **167** (1993) 413
3. Boothe, T.E., McLeod, T.F., Plitnikas, M., Kinney, D., Tavano, E., Feijoo, Y., Smith, P., Szelecsényi F., Commercial and PET radioisotope manufacturing with a medical cyclotron, *Nuclear Instruments and Methods in Physics Research B* **79** (1993) 926
4. Sarkadi É., Kovács Z., Andó L., C izotóppal jelzett metionin előállítására pozitron emissziós tomográffal végzett vizsgálatokhoz, *Izotoptechnika, Diagnosztika* **36** (1993) 18
5. Kopecky, P., Szelecsényi F., Molnár T., Mikecz P., Tárkányi F., Excitation functions of (p, xn) reactions on ^{nat}Ti : Monitoring of bombarding proton beams, *Applied Radiation and Isotopes* **44** (1993) 687

Development of Instruments and Methods

1. Trajber Cs., Simon M., Bohátka S., Futó I., A mass independent pre-filter arrangement for quadrupole mass spectrometer, *Vacuum* **44** (1993) 653
2. Pál K.F., Genetic algorithmus for the traveling salesman problem based on a heuristic crossover operation, *Biological Cybernetic* **69** (1993) 539
3. Deng, H., Bohátka S., Lloyd, D., Enzyme activity in organic solvent as a function of water activity determined by membrane inlet mass spectrometry, *Biotechnology Techniques* **6** (1992) 161
4. Uray I., Heinzelmann, M., On the calibration of large-volume dosimeters with beta radiation, *Radiation Protection Dosimetry* **40** (1992) 27
5. Uray I., A background elimination treatment for TLDs, *Radiation Protection Dosimetry* **40** (1992) 275
6. Szabó Gy., Borbély-Kiss I., PIXYKLM computer package for PIXE analyses, *Nuclear Instruments and Methods in Physics Research B* **75** (1993) 123
7. Lindblad, Th., Székely G., Filtering and unfolding using neural networks, *Nuclear Instruments and Methods in Physics Research A* **328** (1993) 603
8. Kövér L., Némethy A., Cserny I., Varga D., K-shell Auger transitions induced by Mo X-rays, *Surface and Interface Analysis* **20** (1993) 659
9. Kövér L., Cserny I., Calibration of electron spectrometers by using ^{99m}Tc internal conversion electron sources, *Journal of Electron Spectroscopy and Related Phenomena* **63** (1993) 31
10. Bohátka S., Futó I., Gál I., Gál J., Langer G., Molnár J., Paál A., Pintér G., Simon M., Szádai J., Székely G., Szilágyi J., Quadrupole mass spectrometer system for fermentation monitoring, *Vacuum* **44** (1993) 669

11. Denby, B., Lindblad, Th., Lindsey, C.S., Székely G., Molnár J., Eide, Å., Amendolia, S.R., Spaziani, A., Investigation of a VLSI neural network chip as part of a secondary vertex trigger, Nuclear Instruments and Methods in Physics Research **A** 335 (1993) 296
12. Hörnblad, P., Lindblad, Th., Lindsey, C.S., Székely G., Eide, Å., Filtering data from a drift-chamber detector using neural networks, Nuclear Instruments and Methods in Physics Research **A** 336 (1993) 285
13. Minerskjöld, M., Lindblad, Th., Lund-Jensen, B., Székely G., Investigation of the scintillation light from liquid argon doped with xenon, Nuclear Instruments and Methods in Physics Research **A** 336 (1993) 373
14. Lindblad, Th., Klamra, W., Lund-Jensen, B., Székely G., Cennini, P., Lacarrère, D., Moulson, M., Seidel, J.L., Vuillemin, V., Measurements of rise time in liquid argon and xenon gridded ionization chambers, Nuclear Instruments and Methods in Physics Research **A** 324 (1993) 263
15. Bartha L., Kiss Á.Z., Koltay E., Nagy A., Szabó Gy., Félszerfalvi J., Straight acceleration tube of axial gradient modulation using dish-shaped electrodes Nuclear Instruments and Methods in Physics Research **A** 328 (1993) 86
16. Kalinka G., Taniguchi, K., Status of solid state energy dispersive X-ray detection, Nuclear Instruments and Methods in Physics Research **B** 75 (1993) 91

Development of Instrumentation and Methods

1. ...
2. ...
3. ...
4. ...
5. ...
6. ...
7. ...
8. ...
9. ...
10. ...

Conference Contributions and Talks

Nuclear Physics

1. Genevey, J., Nyakó B.M., Zolnai L., et al., A new 5.7-s isomer in ^{131}Pr and low-energy intrinsic states in $A=131,129,127$ Pr and Ce isotopes, Proceedings of the International Conference on Atomic Masses and Fundamental Constants. Bernkastelkues, 1992. Heidelberg, Springer Verlag. International Conference Series No.132, Section 5 (1992) 671
2. Angulo, C., Engstler, S., Schulte, W.H., Somorjai E., Greife, U., Rolfs, C., Trautvetter, H.P., The electron screening effect on boron (p, α) reactions; search for a low energy resonance, Proceedings of the Second International Symposium on Nuclear Astrophysics. Karlsruhe, Germany, 6-10 July, 1992. Ed.:F.Kappeler, K.Wisshak. Bristol, Philadelphia, Institute of Physics Publ. (1993) 147
3. Cseh J., Lévai G, Gupta, R.K., Scheid, W., Semimicroscopic algebraic approach to nuclear clusterization, Anales de Física. Monografias. Eds.: M.A.del Olmo, M.Santander, J.Mateos Guillaude. 1. Group Theoretical Methods in Physics. Proceedings of the XIX International Colloquium, Salamanca, Spain, June 29-July 4,1992. Madrid, Ciemat 2 (1993) 334
4. Maass, R., Cseh J., Schmidt, J., Scheid, W., Molecular structure in the scattering of deformed nuclei - examples $^{24}\text{Mg}+^{24}\text{Mg}$ and $^{12}\text{C}+^{12}\text{C}$, International Conference on Nuclear Structure and Nuclear Reactions at Low and Intermediate Energies. September 15-19,1992, Dubna, Russia. Proceedings. Ed.: E.V. Ivaskevich. Dubna, Joint Institute for Nuclear Research (1993) 321
5. Lévai G., Solvable potentials derived from supersymmetrical quantum mechanics, Quantum inversion theory and applications. Proceedings, Bad Honnef, Germany 1993. Ed.: H.V. von Geramb. Lecture Notes in Physics. Berlin, etc. Springer-Verlag 427 (1993) 107
6. Beck, F.A. , Fülöp Zs., Józsa M., Kiss Á.Z., Nyakó B.M., et al., The first results from EUROGAM: superdeformed structures in ^{151}Tb , 21st International Symposium on Rapidly Rotation Nuclei. Tokyo, Japan, October 26-30,1992. (1992)
7. Cseh J., Relative motion in two-cluster systems and the quantum groups (Abstr. p.27), 2nd International Conference on Atomic and Nuclear Clusters'93. Santorini, Greece, June 28 - July 2, 1993. (1993)
8. Cseh J., The semimicroscopic algebraic cluster model of atomic nuclei (Abstr. p.28), 2nd International Conference on Atomic and Nuclear Clusters'93. Santorini, Greece, June 28 - July 2, 1993. (1993)
9. Angulo, C., Engstler, S., Greife, U., Raimann, G., Rolfs, C., Somorjai E., Trautvetter, H.P., Zahnov, D., Electron screening, European Research Conference "Nuclear Physics: Nuclear Astrophysics". Knossos Royal Village, Limin Hersonissos, Crete, Greece, 29 May - 3 June, 1993. (1993)
10. Lévai G., Solvable potentials derived from supersymmetrical quantum mechanics, International Symposium on Quantum Inversion Theory and Applications. (109. WE-Heraeus Seminar). Bad Honnef, Germany, 17-19 May,1993. (1993)

11. Vertse T., Lind, P., Liotta, R. J., Maglione, E., Description of the continuum in calculating partial decay width of giant resonances, Frontier Topics in Nuclear Physics. Predeal, Romania. Aug.24 - Sept.4,1993. (1993)
12. Cseh J., Semimicroscopic algebraic approach to nuclear clusterization, Half-Day Meeting of Centre for Nuclear Physics. Brighton, U.K., 15 Sept.,1993. (1993)
13. Cseh J., Lévai G, Varga K., Gupta, R.K., Scheid, W., Deformation, clusterization, fission, and SU(3), Frontier Topics in Nuclear Physics. Predeal, Romania. 24 Aug. - 4 Sept., 1993. (1993)
14. Cseh J., Lévai G., Group theoretical approach to clusterization of atomic nuclei, 3rd International Wigner Symposium. Oxford, U.K. 5-11 Sept.,1993 (1993)
15. Dombrádi Zs., Brant, S., Paar, V., Core polarization induced and detected by quasiparticles in In and Sb nuclei (Abstract Booklet p.70), 8th International Symposium on Capture Gamma-Ray Spectroscopy and Related Topics. Fribourg, Switzerland, 20-24 Sept.,1993. (1993)
16. Csótó A., Microscopic dynamical multicluster description of the structure and reactions of light nuclei (Contributed papers pp.94-95), XIV European Conference on Few-Body Problems in Physics. Amsterdam, The Netherlands, 23-27 Aug.,1993. (1993)
17. Lovas R.G., Varga K., Liotta, R. J., Cluster formation and decay in a microscopic model: the alpha decay of ²¹²Po. (Abstr., Institute of Atomic Physics, Buchares., Ed.: M. Dumitriu. p.19), Frontier Topics in Nuclear Physics. Predeal, Romania. Aug.24 - Sept.4,1993. (1993)
18. Varga K., Suzuki, Y., Lovas R.G., Microscopic multicluster description of neutron halos (Book of Abstracts, Cluster'93 p.133), 2nd International Conference on Atomic and Nuclear Clusters'93. Santorini, Greece, June 28 - July 2, 1993. (1993)
19. Varga K., Liotta, R. J., Lovas R.G., Alpha Decay of ²¹²Po (Book of Abstracts, Cluster'93 p.132), 2nd International Conference on Atomic and Nuclear Clusters'93. Santorini, Greece, June 28 - July 2, 1993. (1993)
20. Gizon, J., Józsa M., Nyakó B.M., Zolnai L., et al., Excited superdeformed bands in ¹³²Ce, Perspectives in Nuclear Structure 1993. Copenhagen, Dania, 15 June, 1993. (1993)
21. Santos, D., Józsa M., Nyakó B.M., Zolnai L., et al., Excited superdeformed bands in ¹³¹Ce and ¹³²Ce, EUROGAM Collaboration Meeting, Physics Workshop. Liverpool, UK, 17-19 May, 1993. (1993)
22. Dombrádi Zs., Core polarization induced and detected by (QUASI) particles in In and Sb nuclei (Abstr.: p.70), 8th International Symposium on Capture Gamma-Ray Spectroscopy and Related Topics. Fribourg, Switzerland, 20-24 Sept.,1993. (1993)
23. Zimmerman, B.E., Walters, W.B., Mantica, P.F., Carter, H.K., Kormicki, J., Gácsi Z., Decay of mass-separated ¹¹⁴Te, Spring Meeting of the APS. Washington, USA, 12-15 April,1993. (1993)
24. Dankó I., A ¹¹⁸Sb atommag bomlásának gamma-spektroszkópiai vizsgálata, XXI. Országos Diákköri Konferencia. Szombathely, Magyarország, 1993.ápr.4-6. (1993)
25. Papp Z., Coulomb Sturmian expansion approach to the Faddeev equation with Coulomb interaction (Contributed paper p.182), XIV European Conference on Few-Body Systems in Physics. Amsterdam, The Netherlands, 23-27 Aug.,1993. (1993)

26. Gizon, J., Józsa M., Nyakó B.M., Zolnai L., et al., Excited superdeformed bands in ^{132}Ce , Perspectives in Nuclear Structure 1993. Kopenhagen, Denmark, 14-18 June, 1993. (1993)
27. Papp Z., Separable expansion approach for two- and three-body problems with Coulomb interaction, Universitat Tübingen, Tübingen, Germany, 14 Jan., 1992. (1992)
28. Mahunka I., Low energy cyclotrons in research and training, Ankara Nuclear Research and Training Center. Ankara, Turkey, May 3, 1993. (1993)
29. Csótó A., Shadow-pole structure of the $d + t \rightarrow \alpha + n$ thermonuclear reaction, Physique Nucléaire et Physique Mathématique Université Libre de Bruxelles. Bruxelles, Belgium, 6 June, 1993. (1993)
30. Lévai G., Kvantummechanikai potenciálproblémák vizsgálata a szuperszimmetrikus kvantummechanika és a csoportelmélet segítségével, Budapesti Műszaki Egyetem, Fizikai Intézet. Budapest, Magyarország, 1993.nov.5. (1993)
31. Cseh J., Special aspects of the semimicroscopic algebraic cluster model: multi-channel dynamical symmetry, heavy-cluster radioactivity, quantum-deformed algebras, Institut für Theoretische Physik, Justus-Liebig-Universität. Giessen, Germany. Nov.4, 1993. (1993)
32. Cseh J., Lévai G., The semimicroscopic algebraic cluster model and its application to heavy-ion resonances, Institut für Theoretische Physik, Justus-Liebig-Universität, Giessen, Germany. Oct.28, 1993. (1993)
33. Gácsi Z., The structure of odd-odd nuclei, Department of Physics and Astronomy, University of Kentucky, Lexington, KY. USA, Nov. 11, 1993. (1993)
34. Fényes T., A Ga és As atommagok szerkezete, dinamikus és szuperszimmetriák, MTA Izotópkutató Intézete, Budapest, Magyarország, 1993. november (1993)
34. Fényes T., Szuperszimmetriák atommagokban, Fizikai Szemle 43 (1993) 317

Atomic Physics

1. Sarkadi L., Berényi D., Sixteenth International Conference on X-Ray and Inner-Shell Processes. Debrecen, Hungary. July 12-16, 1993. X'93. Abstracts. Ed.: L. Sarkadi, D. Berényi., Atomki, Debrecen (1993) 373
2. Berényi D., Két nemzetközi atomfizikai rendezvény Debrecenben, Magyar Tudomány 38 (1993) 1381
3. Berényi D., Az atomfizika aktualitása, Eszterházy Károly Tanárképző Főiskola Fizikai Tanszéke. Eger, Magyarország, 1993. március 3. (1993)
4. Závodszy, P.A., Sarkadi L., Kuzel, M., Pálincás J., Gulyás L., Takács E., Tóth L., Berényi D., Groeneveld, K.O., Projectile energy dependence of the ECC electron cusp in $\text{He}^0 \rightarrow \text{Ar}$ collisions, 3rd Debrecen-Uzhgorod-Miskolc Triangle Seminar on Atomic Collision Processes. Uzhgorod, Ukraine, 26 Oct., 1992. (1992)
5. Sarkadi L., Závodszy, P.A., Tanis, J.A., Berényi D., Pálincás J., Plano, V., Gulyás L., Takács E., Tóth L., Projectile energy dependence of the contributions of different mechanisms to cusp electron production in $\text{He}^+ \rightarrow \text{Ar}$ collisions, 3rd Debrecen-Uzhgorod-Miskolc Triangle Seminar on Atomic Collision Processes. Uzhgorod, Ukraine, 26 Oct., 1992. (1992)

6. Plano, V., Sarkadi L., Závodszy, P.A., Berényi D., Pálinkás J., Gulyás L., Takács E., Tóth L., Tanis, J.A., Cusp electron production in 75-300 keV $\text{He}^+ + \text{Ar}$ collisions, VIth International Conference on the Physics of Highly-Charged Ions. Manhattan, Kansas, USA, 28 Sept. - 2. Oct.,1992. (1992)
7. Khemliche, H., Prior, M.H., Plano, V., Haar, R.R., Tanis, J.A., Závodszy, P.A., Sarkadi L., Pálinkás J., Berényi D., Schneider, D., Low-energy electrons from multiple-electron transfer to slow O^{8+} ions. (Abstr.:Bull.of the Amer.Phys.Soc., 38,1993,p.1160 WE74), 1993 Annual Meeting of the Division of Atomic, Molecular and Optical Physics of the American Physical Society. Reno, Nevada, USA, 16-19 May,1993. (1993)
8. Kövér L., Ricz S., High energy- and angular resolution Auger spectroscopy of solid surfaces, free atoms and molecules in a wide energy range, Joint Session of the Hungarian Synchrotron Committee and the Expert Group of ELETTRA Synchrotron (Trieste, Italy). Budapest, Hungary, 28 April,1993 (1993)
9. Biri S., Vámosi J., The Debrecen ECR project (Book of Abstracts, p.20) 11.Workshop on the Physics and Technology of Electron Cyclotron Resonance (ECR) Ion Sources. Groningen, Hollandia. 6-7 May,1993. (1993)
10. Török I., Petukhov, V.P., Závodszy, P.A., Pálinkás J., Sarkadi L., The polarization of the Al K alpha' x-ray satellite in metal and in sapphire (Abstr.: ed. Sarkadi L, Berényi D., pp.166-167), X'93 Sixteenth International Conference on X-Ray and Inner-Shell Processes. Debrecen, Hungary, 12-16 July, 1993. (1993)
11. Tökési K, Hock G., Versatility of the exit channels in the 3-body CTMC method (Abstr. p.52-53), 5th Workshop on Fast Ion-Atom Collisions. Debrecen, Hungary, July 17-19, 1993. (1993)
12. Ricz S., Angular dependence of post-collision interactions (Abstr. p.48), 5th Workshop on Fast Ion-Atom Collisions. Debrecen, Hungary, July 17-19, 1993. (1993)
13. Tökési K, Sarkadi L., Mukoyama, T., Model calculation for the ECC peak at neutral projectile impact (Abstr. p.42), 5th Workshop on Fast Ion-Atom Collisions. Debrecen, Hungary, July 17-19, 1993. (1993)
14. Plano, V., Haar, R.R., Tanis, J.A., Pálinkás J., Sarkadi L., Závodszy, P.A., Berényi D., Khemliche, H., Prior, M.H., Schneider, D., Production of low-energy continuum electrons at 0 degree by 4.4keV/u O^{8+} Ions (Abstr.p.40), 5th Workshop on Fast Ion-Atom Collisions. Debrecen, Hungary, July 17-19, 1993. (1993)
15. Závodszy, P.A., Gulyás L., Vajnai T, Sarkadi L., Szabó Gy., Ricz S., Pálinkás J., Berényi D., Cusp shape studies in $\text{H}^+ - \text{He}$ collision in the energy range 75-1400 keV: experiment and theory (Abstr. p. 39), 5th Workshop on Fast Ion-Atom Collisions. Debrecen, Hungary, July 17-19, 1993. (1993)
16. Skogvall, B., Stolterfoht, N., Grandin, J.P., Lecler, D., Sulik B., Ricz S., Multiple ionization of Li by fast heavy particle impact (Abstr. p.34), 5th Workshop on Fast Ion-Atom Collisions. Debrecen, Hungary, July 17-19, 1993. (1993)
17. Nagy L., Végh L., Shake-off, shake-up and ground state correlation in ionization of molecular hydrogen (Abstr. p.33), 5th Workshop on Fast Ion-Atom Collisions. Debrecen, Hungary, July 17-19, 1993. (1993)
18. Sulik B., Stolterfoht, N., Semiclassical treatment of collisional dielectronic processes (Abstr. p.32), 5th Workshop on Fast Ion-Atom Collisions. Debrecen, Hungary, July 17-19, 1993. (1993)
19. Gulyás L., Szabó Gy., Double electron capture by fast He^{2+} from He (Abstr. p.30), 5th Workshop on Fast Ion-Atom Collisions. Debrecen, Hungary, July 17-19, 1993. (1993)

20. Závodszy, P.A., Sarkadi L., Víkor L., Pálinkás J. Excitation, single and double electron capture in $\text{He}^{0,1,2+}$ collisions on Ar (Abstr. p.29), 5th Workshop on Fast Ion-Atom Collisions. Debrecen, Hungary, July 17-19, 1993. (1993)
21. Mukoyama, T., Hock G., Analytical expressions of potentials and wave functions for atoms and ions (Abstr. p. 26), 5th Workshop on Fast Ion-Atom Collisions. Debrecen, Hungary, July 17-19, 1993. (1993)
22. Stolterfoht, N., Mattis, A., Schneider, D., Schiwietz, G., Skogvall, B., Sulik B., Ricz S., Time-ordering effects in K-shell excitation of 170-MeV Ne^{7+} colliding with gas atoms (Abstr. p. 26), 5th Workshop on Fast Ion-Atom Collisions. Debrecen, Hungary, July 17-19, 1993. (1993)
23. Tóth L., Víkor Gy., Ricz S., Pelicon, P., Miller, R., Study of the Ar LMM spectra by He^+ projectile at 1250, 1500 and 2000 keV bombarding energies (Abstr. p.25), 5th Workshop on Fast Ion-Atom Collisions. Debrecen, Hungary, July 17-19, 1993. (1993)
24. Tökési K, Wang, J., Olson, R.E., Projectile ionization at forward observation angles in intermediate energy H+H collisions (Abstr. p. 24), 5th Workshop on Fast Ion-Atom Collisions. Debrecen, Hungary, July 17-19, 1993. (1993)
25. Takács E., Ricz S., Végh J., Kádár I., Pálinkás J., Sulik B., Tóth L., Berényi D., The role of the shake-off ionization process in the alignment of the $1s2p$ double vacancy states of Ne at high proton impact energies (Abstr. pp.164-165), X'93 Sixteenth International Conference on X-Ray and Inner-Shell Processes. Debrecen, Hungary, 12-16 July, 1993. (1993)
26. Kovács Zs., Kövér L., Pálinkás J., Adachi, H., Interpretation of Al KLV and KVV Auger spectra by the help of a cluster type MO calculation (Abstr. pp.190-191), X'93 Sixteenth International Conference on X-Ray and Inner-Shell Processes. Debrecen, Hungary, 12-16 July, 1993. (1993)
27. Kövér L., Némethy A., P KLL and P KLV Auger spectra of phosphorus oxyanions (abstr. pp.192-193), X'93 Sixteenth International Conference on X-Ray and Inner-Shell Processes. Debrecen, Hungary, 12-16 July, 1993. (1993)
28. Némethy A., Kövér L., Cserny I., Varga D., Barna P.B., KLL and KLM Auger spectra of manganese excited by bremsstrahlung (Abstr. pp.340-341), X'93 Sixteenth International Conference on X-Ray and Inner-Shell Processes. Debrecen, Hungary, 12-16 July, 1993. (1993)
29. Végh L., Macek, J.H., Coherences between autoionizing states of different excitation energies in photoionization (Abstr. p.356), X'93 Sixteenth International Conference on X-Ray and Inner-Shell Processes. Debrecen, Hungary, 12-16 July, 1993. (1993)
30. Végh L., Macek, J.H., About the exchange effect on the angular correlation between photo- and Auger electrons of same energy (Abstr. p.355), X'93 Sixteenth International Conference on X-Ray and Inner-Shell Processes. Debrecen, Hungary, 12-16 July, 1993. (1993)
31. Závodszy, P.A., Sarkadi L., Víkor Gy., Pálinkás J., Cusp electrons in fast $\text{He}^- \rightarrow \text{Ar}$ collisions (Abstr. pp.170-171), X'93 Sixteenth International Conference on X-Ray and Inner-Shell Processes. Debrecen, Hungary, 12-16 July, 1993. (1993)
32. Sarkadi L., Závodszy, P.A., Tanis, J.A., Kuzel, M., Víkor L., Zhu, M., Berényi D., Pálinkás J., Groeneveld, K.O., The role of transfer ionization in the emission of cusp electrons by impact of low-energy protons on argon (Abstr. pp.159-160), X'93 Sixteenth International Conference on X-Ray and Inner-Shell Processes. Debrecen, Hungary, 12-16 July, 1993. (1993)

33. Závodszky, P.A., Sarkadi L., Víkor L., Pálinkás J., Observation of collisionally induced ($1s2p2p'$) $4P_e$ shape resonance of He- (Abstracts of Contributed Papers Vol.II. p.518), XVIIIth International Conference on the Physics of Electronic and Atomic Collisions. Aarhus, Denmark, 21-27 July,1993. (1993)
34. Kuzel, M., Sarkadi L., Pálinkás J., Závodszky, P.A., Maier, R., Berényi D., Groeneveld, K.O., Observation of enhanced ECC cusp yield at impact of metastable neutral He projectiles (Abstracts of Contributed Papers Vol.II. p.620), XVIIIth International Conference on the Physics of Electronic and Atomic Collisions. Aarhus, Denmark, 21-27 July,1993. (1993)
35. Plano, V.L., Haar, R.R., Tanis, J.A., Sarkadi L., Závodszky, P.A., Pálinkás J., Berényi D., Prior, M.H., Khemliche, H., Schneider, D., Production of low-energy electrons by 80-keV O^{8+} ions (Abstracts of Contributed Papers, Vol.II. p.624), XVIIIth International Conference on the Physics of Electronic and Atomic Collisions. Aarhus, Denmark, 21-27 July,1993. (1993)
36. Papp T., Campbell, J.L., Lineshape effects on the determination of coster-kronig probabilities using Si(Li) X-ray detectors (Abstr. pp.308-309), X'93 Sixteenth International Conference on X-Ray and Inner-Shell Processes. Debrecen, Hungary, 12-16 July, 1993. (1993)
37. Papp T., Campbell, J.L., Raman, S., An experimental test of Dirac-Fock versus Dirac-Hartree-Slater L X-ray intensity ratios (Abstr. pp.310-311), X'93 Sixteenth International Conference on X-Ray and Inner-Shell Processes. Debrecen, Hungary, 12-16 July, 1993. (1993)
38. Takács E., Serpa, F.G., Laming, M., Brown, C.M., Gillaspay, J.D., Possibilities for research with the new NIST-NRL EBIT, X'93 Sixteenth International Conference on X-Ray and Inner-Shell Processes. Debrecen, Hungary, 12-16 July, 1993. (1993)
39. Haksela, H., Kabachnik, N.M., Ricz S., Tulkki, J., Theoretical study of angular anisotropy of satellite Auger transitions of neon (Abstr. pp.282-283), X'93 Sixteenth International Conference on X-Ray and Inner-Shell Processes. Debrecen, Hungary, 12-16 July, 1993. (1993)
40. Mayer, I.D., Michelmann, R.W., Ditrói F., Bethge, K., Investigation of the electronic energy loss of light ions for materials analysis, Third European Conference on Accelerators in Applied Research and Technology. (ECAART3). Orleans, France. 30 Aug. - 5 Sept.,1993. (1993)
41. Török I., Terasawa, M., Petukhov, V.P., High resolution PIXE instrumentation survey. Part II. (Abstr. P43), Third European Conference on Accelerators in Applied Research and Technology. (ECAART3). Orleans, France. 30 Aug. - 5 Sept.,1993. (1993)
42. Ricz S., Takács E., Kádár I., Végh J., Tóth L., Sulik B., Berényi D., Angular dependence of the PCI effect in proton-neon collisions (Abstr. of Contributed Papers p.522), XVIIIth International Conference on the Physics of Electronic and Atomic Collisions. Aarhus, Denmark, 21-27 July,1993. (1993)
43. Sulik B., Two-center electron-electron interactions in energetic atomic collisions: an experimental study, XIIIth International Seminar on Ion-Atom Collisions. Stockholm, Sweden, 29-30 July,1993. (1993)
44. Skogvall, B., Chesnel, J., Fremont, F., Lecler, D., Husson, X., Lepoutre, A., Henecart, D., Grandin, J.P., Sulik B., Stolterfoht, N., Double ionization of Li by high velocity N^{7+} ion (Abstracts and Contributed Papers p.485), XVIIIth International Conference on the Physics of Electronic and Atomic Collisions. Aarhus, Denmark, 21-27 July,1993. (1993)

45. Sulik B., Stolterfoht, N., Ricz S., Kádár I., Xiao, L., Schiwietz, G., Grande, P., Köhrbrück, R., Sommer, K., Grether, M., Experimental study of two-center electron-electron interaction in energetic ion-atom collisions (Abstracts and Contributed Papers p.528), XVIIIth International Conference on the Physics of Electronic and Atomic Collisions. Aarhus, Denmark, 21-27 July,1993. (1993)
46. Kövér L., Némethy A., Cserny I., Nisawa, A., Ito, Y., Local electronic structures in phosphorus oxyanions (ECASIAS-93 Abstracts p.98), 5th European Conference on Applications of Surface and Interface Analysis - ECASIA-93. Catania, Italy. Oct.4-8,1993. (1993)
47. Szabó Gy., Wang, J., Burgdörfer, J., Ellipsoidal angular distributions of electrons emitted from Rydberg atoms(14.Arbeitsbericht EAS-14 (1993) p.94), Arbeitsgruppe Energiereiche Atomare Stöße. Riezlern, Germany, 1993. (1993)
48. Moxom, J., Laricchia, G., Chalton, M., Jones, G.O., Kövér Á., Post collision interaction in positron atom collisions (Abstract of Contributed Paper p.400), XVIIIth International Conference on the Physics of Electronic and Atomic Collisions. Aarhus, Denmark, 21-27 July,1993. (1993)
49. Kövér Á., Laricchia, G., Chalton, M., Differention ionisation studies at forward angles (Book of Abstracts p.15), International Workshop on Positron Interaction with Atoms, Molecules and Cluster'. Bielefeld, Germany, July 14-16,1993. (1993)
50. Laricchia, G., Moxom, J., Chalton, M., Kövér Á., Meyerhof, W.E., Near threshold effects in positron-atom (molecule) scattering (Book of Abstracts p.14), International Workshop on Positron Interaction with Atoms, Molecules and Cluster'. Bielefeld, Germany, July 14-16,1993. (1993)

Materials Science and Analysis

1. Munkabizottság tagjaként:, Berényi D., Kövér L., A felületkutatás helyzete hazánkban. Helyzetelemző tanulmány. Készítette a munkabizottság: Barna P., Berényi D., Bertóti I. stb. Szerkesztette: Berényi D., Gergely Gy., Giber J., A szilárdtestkutatás újabb eredményei. Szerkeszti Siklós Tivadar. Bp., Akadémiai K. 24 (1992) 7
2. Kövér L., Varga D., Cserny I., Tóth J., Tökési K, Némethy A., High energy, high resolution Auger spectroscopy using near threshold photoexcitation (abstr.: p.87), Workshop on the International Use of Centres of Excellence and Joint Projects on Materials Science. Budapest, Hungary, 26-27 April,1993. (1993)
3. Varga D., Ricz S., Kövér L., Kövér Á., Kádár I., Cserny I., Végh J., Sulik B., Tóth J., Tökési K., High resolution photo- and Auger electron spectrometers for wide energy range and angular resolved spectroscopy (abstr.: p.98), Workshop on the International Use of Centres of Excellence and Joint Projects on Materials Science. Budapest, Hungary, 26-27 April,1993. (1993)
4. Kövér L., Ricz S., High energy- and angular resolution Auger spectroscopy of solid surfaces, free atoms and molecules in a wide energy range, Joint Session of the Hungarian Synchrotron Committee and the Expert Group of ELETTRA Synchrotron (Trieste, Italy). Budapest, Hungary, 28 April,1993 (1993)
5. Borbély-Kiss I., Fülöp Zs., Gesztelyi T., Kiss Á.Z., Koltay E., Szabó Gy., The PIXE-PIGE method for the classification of late Roman glass sealings (Abstract book 14.4), Eleventh International Conference on Ion Beam Analysis. Balatonfüred, Hungary, July 5-9,1993. (1993)

6. Kiss Á.Z., Biron, I., Calligaro, T., Salomon, J., Thick target yields of deuteron induced gamma ray emission from light elements (Abstract book 2.8), Eleventh International Conference on Ion Beam Analysis. Balatonfüred, Hungary, July 5-9,1993. (1993)
7. Vasváry L., Ditrói F., Takács S., Szabó Z., Szücs J., Kundrák J., Mahunka I., Wear measurement of cutting edge of superhard turning tools using TLA technique (Book of Abstract 4.11), Eleventh International Conference on Ion Beam Analysis. Balatonfüred, Hungary, July 5-9,1993. (1993)
8. Daróczi L., Beke D.L., Posgay G., Kis-Varga M., Bakker, H., Production and magnetic properties of nanocrystalline Fe and Ni (Abstr.: p.60), International Symposium on Mechanisms of Formation of Metastable Microstructures. Cambridge, U.K., July 12-16,1993. (1993)
9. Vad K., Hegman N., Mészáros S., Halász G., Longitudinal and transversal (Hall) voltage in Bi(Pb)SrCaCuO screen printed films, Vortex Fluctuation in Superconductors. Trieste, Italy. 17-20 Aug.,1993. (1993)
10. Hegman N., Mészáros S., Vad K., Flux dynamics study of YBaCuO single crystals by RF susceptibility measurements, Vortex Fluctuation in Superconductors. Trieste, Italy. 17-20 Aug.,1993. (1993)
11. Takács S., Vasváry L., Tárkányi F., Remeasurement and compilation of excitation functions of proton induced reactions on iron for activation techniques, Third European Conference on Accelerators in Applied Research and Technology (ECAART-3). Orléans, France. Aug.31 - Sept.4, 1993. (1993)
12. Ditrói F., Meyer, J.D., Michelmann, R.W., Kislat, D., Bethge, K., Investigation of silicon with (p, p') resonance scattering in $\langle 110 \rangle$ channeling direction, Third European Conference on Accelerators in Applied Research and Technology (ECAART-3). Orléans, France. Aug.31 - Sept.4, 1993. (1993)
13. Mayer, I.D., Michelmann, R.W., Ditrói F., Bethge, K., Investigation of the electronic energy loss of light ions for materials analysis, Third European Conference on Accelerators in Applied Research and Technology. (ECAART3). Orléans, France. 30 Aug. - 5 Sept.,1993. (1993)
14. Török I., Terasawa, M., Petukhov, V.P., High resolution PIXE instrumentation survey. Part II. (Abstr. P43), Third European Conference on Accelerators in Applied Research and Technology. (ECAART3). Orléans, France. 30 Aug. - 5 Sept.,1993. (1993)
15. Szelecsényi F., Boothe, T.E., Tavano, E., Plitnikas, M., Tárkányi F., Nuclear data relevant to the production of ^{67}Ga : A critical comparison of excitation functions / Thick target yield data for the $^{67}\text{Zn}(p,n)$ and $^{68}\text{Zn}(p,2n)$ nuclear reactions (Abstr.: p.9), Fifth International Workshop on Targetry and Target Chemistry. Brookhaven National Laboratory, North Shore University, Hospital, New York, USA. 19-23 Sept.,1993. (1993)
16. Tárkányi F., Takács S., Heselius, S.J., Solin, O., Bergman, J., Study of static and dynamic effects in gas targets (Abstr.:p.11), Fifth International Workshop on Targetry and Target Chemistry. Brookhaven National Laboratory, North Shore University, Hospital, New York, USA. 19-23 Sept.,1993. (1993)
17. Kövér L., Némethy A., Barna P.B., Surface structure of Al-Sn layered systems codeposited in the presence of oxygen (ECASIA-93 Abstracts p.325), 5th European Conference on Applications of Surface and Interface Analysis - ECASIA-93. Catania, Italy. Oct.4-8,1993. (1993)

18. Kövér L., Némethy A., Cserny I., Nisawa, A., Ito, Y., Local electronic structures in phosphorus oxyanions (ECASIAS-93 Abstracts p.98), 5th European Conference on Applications of Surface and Interface Analysis - ECASIA-93. Catania, Italy. Oct.4-8,1993. (1993)
19. Cserny I., Kármán F.H., Kálmán E., Surface study of the effect of bivalent cations on the adsorption of 1-hydroxy-ethane-1,1-diphosphonic acid on polycrystalline iron. (ECASIA-93 Abstracts p.442), 5th European Conference on Applications of Surface and Interface Analysis - ECASIA-93. Catania, Italy. Oct.4-8,1993. (1993)
20. Tárkányi F., Cyclotron utilization programmes in Debrecen, Hungary, National Seminar on Cyclotron in Science and Technology. Cairo, Egypt, 13-17 November, 1993. (1993)
21. Tárkányi F., Small accelerators and cyclotrons as research and teaching tools, National Seminar on Cyclotron in Science and Technology. Cairo, Egypt, 13-17 November, 1993. (1993)
22. Tárkányi F., Analytical applications of cyclotrons and accelerators, National Seminar on Cyclotron in Science and Technology. Cairo, Egypt, 13-17 November, 1993. (1993)
23. Mészáros S., Vad K., Hegman N., Halász G. Electromagnetic properties of HTSC materials, Workshop on the International Use of Centres of Excellence and Joint on Projects on Materials Science. Budapest, Hungary, Apr.26-17,1993. (1993)
24. Uzonyi I., Szluha K.L., Máthé Gy., Determination of Pt concentration in human tissues using XRF, 6th Hungaro-Italian Symposium on Spectrochemistry, Advances in Environmental Sciences. Lillafüred, Hungary, 23-27 Aug.,1993. (1993)
25. Cserny I., Kövér L., Varga D., Kármán F.H., Kálmán E., Várallyai L., Kónya J., Surface study of the effect of bivalent cations on the adsorption of phosphonic acid on polycrystalline iron, Corrosion Conference in memoriam Kurt Schwabe. Tata, Hungary, 24-27 Aug.,1993. (1993)
26. Várallyai L., Kónya J., Kármán F.H., Kálmán E., Cserny I., Kövér L., The investigation of heterogeneous molecule exchange of 1-hydroxy-ethylidene-1,1-diphosphonic acid (HEDP) by nuclear method, Corrosion Conference in memoriam Kurt Schwabe. Tata, Hungary, 24-27 Aug.,1993. (1993)
27. Kármán F.H., Cserny I., Kálmán E., Surface study of corrosion inhibitors, Corrosion Conference. Barcelona, Spain, 12-17.July,1993. (1993)
28. Kálmán E., Kármán F.H., Telegdi J., Cserny I., Kövér L., Varga D., Surface analytical investigation of the influence of calcium ions on the adsorption and on the inhibition of phosphonic acid on mild steel, 4th Meeting of the International Society of Electrochemistry. Berlin, Germany, (1993)
29. Mahunka I., Analytical applications of accelerators and cyclotrons, Ankara Nuclear Research and Training Center. Ankara, Turkey, May 4,1993. (1993)
30. Tárkányi F., Takács S., Heselius, S.J., Solin, O., Bergman, J., Gas targetry. Study of static and dynamic effects in gas targets, Cyclotron Facility, Division of Nuclear Medicine. Mount Sinai Medical Center, Miami Beach, USA, 27 Sept.,1993. (1993)
31. Kövér L., Studies of the local electronic structure by using high energy X-ray excited Auger spectroscopy, Istituto di Metodologie Avanzate Inorganiche C.N.R. Roma, Italy. Oct.11,1993. (1993)
32. Tökési K., Optimal design of electrostatic lens, Electro-Communication University of Osaka. Osaka, Japan, 13.Dec.,1993. (1993)
33. Hertelendi E., Veres M., Oxigénfeltárási eljárás és annak alkalmazási lehetőségei, Alföldi Napok. Debrecen, Magyarország, 1993. május 15. (1993)

Earth and Cosmic Sciences, Environmental Research

1. Raczky P., Hertelendi E., Horváth F., Zur Absoluten Datierung der bronzezeitlichen Tell Kulturen in Ungarn, Bronzezeit in Ungarn. Forschungen in Tell-Siedlungen an Donau und Theiss. Ed.:Fodor I.,Meier-Arendt,W.,Raczky P. Frankfurt a.M., Walter Meier Arendt im Auftrag des Dezernats Kultur und Freizeit der Stadt Frankfurt a.M. (1992) 42
2. Hakl J., Hunyadi I., Csige I., Géczy G., Lénárt L., Töröcsik I., Outline of natural radon occurrences on karstic terrains of Hungary, Radiation Protection Dosimetry **45** (1992) 183
3. Vető I., Nagymarosy A., Hertelendi E., Brukner Wein A., Hetényi M., The cenozoic decrease of the marine photosynthetic carbon isotopic fractionation, Kiel, Germany, 1992. (1992)
4. Vásárhelyi A., Hakl J., Hunyadi I., Soil gas and indoor radon mapping in a Hungarian village located at a geologically active area (Abstr.:p.11.6), Austrian-Italian-Hungarian Radiation Protection Symposium: Radiation Protection in Neighbouring Countries in Central Europe. Obergurgl/Tyrol, Austria. 28-30 April,1993. (1993)
5. Hunyadi I., Hakl J., Vásárhelyi A., Radon monitoring experiences and important facts that may affect dose estimation (Abstr.:p.11.2), Austrian-Italian-Hungarian Radiation Protection Symposium: Radiation Protection in Neighbouring Countries in Central Europe. Obergurgl/Tyrol, Austria. 28-30 April,1993. (1993)
6. Pécskay Z., First data on the age of the volcanic rocks from the Ridanj-Krepoljin zone, Plate Tectonic Aspects of Alpine Metallogeny in the Carpatho-Balkan Region. Budapest, Hungary, 21-29 May, 1993. (1993)
7. Karamata, S., Djordjevic, M., Pécskay Z., Djordjevic, V., Magmatism with associated metallogeny of the Ridanj-Krepoljin belt (Eastern Serbia) and its correlation with northern and eastern analogues, Plate Tectonic Aspects of Alpine Metallogeny in the Carpatho-Balkan Region. Budapest, Hungary, 21-29 May, 1993. (1993)
8. Árkai P., Balogh K., Dunkl I., Timing of low-T metamorphism and cooling in the Paleozoic and Mesozoic of the Bükkium, innermost Western Carpathians, NE-Hungary (Terra abstracts, Abstracts supplement No.1. Terra Nova, Vol.5(1993)413), 7th Meeting of the European Union of Geosciences. Strasbourg, France. 4-8 April,1993. (1993)
9. Szakács E., Seghedi, I., Pécskay Z., Karátson D., Time-space evolution pattern of the Neogene/Quaternary volcanism in the Harghita Mountains, East Carpathians (Terra Abstracts, Abstracts supplement, No.1. Terra Nova, Vol.5(1993)576), 7th Meeting of the European Union of Geosciences. Strasbourg, France. 4-8 April,1993. (1993)
10. Koltay E., Szabó Gy., Borboly-Kiss I., Somorjai E., Kiss Á.Z., Mészáros E., Molnár Á., Bozó L., Characterization of regional atmospheric aerosols over Hungary by PIXE elemental analysis, First Research Co-ordination Meeting on Applied Research on Air Pollution Using Nuclear-Related Analytical Techniques, IAEA, Vienna, Austria. 30 March - 2 Apr.,1993. (1993)
11. Hunyadi I., Csige I., Géczy G., Hakl J., Lénárt L., Töröcsik I., Barlangterápián résztvevők radondózis terhelése Magyarországon (Előadás és poszter kivonatok. Bp., ELTE. p.17.), XVIII.Sugárvédelmi Továbbképző Tanfolyam. Balatonkenese, Magyarország, 1993.május 12-14. (1993)

12. Koltay E., The application of PIXE and PIGE techniques in the analytics of atmospheric aerosols (Abstract Book, 2.1), Eleventh International Conference on Ion Beam Analysis. Balatonfüred, Hungary, July 5-9,1993. (1993)
13. Hakl J., Hunyadi I., Vásárhelyi A., Influence of deep soil gas seepage on the indoor air quality in a Hungarian village located at a geologically active area, International Conference Indoor Air Quality and Climate in Central and Eastern Europe. Cluj Napoca, Romania, 27-28 Sept.,1993. (1993)
14. Hunyadi I., Hakl J., High radon potential in a North-Hungarian village exchanged by natural deep Earth gas upflow, 2nd International Colloquium on Gas Geochemistry. Besancon, France. 5-9 June, 1993. (1993)
15. Hakl J., Hunyadi I., Géczy G., Lénárt L., Experimental and theoretical studies on radon transport based on monitoring in caves, 2nd International Colloquium on Gas Geochemistry. Besancon, France. 5-9 June, 1993. (1993)
16. Józsa S., Majoros Gy., Máthé Z., Árvai-Sós E., Szakmány Gy., Tectonical evolution and magmatism of Tapolca basin (MAEGS8, Abstracts of Papers, Bp.,1993. p.89), 8th Meeting of the Association of European Geological Societies. Bucarest, Hungary, 22-24 Sept.,1993. (1993)
17. Hakl J., Lénárt L., Hunyadi I., Radonmérések a Bükki Nemzeti Park terület barlangjaiban és forrásaiban, A bükki barlangok kutatásának és hasznosításának legújabb eredményei. Miskolc, Magyarország, 1993.nov.11-13. (1993)
18. Pártay G., Németh T., Lukács A., Molnár E., Bujtás K., Csillag J., Bohátka S., 20 csatornás kvadrupól tömegspektrométeres mérőrendszer alkalmazása környezetvédelmi méréseknél (Konferencia kiadvány II.pp.40-46), Nemzetközi Vízügyi Konferencia. Siófok, Magyarország. 1993.május 5-7. (1993)
19. Lakatos G., Makádi M., Kiss M., Oláh M., Szabó M., Bohátka S., Cserháti Cs., Estimation of biocide-treatment effectiveness in industrial water systems using a new SEM-MS method, Sixth International Symposium Toxicity Assessment and On-line Monitoring. Berlin, Germany, 10-14 May,1993. (1993)
20. Benton, E.R., Csige I., Benton, E.V., Depth dependent track density and LET spectrum measurements with plastic nuclear track detectors in the A0015 experiment, Third LDEF Post-Retrieval Symposium. Williamsburg, Virginia, USA, 8-12 Nov.,1993. (1993)
21. Csige I., Frigo, L.A., Benton, E.V., Oda, K., Charge energy and LET spectra of high LET primary and secondary particles in CR-39 plastic nuclear track detectors of the P0006 experiment, Third LDEF Post-Retrieval Symposium. Williamsburg, Virginia, USA, 8-12 Nov.,1993. (1993)
22. Nefedov, N., Csige I., Benton, E.V., Henke, R.P., Benton, E.R., Frigo, L.A., Measurement of trapped proton fluences in main stack of P0006 experiment, Third LDEF Post-Retrieval Symposium. Williamsburg, Virginia, USA, 8-12 Nov.,1993. (1993)
23. Benton, E.V., Csige I., Frank, A.L., Benton, E.R., Frigo, L.A., Parnell, T.A., Watts, J., Harmon, A., Absorbed dose, LET spectra and neutron measurements on LDEF, Third LDEF Post-Retrieval Symposium. Williamsburg, Virginia, USA, 8-12 Nov.,1993. (1993)
24. Uray I., Radiation status in north-east Hungary after the Chernobyl accident, Workshop Chernobyl. Debrecen, Hungary, 29.Oct.,1993. (1993)
25. Uray I., Influence of different factors on external exposure of the population investigated in the Bryansk region, Workshop Chernobyl. Debrecen, Hungary, 29.Oct.,1993. (1993)

26. Uray I., Hille, R., Method for exact measurements of the external exposure around Chernobyl (Abstr.:P-12.6), Radiation Protection in Neighbouring Countries in Central Europe. Obergurgl, Tyrol, Austria. 28-30.Apr.,1993. (1993)
27. Uray I., Hille, R., Some characteristics of the external exposure in territories around Chernobyl (Abstr.: P-12.7), Radiation Protection in Neighbouring Countries in Central Europe. Obergurgl, Tyrol, Austria. 28-30.Apr.,1993. (1993)
28. Uray I., Abhängigkeit der externen Dosis von den Lebensumständen, Abschlussseminar für die Messkampagne des BMU 1993 in der GUS. München, BRD, 16-17 Dec.,1993. (1993)
29. Heinzelmänn, M., Uray I., Izmerenie individual'nykh doz vnesnego oblucheniya s pomoshch'yu termolyuminiscentnykh dozimetrov, Itogi izmeritel'noj programmy, provodimoy spetsialistami Germanii v Respublike Belarus' v 1992-1993 gg. Minsk, Respublika Belarus', 30 avgusta - 1 sentabrya, 1993. (1993)
30. Ramzaev, V.L., Parkhomenko, V.I., Ponomarev, A.V., Tselousov, A.G., Makusnikov, E.V., Trusov, V.V., Krivonosov, S.P., Uray I., Formirovanie doz oblucheniya personala pri tushenii lesnykh pozharov v usloviyakh radioaktivnogo zagryazheniya mestnosti, Opyt raboty po reabilitatsii territorij postradavshikh ot Chernobyl'skoj katastrofy. Novozybkov, Rossijskaya Federatsiya, 30 noyabrya - 2 dekabrya 1993 g. (1993)
31. Konecny, V., Balogh K., Vass, D., Orliczky, O., Lexa, J., Evolution of alkali basalt volcanism in southern Slovakia, based on K/Ar dating (Abstracts of 8th Meeting of EUGS, Bp., Hung.Geol.Soc.1993. p.33), 8th Meeting of the Association of European Geological Societies. Budapest, Hungary, 23 Sept.,1993. (1993)
32. Székyné-Fux V., Tormássy I., Pécskay Z., The Tertiary volcanism of Transdanubia (W-Hungary), MAEGS 8. Evolution of Intramontane Basins on the Example of the Pannonian Basin. Budapest, Hungary, 22-24 Sept.,1993. (1993)
33. Pécskay Z., Balogh K., Székyné-Fux V., Gyarmati P., Crihán, M., Kovacs, M., Bernád, A., Edelstein, O.
K-Ar geochronological studies on Neogene volcanic rocks from the Oas Mts (Romania) and Tokaj Mts. (Hungary). IGS The third Geological Symposium. Baia Mare, 21-23 Oct.,1993. (1993) Romania.
34. Edelstein, O., Pécskay Z., Kovacs, M., Bernád, A., Crihán, M., Gábor M., Halga S., K-Ar and Ar-Ar determination and some aspects of chronology of magmatic and metallogenetic processes from Oas-Tibles Mts., IGS The third Geological Symposium. Baia Mare, Romania, 21-23 Oct.,1993. (1993)
35. Székyné-Fux V., Pécskay Z., Tormássy I., The Tertiary volcanism of Transdanubia (W-Hungary), IGS The third Geological Symposium. Baia Mare, Romania, 21-23 Oct.,1993. (1993)
36. Bartosiewicz L., Tigler A., Hertelendi E., Dating hand-collected fish remains from a prehistoric settlement in Hungary, 7th Meeting of International Council for Archaeozoology. Tervuren, Belgie, Koninklijk Museum voor Midden-Afrika, 1993. (1993)
37. Csige I., Benton, E.V., Benton, E.R., Nefedov, V.I., Frigo, L.A., Frank, A.L., Dosimetric measurements of high LET secondary particles produced by high energy protons in plastic nuclear track detector stacks (Abstr.:p.2.4), Austrian-Italian-Hungarian Radiation Protection Symposium: Radiation Protection in Neighbouring Countries in Central Europe. Obergurgl/Tyrol, Austria. 28-30 April,1993. (1993)

38. Barnabás I., Hertelendi E., Veres M., A Paksi Atomerőmű radiokarbon szennyezésének mérése az erőmű környezetében, XVIII. Sugárvédelmi Továbbképző Tanfolyam. Balatonkenese, Magyarország, 1993.május 12-14. (1993)
39. Kertész R., Sümegi P., Braun M., Hertelendi E., Félegyházi E., Vörös I., Mezőlitische Fundorte auf dem Nördlichen Teil der Grossen Ungarischen Tiefebene, A Neolitikum vitás kérdései Közép-Kelet Európában. Nyiregyháza, Magyarország, 1993.nov.8-11. (1993)
40. Horváth F., Hertelendi E., New data to the chronology of the middle Neolithic in South-Alföld, A Neolitikum vitás kérdései Közép-Kelet Európában. Nyiregyháza, Magyarország, 1993.nov.8-11. (1993)
41. Uray I., Ergebnisse einer KFA-Messreise 1991 in das nach dem Tschernobyl-Unfall hochbelastete Gebiet Brjansk-Thula-Orel/USSR, Uniklinikum. Essen, BRD, 18 Nov.,1991. (1991)
42. Uray I., Ergebnispräsentation der TLD Messungen, Auswertung der Messaktion 1992, Forschungszentrum Jülich GmbH, Jülich, BRD, 4 Dec.,1992. (1992)
43. Pécskay Z., Djordjevic, M., Karamata, S., Knezevic-Djordjevic, V., First data on the age of the volcanic rocks from the Ridanj-Krepoljin zone, Session of Serbian Geological Society. Beograd, Serbia, 24. Dec.,1992. (1992)
44. Balogh K., Cvetkovic, V., Prvi podaci o vremenu i intenzitetu metamorfnih faza u podrucju batocine, Srpsko-Makedonska masa, Session of Serbian Geological Society. Beograd, Serbia, 24. Dec.,1992. (1992)
45. Edelstein, O., Kovács, M., Crihán, M., Bernád, A., Pécskay Z., K-Ar age determination on Neogene volcanic rocks from Oas-Gutii Mountains (East Carpathian, Romania), Institutul de Geologie si Geofizică. Bucharest, Romania, 11.Febr.,1993. (1993)
46. Seghedi, I., Szakács A., Pécskay Z., Geochronology of the volcanic region of the Calimani-Harghita Mountains. (East Carpathian, Romania) in the light of K/Ar data, Institutul de Geologie si Geofizică. Bucharest, Romania, 11.Febr.,1993. (1993)
47. Pécskay Z., Application of K/Ar method in the study of the Tertiary volcanic activity of the Pannonian basin, Institutul de Geologie si Geofizică. Bucharest, Romania, 11.Febr.,1993. (1993)
48. Harangi Sz., Árva-Sós E., A Mecsek hegység és környéke alsó kréta vulkáni kőzeteinek komplex geológiai vizsgálata, Alföldi Napok. Geológiai Ankét, DAB. Debrecen, 1993. május 13. (1993)
49. Máthé Z., Árva-Sós E., A Ny-mecseki neogén tufák ásvány-kőzettani vizsgálata és a K/Ar radiometrikus kora, Alföldi Napok. Geológiai Ankét, DAB. Debrecen, 1993. május 13. (1993)
50. Józsa S., Árva-Sós E., Az É-magyarországi mezozóos bázisos magmás képződmények petrológiai és K/Ar módszeres geokronológiai értékelése, Alföldi Napok. Geológiai Ankét, DAB. Debrecen, 1993. május 13. (1993)
51. Máthé Z., Majoros Gy., Józsa S., Szakmány Gy., Árva-Sós E., A Balatonmária-1.sz. fúrás által harántolt bazalt ásvány-kőzettani vizsgálata és K/Ar kora, Alföldi Napok. Geológiai Ankét, DAB. Debrecen, 1993. május 13. (1993)
52. Balogh K., A Kárpát-medence szarmata utáni bazalt vulkánosságának újabb kronológiai eredményei, Alföldi Napok. Geológiai Ankét, DAB. Debrecen, 1993. május 13. (1993)
53. Árkai P., Felvári Gy., Balogh K., Az alacsony fokú metamorfitok agyagásványainak K/Ar vizsgálata, Alföldi Napok. Geológiai Ankét, DAB. Debrecen, 1993. május 13. (1993)

54. Székyné-Fux V., Pécskay Z., Latitos paleogén vulkanit a Nagy Alföld D-i szegélyéről, Alföldi Napok. Geológiai Ankét, DAB. Debrecen, 1993. május 13. (1993)
55. Kozák M., Pécskay Z., Újabb adatok a Sierra Maestra (Kuba) magmatitjainak korviszonyaihoz, Alföldi Napok. Geológiai Ankét, DAB. Debrecen, 1993. május 13. (1993)
56. Dunkl I., Balogh K., Csontos L., Árkai P., Nagy G., A termikus történetek elemzése a hasadványnyom módszer segítségével - a Bükk kréta utáni kiemelkedésének datálása, Magyarhoni Földtani Társulat, Budapesti Területi Szervezete. Budapest, Magyarország, 1993. ápr. 19. (1993)
57. Hunyadi I., Radon a környezetben, Bolyai Nyári Akadémia. Sepsiszentgyörgy, Románia. 18-25 July, 1993. (1993)
58. Hakl J., Geogas activity in village of Mátraderecske, Hungary, Dip. di Scienze della Terra Università degli Studi di Roma "La Sapienza", Roma, Italy, 26 Oct., 1993. (1993)
59. Hakl J., Underground fluid motions in karstic areas traced by natural radon, Dip. di Scienze della Terra Università degli Studi di Roma "La Sapienza", Roma, Italy, 27 Oct., 1993. (1993)
60. Bilik I., Árva-Sós E., Kontinentális rift-eredetű alsókréta telérrajok a Mecsek hegységben, ELFT, Közettan-Geokémiai Tanszék Szádeczky-Kardoss Elemér Emlékülés. Budapest, Magyarország, 1993. szept. 4. (1993)
61. Pécskay Z., Az Avas-Gutin-Kelemen-Hargita vulkáni vonulat kronológiája a K/Ar koradatok tükrében, ELTE, Magyarhoni Földtani Társulat, Ásványtan-Geokémiai Szakosztály. Budapest, Magyarország, 1993. nov. 16. (1993)
62. Dunkl I., Árkai P., Balogh K., Uplift history of Pannonian basement from fission-track data, Europrobe Meeting. Csopak, Magyarország, 1993. nov. 7-11. (1993)
63. Balogh K., A Kárpát-medence szarmata utáni bazaltvulkánosságának újabb kronológiai eredményei, ELTE Közettan-Geokémiai Tanszék. Szeminárium Szádeczky-Kardoss E. emlékére. Budapest, Magyarország, 1993. szept. 4. (1993)
64. Vető I., Hetényi M., Demény A., Hertelendi E., A hidrogén index, mint az anaerob bakteriális tevékenység mutatója, VEAB Szerveskémiai Albizottság Ülésszaka. Veszprém, Magyarország, 1993. nov. 3. (1993)
65. Hertelendi E., Veres M., A mátraderecskei szivárgó gáz eredete izotópanalitikai vizsgálatok tükrében, ELTE Atomfizikai Tanszék. Budapest, Magyarország, 1993. április 8. (1993)
66. Hámor T., Hertelendi E., Szulfid és szulfátásványok kénizotóp-arány méréseiből levonható következtetések, Alföldi Napok. Debrecen, Magyarország, 1993. május 15. (1993)
67. Szöör Gy., Barta I., Hertelendi E., Sümegi P., Szanyi J., Quarter és neogen mollusca héjak kemotaxonomiai és paleoökológiai elemzése, Alföldi Napok. Debrecen, Magyarország, 1993. május 15. (1993)
68. Hertelendi E., Isotope methods in hydrogeology, Institute of Geology, Zagreb. Zagreb, Croatia, May 17, 1993. (1993)

Biological and Medical Research

1. Csejtei A., Fenyvesi A., Molnár T., Pásti G., Miltényi L., Mahunka I., Kovács P., Francia I., Vincze J., Nagy K., Physical and biological dozimetry with regard to further neutron theory applications at the cyclotron in Debrecen, 24th Annual Meeting of the European Society of Radiobiology. Erfurt, Germany, 4-8 Oct.,1992. (1992)
2. Boothe, T.E., McLeod, T.F., Plitnikas, M., Kinney, D., Tavano, E., Feijoo, Y., Smith, P., Szelecsényi F., Commercial and PET radioisotope manufacturing with a medical cyclotron, 12th International Conference of the Application of Accelerators in Research and Industry. Denton, Texas, USA, 2-5 Nov.,1992. (1992)
3. Hunyadi I., Csige I., Géczy G., Hakl J., Lénárt L., Töröcsik I., Barlangterápián résztvevők radondózis terhelése Magyarországon (Előadás és poszter kivonatok. Bp., ELTE. p.17.), XVIII.Sugárvédelmi Továbbképző Tanfolyam. Balatonkenese, Magyarország, 1993.május 12-14. (1993)
4. Mikecz P., Tóth Gy., Quality control of radiopharmaceuticals in the Atomki, Cost-Action B3. Meeting of the Management Committee and Associated Workshop. Budapest, Hungary, 24-25 June, 1993. (1993)
5. Szelecsényi F., Boothe, T.E., Tavano, E., Plitnikas, M., Tárkányi F., Nuclear data relevant to the production of ⁶⁷Ga: A critical comparison of excitation functions / Thick target yield data for the ⁶⁷Zn(p,n) and ⁶⁸Zn(p,2n) nuclear reactions (Abstr.: p.9), Fifth International Workshop on Targetry and Target Chemistry. Brookhaven National Laboratory, North Shore University, Hospital, New York, USA. 19-23 Sept.,1993. (1993)
6. Tárkányi F., Takács S., Heselius, S.J., Solin, O., Bergman, J., Study of static and dynamic effects in gas targets (Abstr.:p.11), Fifth International Workshop on Targetry and Target Chemistry. Brookhaven National Laboratory, North Shore University, Hospital, New York, USA. 19-23 Sept.,1993. (1993)
7. Bohátka S., Csatlós M., Lakatos Gy., Makádi M., Ecophysiological measurements with quadrupole mass spectrometer, 11th Internal Meeting on Mass Spectrometry. Budapest'93. Budapest, Hungary, 26-28 April,1993. (1993)
8. Tárkányi F., Cyclotron utilization programmes in Debrecen, Hungary, National Seminar on Cyclotron in Science and Technology. Cairo, Egypt, 13-17 November, 1993. (1993)
9. Tárkányi F., Small accelerators and cyclotrons as research and teaching tools, National Seminar on Cyclotron in Science and Technology. Cairo, Egypt, 13-17 November, 1993. (1993)
10. Uzonyi I., Szluha K.L., Bacsó J., Determination of Pt concentration in human tissues using XRF, 6th Hungaro-Italian Symposium on Spectrochemistry, Advance in Environmental Sciences. Lillafüred, Hungary, 23-27 Aug.,1993. (1993)
11. Bacsó J., MacPherson, A., Hair calcium concentration as a marker of atherosclerosis (Abstract p.123), World Congress of Gerontology. Budapest, Hungary, 4-9 July, 1993. (1993)
12. Szluha K.L., Péter M., Lampé L., Hernádi Z., Czifra I., Bacsó J., Uzonyi I., és mások, Gyógyszereloszlás vizsgálatainak új lehetőségei előrehaladott cervixrák neoadjuvans cisplatin kezelésénél (Abstract Book p.44), XIII.Magyar Onkológus Kongresszus. Budapest, Magyarország, 1993.nov.3-5. (1993)

13. Szluha K.L., Péter M., Lampé L., Hernádi Z., Bacsó J., Uzonyi I., et al., Assessment of the distribution of CDDP in the tumor of cervical cancer patients treated by intra-arterial and i.v. administration (Regional Cancer Treatment 1993.S.1.48), ICRC Kongress Wiesbaden. Wiesbaden, Germany, 12-14 July, 1993. (1993)
14. Sarkadi É., Kovács Z., Andó L., C izotóppal jelzett metionin előállítására pozitron emissziós tomográffal végzett vizsgálatokhoz, MONT 8.kongresszusa. Szeged, Magyarország, 1993.aug.30-sept.1. (1993)
15. Nagy K., Dajkó G., Uray I., Nagy Zs., Comparativ studies on the free radical scavenger properties of two nootropic drugs, CPH and BCE-001, 5th Conference on the International Association of Biomedical Gerontology. Budapest, Hungary, 1-3 July, 1993. (1993)
16. Bacsó J., Application of XRF in bio-medical research, Universitatea Babes, Bolyai, Facultatea de Fizica. Kolozsvár, Románia, 1993.jun.2. (1993)
17. Bacsó J., XRF and its applications on interdisciplinary field, Universitatea Babes, Bolyai Facultatea de Fizica. Kolozsvár, Románia, 1993.jun.3. (1993)
18. Mahunka I., Radionuclide productions with cyclotrons, Ankara Nuclear Research and Training Center. Ankara, Turkey, May 5, 1993. (1993)
19. Mikecz P., Developments in the field of isotope production at Debrecen, Hammer-smith Hospital, MRC Cyclotron Unit. London, U.K. 12 March, 1993. (1993)
20. Tárkányi F., Takács S., Heselius, S.J., Solin, O., Bergman, J., Gas targetry. Study of static and dynamic effects in gas targets, Cyclotron Facility, Division of Nuclear Medicine. Mount Sinai Medical Center, Miami Beach, USA, 27 Sept., 1993. (1993)
21. Kovács Z., Tárkányi F., Production of radiohalogens with the CV-28 cyclotron in the frame of Jülich-Debrecen cooperation, KLTE Kísérleti Fizika Tanszék, Debrecen, Magyarország, 1993.szept.24. (1993)
22. Kovács Z., Automated syntheses in labeling procedures with PET isotopes, NKK Corporation. Kawasaki, Japan, 17 Nov, 1993. (1993)
23. Kovács Z., Radioisotope production for medical purposes, Nisina Memorial Cyclotron Centre. Morioka, Japan, 11. Nov., 1993. (1993)
24. Mahunka I., Recent developments in the medical application at the Debrecen cyclotron, NKK Corporation, Cyclotron team. Kawasaki, Japan, Nov. 17, 1993. (1993)

Development of Instruments and Methods

1. Biri S., Gyorsítóberendezések nehézionforrásai, Az atomenergia- és magkutató újabb eredményei. Szerk. Koltay E. Bp., Akadémiai K. 10 (1993) 137
2. Molnár J., Implementing Intel 80170 on VME, "IMANN Two" Informal Meeting on Artificial Neural Networks 2. Stockholm, Sweden, 25 Nov., 1992. (1992)
3. Parkhomenko, V.I., Trusov, V.V., Gorodnaya, T.A., Hille, P., Uray I., Metodicheskie osobennosti povysheniya chuvstvitel'nosti termolyuminestsennykh dozimetrov na osnove LiF i rezul'taty obsledovaniya naseleniya Bryanskoj oblasti (Ukrainskij Nauchnyj Tsentri Radiatsionnoj Meditsiny MZ i AN Ukrainy, Kiev), Aktual'nye voprosy retrospektivnoj, tekushchej i prognoznoj dozimetrii oblucheniya v rezul'tate chernobyl'skoj avarii. Kiev, Ukraina, 27-29 okt. 1992. (1992)
4. Biri S., Vámosi J., The Debrecen ECR project (Book of Abstracts, p.20), 11. Workshop on the Physics and Technology of Electron Cyclotron Resonance (ECR) Ion Sources. Groningen, Hollandia. 6-7 May, 1993. (1993)

5. Rosengard, U., Leontein, S., Nilsson, A., Paál A., Filevich, A., Székely G., Beam diagnostics in CRYRING, First European Workshop on Beam Instrumentation and Diagnostics for Particle Accelerators, DIPAC 1993. Montreaux, Switzerland, 3-5 May, 1993. (1993)
6. Székely G., Filtering detector signals using neural networks, Informal Meeting on Artificial Neural Networks 3. Manne Siegbahn Institute of Physics. Stockholm, Sweden, 24.Febr,1993. (1993)
7. Molnár J., An "Universal" hardware implementation, "IMANN Three" Informal Meeting on Artificial Neural Networks 3. Stockholm, Sweden, 24 Febr.,1993. (1993)
8. Vasváry L., Ditrói F., Takács S., Szabó Z., Szücs J., Kundrák J., Mahunka I., Wear measurement of cutting edge of superhard turning tools using TLA technique (Book of Abstract 4.11), Eleventh International Conference on Ion Beam Analysis. Balatonfüred, Hungary, July 5-9,1993. (1993)
9. Ditrói F., Meyer, J.D., Michelmann, R.W., Kislak, D., Bethge, K., Investigation of silicon with (p,p') resonance scattering in <110> channeling direction, Third European Conference on Accelerators in Applied Research and Technology (ECAART-3). Orléans, France. Aug.31 - Sept.4, 1993. (1993)
10. Török I., Terasawa, M., Petukhov, V.P., High resolution PIXE instrumentation survey. Part II. (Abstr. P43), Third European Conference on Accelerators in Applied Research and Technology. (ECAART3). Orléans, France. 30 Aug. - 5 Sept.,1993. (1993)
11. Bohátka S., Futó I., Gál I., Gál J., Langer G., Molnár J., Paál A., Pintér G., Simon M., Szádai J., Székely G., Szilágyi J., Mass spectrometer system for monitoring fermentation processes (Abstract Book Vol.II. TU378), 6th European Congress on Biotechnology. Firenze, Italy, 13-17 June, 1993. (1993)
12. Szilágyi J., Sántha Gy., Seres P., Ágoston A., Pólya K., Bohátka S., Langer G., Futó I., Simon M., Quadrupole mass spectrometric measurements of volatile and nonvolatile fermentation components (Abstract Books Vol.II.TU158), 6th European Congress on Biotechnology. Firenze, Italy, 13-17 June, 1993. (1993)
13. Tárkányi F., Cyclotron utilization programmes in Debrecen, Hungary, National Seminar on Cyclotron in Science and Technology. Cairo, Egypt, 13-17 November, 1993. (1993)
14. Kormány Z., Energiemess system für das Kompaktzyklotron in der KFA Jülich, Zyklotron - Workshop. Rossendorf, Germany, Sept.30 - Oct.1,1993. (1993)
15. Máthé Gy., Microminiature cryocooler, Hungarian-Korean Technical Cooperation Center Conference. Balatonfüred, Hungary, 31 March, 1993. (1993)
16. Papp Z., Faddeev-equations with Coulomb-interaction, Karl-Franzens Universität Graz. Graz, Austria, 11-13 April, 1993. (1993)
17. Uray I., Hille, R., Method for exact measurements of the external exposure around Chernobyl (Abstr.:P-12.6), Radiation Protection in Neighbouring Countries in Central Europe. Obergurgl, Tyrol, Austria. 28-30.Apr.,1993. (1993)
18. Uray I., Hille, R., Some characteristics of the external exposure in territories around Chernobyl (Abstr.: P-12.7), Radiation Protection in Neighbouring Countries in Central Europe. Obergurgl, Tyrol, Austria. 28-30.Apr.,1993. (1993)
19. Dajkó G., Tóth J., Microfilter equipment applying track membranes, Third International Conference on Particle Track Membranes. Jahranka, Poland,26-30 Oct.,1993. (1993)
20. Mahunka I., Radionuclide productions with cyclotrons, Ankara Nuclear Research and Training Center. Ankara, Turkey, May 5, 1993. (1993)

21. Mahunka I., Analytical applications of accelerators and cyclotrons, Ankara Nuclear Research and Training Center. Ankara, Turkey, May 4,1993. (1993)
22. Kövér L., Studies of the local electronic structure by using high energy X-ray excited Auger spectroscopy, Istituto di Metodologie Avanzate Inorganiche C.N.R. Roma, Italy. Oct.11,1993. (1993)
23. Futó I., Deng, H., Effect of pressure on membrane inlet mass spectrometry, Technical University Center of Biotechnology Research (Annual Meeting). Copenhagen, Dania, 15.Nov.,1993. (1993)
24. Mahunka I., Multipurpose use of the MGC cyclotron in Debrecen, Nisina Memorial Cyclotron Centre. Morioka, Japan, Nov.11,1993. (1993)
25. Kövér L., Tökési K, Varga D., Elektrosztatikus elektronspektrométer modul, közös tengelyű elrendezésben való alkalmazása *Patent submitted*: in Hungary, on 03-20-1989; *accepted*: on 12-23-1992; Nr. 207 606 (1992) 13

Theses completed

Academic Doctor of Sciences Degree

1. L. Sarkadi, **Atomic collision processes of high energy** (in Hungarian), Atomki, Debrecen (1991) 92

Academic Candidate of Sciences Degree

1. Z. Papp, **Approximate method to describe charged, quantummechanical systems in an asymptotically correct way in the case of two-body final states** (in Hungarian), Atomki, Debrecen (1992) 58

University Doctoral Degree (PhD)

1. Zs. Fülöp, **Study of bound and resonant states of *sd*-shell nuclei** (in Hungarian), Atomki, Debrecen (1993) 84
2. J. Hakl, **Study of radon transport** (in Hungarian), Atomki, Debrecen (1992) 72

Diploma Works

1. J. Tassy, **Origin of bankfiltrated water supply** (in Hungarian), Supervisor: E. Hertelendi, Atomki, Debrecen (1993) 37
2. L. Urbán, **Study of origin and composition of gases leaking in the region of Mátradercske** (in Hungarian), Supervisor: E. Hertelendi, Atomki, Debrecen (1993) 20
3. I. Lente, **Radiocarbon chronology of late-neolithic settlements in Kislőd** (in Hungarian), Supervisor: E. Hertelendi, Atomki, Debrecen (1993) 39
4. I. Rajta, **Electron-optic calculations in electrostatic fields** (in Hungarian), Supervisor: K. Tökési, Atomki, Debrecen (1993) 48
5. I. Cseh, **Modelling and experimental study of the formation of Si(Li) Röntgen spectra** (in Hungarian), Supervisor: M. Kiss-Varga, Atomki, Debrecen (1993) 63
6. M. Nyitrai, **Theory, construction, and use of microminiature cryocooler based on the Joule-Thomson effect** (in Hungarian), Supervisor: Gy. Máthé, Atomki, Debrecen (1993) 52
7. S. Széles, **Study of Hall-effect in high- T_C superconductors** (in Hungarian), Supervisor: K. Vad, Atomki, Debrecen (1993) 42

8. P. Végh, **Study of trace-element composition of the atmospheric dust particles with Röntgen-emission analysis: Analysing the lead content of the air in the city Debrecen and its surroundings** (in Hungarian), Supervisor: J. Bacsó, Atomki, Debrecen (1993) 58
9. G. Szekrényes, **Röntgen-emission-analytic study of Ca content in human hair** (in Hungarian), Supervisor: J. Bacsó, Atomki, Debrecen (1993) 49
10. Sz. Vattamány, **Algebraic description of $^{28}\text{Si}+\alpha$ and $^{28}\text{Si}+^{28}\text{Si}$ systems** (in Hungarian), Supervisor: J. Cseh, Atomki, Debrecen (1993) 52
11. I. Dankó, **Study of ^{112}Sb nucleus in cyclotron beams** (in Hungarian), Supervisors: T. Fényes, J. Gulyás, Atomki, Debrecen (1993) 59

HEBDOMADAL SEMINARS

January 7

Developments and first measurements at the MSI (Stockholm) heavy-ion storage ring

A. Paál

January 14

Giant dipole resonances in hot thorium and californium nuclei

I. Diószegi (Institute of Isotopes, Budapest)

January 21

Investigation of Hungarian magmatic structures by *K-Ar* method

E. Sós

January 28

Structure of *Ga* and *As* nuclei, dynamical- and supersymmetries

T. Fényes

February 4

Medical NMR-spectroscopy

J. Széles, (II. Chirurgische Universitätsklinik, Vienna)

February 11

Tshernobyl paradoxons (A reportage from the infected territories)

Í. Uray

February 18

Determination of relative intensity of radiative electron transitions from wave dispersive Röntgen spectra

J. Lábár, Institute of Technical Physics Research, Budapest

February 25

Investigation of Hungarian vulcanic minerals by *K-Ar* method

Z. Pécskay

March 11

Nanocrystallic materials

D. Beke (Kossuth University, Debrecen)

March 18

Quantummechanical three-body problem with Coulomb interaction

Z. Papp

March 25

Nuclear structure research with the (e,e'p) reaction
H. P. Blok (Free University, Amsterdam)

April 1

Artificial neural networks applied to physics experiment and analysis
Th. Lindblad (Manne Siegbahn Institute, Stockholm)

April 8

Revolution in chemistry: the discovery of fullerenes
M. Beck (Kossuth University, Debrecen)

April 16

Structure of the low-energy excited states of ^{66}Ga and ^{68}Ga nuclei
J. Tímár

April 20

Semimicroscopical description of nuclear clusterization
J. Cseh

April 29

Record of cosmogenic nuclides in meteorits and Moon
U. Herpers (University of Köln)
Modelling of interaction of cosmic rays with matter
R. Michel (University of Hannover)

May 6

Superactive groups of sun-spots and evolution of their magnetic fields
B. Kálmán (Observatory of the Hungarian Academy of Sciences, Debrecen)

May 13

Resonant post-collision interactions in proton-neon ionization processes
S. Ricz

May 20

Effect of the nuclear core on splitting of proton-neutron multiplets in $^{104-116}\text{In}$
and $^{116-124}\text{Sb}$ nuclei
Zs. Dombrádi

May 27

Operation of ECR source and K130 cyclotron at University of Jyväskylä
J. Ärje (University of Jyväskylä)

June 3

On the institute's ECR project and an account about the 11. ECR conference
S. Biri

June 10

PIXE measurements at the 5 MeV Van de Graaff generator

I. Borbélyné Kiss

June 17

Genetical algorithms and the problem of the travelling salesman

K. F. Pál

June 24

Structure of ^{106}In and ^{118}Sb nuclei

J. Gulyás

June 30

X-ray satellite lines in charged particle excitations

I. Török

August 17

Structure of ^{114}Sb , ^{116}Sb and ^{116}Sn nuclei

Z. Gácsi

September 2

Life-time measurements by small recoil velocity Doppler shift in ^{96}Zr , ^{134}Ba and ^{144}Sm nuclei

T. Belgya

September 8

The roles of sample processes and excitation modes in the ED Roentgen fluorescence analysis

M. Kis-Varga

September 9

Multivalued wave functions and the Aharanov-Bohm effect

H. Miyazawa (Kanagawa University)

September 16

Nuclear accelerator in the Louvre

Á. Kiss

September 23

Continuum effects in the description of giant resonances

T. Vertse

September 30

Decay mode of the isobaric analogue state and isospin impurity

M. N. Harake (KVI, Groningen)

October 6

Investigation of quantumechanical potential problems by methods of supersym-

metric quantum mechanics and group theory

G. Lévai

October 7

Water-jet technology

M. M. Vijay (Int. Soc. of Water-Jet Technology, Canada)

October 14

Measurement of double differential ionization cross sections for proton-argon collisions

Á Kövér

October 21

Charge-exchange modes: Collectivity and microscopic structures

S. Y. van der Werf (KVI, Groningen)

October 28

Active and passive electrons in ion-atom collisions

B. Sulik

November 11

Determination of magnetic moments of Coulomb-excited nuclear states in ^{150}Sm nucleus

T. Vass

December 2

Description of strongly correlated systems by variational wave functions

Zs. Gulácsi (Kossuth University, Debrecen)

December 15

Detection of neutrons by solid-state track detectors

G. Dajkó

December 16

Recent advances in radiopharmaceutical development for emission tomography

G. Stöcklin (Inst. für Nuklearchemie Forschungszentrum, Jülich)

Author Index

- Adachi *H. 53, 73
Adamides *E. 24
Adamik *M. 79
Algora A. 16, 19
Ali *A. 114, 116
Andó L. 147, 148
Atac *A. 24
- Árva-Sós E. 104
- Bacsó J. 114, 116, 129, 131
Balogh K. 104
Barna *P.B. 51, 79
Barnabás *I. 124
Bartha L. 166
Bartosiewicz *L. 126
Beke *D.L. 97, 158
Benton *E.R. 108
Benton *E.V. 108
Berényi D. 41, 47, 62
van den Berg *A.M. 143
Bergman *J. 81, 83
Bethge *K. 88
Biri S. 162, 164
Biron *I. 6
Bohátka S. 101
Boothe *T.E. 133, 134
Borbély-Kiss I. 96, 114, 118, 120, 121
Bozó *L. 118, 121
Brant *S. 10
- Calligaro *T. 6
Campbell *J.L. 64, 66
Cederwall *B. 24
Charlton *M. 58
Czifra *I. 131
- Csaba *E. 124
Csatlós M. 28, 30, 154
Cseh J. 37, 38
Cserny I. 51, 53
Csige I. 108
- Dajkó G. 156
Dankó I. 26, 27
Daróczi *L. 97
Deák *J. 128
Degn *H. 160
Diószegi I. * 30
Ditrói F. 81, 85, 87, 88
Dombi I. 147
Dombrádi Zs. 10, 19, 22, 24
- Engstler *S. 1
- Fahlander *C. 24
Fainstein *P.D. 77
Fayez F.M. Hassan 26, 27
Feijoo*Y. 133, 134
Fenyvesi A. 81, 85, 156
Fényes T. 10, 12, 14, 16, 19
Figler *M. 126
Futó I. 160
Fülöp Zs. 5, 8, 21
- Gácsi Z. 22, 23
Gál I. 145, 158
Gál J. 140, 142, 158
Grodén *B.M. 129
Groeneveld *K.O. 41, 62
Gulyás J. 26, 27
Gulyás L. 77
- Haar *R.R. 47
Hakl J. 110, 112
Halász G. 99
Harakeh *M.N. 145
Hegman N. 99
Hegyési Gy. 158
Henke *R.P. 108
Hertelendi E. 124, 126, 128
Heselius *S.-J. 81, 83
Horváth *F. 126
Hunyadi I. 5, 110, 112
Hunyadi M. 30

- Ideguchi *E. 24
- Johnson *A. 24, 140, 142
- Józsa M. 24
- Julin *R. 24
- Juutinen *S. 24
- Kalinka G. 56, 94, 137, 140, 142
- Karczmarczyk *W. 24
- Keinonen *J. 8
- Kerek *A. 24, 140, 142, 156
- Khemliche *H. 47
- Kislat *D. 88
- Kiss Á.Z. 5, 6, 8, 21, 118, 166
- Kis-Varga M. 97, 158
- Koltay E. 114, 118, 120, 121, 166
- Kovács P. 158
- Kovács Z. 85, 148
- Kovács Zs. 73
- Kownacki *J. 24
- Kövér Á. 58, 152
- Kövér L. 51, 53, 73, 79
- Krasznahorkay A. 28, 30, 145, 154
- Kruppa A.T. 28
- Kuzel *M. 41, 62
- Lakatos *Gy. 101
- Lampé *L. 131
- Laricchia *G. 58
- Lénárt *L. 128
- Lévai G. 1, 37, 38
- Lind *P. 32
- Liotta *R.J. 32, 40
- Lovas R.G. 35
- Macek *J.H. 68
- MacPherson *A. 129
- Maglione *E. 32
- Mahunka I. 87, 147
- Maier *R. 41
- Makádi *M. 101
- Máté Z. 28, 140, 142
- Medve *F. 114
- Meyer *J.D. 88
- Mészáros *E. 118, 121
- Mészáros S. 99
- Michelmann *R. 88
- Mikó *L. 128
- Miller *R. 60
- Mitrai *S. 24
- Molnár Á. 118, 121
- Molnár J. 150, 152, 154, 156
- Molnár M. 158
- Molnár T. 85, 134
- Monnin *M. 110
- Morin *J.P. 110
- Mórik Gy. 166
- Mukoyama *T. 71, 90, 92
- Nagy A. 147
- Nefedov *N. 108
- Némethy A. 51, 53, 79
- Norlin *L-O. 24
- Nyakó B.M. 24, 30, 140, 142
- Nyberg *J. 24
- Ormai *P. 124
- Paar *V. 10
- Papp T. 64, 66
- Pál K.F. 3
- Pálinkás J. 41, 43, 45, 47, 49, 62, 73, 75
- Pelikon *P. 60
- Perez G.E. 24, 140, 142
- Petukhov *V.P. 49
- Pécskay Z. 104
- Péter *M. 131
- Piiparinen *M. 24
- Plano *V.L. 47
- Plitnikas *M.E. 133, 134
- Podolyák Zs. 12, 18
- Posgay *G. 97
- Prior *M.H. 47
- Raczky *P. 126
- Raman *S. 64, 66
- Rauhala *E. 5
- Räisänen *J. 5

Ricz S. 60, 152
Rolfs *C.E. 21

Salin *A. 77
Salomon *J. 6
Sarkadi É. 148
Sarkadi L. 41, 43, 45, 47, 62, 71, 75
Schippers *J.M. 145
Schmidt *W. 131
Schneider *D. 47
Schubart *R. 24
Seidel *J.L. 110
Seweryniak *D. 24
Simon M. 101
Sletten *G. 24
Sohler D. 14, 18
Solin *O. 81, 83
Somorjai E. 5, 8, 21, 118, 166
Sulik B. 152
Suzuki *Y. 34, 35
Süveges *M. 128
Šimičić *Lj. 10

Szabó Gy. 96, 114, 118, 120, 121, 166
Szádai J. 147
Szelecsényi F. 85, 133, 134
Szluha *K.L. 131
Szűcs I. 147
Szűcs Z. 85, 133, 136

Takács S. 81, 82, 83, 85, 133, 134,
147, 148
Tanis *J.A. 47, 62
Tavano *E. 133, 134
Tárkányi F. 81, 82, 83, 85, 133, 134,
147, 148
Tikkanen *P. 8
Timár J. 10
Tóth *L. 60
Törmänen *S. 24
Török I. 49
Tökési K. 71, 90, 92
Trautvetter *H.P. 21

Uchrin *Gy. 124

Uray I. 105
Uzonyi I. 116, 131

Vad K. 99
Valek A. 167
Varga D. 51
Varga K. 34, 35, 40
Varga *Z. 140, 142
Vass T. 140, 142
Vasváry L. 82
Vámosi J. 162, 164
Várhegyi *A. 110
Vásárhelyi A. 112
Veres M. 124, 126, 128
Vertse T. 32
Végh J. 150, 152, 154, 156
Végh L. 68, 70
Villena *C. 131
Virtanen *A. 24
Viktor *L. 43, 45, 60, 62
Volent *G. 124

Wyss *R. 24

Závodszy P.A. 41, 43, 45, 47, 49,
62, 75
Zhu *M. 62

(* denotes author from other estab-
lishment)

Kiadja a
Magyar Tudományos Akadémia Atommag Kutató Intézete
A kiadásért és szerkesztésért felelős
Dr. Pálinkás József, az Intézet igazgatója
Készült a PÉJÉ Bt. vállalkozás nyomdájában
Törzsszám: 65785
Debrecen, 1994. március.

